Protocols for Collecting and Using Traffic Data in Bridge Design

REVISED DRAFT FINAL REPORT

Prepared for

National Cooperative Highway Research Program
Transportation Research Board
National Research Council

Bala Sivakumar
Michel Ghosn
Fred Moses

Research Agency:
Lichtenstein Consulting Engineers, Inc.
45 Eisenhower Drive
Paramus, New Jersey 07652

July 2008

TABLE OF CONTENTS

ACKNOWLEDGMENTS

ABSTRACT

This report documents and presents the results of a study to develop a set of protocols and methodologies for using available recent truck traffic data to develop and calibrate live load models for LRFD bridge design. The HL-93, a combination of the HS20 truck and lane loads, was developed using 1975 truck data from the Ontario Ministry of Transportation to project a 75-year live-load occurrence. Because truck traffic volume and weight have increased and truck configurations have become more complex, the 1975 Ontario data do not represent present U.S traffic loadings. The goal of this project, therefore, was to develop a set of protocols and methodologies for using available recent truck traffic data collected at different US sites and recommend a step-by-step procedure that can be followed to obtain live load models for LRFD bridge design. The protocols are geared to address the collection, processing and use of national WIM data to develop and calibrate vehicular loads for LRFD superstructure design, fatigue design, deck design and design for overload permits. These protocols are appropriate for national use or data specific to a state or local jurisdiction where the truck weight regulations and/or traffic conditions may be significantly different from national standards. The study also gives practical examples of implementing these protocols with recent national WIM data drawn from states/sites around the country with different traffic exposures, load spectra, and truck configurations.

EXECUTIVE SUMMARY

Protocols for Collecting and Using Traffic Data in Bridge Design

This report documents and presents the results of a study to develop a set of protocols and methodologies for using available recent truck traffic data to develop and calibrate live load models for LRFD bridge design. The HL-93, a combination of the HS20 truck and lane loads, was developed using 1975 truck data from the Ontario Ministry of Transportation to project a 75-year live-load occurrence. Because truck traffic volume and weight have increased and truck configurations have become more complex, the 1975 Ontario data do not represent present U.S traffic loadings. The goal of this project, therefore, was to develop a set of protocols and methodologies for using available recent truck traffic data collected at different US sites and recommend a step-by-step procedure that can be followed to obtain live load models for LRFD bridge design. The protocols are geared to address the collection, processing and use of national Weigh-In-Motion (WIM) data to develop and calibrate vehicular loads for LRFD superstructure design, fatigue design, deck design and design for overload permits. These protocols, comprised of thirteen steps with detailed instructions on their application, are appropriate for national use or use with data specific to a state or local jurisdiction where the truck weight regulations and/or traffic conditions may be significantly different from national standards. The study also gives practical examples of implementing these protocols with recent national WIM data drawn from states/sites around the country with different traffic exposures, load spectra, and truck configurations.

Project recommends that truck traffic data should be collected through Weigh-In-Motion systems that can collect simultaneously headway information as well as truck weights and axle weights and axle configurations while remaining hidden from view and unnoticed by trucks drivers. Truck data surveys collected at truck weigh stations and publicized locations are not accurate, because, they are normally avoided by illegal overweight vehicles that could control the maximum loads applied on bridge structures. The selection of WIM sites should focus on sites where the owners maintain a quality assurance program that regularly checks the data for quality. WIM devices used for collecting data for live load modeling should be required to meet performance specifications for data accuracy and reliability. A year's worth of recent continuous data is generally recommended for live load modeling. Quality information is just as important as the quantity of data collected. It is far better to collect limited amounts of well-calibrated data than to collect large amounts of data from poorly calibrated scales. Even small errors in vehicle weight measurements caused by poorly calibrated sensors could result in significant errors in measured loads.

High speed WIM is prone to various errors, which need to be recognized and considered in the data review process to edit out unreliable data and unlikely trucks to ensure that only quality data is made part of the load modeling process. It is also important to recognize that unusual data is not all bad data. The WIM data should therefore be scrubbed to include only the data that meet the quality checks. Error filtering procedures provided in these protocols should be applied for screening the WIM data prior to use in the live load modeling and calibration processes.

In many spans, the maximum lifetime truck-loading event is the result of more than one vehicle on the bridge at a time. Refined time stamps are critical to the accuracy of multiple presence (MP) statistics for various truck loading cases, including: single, following, side-by-side, and staggered. Many modern WIM data loggers currently in use in the U.S. have the

capability to record and report sufficiently accurate truck arrival times for estimating multiple presence probabilities. Studies have also shown that multiple presence statistics are mostly transportable from site to site with similar truck traffic volumes and traffic flow. Load effects for single lane and two lane loadings may be obtained directly from the WIM data when accurate time arrival stamps are collected. Generalized MP statistics may be used for simulation of maximum load effects where accurate truck arrival time stamps are not available. Trucks arriving at a bridge span are grouped into bins by travel lane and run through moment and shear influence lines with their actual relative positions and the resulting load effects are normalized by dividing by the corresponding load effects for HL-93. Legal loads and routine permits are grouped under STRENGTH I. Heavy special permits are grouped under STRENGTH II.

There are several possible methods available to calculate the maximum load effect L_{max} for a bridge design period (75 years) from truck WIM data collected over a shorter period of time (one year). The one implemented in these protocols is based on the assumption that the tail end of the histogram of the maximum load effect over a given return period approaches a Gumbel distribution as the return period increases. The method assumes that the WIM data is assembled over a sufficiently long period of time, preferably a year, to ensure that the data is representative of the tail end of the truck weight histograms and to factor in seasonal variations and other fluctuations in the traffic pattern. Sensitivity analyses have shown that the most important parameters for load modeling are those that describe the shape of the tail end of the truck load effects histogram. The protocols therefore recommend that a year's worth of recent continuous data at each site be collected for use in live load modeling.

Various levels of complexity are available for utilizing the truck weight and traffic data to calibrate live load models for bridge design. A simplified calibration approach (Method I) is first proposed that focuses on the aforementioned maximum live load variable, L_{max} for updating the live load factor for current traffic conditions, in a manner consistent with the LRFD calibration. The ratio, r for one-lane and for two-lanes is used to adjust the LRFD design live load factor. The ratio, r is defined as follows:

$$r_1 = \frac{L_{max} \text{ from WIM data projections for one-lane}}{L_{max} \text{ used in existing LRFD calibration for one-lane}} \qquad (30)$$

$$r_2 = \frac{L_{max} \text{ from WIM data projections for two-lanes}}{L_{max} \text{ used in existing LRFD calibration for two-lanes}} \qquad (31)$$

The LRFD calibration report (NCHRP Report 368) provides mean maximum moments and shears for 75-years for simple and continuous spans. An increase in maximum expected live load based on current WIM data can be compensated in design by raising the live load factor in a corresponding manner. This simple procedure assumes that the present LRFD calibration and safety indices are adequate for the load data and site-to-site scatter or variability statistics for the WIM data is consistent with values assumed in the LRFD calibration.

When implementing the draft protocols using recent WIM data from various states, it became evident that this procedure, while simple to understand and use, had certain limitations when applied to statewide WIM data. Using a single maximum or characteristic value for L_{max} for a State would be acceptable if the scatter or variability in L_{max} from site-to-site for the state was equal to or less than the COV assumed in the LRFD calibration. If the variability in the WIM data is much greater than that assumed in the calibration, then the entire LRFD calibration to achieve the target 3.5 reliability index may no longer be valid for that state and a simple adjustment of the live load factor as given above should not be done. The site-to-site scatter in the L_{max} values obtained from recent WIM data showed significant variability from span to span, state to state, and between one-lane and two-lane load effects. Therefore, a second more robust reliability-based

approach (Method II) is also presented that considers both the recent load data and the site-to-site variations in WIM data in the calibration of live loads for bridge design.

The draft recommended protocols were implemented using recent traffic data (either 2005 or 2006) from 26 WIM sites in five states across the country. The states were: CA, TX, FL, IN, and MS. The states and WIM sites were chosen to capture a variety of geographic locations and functional classes, from urban interstates, rural interstates and state routes. An aim of this task was to give practical examples of using these protocols with national WIM data drawn from sites around the country with different traffic exposures, load spectra, and truck configurations. Adjustments and enhancements were made to the protocol steps based on the experience gained from this demonstration task.

Both calibration methods indicate that the lifetime maximum loading for the one lane loaded case will govern over the maximum loading for a two-lanes loaded case. This could be attributable to the increasing presence of heavy exclusion vehicles and/or routine permits in the traffic stream. The load limit enforcement environment in a state will also have a more discernible influence on the maximum single-lane loading than the maximum two-lane loading, which results from the presence of two side-by-side trucks. Additionally, with long-term WIM data with accurate truck arrival time stamps currently available, the projections of L_{max} for two-lane events as undertaken in this study are based on actual side-by-side events rather than based on simulations using conservative assumed side-by-side multiple-presence probabilities as done during the AASHTO LRFD code calibration. The WIM data collected as part of this study show that the actual percentage of side-by-side multiple truck event cases is significantly lower than assumed by the AASHTO LRFD code writers who had to develop their models based on a limited set of multiple presence data.. Knowing the truck weight distribution in each lane allowed the determination of the actual relationship between the trucks weights in the main traffic lane (drive lane) and adjacent lanes and if there is a correlation between the truck properties. This study seems to indicate that there is some negative correlation between the weights of side-by-side trucks. This means that when a heavy truck is in one lane, the other lane's truck is expected to be lighter. Here again, the conservative assumptions used during the LRFD calibration were not adequately supported by field measurements.

LRFD did not specifically address deck components in the calibration. The proposed approach to calibration of deck design loads is to assume the present LRFD safety targets are adequate for the strength design of decks and establish new nominal loads for axles based on recent WIM data. The LRFD live load factors will remain unchanged, but the axle loads and axle types will be updated to be representative of current traffic data.

Updating the LRFD fatigue load model using recent WIM data is described in the protocols. Damage accumulation laws such as Miner's rule can be used to estimate the fatigue damage for the whole design period for the truck population at a site. Based upon the results of the WIM study changes may be proposed to the LRFD fatigue truck model, its axle configuration and/or its effective weight.

The protocols and methodologies recommended in this report can be followed to obtain live load models for bridge design using available truck traffic data collected at different US WIM sites. The models will be applicable for ultimate capacity and cyclic fatigue for main members and for bridge decks. The project was not intended to assemble sufficient data to permit recommendations about revisions to the AASHTO HL-93 design load.

CHAPTER 1

BACKGROUND

PROBLEM STATEMENT AND RESEARCH OBJECTIVE

A new vehicular live-load model was developed for the AASHTO LRFD Bridge Design Specifications because the HS20 truck from the Standard Specifications for Highway Bridges did not accurately represent service-level truck traffic. The HL-93, a combination of the HS20 truck and lane loads, was developed using 1975 truck data from the Ontario Ministry of Transportation to project a 75-year live-load occurrence. Because truck traffic volume and weight have increased and truck configurations have become more complex, the 1975 Ontario data do not represent present U.S traffic loadings. Other design live loads were based on past practice and did not consider actual or projected truck traffic and may not be consistent with the LRFD philosophy.

The present HL-93 load model, and in fact the calibration of the AASHTO LRFD specifications, is based on the top 20% of trucks in an Ontario truck weight database assembled in 1975 from a single site over only a two-week period. It reflects truck configurations and weights taken in the mid-1970s, which primarily consisted of five-axle semi trailer trucks. In the past 30 years, truck traffic has seen significant increases in volume and weight.

Updating bridge live load models needs representative samples of unbiased truck weight data that meet accepted quality standards. One method that has been developed over the last three decades to capture truck loads in an undetected manner and obtain a true unbiased representation of actual highway loads, is known as the Weigh-In-Motion, or WIM technology. Although the quality and quantity of traffic data has improved in recent years, it has not been used to update the bridge design loads. Besides information on truck weights and configurations, the design live load is highly influenced by the simultaneous presence of multiple trucks on the bridge. Such information, usually assembled from headway data, has not been traditionally collected in a manner suitable for the development of design live loads.

The goal of this project is to develop a set of protocols and methodologies for using available truck traffic data collected at different US sites and recommend a step-by-step procedure that can be followed to obtain live load models for bridge design. The models will be applicable for the design of bridge members, for both ultimate capacity and cyclic fatigue. The models will be applicable for both main structural members as well as the design of bridge decks.

SCOPE OF STUDY

The original Ontario weight data from one static scale contained 10,000 truck events (2-week sample), which is a relatively small sample. More important for highway truck weight forecasting than the small sample size are the considerable site-to-site, seasonal, and other time variations in the truck weight description. These variations are not modeled in a single realization of data from one site. Heavy trucks may have avoided the static weigh station, and the degree to which this avoidance occurred in the recorded sample is also unknown. The Ontario site was assumed to have a high ADTT of 5000. With data from only one site, the influence of volume on traffic loading is also unknown.

In the LRFD development, it was seen that for two-lane bridges, loading events consisting of two side-by-side trucks govern the maximum load effect. It was calculated that the maximum load effect is equivalent to the effect of a side-by-side occurrence where each truck is about 85% of the mean maximum 75-year truck. A truck having 85% of the weight of the 75-year truck also closely corresponds to the maximum 2-month truck. The calibration of the HL93

4

load model used the following assumptions for side-by-side vehicle crossings (NCHRP Report 368):

- ❑ The total ADTT is assumed to be 5000 trucks/day.
- ❑ One out of every five trucks is a heavy truck.
- ❑ One out of every 15 heavy truck crossings occurs with two trucks side-by-side.
- ❑ Of these multiple truck events on the span, one out of 30 occurrences has completely correlated weights.
- ❑ Using the product of 1/15 and 1/30 means that approximately 1/450 crossings of a heavy truck occurs with two identical heavy vehicles alongside each other.
- ❑ No field data on multiple presence probabilities and truck weight correlation were provided in the LRFD calibration report. Available literature and published reports show that there is practically little field data to support these assumptions.
- ❑ No data on site-to-site variations was provided.
- ❑ There was no determination of the extent to which overloaded trucks may have by-passed the static weighing operations.

This project will aim to overcome the above-stated limitations in the previous load modeling study and determine the data required for establishing a representative live load model.

The first condition that any set of traffic data should meet before being used for the development of load models is the elimination of bias. Truck data surveys collected at truck weigh stations and publicized locations are not accurate, because, they are normally avoided by illegal overweight vehicles that could control the maximum loads applied on bridge structures. Furthermore, an important parameter that controls the load imposed on the structure is related to the number of simultaneous vehicles on the bridge, which is determined through data on truck headways under operating conditions. Accurate headway information cannot be obtained from fixed weigh-stations or from truck data collected at highway bypasses. For these reasons it is determined that truck traffic data should be collected through Weigh-In-Motion (WIM) systems that can collect simultaneously headway information as well as truck weights and axle weights and axle configurations while remaining hidden from view and unnoticed by trucks drivers. Simultaneous data on headways and weights is necessary to determine possible correlations between truck positions or the lanes they occupy and their weights or other characteristics such as truck type, size and numbers of axles. The 1/15 multiple presence assumption was made because of the lack of sufficient real data at the time of the LRFD calibration. Fortunately, the data needed for multiple presence estimates is presently available and already contained in the raw data files captured by many WIM data loggers.

The quality and quantity of WIM data has greatly improved in recent years. Due to the development of various weigh-in-motion technologies, unbiased truckloads are now being collected at normal highway speeds, in large quantity, and without the truck driver's knowledge. The more advanced load modeling processes will require a more complete set of input data as discussed herein. The maximum lifetime loading requires as an input the percentage of trucks that cross the bridge side-by-side and the lane-by-lane distribution of truck weights. Assuming that the trucks in each lane have identical distribution, as in past simplified approaches, can introduce unnecessary conservatism. Using WIM data could easily improve past estimates or assumptions of various load uncertainties. Some of these uncertainties are now elaborated:

1. Knowing the truck weight distribution in each lane, including mean, COV, and distribution type can improve the input parameters needed for the load modeling process.
2. Estimation of expected maximum loading may require different distributions such as an extremal probability distribution derived from the WIM truckload histograms, rather than the normal distribution.

3. Site-to-site variability of truckloads should be incorporated. LRFD used data from only one site in Ontario.
4. Using unbiased data is very important for the estimation of the maximum load. The data used for the LRFD calibration was obtained using a static scale operated by the Canadian province, and some trucks with excessive overloads may have deliberately bypassed the scales. The data must also not be biased by the presence of weight enforcement activity in the vicinity of the data collection site.
5. With additional WIM data, improved estimates of the tail of the probability distribution of the maximum lifetime effect can be made using Extremal distributions and other advanced reliability tools. Determining the probability distribution of the maximum effect is needed for the calibration of the live load factors. The WIM data must also be separated out — WIM measurement scatter from the actual truck weight scatter.
6. Developing and calibrating bridge live load models requires large amounts of quality WIM data. High speed WIM is prone to various errors, which need to be recognized and scrubbed / filtered out in the data review process.
7. A major advance in recent WIM operations is their ability to collect improved headway data for trucks. Clearly the headway assumptions used during the LRFD calibration were not based on actual measurements of multiple presence. Field measurements of truck arrival data to a 0.01 second resolution performed in this project and in NCHRP 12-63 consistently showed much lower side-by-side cases than those assumed in the LRFD. These new multiple presence values, can be easily incorporated in a simulation model or a simplified model for estimating the maximum lifetime loading.
8. The data must adequately represent daily and seasonal variations in the truck traffic. Hence, it should be collected for a period of one year or at random intervals over extended periods of time.
9. The relationship between the trucks weights in the main traffic lane (drive lane) and adjacent lanes must be established to determine whether passing trucks characteristics are similar to those in the main traffic lane and if there is a correlation between the truck properties. Here again, the assumptions used during the LRFD calibration were not adequately supported by field measurements. The availability of the current WIM data along with headway information and lane of occupancy will allow us to determine the level of correlation (if any) between the trucks in each lane. The relationship between truck traffic patterns and headways should be related to ADTT. Specifically, data should be collected to determine how the number of side-by-side events varies with ADTT.

The goal of this project is to develop a set of protocols and methodologies for using available current truck traffic data collected at different US sites and recommend a step-by-step procedure that can be followed to obtain live load models for bridge design. The protocols are geared to address the collection, processing and use of national WIM data to develop and calibrate vehicular loads for LRFD superstructure design, fatigue design, deck design and design for overload permits. Various levels of complexity are available for utilizing truck weight and traffic data to calibrate live load models for bridge design. A simplified calibration approach that focuses on the maximum live load variable, L_{max} for updating the load factor and a more robust reliability-based approach that considers the site-to-site variations in WIM data in the calibration of live loads are proposed.

The study also gives practical examples of implementing these protocols with recent national WIM data drawn from states/sites around the country with different traffic exposures, load spectra, and truck configurations. This will give a good cross-section of WIM data for illustrative purposes. This task also allowed the updating and/or refinement of the protocols based on its applicability to WIM databases of varying quality and data standards currently being

collected by the states. This report discusses the results of the demonstration studies in more detail.

INTRODUCTION TO THE FINAL REPORT

This Final Report prepared in accordance with Task 9 requirements for this project, documents the findings of Tasks 1 through 8. It contains four chapters and three Appendices. Chapter 1 gives a review of the problem statement, the research objective and scope of study. Chapter 2 describes the research tasks, findings of the literature search and survey of states, a state-of-the-art summary, and the process to develop and calibrate bridge design live load models. Chapter 3 provides the draft recommended protocols for using traffic data in bridge design and the results of the demonstration of the draft protocols using national WIM data. Chapter 4 contains the conclusions and recommendations for future research.

Appendix A includes the results of the demonstration of the draft protocols performed in Task 8 using recent national WIM data from five states. Appendix B summarizes the main features of technical publications most relevant to this project that were compiled during the literature search. Appendix C contains the questionnaires used in the surveys and tabulated responses. Appendix D summarizes the findings of Task 2, which investigated potential processes for developing live load models for bridge design. Appendix E illustrates an implementation of the error filtering algorithm described in the protocols, using recent WIM data.

CHAPTER 2

RESEARCH APPROACH

RESEARCH TASKS

The research effort was organized according to the following nine tasks:

Task 1. *Review relevant practice, data, existing specifications, and research findings from both foreign and domestic sources on the collection and analysis of truck weight data with particular emphasis on evaluating the stresses and deformations induced in highway bridges. This information shall be assembled from both technical literature and unpublished experiences. Information on the quantity and quality of existing WIM data from studies on or near U.S. Interstate bridges is of particular interest.*

Task 2. *Describe existing and potential processes to develop and calibrate vehicular loads for superstructure design, fatigue design, deck design, and overload permitting.*

Task 3. *Develop the vehicular traffic data requirements (type, quantity, and quality) for each of the processes identified in Task 2. The data requirements should be validated by a sensitivity analysis of each data element.*

Task 4. *Assess the statistical adequacy of existing traffic data to meet the requirements developed in Task 3. Recommend means to eliminate any inadequacies.*

Task 5. *Using the information from Tasks 1 through 4, recommend candidate protocols for collecting and processing traffic data to calibrate national bridge live-load models. The protocols should include guidance on selecting default values for use when the traffic data do not meet the requirements developed in Task 3. Prepare an updated, detailed work plan for developing and demonstrating the application of the protocols.*

Task 6. *Submit an interim report within 6 months of the contract start that documents the results of Tasks 1 through 5 and includes the updated and expanded work plan for developing and demonstrating the protocols for collecting and processing traffic data. The contractor will be expected to meet with the NCHRP approximately 1 month later. Work may not proceed on subsequent tasks without NCHRP approval of the work plan.*

Task 7. *Develop the protocols in accordance with the approved work plan.*

Task 8. *Demonstrate the application of the protocols using existing national data to develop and calibrate vehicular loads for superstructure design, fatigue design, deck design, and overload permitting.*

Task 9. *Submit a final report that documents the entire research effort.*

OVERVIEW OF DATA COLLECTION AND REVIEW

The first step in the live load model development process was to assemble and review recent developments and relevant information on practice, specifications, bridge live load models, weigh-in-motion systems, weigh-in-motion data, and studies of truck weights. A purpose of this

task was to understand the state-of-the-art and the practice of collecting and utilizing traffic data in bridge design in the U.S., and in other countries. It included a survey of state highway agencies in the U.S. A search of published technical literature in the U.S. and other countries was conducted for information applicable to this research.

Survey: A survey questionnaire was e-mailed to the traffic monitoring divisions of all state DOTs. The purpose of this questionnaire was to obtain detailed information and document practices on issues central to this research, such as: types of WIM equipment in use in each state and the locations of WIM sites; WIM equipment calibration procedures; the types of traffic data being collected and how they are being used. A copy of the survey questionnaire is contained in Appendix C. The questionnaire consisted of the following five sections:

> SECTION 1 -- Weigh-In-Motion (WIM) Program
> SECTION 2 – WIM Sites
> SECTION 3 – WIM Data
> SECTION 4 – WIM Data Validation and WIM System Calibration
> SECTION 5 – WIM Data Analysis & Applications

Completed questionnaire were received from 26 states. Responses were received from: Alaska, Arkansas, California, Connecticut, Florida, Georgia, Hawaii, Idaho, Indiana, Iowa, Kansas, Louisiana, Michigan, Minnesota, Mississippi, Missouri, Nevada, New Jersey, New Mexico, New York, North Dakota, Ohio, Oregon, South Dakota, Virginia, Washington, Wyoming. It is believed that states with significant WIM programs have responded to the questionnaire.

STATE OF-PRACTICE SUMMARY

State DOT Survey

Tabulated responses to all survey questions are contained in Appendix C. Responses to certain key questions are presented in the tables below.

Table 1 WIM Program details

State DOT	WIM Program?	How Long Has the WIM Program Been in Operation?	Total Number of High Speed WIM Sites	Number of WIM Sites on Interstates	Do you Have WIM Data Available for a Whole Year?
Alaska	Yes	10+ years	7	4	Yes
Arkansas	No				Yes
California	Yes	15 years	137	58	Yes
Connecticut	Yes	9 years	36 bi-directional +4 LTPP	21 bi-directional +2 LTPP	Yes
Florida	Yes	32 years	40	14	Yes
Georgia	Yes	10 years	90	30	No
Hawaii	Yes	18 years	7	2	Yes
Idaho	Yes	12 years	16	6	Yes. Lots of available WIM data.
Indiana	Yes	15 years	52	24	Yes
Iowa	Yes	15 years	28	9	Yes
Kansas	Yes	14 years	9 Perm 70 Portable	3 Perm 25 Portable	Yes
Louisiana	Yes	7 years	3	3	No
Michigan	Yes	14 years	41	21	Yes
Minnesota	Yes	22 years	6	2	Yes
Mississippi	Yes	14 years	15	7	Yes
Missouri	Yes	10 years	13	7	Yes
Nevada	Yes	20 years	4	4	Yes
New Jersey	Yes	13 years	64	14	Yes
New Mexico	Yes	17 years	18	7	Yes
New York	Yes	10+ years	21	11	Yes
North Dakota	Yes	3 years	12	4	Yes. Possibly.
Ohio	Yes	15 years	44	21	Yes
Oregon	Yes	8 years	22	18	Yes. In a text format
South Dakota	Yes	15 years	14	6	Yes
Virginia	Yes		3	2	Yes
Washington	Yes	16 years	37	10	Yes
Wyoming	Yes	8 years	5	3	Yes

NR - No Response

The responding states have maintained a WIM program over the past 3 to 32 years. The number of high-speed WIM sites varied from 3 to 137, distributed among Interstate and non-Interstate routes. Most states also indicated that they can provide a whole year's worth of WIM data for statistical analyses. This will be an important consideration in the selection of WIM sites for load modeling data as it incorporates any seasonal variability in the traffic data. The types of sensors used at each WIM site, date installed, date last calibrated, number of traffic lanes, and the number of WIM lanes are given in Appendix C. These details were valuable when selecting WIM sites for demonstrating the use of the protocols in this project in Task 8.

Table 2   Accuracy of Truck Arrival Time Stamps

Question 3.4. What is the accuracy of truck arrival time stamps reported in the data set (1 sec, 0.01 sec, etc.)? Are time stamps available for more than one lane at a site? What is the highest resolution possible for truck arrival times? Please explain.	
State DOT	**Time Stamp Accuracy**
Alaska	The accuracy of the truck time arrival is .01 for all lanes of data. The time stamp is on each vehicle record (PVR). This was an Alaska requirement to ensure that duplicate records were not loaded to the data base. This is the highest resolution possible for truck arrival times.
California	0.01 sec. Yes.
Connecticut	Truck arrival time stamps are reported for each lane at a site and are recorded by 1 second. The IRD software shows the data time stamp recorded to one hundredth of a second (0.01) in the individual vehicle viewing software. Additional work would be needed to determine the resolution of the data that is reported in the output file formats.
Florida	Times are recorded to the nearest full second, for all lanes.
Georgia	Accurate to the .01 second and we weight in one lane of the roadway. At 10 locations we collect truck traffic in the two outside lanes.
Hawaii	Time stamps are not checked for minute/second accuracy. We check them for date accuracy, and we check the WIM system clock at least once per month. Observed accuracy for those can range from within 1-2 seconds to 1-2 minutes.
Idaho	ECM WIM system equipment has a time resolution of one tenth of a second. The IRD/Diamond WIM systems have a "scientific" mode setting which allows for data collection with a time stamp of one hundred thousands of a second.
Indiana	The timestamps for the vehicle records are to the 1/100 of a second. The ascii report, however, will alone show the timestamp to the nearest second. This is a shortcoming that has been identified and will be corrected in future versions of the software.
Iowa	They are stored by the hour. We can view the info real time to the second and can be viewed for all lanes at the site.
Kansas	Accuracy varies because the on-site clock is not externally synchronized. Precision of the arrival time is 1 second, which is the finest resolution available from the equipment. Time stamps are available for each truck, regardless of lane.
Michigan	The time stamp is down to the second for each lane of travel. So we have the hour, minute and second the vehicle started to cross the sensor.
Minnesota	whole second
Mississippi	We store the data on an hourly basis in the cardw, but the img file has a time stamp associated with each vehicle. We collect WIM data on all lanes at a permanent site.
Missouri	Year, month, day, hour
Nevada	We have never had the need to investigate this but from my experience it is within a second
New Jersey	Truck arrival time stamps using the "View Vehicle" menu of the IRD office software shows a time stamp of up to 0.01 of a second; processed weight data from the W-record cards only up to one minute.
New Mexico	Hourly, for all lanes.
New York	All lanes are monitored and trucks are time stamped to 0.01 seconds.
North Dakota	1 second resolution – Yes, time stamps available on all lanes at all times
Ohio	Mettler-Toledo's time stamp is now sub second at .01 sec. The TMG does not have this resolution and needs to be changed. The time stamp is on each vehicle so it would be by lane. Peek or Pat/IRD do not provide time stamps to the .01 second level.
Oregon	Time stamp accuracy is within .01 seconds. Time stamps are available for each lane in multi-lane systems.
South Dakota	unknown on accuracy of arrival time and are by lane
Virginia	time stamps are to the nearest second, and are available for all lanes
Washington	12:00:00:00
Wyoming	Time stamps are to the second and are by lane.

There is great variability in the truck arrival time data recorded by the various systems. The range is from 0.01 second to the hour. The fact that many systems record time stamps to 0.01 second

accuracy indicates that there is sufficient availability of refined time stamps for estimating multiple-presence probabilities for truck crossings as discussed in the following chapter.

Table 3 Multi-Year Traffic Data

State DOT	Availability of WIM Data for a Number of Years at the Same Site?	Use of WIM data for bridge design applications?
Alaska	Yes	No
Arkansas		
California	Yes	Yes. Caltrans has started using WIM data for bridge design recently.
Connecticut	No. See answer for previous question.	No. Based loads permitted through the state.
Florida	Yes	No
Georgia	No	No
Hawaii	Yes	No
Idaho	Yes	Yes. We provide some commercial vehicle weight data and reports to our bridge design people.
Indiana	Yes	No. The data is not provided directly to them. However through Purdue University or our research section they maybe utilizing the data.
Iowa	Yes	No
Kansas	Yes	No
Louisiana	No	No
Michigan	Yes	No. Not to my knowledge.
Minnesota	Yes	No
Mississippi	No	No
Missouri	Yes	No
Nevada	Yes	No
New Jersey	Yes	No
New Mexico	Yes	No
New York	Yes	
North Dakota	Yes. Possibly.	No
Ohio	Yes	Yes. Maumee River crossing design & I think for a few other applications a few years back.
Oregon	Yes. From "official" state weigh records. These are available from every weigh station location, not just WIM sites.	Yes – currently the ODOT Bridge Section is conducting an analysis for Bridge re-design, and engineering standards.
South Dakota	Yes	Unknown
Virginia	No	No
Washington	Yes	No at least not to our knowledge
Wyoming	Possibly	Not to my knowledge

The responses show that that many states have traffic data of similar quality for a number of years at the same site that may be helpful in estimating trends in truck loadings. It is also interesting to note that of the 26 responding states only CA and OR have begun using WIM data for bridge design applications. These initiatives appear to be in the early states of implementation.

Table 4   WIM Data Quality Assurance

*Question 4.5 Do you have a Quality Assurance Program in place for your WIM systems to check data accuracy?	
State DOT	
Alaska	No
Arkansas	
California	No
Connecticut	Yes. Through the office checks and the LTPP checks conducted by the FHWA Regional contractors.
Delaware	
Florida	Yes
Georgia	No
Hawaii	No
Idaho	Yes. This is a daily ongoing part of our WIM maintenance and processing program.
Illinois	NR
Indiana	Yes
Iowa	Yes
Kansas	No
Louisiana	Yes
Michigan	Yes
Minnesota	Yes
Mississippi	Yes
Missouri	Yes
Nevada	Yes
New Jersey	Yes
New Mexico	Yes
New York	Yes
North Dakota	No. Still under development.
Ohio	Yes. TKO
Oregon	Yes. A trouble Report system.
South Dakota	Yes
Virginia	Yes
Washington	Yes
Wyoming	The procedures explained in Section 4.1 assure data quality.

WIM data quality testing and validation is important to ensure that only quality data is made part of the load modeling process. Although WIM systems can provide massive amounts of valuable data in a relatively efficient manner, the data must be checked for accuracy. This accuracy check is a WIM user's quality assurance (QA) program. Most states have implemented QA programs for their WIM systems to check data accuracy. A QA program adds confidence to the validity of the WIM data and alerts the data analyst to problems occurring at the WIM site. The purpose of a QA procedure is to help WIM users check data for accuracy and precision.

Literature Review

An investigation of published technical literature for the monitoring, collection, and analysis of bridge-related weigh-in-motion data has been performed utilizing transportation organization websites including the following resources: the TRIS, NTIS, USDOT, FHWA, and TRB. In addition, transportation engineering websites and databases, and the websites of state departments of transportation and other United States, Canadian, European, Asian, and Australian transportation institutes were explored for relevant material regarding the use of WIM data.

This literature search concentrated on the following WIM research topics:

- The use of WIM to model bridge loads
- The use of WIM to study the growth or trends in truck weights
- The use of WIM to study the multiple presence of trucks
- The use of WIM to study site-specific bridge loads

The technical literature search resulted in the compilation of a reference list consisting of approximately 250 abstracts, research papers, journal articles, conference papers, and reports with applicability to the project research.

The collected material was reviewed for pertinence to the areas of research under consideration. The documents determined to be the most relevant were obtained and a scan of the material was performed. Of the examined material, approximately 70 applicable documents were selected for further evaluation and possible summary preparation.

A tabulated summary of approximately 40 documents was prepared from the reviewed material (See Appendix B). Contained in each document summary is a brief study description, the study findings (if any), and recommendations for further research suggested by the authors.

A review of the summarized material (Appendix B) reveals that WIM data has been employed in numerous bridge-related applications in North America and abroad.

WIM data has been used to assess current bridge design live loads and to model new design live loads. Several studies have found that the current load models were insufficient for the actual loading experienced by the bridge population. WIM data has also been applied to the development of new fatigue models and the assessment of existing models. The results of the investigations reveal that fatigue evaluation is highly site specific and that the actual fatigue damage resulting from the use of WIM data is often underestimated or overestimated by the code-specified fatigue truck.

Truck load growth trends have been assessed utilizing WIM data. For instance, a large-scale California study has established that truck volumes have increased over time, however the gross vehicle weight in the state has remained unchanged. This study also investigated the possibility of applying WIM data that was collected at a bridge site to other nearby bridge locations. The forecasting of truck load spectra as a result of changing truck weight limits has also been investigated by the application of WIM data

The examination of truck multiple presence on bridges has employed WIM data to simulate multi-lane traffic critical loading events and extreme load effects. The studies differ in bridge span length and number of lanes investigated, however it was generally noted that as the span length increases, the critical loading event is governed by an increasing number of trucks. One study indicated that traffic density should be a deciding factor in the development of multiple presence reduction factors.

Numerous studies have investigated WIM-derived site-specific bridge loads for evaluation and design purposes. Generally, it was determined that truck loads are strongly site specific, influenced by factors such as traffic volume, gross vehicle weight, axle weight, local industry, and law enforcement effort, and that current load models for design are often not representative of actual site loading.

WIM Technology: Over the last two decades, highway agencies have recognized the advantages of having automated data collection systems that can provide information on truck weights and truck traffic patterns for economic analysis, traffic management and various other purposes. The quality and quantity of WIM data has greatly improved in recent years. Due to the development of various weigh-in-motion technologies, unbiased truckloads are now being collected at normal highway speeds, in large quantity, and without truck driver's knowledge.

WIM systems that are utilized to provide high-speed weighing of trucks and other traffic are: Bending Plates, Load cells, Piezoelectric cables, Quartz cables, and Bridge WIM systems. One major WIM system vendor alone has approximately 500 permanent WIM sites in operation in forty seven states: 246 Piezo; 180 Bending Plate (BP); 42 Single Load Cell (SLC); 24 Kistler Quartz (Table 5). The electronics, software, and storage technologies of WIM data loggers have also advanced in pace with the sensor technology.

Weigh-in-motion equipment currently used in the United States can collect data on truck volumes, axle configurations, truck arrival times and load spectra. They usually classify the vehicles into at least the 13 FHWA classifications (bins). The majority of WIM data collection is done with permanently installed weight sensors, although some states may not collect weight data continuously at these sites. Permanent WIM stations provide more extensive datasets at geographically diverse locations over long periods. On a national or regional basis, WIM data is easily obtained from the wide network of permanent sites. If more localized site-specific characteristics are desired it may be necessary to utilize portable WIM systems for data collection. Portable devices allow flexibility in collecting site-specific traffic data at locations of interest, such as a bridge where significant illegal overloads are suspected.

There are several types of WIM technologies with varying performance and cost considerations (Table 6). Piezoelectric sensor based systems offer acceptable accuracy (usually ± 15% for gross weights) at a low cost that their use has become quite widespread for data collection purposes. They can be used as temporary or permanent sites. Strain based WIM scales and load cell WIM systems provide more accuracy at a higher cost. Strain and load-cell based systems are used primarily in permanent applications. New WIM technologies continue to be developed and brought to the market. Piezoquartz sensors were recently introduced in the United States. They are less sensitive to changes in temperature than the piezo-style sensors, and therefore generally more accurate.

Table 5 WIM Sites and Lanes (maintained by one vendor)

State/Province	Piezo		SLC		IRD BP		PAT BP		Kistler Quartz	
	Sites	Lanes	Sites	Lanes	Sites	Lanes	Sites	Lanes	Sites	Lanes
Alabama	11	40								
Alaska	19	48			8	22				
Arizona	5	5					4	8		
Arkansas										
California	16	54			100	345				
Colorado							1	1		
Connecticut	7	38							1	4
DC (Washington)			3	10					1	4
Delaware					1	1				
Florida							13	19		
Georgia										
Hawaii	5	14					2	6		
Idaho	3	12								
Illinois							1	1		
Indiana		20	32	100						
Iowa										
Kansas							2	2		
Kentucky			2	12						
Louisiana							1	1		
Maryland							1	1		
Massachusetts	3	10								
Michigan	1	4			3	14	5	14		
Minnesota	6	12							4	16
Missouri	7	28								
Mississippi							1	4		
Montana										
Nebraska										
Nevada							1	2	6	24
New Hampshire			1	4						
New Jersey	53	131			9	18				
New Mexico					3	12			1	4
New York	20	70								
North Carolina										
North Dakota										
Nova Scotia	8	3								
Ohio	2	2					2	8		
Oklahoma	20	60								
Oregon	10	20	2	6						
Pennsylvania	2	2							10	12
Rhode Island	5	16								
South Dakota					12	34			1	2
Texas					10	40				
Utah	7	36								
Vermont	16	58								
Virginia										
Washington	20	96								
Wisconsin										
Wyoming			2	4						

Table 6   Sensors commonly used for Permanent WIM Sites

Type of Sensor	Strengths	Concerns
Piezoelectric (BL)	Easier, faster installation than many other WIM systems. Generally lower cost than most other WIM sensors. Well supported by industry. Can be used for temporary WIM systems	Sensitive to temperature change. Accuracy affected by structural response of roadway. Above average maintenance requirement. Requires multiple sensors per lane
Piezoquartz	Easier, faster installation than many other WIM systems. May be more cost-effective (long term) if sensors prove to be long lived. Very accurate sensor. Sensor is not temperature sensitive. Growing support by industry.	More expensive that other piezo technologies. Requires multiple sensors per lane. Above average maintenance requirement. Sensor longevity data not available. Accuracy affected by structural response of roadway.
Bending Plate	Frame separates sensor from pavement structure. Entire tire fits onto sensor. Moderate sensor cost. Sensor is not temperature sensitive. Extensive industry experience with the technology.	Longer installation time required than piezo systems. Some systems have experienced premature failure, while others have been very long lived.
Load Cell	Entire tire fits onto sensor. Frequently considered the "most accurate" of conventional WIM technologies. Some systems have demonstrated very long life spans.	Most expensive WIM system. Requires significant construction effort to install. Cost effective if constructed and maintained for a long life span.

Use of In-Service Strain Measurements: Procedures for using in-service peak strain measurements to directly evaluate the safety (using the LRFR method) of existing bridges have been proposed by some researchers. A considerable part of this effort involves the statistical characterization of the live load effect using an extreme-value theory. The strains due to ambient traffic are monitored and recorded to represent the distribution of maximum load effects. The maximum load effect distribution is then projected for longer periods up to 10 years for determining the maximum expected load effect for evaluation. Because it is based on actual bridge response it eliminates a substantial part of live load modeling uncertainties, such as those related to dynamic impact and girder distribution factors. Used in combination with pavement WIM systems, this method has potential applications in other load modeling applications, particularly for fatigue design and assessment. Combining WIM data with bridge response data could significantly reduce uncertainties inherent in high speed WIM data. One problem involved in such procedures is that the projection is valid for only the stresses at the point where the stain measurements are recorded and the information cannot be generalized for stresses and strain at other locations of the same bridge let alone for application to other bridges. In any case, it is not the aim of this project to develop or recommend new WIM systems. Rather, efforts will concentrate on data now produced by operational WIM networks.

LRFD Fatigue Design: Fatigue criteria for steel bridges are an important consideration for designing for heavy traffic and long expected design lives as well as for assessment of remaining life for existing bridges. As truck weight and volume increase and bridges are maintained in service for increasingly longer periods of time, the fatigue design and assessment issues becomes even more important.

  The present AASHTO fatigue truck, which is based on reliability analyses, was developed by Moses, et al, in NCHRP Project 12-28 (3). The truck traffic load input was taken for some 30 WIM sites in about 8 states collected in the 1980s. For a suite of bridges, each of over 20,000 trucks was used to calculate the stress ranges and then the fatigue damage averaged according to the fatigue damage law (cubic power). The number of cycles to failure depends on the cube of the stress range and comparison with lab test data for various welded details. A variety of random variables were considered to account for material, analysis and load uncertainties. This information is used to calibrate the fatigue process to a target β for redundant and non-redundant cases. Moses, et al, describes the details of this derivation in NCHRP Report 299. The results were incorporated into two AASHTO Guide specifications for fatigue design and fatigue evaluation, respectively. Further, the fatigue truck developed for the nominal loading (54 kip, 5-axle truck) in these Guide Specifications was also incorporated into the AASHTO LRFD Specifications and the LRFR manual.

  Most of the fatigue damage in a bridge is caused by passages of single trucks across the bridge. The total number of truck passages in the 75 year life of a bridge can exceed 100 million. Static strength design must be based on the most severe load effect expected to occur over the life of the bridge. Fatigue design, on the contrary, should be based on typical conditions that occur, because many repetitions are needed to cause a fatigue failure. (Ref NCHRP Report 399).

  The fatigue load specified in the steel structures section of the LRFD Specifications also produces a lower calculated stress range than that of the Standard Specifications. The fatigue provisions of the new specifications are more reflective of the fatigue loads experienced by highway bridges.

  In LRFD, a special vehicle is used for fatigue analysis. It consists of one design truck, as specified above, but with the rear (32-kip) axle spacing fixed at 30.0 FT and without an accompanying uniform load (Figure 1). The fatigue load is used to represent the variety of trucks of different types and weights in actual traffic. For the purposes of fatigue design, a truck is defined as any vehicle with more than either two-axles or four wheels. The constant axle spacing approximates that for a 5-axle semi-trailer truck that do most of the fatigue damage to steel

18

bridges. The specified fatigue loading in LRFD produces a lower calculated stress range than produced by the loadings in the Standard Specifications. This reduction in calculated stress range is offset by an increase in the number of cycles of loading to be considered in the LRFD Specifications. The lower stress range and increased number of cycles are more reflective of the actual conditions experienced by bridges. If the maximum stress a detail experiences in its lifetime is less than the constant amplitude fatigue threshold for that detail, the detail is considered to have infinite fatigue life.

In the FATIGUE load combination given in the LRFD specifications, a load factor of 0.75 is applied to the fatigue load. The factored fatigue load is equivalent to the AASHTO HS15 loading. A revision to Article 3.4.1 was adopted in 2008 to specify two separate fatigue load combinations. For infinite life design under higher traffic volume conditions, the FATIGUE I load combination would be used. In the new FATIGUE I load combination, the stress range caused by the fatigue design truck is multiplied by a load factor of 1.50 (or 2.0 * 0.75). For finite life design under lower traffic volume conditions, the FATIGUE II load combination would be used. The FATIGUE II load combination retains the load factor of 0.75 applied to the stress range caused by the fatigue design truck.
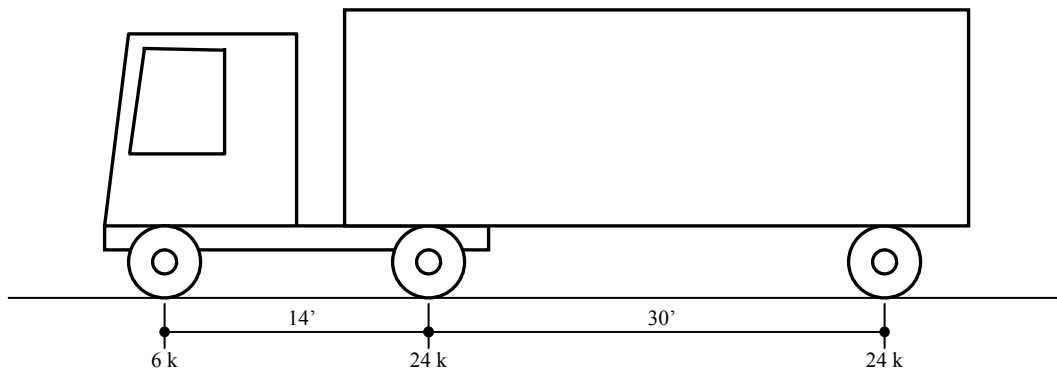
Figure 1   LRFD Fatigue Truck (includes 0.75 load factor)

Where the bridge is analyzed using approximate analysis methods, the specified lateral live load distribution factors for one lane loaded are used in the fatigue check, without the multiple presence factor of 1.2. Where the bridge is analyzed by any refined method, a single fatigue truck is positioned transversely and longitudinally to maximize the stress range at the detail under consideration. A reduced dynamic load allowance of 15 percent is applied to the fatigue load.

Since fatigue is defined in terms of accumulated stress-range cycles over the anticipated service life of the bridge, the fatigue load should be specified along with the frequency of load occurrence / stress cycles. For the purposes of determining the number of stress cycles per truck passage LRFD Table 6.6.1.2.5-2 may be used (Table 7).

Table 7 Stress Cycles per Truck Passage

Longitudinal Members	Span > 40 ft	Span ≤ 40 ft
Simple span girders	1.0	2.0
Continuous span girders near supports	1.5	2.0
Continuous span girders elsewhere	1.0	2.0
Transverse Members	Spacing > 20 ft	Spacing ≤ 20 ft
	1.0	2.0

The frequency of the fatigue load is taken as the single lane average daily truck traffic. The number of cycles to be considered is the number of cycles due to trucks actually anticipated to cross the bridge in the most heavily traveled lane over its design life. The frequency of the fatigue load is taken as the single-lane average daily truck traffic ($ADTT_{SL}$). In the absence of better information, the single-lane average daily truck traffic shall be taken as:

$$ADTT_{SL} = p \times ADTT \tag{1}$$

Where:
> ADTT = the number of trucks per day in one direction averaged over the design life
> p = fraction of truck traffic in a single lane.

Because of the importance of the lifetime average daily truck volume parameter in fatigue design, the engineer should use whatever site data may be available for making this estimate. It should be made excluding 2-axle trucks consistent with the procedure used in calculating the fatigue truck weight. Traffic volume usually grows at an annual rate of about 2 to 5 percent until they reach a very high limiting value. It is unrealistic to project traffic growth indefinitely into the future. ADT, including all vehicles, is physically limited to about 20,000 vehicles per day per lane.

AASHTO Fatigue Guide Specifications (1989, 1990): The 1989 AASHTO *Guide Specifications for Fatigue Design of Steel Bridges* and the 1990 AASHTO *Guide Specifications for Fatigue Evaluation of Existing Steel Bridges* specified a three-axle fatigue tuck having a gross weight of 54 kips to represent the variety of trucks in actual traffic seen in the WIM data collected in the early 1980s. The fatigue truck is similar to the LRFD fatigue load once the loads are scaled down using the 0.75 load factor. One key difference was that the Guide Spec allowed a variable spacing of 14 ft to 30 ft instead of the standard 30 ft main axle spacing. If used, the reduced axle spacing would have resulted in increased fatigue design stresses.

To recognize the considerable region-to-region and site-to-site differences in truck weight population, alternatives for determining the gross weight of the fatigue truck were permitted. Where the gross-weight histogram for truck traffic (excluding 2-axle trucks) was available, the guide allowed the determination of the gross weight of the fatigue truck from:

$$W = \left(\sum f_i W_i^3 \right)^{1/3} \tag{2}$$

> f_i = fraction of gross weights within an interval i
> W_i = gross weight at mid-width of interval i

The fatigue design was based on the passage of a single fatigue truck across the bridge in the lane under consideration. The net effect of closely spaced trucks was considered to be small for normal traffic conditions (NCHRP Report 299). Therefore, the effect of truck superpositions was neglected for span lengths typically covered by the AASHTO Standard Specifications. If unusual bunching of trucks is expected at a site, a 15% increase of the fatigue truck weight was specified.

Fatigue Load Research: Research studies have been conducted to establish improved fatigue load models that will cause the same cumulative fatigue damage as the normal truck traffic distribution obtained by WIM measurements in various states. Laman and Nowak (1996) developed a fatigue load model for girder bridges from WIM measurements at five bridge sites in Michigan (Figure 2). Stress cycles were also measured at the midspan of all girders. A new three axle fatigue truck was proposed to model vehicles with 3 to 7 axles. The fatigue damage caused by the traffic consisting of 3 to 7 axles is equivalent to the damage caused by an equal number of passes of the 3 axle fatigue truck. A four axle fatigue truck was proposed for sites with 10 and 11

axle trucks common in Michigan. The AASHTO fatigue truck was not adequate to model the traffic at these sites. It was found that a high percentage of the fatigue damage was dominated by 10 and 11 axle trucks, though they did not dominate the distribution of truck types. It was found that for these sites, two site-specific fatigue trucks could provide relatively accurate estimates of fatigue damage accumulation over a range of bridge spans. This illustrates that truck load spectra are strongly site-specific.

Chotickai and Bowman (2006) developed a new fatigue load model based on WIM data collected from three different sites in Indiana (Figure 3). The recorded truck traffic was passed over simulated bridge spans to investigate moment range responses in simple and continuous span bridges. Based on Miner's hypotheses, fatigue damage accumulations were compared with the damage predicted for the 54 Kip AASHTO fatigue truck, a modified AASHTO fatigue truck with an equivalent effective gross weight, and other fatigue truck models. The simulation results indicate that the use of the 54 Kip gross weight in an evaluation of bridge structures can result in a considerable overestimation or underestimation of the extent of the actual fatigue damage. It was also shown that the fatigue trucks given by Laman and Nowak (1996) do not provide an accurate estimate of the fatigue damage accumulation for a wide range of span lengths when compared with fatigue damage estimated using the WIM database. Based upon the results of the Indiana WIM study, a new three axle fatigue truck and a four axle fatigue truck were proposed. The front and rear axle spacing of the new three axle fatigue truck are wider than the AASHTO fatigue truck. In addition, a higher percentage of the gross weight is distributed to the front axle compared with the AASHTO fatigue truck. These adjustments were considered to be consistent with statistics of the axle configurations of truck traffic observed. The new four-axle fatigue truck was most effective when a significant number of 8 to 11 axle trucks pass over a bridge, while the new three-axle fatigue truck was most effective otherwise.
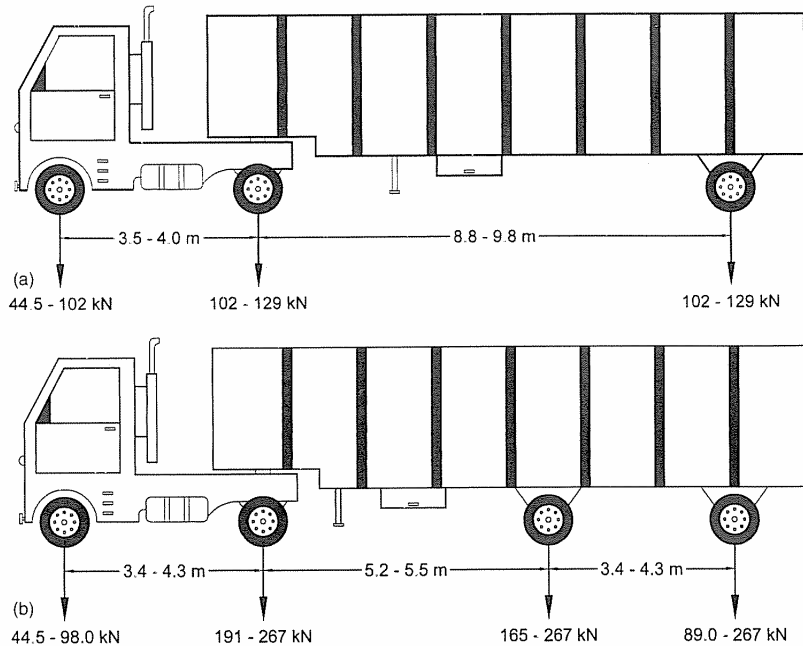
Figure 2   Fatigue Trucks – Laman and Nowak (1996)

21
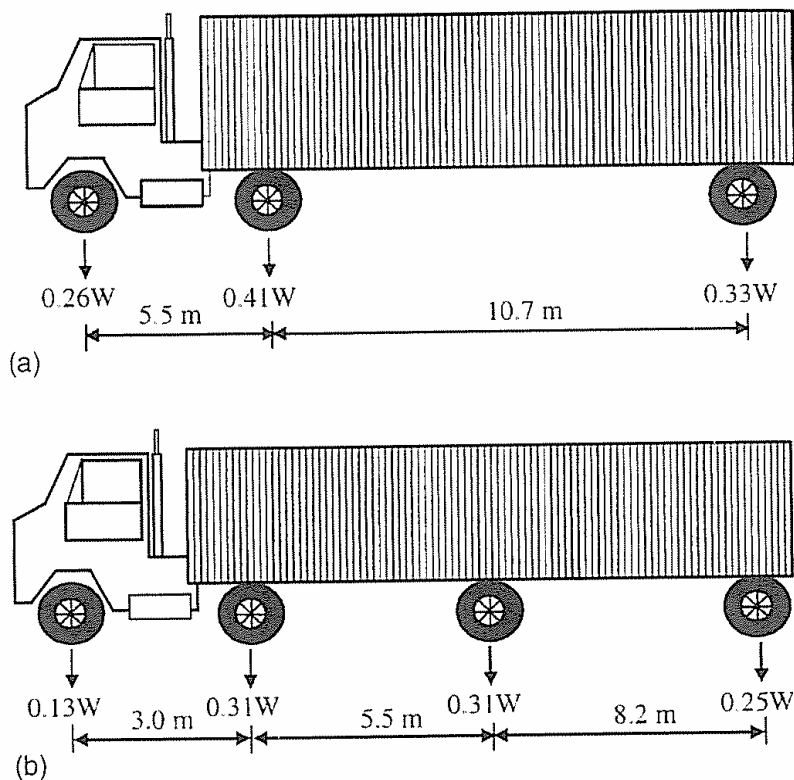
Figure 3   Fatigue Trucks -- Chotickai and Bowman (2006)

LRFD Deck Design: In the LRFD Specifications, design load for decks and top slabs of culverts using the transverse strip method is the axle load, represented by a 32 kip axle of the design truck or the design tandem consisting of a pair of 25.0 Kip axles spaced 4.0 ft apart, whichever creates the most extreme force effect (Fig. 4). The two design vehicles should not be considered in the same load case — consider all trucks of one kind, design truck or design tandem, not a mix of the two. The design truck has the same weights and axle spacing as the HS20 load model, which was adopted in 1944 for bridge design, and has been carried over from the Standard Specifications. Only the truck load is required for decks and not the truck + distributed loads as required for girders.

The slab may be designed by three methods: 1) Traditional strip method 2) Empirical design 3) Yield-line method. In the traditional strip method, the deck is subdivided into equivalent strips perpendicular to the supporting components. The width of equivalent strips is given in LRFD Table 4.6.2.1.3-1. The strips are analyzed as continuous beams using one or more loaded lanes to determine maximum live load moments. The empirical design requires that the designer satisfy a few simple rules regarding deck thickness and reinforcement details. An analysis for load effects is not required. Though newer deck design methods were introduced, design load effects on bridge decks have remained essentially the same in the LRFD specifications compared with the requirements of the standard Specifications. The live load modeling in LRFD did not specifically address the increasing load effects on bridge decks from the heavier and more complex axle configurations of current truck traffic.

22

DECK DESIGN — LRFD CODE PROVISIONS

32 k   **DESIGN AXLE**

25 k   25 k   **DESIGN TANDEM**

4'

APPROXIMATE STRIP METHOD OF ANALYSIS:

$+M = 26.0 + 6.6S$

$-M = 48.0 + 3.0S$
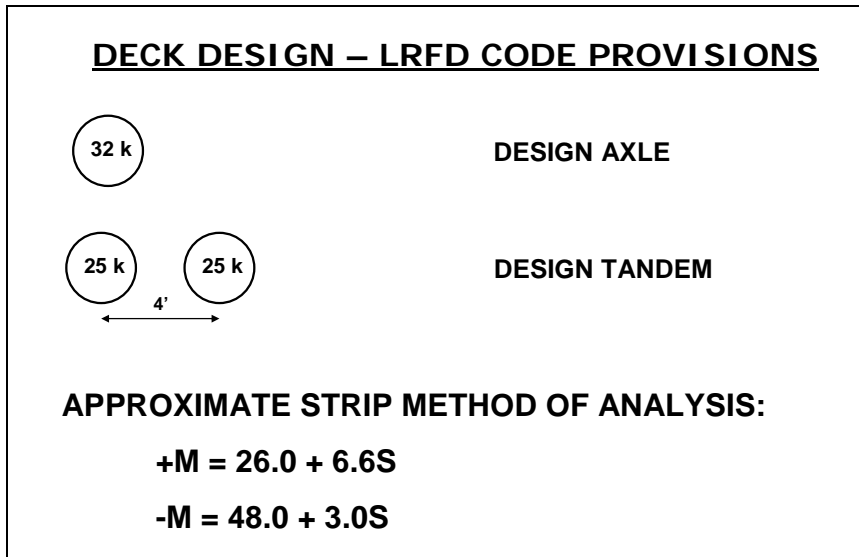
Figure 4   LRFD Deck Design Loads and Strip Widths.

Axle groups with more than two axles are currently not considered for deck design in LRFD. However, LRFD commentary C3.6.1.3.3 states "*Individual owners may choose to develop other axle weights and configurations to capture the load effects of the actual loads in their jurisdiction based upon local legal load and permitting policies. Triple axle configurations of single unit vehicles have been observed to have load effects in excess of the HL-93 tandem axle load*".

W2 W2   **TANDEM**

S2

W3 W3 W3   **TRIDEM**

S3   S3

W4 W4 W4 W4   **QUAD**

S4   S4   S4
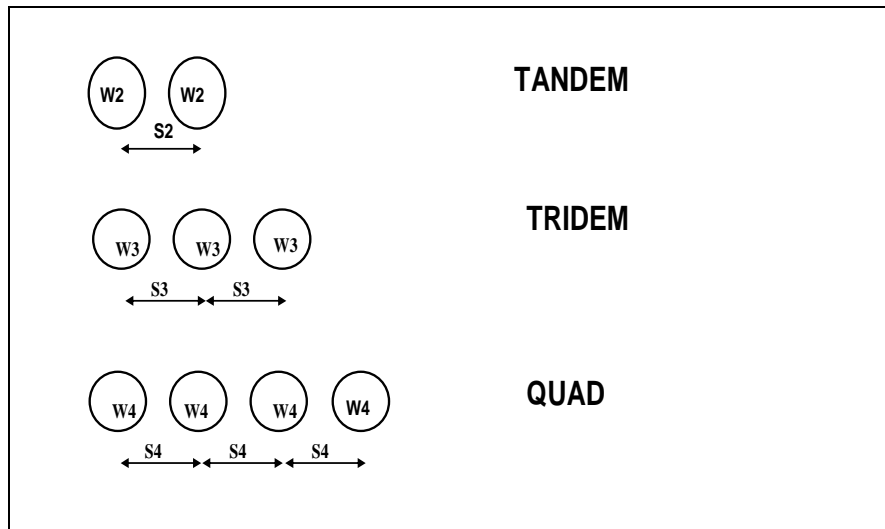
Figure 5   Typical Multi-Axle Loads

Figure 6   Concrete Ready-Mix Truck with Quad Axle

Multi-Axle Specialized Hauling Vehicle

To increase load carrying capacity and maximize productivity, the trucking industry has in recent years introduced specialized commercial vehicles with closely-spaced multiple axles (Figures 6, 7 & 8). This was the focus of the NCHRP 12-63 project (NCHRP Report 575). States have adopted a variety of short multi-axle vehicles as posting loads in response to their potential for overstressing shorter span bridges and bridge decks (Figs 9 and 10). Additionally short dump trucks are allowed loads of 60K or more in the rear tri-axle group in many states, as seen in Fig 9. Similar exemptions are granted for tandem axles on concrete mixer trucks and other work trucks (> 50 K allowed on a tandem). Such axle groups usually include lift axles, which are required to be lowered when the truck is loaded, but are not always used in this manner. This further exacerbates the overstress problem on decks and short span bridges. NCHRP 12-63 has compiled a database of over 70 trucks with complex axle configurations currently in use as legal loads in the various states. Many states exempt short hauling vehicles from Federal Formula B and axle weight limits under the grandfather rights granted when the federal weight laws were first enacted. This information intended for developing new AASHTO load models for evaluation in NCHRP 12-63 can be a valuable resource for developing new axle loads for deck design as the data represents service loads that the new decks will be subjected to on a routine basis. This has implications for the strength and fatigue design provisions for decks in the current LRFD Specifications. Current provisions may be grossly underestimating the maximum and repetitive load effects on bridge decks. Furthermore, the multiple presence probabilities for side-by-side axles could be considerably different than truck multiple presence probabilities for trucks. The former influences deck design, which could be much higher than the side-by-side probabilities for trucks as each truck may have several axle groups that could increase multiple-presence. This issue has not been adequately investigated in past calibrations of the bridge code.

Figure 7   Multi-Axle Specialized Hauling Vehicle (Ref: NCHRP Report 575)

Figure 8   Truck with Tridem and Quad Axles
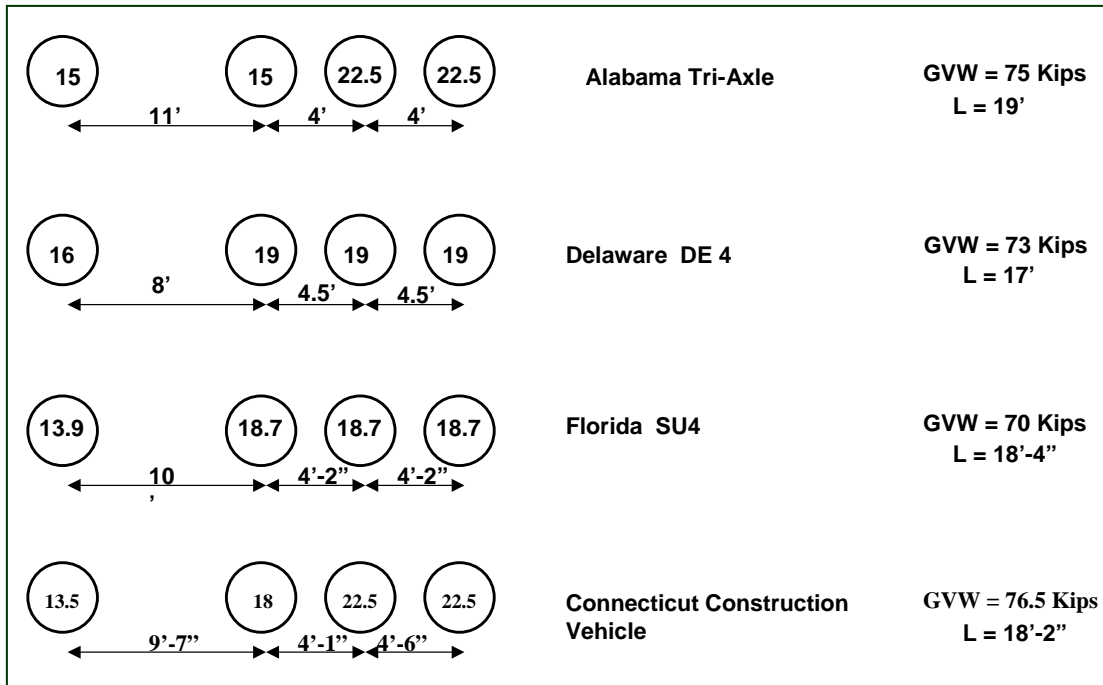
Figure 9   State Legal Loads that Exceed Federal Weight Limits (Ref: NCHRP Report 575)

SINGLE VEHICLE (SV)		TRUCK TRACTOR SEMI-TRAILER (TTST)	
REF. #	SCHEMATIC	REF. #	SCHEMATIC
SH	5K 20K 25K; 12.5 TON; 14'	T4A	12.1K 12.05K 19K 19K; 9' 9' 4'; 22'; 62.15K 31.075 TON
S3A	12.05K 19K 19K; 50.05K 25.025 TON; 9' 4'; 13'	T5B	7.15K 19K 19K 12.625K 12.625K; 9' 4' 9' 4'; 26'; 70.4K 35.2 TON
S3C	5K 19K 19K; 43K 21.5 TON; 11' 4'; 15'	T6A	12.1K 8.2K 19K 19K 10.45K 10.45K; 9' 4' 4' 9' 4'; 30'; 79.2K 39.6 TON
S4A	12.65K 8.2K 19K 19K; 58.85K 29.425 TON; 9' 4' 4'; 17'	T7A	4.1K 4K 19K 19K 11.3K 11.3K 11.3K; 9' 4' 4' 9' 4' 4'; 34'; 80K 40 TON
S5A	12.1K 8.5K 19K 19K 8.5K; 67.1K 33.55 TON; 9' 4' 4' 4'; 21'	T7B	4.1K 10.5K 10.5K 8.45K 8.45K 19K 19K; 9' 4' 9' 4' 4' 4'; 34'; 80K 40 TON
S6A	12.1K 8.6K 8.6K 19K 19K 8.6K; 75.9K 37.95 TON; 9' 4' 4' 4' 4'; 25'		
S7A	5.2K 8.59K 8.6K 19K 19K 8.6K 11K; 9' 4' 4' 4' 4' 9'; 34'; 80K 40 TON		
S7B	4.4K 9.4K 9.4K 19K 19K 9.4K 9.4K; 9' 4' 4' 4' 4' 4'; 29'; 80K 40 TON		

7/18/95

Figure 10 North Carolina Legal Loads (Ref: NCHRP Report 575)

LRFD Overload Design: In addition to routine service loads, bridge owners usually have established procedures that allow the passage of vehicles above the legally established weight limitations on the highway system. Depending upon the authorization, these permit vehicles may be allowed to mix with normal traffic or may be required to be escorted in a manner which controls their speed and/or lane position, and the presence of other vehicles on the bridge. The multiple-presence probabilities for permit trucks are significantly different from those used for normal traffic. In the LRFD, the STRENGTH II limit state is specified for checking an owner-specified special design vehicle or permit vehicle during the design process with a reduced load factor of 1.35. No further guidance is given in the LRFD Specifications on how this load factor was derived, the level of safety represented by this limit state, site traffic, or how the load factor might be adjusted when design live loading characteristics (such as the gross weight of the permit load, likelihood of trucks exceeding the permitted weight, and multiple presence likelihood) differ significantly from the calibration assumptions. These kinds of information need to be obtained

locally or regionally through WIM measurements and considered in the STRENGTH II design process since the data used for calibration of national codes are unlikely to be representative of all jurisdictions.

LRFD Superstructure Design: The notional live load model used in the LRFD Specification for the design of bridges, designated HL-93, consists of a combination of the:

- ❑ Design truck or design tandem, and
- ❑ Design lane load

Each design lane under consideration shall be occupied by either the design truck or tandem, coincident with the lane load, where applicable.

The HL-93 live load model was initially developed as a notional representation of shear and moment produced by a group of vehicles routinely permitted on highways of various states under "grandfather" exclusions to weight laws. The vehicles were based on a 1990 study conducted by the Transportation Research Board, which identified twenty-two representative configurations of vehicles allowed by states as exceptions to weight laws. The smallest and largest of which were a three-axle 48 Kip single truck and an eleven axle 149 Kip trailer truck (Kulicki 1994). The notional load model was subsequently compared to the results of truck weight studies, selected WIM data (Ontario), and the 1991 OHBDC live load model. These comparisons showed that the notional load could be scaled by appropriate load factors to be representative of these other load spectra.

Comparisons of moments and shears in simple spans and two-span continuous girders raging in span from 20 to 150 feet produced by HS20 and the envelope of results produced by the 22 representative exclusion vehicles indicated that the HS20 design loading was not representative of vehicles on U.S. highways. Five candidate notional loads were identified in the live load development for the AASHTO LRFD Specification (Kulicki 1994). Ratios of force effects for each of these live load models divided by the corresponding force effect from the envelope of exclusion loads indicated that the load model involving a combination of either a pair of 25-Kip tandem axles and the uniform load, or the HS20 and the uniform load, seem to produce the best fit to the exclusion vehicles. The tight clustering of force effect ratios for all span lengths, forming bands of data which are essentially horizontal, indicates that the live load model and load factor can be independent of span length. Thus, the combination of the tandem with uniform load and the HS20 with the uniform load, were shown to be an adequate basis for a notional design load in the LRFD Specification.

The LRFD Specification allows site-specific modifications to the design truck, design tandem, and/or the design lane load under the following conditions:

- ❑ the legal load of a given jurisdiction is significantly greater than typical
- ❑ the roadway is expected to carry unusually high percentages of truck traffic
- ❑ flow control, such as stop sign, traffic signal, or toll booth, cause trucks to collect on certain areas of a bridge, or
- ❑ special industrial loads are common due to the location of the bridge.

The dynamic load model was determined to be a function of three major parameters: road surface roughness, bridge dynamics (frequency of vibration) and vehicle dynamics (suspension system). The actual contribution of road roughness, bridge dynamics and vehicle dynamics varies from site to site and are difficult to predict. Therefore, the dynamic load allowance in the LRFD was specified as a constant percentage of live load (Nowak 1993).

PROPOSED PROCESS TO DEVELOP VEHICULAR LIVE LOAD MODELS

The design and load capacity evaluation of a bridge member depends on the live load model and the live load factor used in the design check equation. The live load factor γ_L=1.75 for Strength I provided in the AASHTO LRFD Specifications has been calibrated for use along with the HL-93 design load such that bridge members designed with the AASHTO LRFD Specifications would achieve a uniform target reliability index β=3.5. In actuality, conservative rounding up of the originally calibrated live load factor indicate that the AASHTO LRFD will produce members with reliability index values higher than 3.5. The reliability index calculations use as input a live load model that estimates the maximum expected live load effect on a bridge member. (L_{max} is the expected lifetime maximum load effect on a bridge). The model includes the mean value of the maximum expected live load effect along with the standard deviation and the probability distribution type. The live load model used during the AASHTO LRD calibration was obtained from a generic set of truck weight and load effect statistics that are presumed to be valid for any typical bridge site in the U.S. Because of its generic nature, the live load model may not represent the actual loading conditions at a particular bridge site or bridges in a state where the truck weights or traffic conditions do not follow the expected typical model. Under these conditions, site-specific or state-specific live load models may need to be developed based on actual truck weight and traffic data collected at the site or within the state. Several states are currently using Weigh-In-Motion (WIM) systems to collect vast amounts of truck weight and traffic data that can be used to obtain site-specific and state-specific live load models for bridge design and load capacity evaluation. This would allow individual states to adjust the AASHTO live load factors to take into consideration the particular truck traffic conditions throughout a state, a region, or on a particular route.

Task 2 of this research project was focused on existing and potential processes to develop and calibrate vehicular loads for superstructure design, fatigue design, deck design, and overload permitting. The findings are summarized in Appendix D. Several procedures of various levels of complexity exist to estimate the maximum expected load effect on a highway bridge. This section describes the recommended procedure that utilizes site-specific truck weight and traffic data to obtain estimates of the maximum live load for a specified return period. The return period for the design of a new bridge is specified to be 75 years as per the AASHTO LRFD code for Strength I limit state. A two-year return period has been used for the load capacity evaluation of existing bridges during the calibration of the AASHTO LRFR, and a one-period has been proposed for estimating the maximum live load effect for the AASHTO LRFD Strength II limit state. It should be clearly stated that it is not possible to obtain exact values of the maximum expected 75-year load due to the limitations in the available data. In fact, to obtain accurate results, one would need several cycles of WIM data collected over 75 years for each cycle which is an impossible task. Even the development of live load models for one year and two year return periods would require several cycles of one year and two year data which are currently not available due to the relative recent adoption of WIM technology in the U.S. Hence, some form of statistical projection will be needed for any practical load modeling effort as will be described in this section. The approach described in this section uses a Normal probability distribution to project the tail end of the collected WIM data histograms. The properties of the Normal distribution can then be used to obtain the statistics of the maximum load effects for any return period using extreme value distributions.

This section presents the theoretical background for the proposed procedure for modeling the maximum live load effect on a highway bridge. The proposed approach for obtaining the live load model requires as input the WIM data collected at a site after being "scrubbed" and processed to remove data outliers as described in other sections of this report. For state-specific load models, data from several representative sites should be assembled. The statistics of the maximum live load effects can then be used to adjust the AASHTO live load factors so that the

29

Strength I and Strength II limit state designs would achieve safety levels similar to those intended by the AASHTO code writers while simultaneously accounting for the state-specific loading conditions.

1. Probability density function and frequency histogram of truck load effects

For the single lane loading of short span bridges, a truck loading event is defined as the occurrence of a single truck on the bridge. For multiple truck presence in multi-lanes, the loading event may consist of two or more trucks simultaneously on the bridge. While all currently used WIM systems are capable of providing axle weights and axle spacings for each truck crossing, only WIM systems capable of taking continuous uninterrupted data at normal highway traffic speeds with accurate time stamps are able to identify multilane loading events and provide the axle weights, axle spacings and relative positions of all the trucks involved in each multilane loading event. For the cases when uninterrupted multilane data with accurate time stamps are not available, multilane loading events can be obtained from simulations based on estimates of the number of side-by-side and information on Average Daily Truck Traffic data. This could be achieved using an approach that will be described in Chapter 3.

In a first step, using the WIM data files, the shear force or bending moment effect of each truck loading event in the WIM record is calculated by passing the trucks through the proper influence line. For multilane loadings the combined shear force or moment effect from the trucks that are simultaneously on the bridge is obtained. The shear or moment for each truck load event is then normalized by dividing the calculated value by the shear or moment of the HL-93 load model.

The shear and moment data for the single lane loading and the multilane lane loading events are collected into separate percent frequency histograms. Each histogram provides a discretized form of the probability density function (pdf) of the shear or moment effects for the site. The histogram is designated as $H_x(X)$ while the pdf is designated as $f_x(X)$. The relation between $H_x(X)$ and $f_x(X)$ is given by:

$$H_x(X) = \int_{X_l}^{X_u} f_x(x)dx \tag{1}$$

where X_l and X_u give the upper and lower bounds of the bin within which X lies. If the bin size is small, then $f_x(X)$ can be assumed to be constant within the range of X_l to X_u and Equation (1) becomes:

$$H_x(X) = f_x(X)\Delta X = f_x(X)(X_u - X_l) \tag{2}$$

where ΔX is the bin size.

2. Cumulative distribution functions and cumulative frequency histograms.

Using the histograms and the probability density functions $f_{x1}(\ldots)$, $f_{x2}(\ldots)$, $f_{xs}(\ldots)$ and $f_z(\ldots)$ the cumulative distributions for the shear or moment effects of single or multilane loading events can be obtained. The cumulative distribution is assembled from the pdf using the equation:

$$F_z(Z) = \int_{-\infty}^{z} f_z(y)dy \tag{3}$$

30

In essence, Equation (3) assembles all the bins of the histogram below a certain value Z into a single bin at Z. This is repeated for all possible values of Z. Thus, $F_z(Z)$ will give the probability that a loading event will produce a load effect less or equal to Z.

3. Cumulative probability function for the maximum load effect over a return period of time, t_{return}.

For the AASHTO Strength I limit state, a bridge structure should be designed to withstand the maximum load effect expected over the design life of the bridge. The AASHTO LRFD code specifies a design life of 75 years. The LRFR bridge load rating also requires checking the capacity to resist the maximum load effects for a two-year return period. The AASHTO LRFD Strength II limit state implicitly assumes a one-year return period associated with special permit trucks. It is simply impossible to collect enough data to determine the maximum load effect expected over 75 years of loading. Even getting sufficient data for the one-year and two-year return periods would require several cycles of one-year and two-year data which are not currently available. Therefore, some form of statistical projection should be performed. The proposed calculation procedure uses the cumulative distribution function for individual loading events and then applies a statistical projection to obtain the information required for a one-year, two-year, or 75-year return period.

To find the cumulative distribution for the maximum loading event in a period of time t_{return} we have to start by assuming that N loading events occur during this period of time. These events are designated as S_1, S_2, … S_N. The maximum of these N events, call it $S_{max,N}$, is defined as:

$$S_{max,N} = max\ (S_1, S_2, …\ S_N) \qquad (4)$$

We are interested in finding the cumulative probability distribution of $S_{max,N}$. This cumulative probability distribution, $F_{s\ max\ N}(S)$, gives the probability that $S_{max,N}$ is less than or equal to a value S. If $S_{max,N}$ is less than S, this implies that S_1 is less than S, and S_2 is less than S, … and S_N is less than S. Hence, assuming that the loading events are independent, the probability that $S_{max,N} \le S$ can be calculated from:

$$F_{s_{max\ N}}(S) = F_{s_1}(S).F_{s_2}(S)...F_{s_N}(S) \qquad (5)$$

If S_1, S_2, ... S_N are independent random variables that are drawn from the same probability distribution, then:

$$F_{s_1}(S) = F_{s_2}(S) = ... = F_{s_N}(S) = F_s(S) \qquad (6)$$

and Equation (5) reduces to

$$F_{s_{max\ N}}(S) = \left[F_s\ (S)\right]^N \qquad (7)$$

Note that Equation (7) assumes that the number of events is a known deterministic value. A sensitivity analysis performed as part of this study has however demonstrated that the results of Equation (7) are not highly sensitive to small variations in N as N becomes large.

The application of Equation (7) requires high precision in $F_s(S)$. For example, given 3000 trucks per day over a 75-year return period the number of single truck events N would be over 82 million. Thus, to obtain the median value of the maximum event $S_{max\ N}$ corresponding to

$F_{S_{\max N}}(S)$=0.5 would require $F_s(S)$ to have precision up to the 9th decimal point which is not possible to obtain without executing some form of statistical projection. To perform the statistical projection a careful analysis of the tail end of $F_s(S)$ is required.

4. Statistical fit of tail end of probability distribution of load effect of a single loading event.

The probability distribution of the single loading event does not follow any known probability distribution type. However, careful observations of the tail ends of the WIM data histograms assembled from several sites indicate that the tail ends match the tail ends of Normal probability distributions. For example, Figure 1 shows the plot of the data collected at the I-81 site in upstate New York on a Normal probability scale. A Normal probability plot is executed by taking the Normal inverse of $F_s(S)$ represented by $\Phi^{-1}[F_s(S)]$ and plotting versus S. The plot would produce a straight line if S follows a Normal distribution. In this case, the mean of S would correspond to the abscissa for which $\Phi^{-1}[F_s(S)]$ is zero. The mean plus on standard deviation would correspond to the abscissa for which $\Phi^{-1}[F_s(S)]$ is equal to 1.0.

The plot of the WIM data shows that the data as a whole does not follow a Normal distribution as the curve does not follows a straight line. However, the figure shows that the upper 5% of the data (plotted in red) does approach a straight line indicating that the tail end of the data resembles the tail end of a hypothetical Normal distribution. A linear fit on the Normal probability plot of the upper 5% of the data collected at this I-81 site will produce a slope, m, and an intercept, n, which will give the mean of the equivalent Normal distribution that best fits the tail end as μ_{event}= -n/m. The standard deviation of the best-fit Normal is σ_{event}=1/m. For the I-81 data, single truck events give μ_{event}=0.0232 and σ_{event}=0.333. The regression analysis of the upper 5% of the data produces a regression coefficient R^2=0.997 indicating a good linear fit.
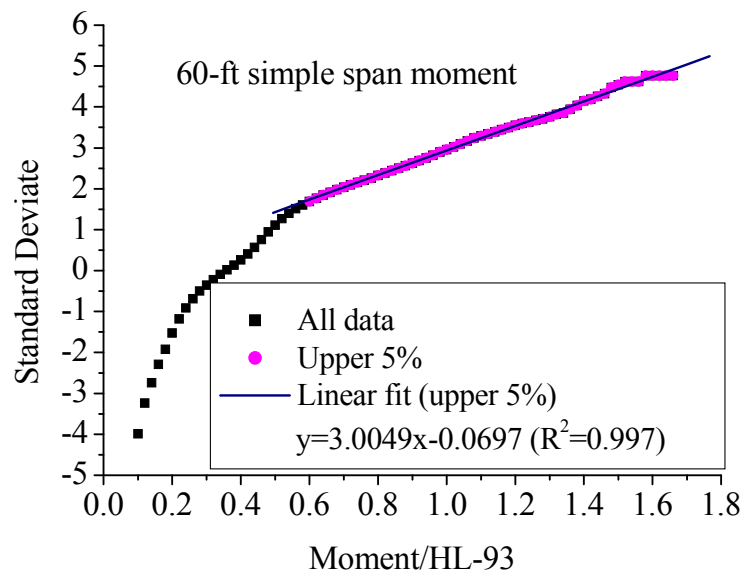
Figure 1. Normal probability plot for moment effect of trucks in drive lane of I-81 NB

5. Cumulative distribution of maximum load effect.

To verify that the Normal fit of the tail end of the data is sufficient to obtain good estimates of the maximum load effect for long return periods, the results of Eq. (7) are plotted in Figure 2 for two cases. Cases 1 uses as input the cumulative distribution $F_s(S)$ obtained from the WIM data for single loading events and case 2 plotted in red uses the $F_s(S)$ that corresponds to the Normal distribution with μ_{event}=0.0232 and σ_{event}=0.333. The application of Eq. (7) uses different return periods varying from one day to 75 years. The number of events for the I-81 site are obtained as N_{day}=3200 single truck events.

Figure 2 shows good agreement between the projections obtained from the Normal fit of the tail (in red) and the WIM data for the one-day, one-week and the one-month return periods. The figure also shows that the WIM data is not sufficient to obtain the maximum load effect for return periods greater than one month. However, the use of the Normal distribution to model the tail end of WIM data would allow for obtaining the maximum load effect distribution for extended return periods.

Cumulative Moment Distribution for Maximum Truck Effect in Different Return Periods
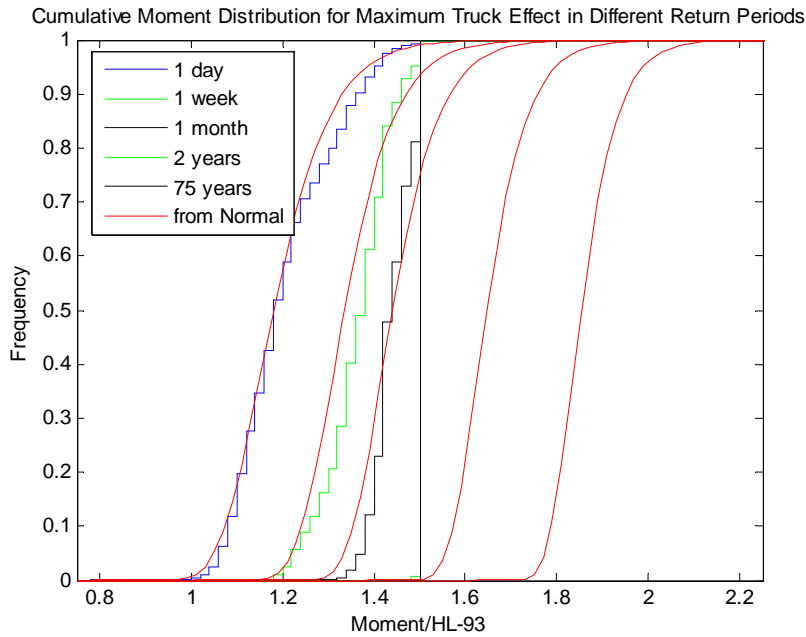
Figure 2. Cumulative distribution of maximum load effect of single lane events for different return periods.

6. Extreme value distribution of maximum load effect.

Although the application of Eq. 7 can be executed numerically for any parent probability distribution, the fact that the tail end of the WIM data matches that of a Normal distribution allows for the application of extreme value theory to obtain the statistics of the maximum load effect in closed form. The approach is based on the following known concept as provided in Ang and Tang (2007): "if the parent distribution of the initial variable S has a general Normal distribution with mean μ_{event} and standard deviation σ_{event}, then the maximum value after N

repetitions approaches asymptotically an Extreme Value Type I (Gumbel) distribution" with a dispersion α_N given by:

$$\alpha_N = \frac{\sqrt{2\ln(N)}}{\sigma_{event}}$$

(8)

and a most probable value u_N given by:

$$u_N = \mu_{event} + \sigma_{event}\left(\sqrt{2\ln(N)} - \frac{\ln(\ln(N)) + \ln(4\pi)}{2\sqrt{2\ln(N)}}\right)$$

(9)

α_N and u_N can be used to find the mean of the maximum load effect, L_{max}, and its standard deviation, σ_{max}, for any return period having N repetitions as:

$$\overline{L}_{max} = \mu_{max} = u_N + \frac{0.577216}{\alpha_N}$$

(10)

and

$$\sigma_{max} = \frac{\pi}{\sqrt{6}\alpha_N}$$

(11)

Monte Carlo Simulation

An alternative to the statistical projections approach consists of using a Monte-Carlo simulation to obtain the maximum load effect. In this approach, results of WIM data observed over a short period can be used as a basis for projections over longer periods of time. A Monte Carlo simulation requires the performance of an analysis a large number of times and then assembling the results of the analysis into a histogram that will describe the scatter in the final results. Each iteration is often referred to as a cycle. The process can be executed for the single lane-loading situation or the side-by-side loading. A step-by-step procedure for Monte Carlo Simulation is described in Step 12.3 of the Draft protocols, in the next chapter.

Monte Carlo simulation will not be accurate for large projections periods because of the limitations in the originally collected data. Also, the Monte Carlo simulation will be extremely slowed down when the number of repetitions K is very high. Furthermore, one should make sure not to exceed the random number generation limits of the software used, otherwise the generated numbers will not be independent and the final results will be erroneous. Hence, statistical projections must be made to estimate the maximum load effects for long return periods. Alternatively, one can use a smoothed tail end of the WIM histogram by fitting the tail with a known probability distribution function (such as the Normal distribution) and use that fitted distribution with the Monte Carlo simulation. It should be emphasized however, that the Monte Carlo simulation would still be very inefficient for projections over long return periods.

CHAPTER 3

FINDINGS AND APPLICATIONS.

BACKGROUND TO DEVELOPMENT OF DRAFT RECOMMENDED PROTOCOLS

LRFD Background

The HL-93 live load model was initially developed as a notional representation of shears and moments produced by a group of vehicles routinely permitted on highways of various states under "grandfather" exclusions to weight laws. The notional load model was subsequently compared to the results of truck weight studies, selected WIM data (Ontario), and the 1991 OHBDC (Ontario Code) live load model. These comparisons showed that the notional load could be scaled by appropriate load factors to be representative of these other load spectra.

The calibration of the AASHTO LRFD Specifications, is based on the top 20% of trucks in an Ontario truck weight database assembled in 1975 from a single site over only a two-week period. In the past 30 years, truck traffic has seen significant increases in volume and weight.

The goal of this project is to develop a set of protocols and methodologies for using available current truck traffic data collected at different US sites and recommend a step-by-step procedure that can be followed to obtain live load models for bridge design. The protocols are geared to address the use of national WIM data to develop and calibrate vehicular loads for LRFD superstructure design, fatigue design, deck design and design for overload permits.

Various levels of complexity are available for utilizing the site-specific truck weight and traffic data to calibrate live load models for bridge design. A simplified calibration approach is proposed that focuses on the maximum live load variable, L_{max} for updating the live load model or the load factor for current traffic conditions, in a manner consistent with the LRFD calibration. A more robust reliability-based approach is also presented that considers the site-to-site variations in WIM data in the calibration of live loads. Some key issues and traffic parameters that influence the estimation of traffic statistics and the maximum load effect are summarized as given below.

Use of High-Speed WIM Sites

The first condition that any set of traffic data should meet before being used for the development of load models is the elimination of bias. Truck data surveys collected at truck weigh stations and publicized locations are not accurate, because, they are normally avoided by illegal overweight vehicles that could control the maximum loads applied on bridge structures. Furthermore, an important parameter that controls the load imposed on the structure is related to the number of simultaneous vehicles on the bridge, which is determined through data on truck headways under operating conditions. Accurate headway information cannot be obtained from fixed weigh-stations or from truck data collected at highway bypasses. For these reasons it is determined that truck traffic data should be collected through Weigh-In-Motion systems that can collect simultaneously headway information as well as truck weights and axle weights and axle configurations while remaining hidden from view and unnoticed by truck drivers.

WIM Data Quality

WIM data collection should not sacrifice quality for quantity. The selection of WIM systems sites should focus on sites where the owners maintain a quality assurance program that regularly checks the data for quality and requires system repair or recalibration when suspect data

is identified. Weighing accuracy is sensitive to roadway conditions. Roadway conditions at a WIM site can deteriorate after a system is installed and calibrated. Regular maintenance and recalibrations are essential for reliable WIM system performance. Vehicle dynamics plays a significant role in the force actually applied by any given axle at any given point on the roadway. Site-specific calibration is the only way that the dynamic effects of the pavement leading to the scale can be accounted for in the WIM scale calibration. The dynamic motion of trucks is also influenced by the vehicle design, gross weight, and suspension systems. The calibration approach should account for the vehicle dynamics and the truck traffic characteristics of each data collection site.

Physical and software-related failures of equipment, and transmission failures are common sources of traffic data quality problems. Transmission problems can lead to gaps in the data (i.e., missing data) even though data may be continuously collected in the field. Data quality checks should be implemented to detect and fix "bad data" before processing.

WIM Scale Calibration

Heavy emphasis is placed on the calibration of WIM data collection equipment. Quality information is more important than the quantity of data collected. It is far better to collect small amounts of well-calibrated data than to collect large amounts of data from poorly calibrated scales. Even small errors in vehicle weight measurements caused by poorly calibrated sensors could result in significant errors in measured loads. Key issues concerning the use of WIM equipment are: 1) the calibration of WIM equipment and 2) the monitoring of the data reported by WIM systems as a means of detecting drift in the calibration of weight sensors. Recommendations for WIM sensor calibration and monitoring of data are given in Appendix 5-A of the Traffic Monitoring Guide (USDOT 2001).

Auto-calibration is the practice by which software calculates and applies an adjustment to the scale calibration factor based on a comparison of the average of a number of measurements of front axle weights against its expected value. There are drawbacks to auto-calibration techniques currently used by some states to offset calibration errors, and it is recommended that direct WIM scale calibration be implemented. Only direct calibration of a WIM scale after it has been installed at a site ensures that it is measuring axle weights correctly. This includes a comparison of static axle weights with axle weights that are estimated from multiple vehicle passes with more than one vehicle. Comparison of static weights and dynamic weights will provide an effective check of system accuracy with regard to sensor errors and errors due to vehicle dynamic effects. For long duration counts, the scale should be calibrated initially, the traffic characteristics at that site should be recorded, and the scale's performance should be monitored over time. The State should also perform additional, periodic on-site calibration checks (at least two per year). These steps will ensure that the data being collected are accurate and reliable.

WIM data scatter for axles is different from gross weight scatter and is usually much larger. This axle scatter should be assembled separately from the equipment calibration and should be used to modify the measured axle loads.

Filtration of WIM measurement Errors

Sensitivity analyses have shown that the most important parameters affecting maximum bridge loads are those parameters that describe the shape of the tail end of the truck load effects histogram. Current WIM technology is known to have certain levels of random measurement errors that may affect the accuracy of the load modeling results. These errors are due to the inherent inaccuracies of the WIM system itself, the difference between the dynamic weight measured and the actual static scale weight, as well as the effect of tire pressure, size and

configuration on the WIM results. Hence, it is advisable to use a statistical algorithm to filter out these errors. A standardized approach to executing the error filtering procedure will bring uniformity in the load modeling process that will utilize WIM data from various sites.   To execute the filtering process, a calibration of the results of the WIM system should be made by comparing the results of the WIM to those of a static scale. This calibration process should be executed for a whole range of truck and axle weight types and configurations. The ratio of the measured weight to the actual weight (bias) for a large sample of readings is the calibration statistics that should be assembled into a histogram. A procedure for error filtering utilizing the scale calibration data is recommended as part of the load modeling protocols.

Site-to-Site Variability

One of the largest variability in truck traffic is the site-to-site variability. Site-to-site variability of truckloads should be incorporated as the calibration of the AASHTO LRFD Specifications used data from only one site in Ontario, Canada (U.S. sites were not considered). Dividing truck routes into three functional classifications will allow a systematic assessment of truck load spectra within a state. Each route within a functional classification group is taken to experience truck weights per vehicle type that are similar to those of other routes within that group. The classification groups routes into Interstate and Non-Interstate highways. Many states allow heavier loads on non-Interstate routes under grandfather exemptions to weight laws. Interstates are further divided into urban vs. rural as many urban areas have been known to experience heavier truck loads and volume due to increased commercial activity, lack of alternate modes of freight movement and a general lack of truck weight enforcement.

Truck data will be collected from WIM sites on principal arterials. The routes on the principal arterial system are sub classified as Interstate and other principal arterials (Table 8). Urban and rural areas could have fundamentally different traffic characteristics. Consequently, this workplan provides for separate classification of urban and rural functional systems.

Table 8 Proposed Classification Scheme for Truck Weight Data Collection

Protocols Functional Class	Description	FHWA functional Class(es)
A	Rural Interstate Principal Arterial	1
B	Urban Interstate Principal Arterial	11
C	Other Principal Arterial	2, 12, 14

Seasonal Variability in the Traffic Stream

Traffic varies over time. Traffic varies over a number of different time scales, including:

- Time of day
- Day of week
- Season (month) of the year.

Most trucks follow a traditional urban pattern where weekday truck volumes are fairly constant, but on weekends, truck volumes decline considerably. Long-haul trucks are not concerned with the "business day"; they travel equally on all seven days of the week. WIM sites should operate continuously throughout the year to measure temporal changes in the loads carried

by trucks. Where possible, more than one site within a functional group should be monitored continuously to provide a more reliable measure of seasonal change. Tracking of seasonal changes in truck traffic is necessary to obtain representative truck weight histograms needed for various analyses.

Directional Variation

Most roads exhibit differences in flow by direction. Truck weights, volumes and characteristics can also change by direction. One "classic" example of directional differences in trucks is the movement of loaded trucks in one direction along a road, with a return movement of empty trucks. This is often the case in regions where mineral resources are extracted or near port facilities. Tracking these directional movements is important to obtain the load spectra for bridge load modeling.

Lane-By-Lane Variation

Vast majority of trucks (80% or more) travel in the right (drive) lane. The expected maximum gross vehicle weight and, therefore, the expected maximum moments and shears of the trucks in the drive lane are different than those of the trucks in the passing lane. The degree of this difference seems to be dependant on the site and travel direction. The maximum lifetime loading requires as an input the percentage of trucks that cross the bridge side-by-side and the lane-by-lane distribution of truck weights. Assuming that the trucks in each lane have identical distribution (as in past simplified approaches) can introduce unnecessary conservatism. Using WIM data could easily improve past estimates or assumptions of various load uncertainties for trucks in each lane. Knowing the truck weight distribution in each lane, including mean, COV, and distribution type can improve the input parameters needed for the load modeling process.

Permit Traffic vs. Non-Permit Traffic

In most states permit records are either not specific enough or detailed enough to allow separation of permit loads from non-permit loads in a large WIM database. Routine permits are not route-specific and are allowed unlimited trips. For LRFD bridge design it is not necessary to separate legal loads from Routine Permits as both are classified as unanalyzed truck loads, that should be enveloped by the HL-93 design loading. Protocols require that legal loads and routine permits be grouped under STRENGTH I and heavy special permits be grouped under STRENGTH II. The following approach was developed to grouping trucks that would be consistent from site to site:

- Do not attempt to classify trucks as permit or non-permit as customarily the permit records are not reliable enough or readily accessible to do this.
- Group all trucks with six or fewer axles in the STRENGTH I calibration. These vehicles include legal trucks and routine permits or divisible load permits. These vehicles are considered to be enveloped by the HL-93 load model.
- Group all trucks with seven or more axles in the STRENGTH II calibration. These vehicles should include the heavy special permit loads, typically in the 150 Kip GVW and above category.

For a state that maintains easily accessible permit records with a well established and enforced overweight permits program it would be possible to obtain the records for authorized permits or permit vehicles for a route for a specific data collection period and separate out these heavy vehicles (STRENGTH II) from the illegal overloads (STRENGTH I), both of which populate the

upper tail of the histogram. With many states moving to on-line and web-based permits processing, electronic records for permits should become more readily available in the future.

Multiple-Presence Probabilities

In many spans, the maximum lifetime truck-loading event is the result of more than one vehicle on the bridge at a time. An important step in defining nominal design load models is the modeling of multiple presence probabilities. Many modern WIM data loggers currently in use in the U.S. have the capability to record and report sufficiently accurate truck arrival times for estimating multiple presence probabilities. Many traffic counters routinely record data to 1/100 of a second or even a millisecond in their binary files. These time stamps allow the determination of headway separation of trucks in adjacent lanes or in the same lane and the occurrence of simultaneous or near-simultaneous load events in each lane. The sensitivity analysis has demonstrated that small changes in the number of multiple presence events do not have a significant effect on the estimated maximum load effect over the 75 year design life.

Studies done using New York WIM data during this project show that there is a strong correlation between multiple presence and ADTT. From Figure 12 it is evident that the number of multiple presences sees a sharp drop off on days when the ADTT is low (such as weekends). Though not linear, the graph demonstrates that multiple presence statistics are related to the site traffic conditions. A recent study of truck multiple-presence at twenty-five (25) sites across NJ over a period of 11 years has also provided valuable data on the relationship between truck volume and truck multiple-presence. (Gindy, M. and Nassif, H. (2006))

Obtaining reliable multiple presence statistics requires large quantities of continuous WIM data with refined time stamps, which may not be available every site. The site ADTT could serve as one key variable for establishing a site multiple presence value. A single WIM site can provide multiple presence data for varying ADTT values due to daily variation in ADTT.
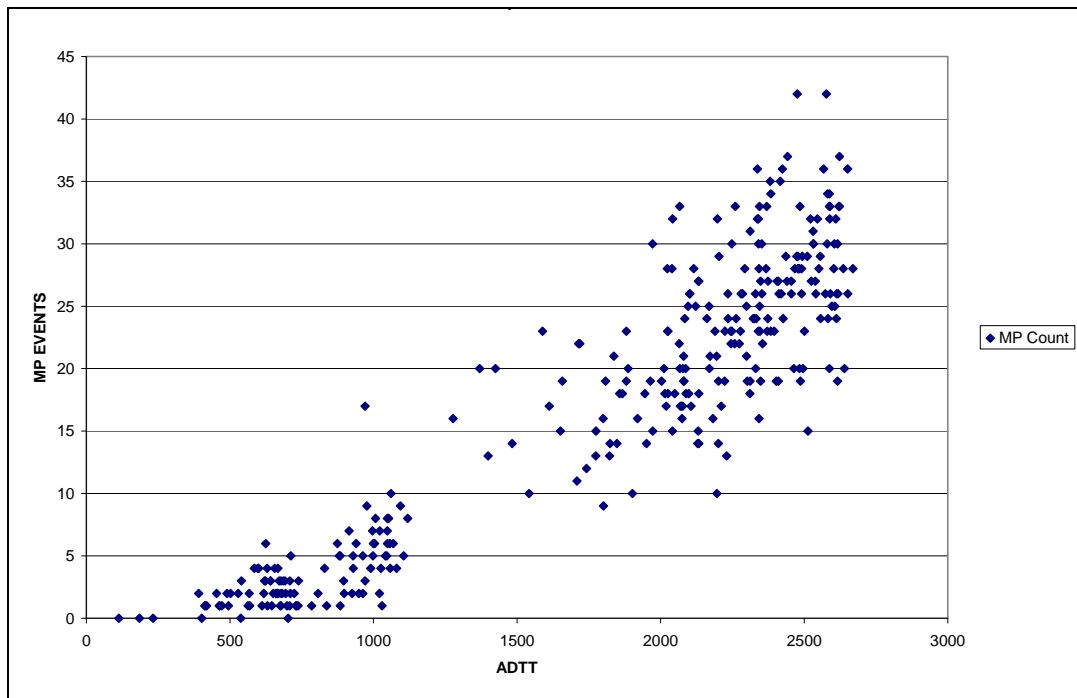
Figure 12   Side-by-Side Events vs. ADTT -- I-81 NB New York

Multiple-Presence Probabilities for Permit Loads

The multiple-presence probabilities for permit trucks are significantly different from those used for normal traffic. In the LRFD, the STRENGTH II limit state is specified for checking an owner-specified permit vehicle during the design process with a reduced load factor of 1.35. Though no guidance is given in the LRFD Specifications on how this load factor was derived, a reduced load factor is considered appropriate due to the reduced likelihood of permit trucks exceeding the authorized weight, the reduced multiple presence likelihood and the reduced exposure period of one year. The permit live load factors are derived to account for the possibility of simultaneous presence of non-permit heavy trucks on the bridge when the permit vehicle crosses the span. Information on loads and multiple-presence probabilities for permits need to be obtained locally or regionally through WIM measurements and considered in the STRENGTH II design process since the data used for calibration of national codes are unlikely to be representative of all jurisdictions.

LRFD Fatigue Design

Since fatigue is defined in terms of accumulated stress-range cycles over the anticipated service life of the bridge, fatigue design is based on typical conditions that occur as many cycles are needed to cause a fatigue failure. The present AASHTO fatigue truck, which is based on reliability analyses, was developed using truck traffic load data taken for some 30 WIM sites in about eight states collected in the 1980s. Over 20,000 trucks were used to calculate the stress ranges and then the fatigue damage averaged according to the fatigue damage law (cubic power). The number of cycles to failure was compared with lab test data for various welded details. The fatigue truck developed (54 kip, 5-axle truck) from these studies has been incorporated into the AASHTO LRFD Specifications and the AASHTO LRFR manual.

As truck weight and volume increase and bridges are maintained in service for increasingly longer periods of time, the fatigue design and assessment issues becomes even more important. The AASHTO fatigue load is used to represent the variety of trucks of different types and weights in actual traffic. Applying a single truck model that may not be representative of current traffic as a standard for all fatigue design may be inaccurate or potentially unsafe. Code-based load models based on past WIM data may not adequately represent modern traffic conditions in many jurisdictions.

DRAFT RECOMMENDED PROTOCOLS FOR USING TRAFFIC DATA IN BRIDGE DESIGN

Protocols recommended for collecting and using traffic data in bridge design can be categorized into the following steps:

STEP 1   DEFINE WIM DATA REQUIREMENTS FOR LIVE LOAD MODELING
STEP 2   SELECTION OF WIM SITES FOR COLLECTING TRAFFIC DATA FOR BRIDGE DESIGN
STEP 3   QUANTITIES OF WIM DATA REQUIRED FOR LOAD MODELING
STEP 4   WIM CALIBRATION & VERIFICATION TESTS
STEP 5   PROTOCOLS FOR DATA SCRUBBING, DATA QUALITY CHECKS & STATISTICAL ADEQUACY OF TRAFFIC DATA
STEP 6   GENERALIZED MULTIPLE-PRESENCE STATISTICS FOR TRUCKS AS A FUNCTION OF TRAFFIC VOLUME
STEP 7   PROTOCOLS FOR WIM DATA ANALYSIS FOR ONE-LANE LOAD EFFECTS FOR SUPERSTRUCTURE DESIGN
STEP 8   PROTOCOLS FOR WIM DATA ANALYSIS FOR TWO-LANE LOAD EFFECTS FOR SUPERSTRUCTURE DESIGN
STEP 9   ASSEMBLE AXLE LOAD HISTOGRAMS FOR DECK DESIGN
STEP 10   FILTERING OF WIM SENSOR ERRORS / WIM SCATTER FROM WIM HISTOGRAMS
STEP 11   ACCUMULATED FATIGUE DAMAGE AND EFFECTIVE GROSS WEIGHT FROM WIM DATA
STEP 12   LIFETIME MAXIMUM LOAD EFFECT L_{max} FOR SUPERSTRUCTURE DESIGN
STEP 13   DEVELOP AND CALIBRATE VEHICULAR LOAD MODELS FOR BRIDGE DESIGN

The above steps to be followed are described below in detail:

STEP 1   DEFINE WIM DATA REQUIREMENTS FOR LIVE LOAD MODELING

An aim of these processes is to capture weight data appropriate for national use or data specific to a state or local jurisdiction where the truck weight regulations and/or traffic conditions may be significantly different from national standards. The objective is to use data from existing WIM sites to develop live load models for bridge design. The models will be applicable for the strength and fatigue design of bridge members, including bridge decks and design vehicles for overload permitting. The traffic data needs for live load modeling are summarized below:

Step 1.1   Data needed for calibration of superstructure (STRENGTH I) design load models include:

❑ Lane by lane truck type distribution, total weights, and axle weights and spacings with particular emphasis on the tails of the weight histograms.
❑ Headways and multi-presence for single, two, or more lanes including side-by-side, staggered and following trucks which are of particular interest for multi-span or longer single span bridges. How headways are affected by truck volumes is important for developing models that take into consideration local or regional traffic patterns.

❑ Calibration statistics for the WIM scale to filter out sensor errors.

Step 1.2   Data needed for overload permitting (STRENGTH II) include:

❑ State permit policies and routine permit types authorized for a specific route.
❑ Where available, record of special permits authorized for a specific route during the data collection period, including truck descriptions, axle weights and axle spacing
❑ Information on multiple presence for permit loads – two permits trucks side-by-side or permit truck with a non-permit truck.
❑ WIM calibration data using overloaded test trucks, if available. If not, utilize same calibration data as for STRENGTH I.

Step 1.3   Data needed for calibration of deck design load models include:

❑ Common axle configurations and axle weight distributions of legal trucks and permit trucks.
❑ Frequencies of occurrences of common axle configurations.
❑ Other multi-axle axle configurations with fixed and variable axles.
❑ Headway information for side-by-side effects of axle groups or single axles.
❑ WIM scale calibration statistics for axle loads

Step 1.4   Data needed for calibration of fatigue load models (FATIGUE) include:

❑ Truck type distribution, total weights, and axle weights and spacings with emphasis on the most common vehicles rather than on the tails. This is because the fatigue process is due to the accumulation of damage from every truck crossing and is less dependent on the extreme loading events.
❑ Frequencies of occurrences of common truck configurations.
❑ WIM scale calibration statistics

STEP 2   SELECTION OF WIM SITES FOR COLLECTING TRAFFIC DATA FOR BRIDGE DESIGN

❑ Select remote WIM sites away from weigh stations. This is very important for obtaining unbiased data. Traffic monitoring unknown to the truck drivers' is key.
❑ Select sites that do not experience significant breakdowns and provide reliable year-round operation. Select sites that can provide a year's worth of continuous data.
❑ Select WIM sites that have been recently calibrated and are subject to a regular maintenance and quality assurance program. A review of recent WIM data will indicate if there is an obvious problem with the calibration. Perform a calibration check of the system. Accuracy of the weight data and the time stamps should be verified. Request a manual recalibration using a group of trucks of known weight and configuration if the system does not meet specified tolerances. Calibration data must be available for filtering out measurement errors. The project will recommended data quality requirements for WIM sites used for data collection.
❑ Select WIM sites with free flowing traffic, where trucks usually maintain their lanes and travel speed (>10 mph), that do not experience any significant stop-and-go traffic or traffic backups. The sites should be away from exits, on level grade, with smooth roadway surfaces near the WIM installation. Avoid sites with numerous traffic stoppages.
❑ Select sites with WIM sensors in right lane and passing lanes, in both directions. Some sites have sensors only in the drive lane.

- ❑ The user should have a good understanding of the state's overweight permit policies that apply to the specific routes. It would be difficult to identify continuous or routine permits in the traffic stream in most states. These permits are not route-specific and are allowed unlimited trips within the period of duration for the permit. Special permits that are issued for very heavy loads are subject to restrictions on the route taken and the number of crossings made. Use records of Special permits (usually available from the permit office), to identify and remove these vehicles that populate the extreme end of the load data prior to statistical processing of "random" traffic.
- ❑ Select sites equipped with current sensor and equipment technologies. Regular maintenance and periodic recalibration of any WIM system is critical for obtaining reliable traffic data. It is also important to filter out WIM data measurement errors so that they do not affect the accuracy of the load modeling results. The calibration of the WIM system will provide information on the calibration factor, ε, for use in the filtering process.
- ❑ Preferably, the WIM system should be able to capture and record truck arrival times to the nearest $1/100^{th}$ of a second or better to allow the determination of truck headway separations.

In general, the selection of WIM sites for bridge load modeling will depend on the geographic spread of the truck load data represented by the model.

Step 2.1   Sites for National Design Live Load Modeling

- Study of truck loads can be conveniently handled by dividing the country into five regions as shown in Figure 14 below. (FHWA 2001)
- Ten states with the high truck populations are: CA, IL, TX, OH, FL, PA, OK, NY, NC, and IN (Table 9).
- Select one representative state from each region. The state should have a well established and maintained WIM program that has been in place for a number of years that could provide the data needed for load modeling. The five recommended states, one from each region are: California, Florida, Indiana, New York and Texas.
- For each representative state, select the sites and routes for WIM data collection based on functional classifications defined in Table 8.
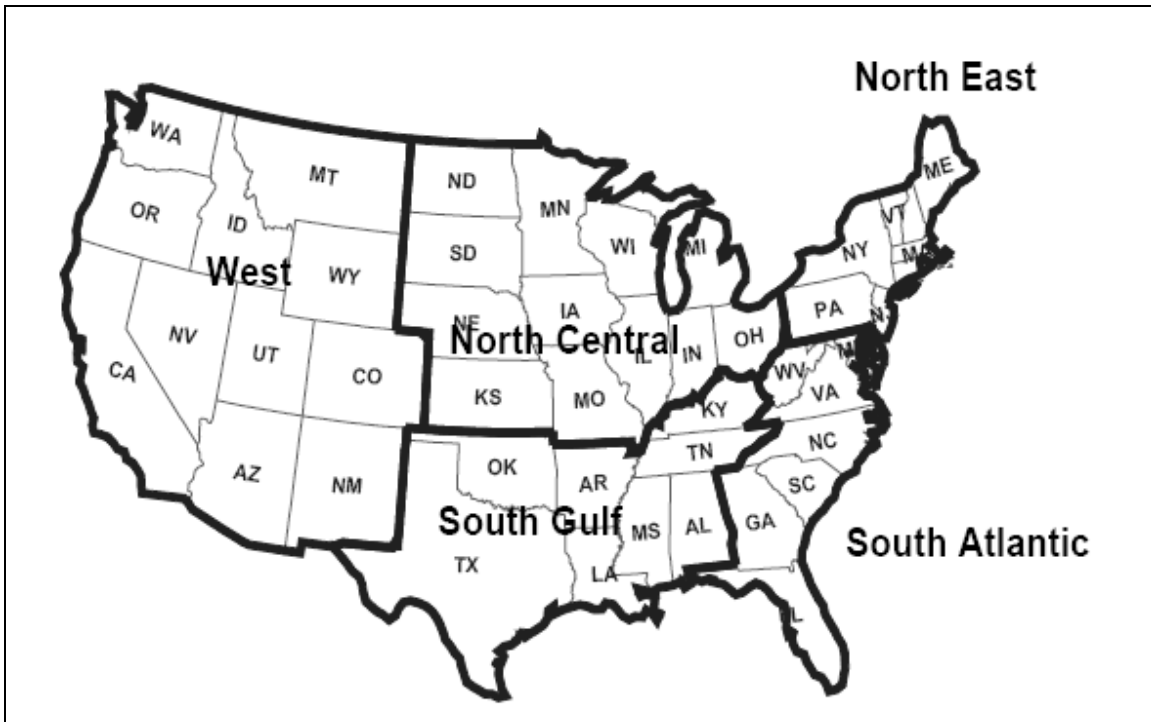
Figure 14   U.S. Regions for Truck Loads.

Table 9   Candidate States for National Data Collection for Live Load Modeling.

State	State Ranking Based on Truck Population	Region (See map Fig 2)	How Long Has the WIM Program Been in Operation?	Total Number of High Speed WIM Sites	Number of WIM Sites on Interstates	WIM Data Available for a Whole Year?
California	1	WE	15 years	137	58	Yes
Florida	5	SA	32 years	40	14	Yes
Indiana	10	NC	15 years	52	24	Yes
Michigan	11	NC	14 years	41	21	Yes
Missouri	15	NC	10 years	13	7	Yes
New Jersey	19	NE	13 years	64	14	Yes
New York	8	NE	10+ years	21	11	Yes
Ohio	4	NC	15 years	44	21	Yes
Oregon	23	WE	8 years	22	18	Yes.
Texas	3	SG	21 years	18	6	yes

Table 10 Recommended Five States from Each of the Five Regions (see Fig. 14).

State	State Ranking Based on Truck Population	Region	How Long Has the WIM Program Been in Operation?	Total Number of High Speed WIM Sites	Number of WIM Sites on Interstates	WIM Data Available for a Whole Year?
California	1	WE	15 years	137	58	Yes
Florida	5	SA	32 years	40	14	Yes
Indiana	10	NC	15 years	52	24	Yes
New York	8	NE	10+ years	21	11	Yes
Texas	3	SG	21 years	18	6	yes

For each functional classification select two WIM sites, guided by the following considerations, as applicable:

- o Heavy freight routes or routes known to have significant permit traffic.
- o Bulk cargo shipping routes
- o Logging routes
- o Specialized equipment shipping routes
- o WIM sites near ports, railroad terminals or other truck origination points.
- o WIM sites near industrial facilities or mining operations.
- o WIM sites near landfills or waste transfer sites.
- o WIM sites near military installations
- o WIM sites should preferable be geographically dispersed within a state
- o WIM sites should preferable have varied truck volumes.

Table 11 Sites by Functional Classification for WIM Data Collection

Functional Class	FHWA Functional Classes	Description	WIM Sites
A	1	Rural Interstate Principal Arterial	2
B	11	Urban Interstate Principal Arterial	2
C	2, 12, 14	Other Principal Arterial	2

Step 2.2 Sites for State-Specific Design Live Load Modeling

It is important to recognize that there can be significant variations in traffic conditions within a state that should be accounted for in truck weight studies. For calibrating design load models for a specific state, some broad guidelines may be given as follows:

- Two sites from each of the three highway functional classes. Where WIM sites exist, verify that WIM data from all major truck routes within a state are included.
- Each site in a functional class should preferably be from a different region of the state.
- The guidelines for selecting individual WIM sites should be as discussed above under national design live load modeling.

Step 2.3   Sites for Design Live Load Modeling for a Metro-Area or Transportation Hub

- For calibrating load models for a city or a transportation hub within a state, select at least six WIM sites from within a 25-mile radius of the city or region. Where WIM sites exist, verify that WIM data from all major truck routes within the area of interest are included.
- The guidelines for selecting individual WIM sites should be as discussed above under national design live load modeling.
- Where enough permanent WIM sites are not in operation, temporary WIM sites for short-term data collection may be employed. Data should be collected to capture likely seasonal variability in truck traffic.

Step 2.4   Sites for Route-Specific Design Live Load Modeling

- For calibrating live load models for a designated hauling route, select a minimum of three WIM sites on that route or on feeder routes.
- The guidelines for selecting individual WIM sites should be as discussed above under national design live load modeling.
- Where enough permanent WIM sites are not in operation, temporary WIM sites for short-term data collection may be employed. Data should be collected to capture likely seasonal variability in truck traffic.

Step 2.5   Sites for Site-Specific Design Live Load Modeling

- This would be particularly relevant to major bridge design and/or evaluation.
- For calibrating site-specific load models for a specific bridge, select three WIM sites on that route or feeder routes, preferable within a distance of 25 miles of the bridge.
- If permanent WIM sites are not available, a temporary WIM site may be deployed at the approaches to the bridge. Data should be collected to capture likely seasonal variability in truck traffic. WIM data shall be gathered in both travel directions.

For the purposes of picking WIM data collection sites for the demonstration of the protocols for this project, one site for each functional classification in two states is proposed. In this regard, the resources available on this project were also a consideration.

STEP 3   QUANTITIES OF WIM DATA REQUIRED FOR LOAD MODELING

Some recommendations for the quantity of WIM data to be collected from each site to capture the variability in traffic loads include:

     i. A year's worth of recent continuous data at each site to observe seasonal changes of vehicle weights and volumes is preferable.
     ii. If continuous data for a year is unavailable seek a minimum of one month data for each season for each site.
     iii. Data from all lanes in both directions of travel.

STEP 4   WIM CALIBRATION & VERIFICATION TESTS

To ensure that high quality data will be collected for use in bridge live load modeling, all WIM devices used for this purpose should be required to meet performance specifications for

data accuracy and reliability. Because collection of accurate traffic loading rates throughout the year is necessary to provide the load data needed, the WIM systems used in this effort must meet the ASTM criteria all year long. Historically, many WIM systems have had problems accurately weighing vehicles when environmental conditions have changed from those that were present when the equipment was last calibrated. Changes in pavement condition at the scale location are also known to cause problems with WIM system sensor accuracy.

Pavement design procedures compute equivalent single-axle loads (ESALs) from measured axle weights using a mathematical formula developed by AASHTO. The fourth-order relationship in this formula heavily magnifies the effects of poor scale calibration, which can lead to significant errors in determining the load experienced by a pavement and thus computing the expected pavement life. Bridge design however is controlled by shear and moment effects which bear a linear relationship to axle loads and axle spacings. Therefore, errors in scale calibration are not magnified to the same extent as in pavement design.

Many States attempt to work around the cost of scale calibration by relying on a variety of auto-calibration techniques provided by WIM equipment vendors. Auto-calibration is the practice by which software calculates and applies an adjustment to the scale calibration factor. This is a common technique utilized on piezo systems to account for changing sensitivity of the scale sensors to changing environmental conditions. It is based on a comparison of the average of a number of measurements of some specific variable against its expected value. Some of these techniques adjust scale-calibration factors to known sensitivities in axle sensors for changing environmental conditions, "known" truck conditions, and equipment limitations. Although these techniques have considerable value, they are only useful after the conditions being monitored at the study site have been confirmed. State must determine whether the auto-calibration procedure used is based on assumptions that are true for a particular site and whether enough test trucks are crossing the sensor during a given period to allow the calibration technique to function as intended. Auto-calibration may not be particularly suited to low truck volume sites. Field tests to verify that a WIM system is performing within the accuracy required is an important component of data quality assurance for bridge load modeling applications.

Steps to ensure that the data being collected are accurate and reliable are:

Step 4.1   **Initial Calibration**: Initial calibration of WIM equipment should follow LTPP calibration procedures or ASTM 1318 standards.

Step 4.2   **Periodic Monitoring:** Periodic monitoring of the data reported by WIM systems as a means of detecting drift in the calibration of weight sensors.

Step 4.3   **Periodic On-Site Calibration Checks**: For long duration counts, the scale should be calibrated initially, the traffic characteristics at that site should be recorded, and the scale's performance should be monitored over time. The State should also perform additional, periodic on-site calibration checks (at least two per year). Only direct calibration of a WIM scale after it has been installed at a site ensures that it is measuring axle weights correctly. This includes a comparison of static axle weights with axle weights that are estimated from multiple vehicle passes with more than one vehicle.

Assemble calibration statistics for WIM site for filtration of sensor errors during the load modeling process (see Step 11). This calibration process should be executed for a range of truck and axle weight types and configurations operating at normal highway speeds. The ratio of the measured weight to the actual weight for a large sample

of readings is the calibration factor that should be assembled into a histogram. WIM data scatter for axles is different from gross weight scatter and is usually much larger. This axle scatter should be assembled separately from the equipment calibration and should be used to modify the measured axle loads.

STEP 5   PROTOCOLS FOR DATA SCRUBBING, DATA QUALITY CHECKS & STATISTICAL ADEQUACY OF TRAFFIC DATA

Step 5.1   Data Scrubbing

The key to developing and calibrating bridge live load models is quality of WIM data and not quantity. High speed WIM is prone to various errors, which need to be recognized and considered in the data review process. It is important to review the WIM data to edit out "bad or unreliable data" containing unlikely trucks to ensure that only quality data is made part of the load modeling process. It is also important to recognize that unusual data is not all bad data as truck configurations are becoming increasingly more complex and truck weights are getting heavier. Slow moving traffic (<10 mph) and stop-and-go traffic could cause difficulty in separating vehicles. Two or more trucks may be read as one truck. It is therefore important to check speed data. Trucks with very large axle spacings and excessive total wheelbase may be combining separate trucks. Maximum likely axle spacing must be specified. This could be done by importing the WIM text files into a database. The filters can be used the screen the database for bad data or unlikely trucks during the data transfer process.

The WIM survey data should be scrubbed to include only the data that meet the quality checks. The following is a filtering protocol that was applied for screening the WIM data used in this project. Truck records that meet the following filters were eliminated:

- Speed < 10 mph
- Speed > 100 mph
- Truck length > 120 ft
- Total number of axles < 3
- Record where the sum of axle spacing is greater than the length of truck.
- GVW < 12 Kips (and max as required).
- Record where an individual axle > 70 Kips
- Record where the steer axle > 25 Kips
- Record where the steer axle < 6 Kips
- Record where the first axle spacing < 5 feet
- Record where any axle spacing < 3.4 feet
- Record where any axle < 2 Kips
- Record which has GVW +/- sum of the axle weights by more than 10%. This may indicate that the axle records provided may not be complete or accurate.

The data scrubbing rules have been refined and updated as WIM data from typical sites were processed during the course of this study. Adjustments to the data scrubbing rules may need to be made to accommodate differences in traffic characteristics, truck configurations and weight limit compliance from state to state. Some newer trucks with complex axle configurations may need rules specifically tailored to fit their use. The rules do not propose a maximum GVW limit. This

ensures that trucks are not excluded just because they are very heavy. The test is to see if a truck configuration is "realistic" based upon an understanding of feasible axle configurations.

Step 5.1.1   Review of Eliminated Suspect Data

Reviewing a sampling of trucks that were eliminated during the data scrubbing process is recommended to check if the process is performing as intended and that real trucks have not been inadvertently removed from the dataset. This is a valuable quality assurance check of the data scrubbing process. Comparing WIM data with permit data or data from any nearby weigh station would provide an additional check. Where feasible, short-duration monitoring of trucks using real time WIM data could be helpful to verify scale performance and the accuracy of truck classifications. Stopping of trucks for static weighing is not recommended during such monitoring as it may bias the WIM data, as the heavy overweight trucks may find an alternate route to avoid detection.

Step 5.2   Quality Control Checks for Scrubbed WIM Data

This section describes simple quality checks performed on WIM data to quickly confirm that a properly calibrated data collection device is working as intended. It should not be confused with calibration tests.

Perform the following quality control checks for each WIM site for each lane, for each month of data collection:

1. Check vehicle classification statistics (truck percentages by class) and compare results with historical values or manual counts where available for the site/route. Large deviations from expected values could indicate sensor problems.
2. Produce a GVW histogram of Class 9 trucks (5-axle semi-trailer trucks) using a 4 kip increment. Most sites will have two peaks in the GVW distribution (unloaded peak usually falls between 28 Kips and 32 Kips; the loaded peak falls somewhere between 72 Kips and 80 Kips). A shift in the peaks could indicate that the scale calibration may be changing or the scale may be malfunctioning. If both peaks have shifted, the scale is probably out of calibration.
3. Compute the number and percentage of Class 9 trucks over 100 Kips. If the percentage of Class 9 trucks over 100 Kips is high the scale calibration may be questionable, unless such readings could be explained by a State's weight and permitting laws or by known movement of heavy commodities on a route. Such readings may indicate operational problems with the sensor.
4. Produce a histogram of steer axle weights for Class 9 trucks. The average front axle weight for Class 9 trucks is fairly constant for most sites. It ranges between 9 Kips and 11 Kips. Some variations are possible due to truck characteristics and GVW. Significant deviation of steer axle weights is a sign of scale operational problems.
5. Produce a histogram of Class 9 drive tandem axle weights. Compare with mean drive axle weight for Class 9 trucks given in NCHRP Report 495 (estimates wheel weights as a function of truck GVW).
6. Produce a histogram of spacing between front axles and drive tandem axles. Check mean spacing between drive tandem axles. Compare results to historical values available for class 9 trucks.

Step 5.3   Assess the Statistical Adequacy of Traffic Data

The proposed protocols for calculating the maximum 75-year live load effect, L_{max}, is based on the WIM truck weight and truck traffic database assembled at various sites within the jurisdiction for which the L_{max} estimates are required. The protocols are based on collecting truck weight and truck traffic WIM data over a period of a year in order to cover all possible seasonal variations and other short-term fluctuations in truck traffic patterns.

The models used in this study assume that the WIM data is stationary in the sense that the one-year data is representative of all subsequent years within the 75-year design life of a bridge site. Possible growth in truck weights and traffic intensities must be considered using an economic projection analysis, which is beyond the scope of this study.

Furthermore, the proposed protocols assume that the tail end of the truckload effect histogram for a bridge span follows a Normal distribution the statistical properties of which are obtained from a regression analysis of the upper 5% of the data plotted on a Normal probability curve. Normal probability plots of truckload effects obtained from WIM data collected at several different sites have confirmed that the upper 5% of the data approaches a straight line with a regression coefficient R^2 on the order of 0.97 to 0.99 indicating that the Normal distribution does reasonably well model the upper tail of the truck load effect histograms. The slope and intercept of the regression fit of the upper tail on the Normal probability plot can then be used to find the mean and standard deviation of the Normal distribution. However, the values of the slope and intercept depend on the estimates of the frequency of trucks in each bin of the histogram. In particular, the Normal probability plot uses the cumulative frequencies as the basis for the calculation of the slope and intercept of the regression line and thus the mean and standard deviation of the equivalent Normal distribution. The calculated values for the mean and standard deviation provide "best estimates" of these parameters. However, the process does not provide any information about the accuracy of these estimates except our understanding that these estimates will improve as the sample size increases. In order to provide some quantitative measure of the accuracy of these estimates, it is herein proposed to use statistical confidence intervals. A confidence interval of a parameter defines a range with lower and upper limits within which the true value of the parameter will lie with a prescribed probability. These confidence intervals will reflect the effect of the sample size and the number of samples that are found to lie within a bin of the truckload effect. Obviously the more data is collected, the more confidence the engineer will have in the estimated truck load effect frequencies in each category and the higher will be the accuracy of the calculated mean and standard deviations of the equivalent Normal distribution.

Confidence Intervals on the Cumulative Frequencies

Let us assume that the percent cumulative frequency in a particular bin of the load effect histogram at a given site is given as "p_i" which is calculated as the total number of trucks that produced moments within the bin "i" divided by the total number of trucks, n. It can be proven that statistically speaking, this p_i is an unbiased estimate of the true value p_i. Thus, (according to Ang & Tang (2007)), the $(1-\alpha)$ lower and upper confidence intervals of p_i can be obtained from:

Lower limit: $$p_{i \ \alpha/2} = \hat{p}_i + k_{\alpha/2}\sqrt{\frac{\hat{p}_i(1-\hat{p}_i)}{n}} \qquad (14)$$

Upper limit:
$$p_{i \ \alpha/2} = \hat{p}_i + k_{(1-\alpha/2)}\sqrt{\frac{\hat{p}_i(1-\hat{p}_i)}{n}}$$
(15)

where $k_{\alpha/2} = -\Phi^{-1}(1-\alpha/2)$, and $k_{(1-\alpha/2)} = \Phi^{-1}(1-\alpha/2)$, $\Phi^{-1}(...)$ is the inverse cumulative function of the Normal standard distribution. If the 95% confidence limits are desired, then 1-α=95% leading to $k_{\alpha/2} = -1.96$ and $k_{(1-\alpha/2)} = +1.96$.

To get the 95% confidence interval on the projected maximum live load effect L_{max}, follow Step 12.2.1 but use the upper and lower limits of the cumulative frequency p_i rather than the value obtained directly from the WIM data. The evaluating engineer should decide whether the resulting confidence interval L_{max} are sufficiently narrow. If the intervals are not adequate, more WIM data should be collected to further narrow the intervals.

STEP 6   GENERALIZED MULTIPLE-PRESENCE STATISTICS FOR TRUCKS AS A FUNCTION OF TRAFFIC VOLUME.

In many spans, the maximum lifetime truck-loading event is the result of more than one vehicle on the bridge at a time. Refined time stamps are critical to the accuracy of MP statistics. Accurate multiple presence data requires time stamps of truck arrival times to the hundredth of second. Many states typically report arrival times to the nearest second. A time stamp which records to the nearest second could result in an error of over a truck length for trucks traveling at highway speeds. With time stamps recorded to the nearest hundredth-of-a-second headway separations will be accurate to within a foot. As noted, multiple-presence statistics need not be developed for each site as there is a correlation between multiple presence and ADTT. There may also be a correlation between MP and the functional class of the highway. Higher MP probabilities may be more likely at urban WIM sites due to slower traffic speeds and increased congestion.

Multiple presence statistics are mostly transportable from site to site with similar truck traffic volumes and traffic flow. A single WIM site can provide multiple presence data for varying ADTT values due to daily variation in ADTT. In this study, few sites with large quantities of continuous WIM data that include refined time stamps to a resolution of 0.01 second or better were investigated. A relationship between MP and traffic volume was developed to utilize the MP values from national data to any given site without performing a site-specific analysis. Where accurate time stamps are not available multiple presence events may be evaluated using MP statistics from other sites with similar traffic conditions and functional classifications. MP statistics are obtained as a function of headway separation for side-by-side and following trucks.

Definitions:

- Headway: the distance between front axles of side-by-side trucks.
- Gap: the distance between the rear axle of the first truck and the first axle of the following truck. If the gap exceeds the span length, then there is no multiple-presence on the bridge span.
- Light Volume: ADTT ≤ 1000
- Average Volume: 1000 < ADTT ≤ 2500
- Heavy Volume: 2500 < ADTT ≤ 5000
- Very Heavy Volume: ADTT > 5000

Trucks can occur on a bridge in many different arrangements. Five loading patterns are defined as follows:

Single   -- only one truck is present on the bridge in any lane.
Following   – two trucks in the same lane, with varying headway distances with a gap less than the span length.
Side-by-Side -- two trucks in adjacent lanes with an overlap of more than one-half the truck length of the first truck.
Staggered   -- two trucks in adjacent lanes with an overlap of less than one-half the truck length of the first truck and a gap less than the span length (Figure 15)
Multiple   --- Simultaneous presence of trucks in adjacent lanes and in same lane
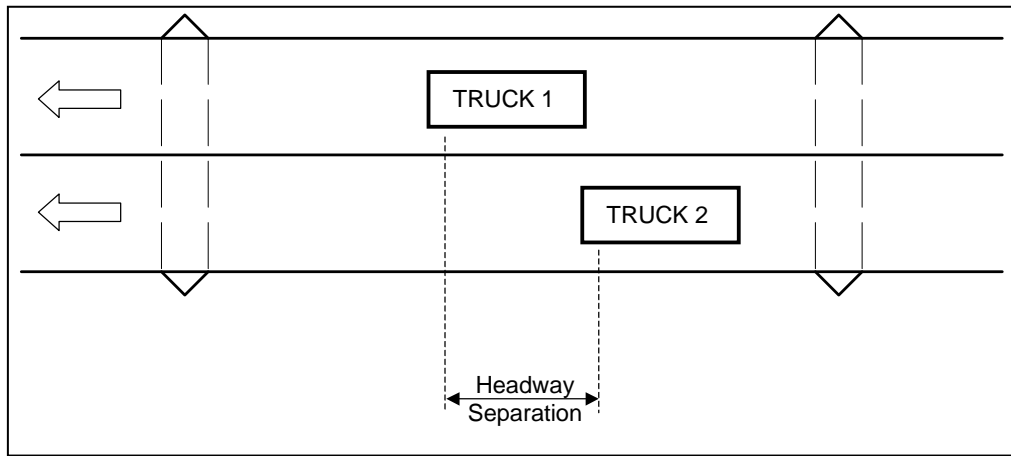
Figure 15 Staggered Truck Event with Overlap Less than One-Half Truck Length

For each WIM site with refined time stamp data, the cumulative frequencies for side-by-side, staggered and following events are obtained for headway separation from 0 ft. to 300 ft. in 20 ft increments. Report MP probabilities for each day for each site as a function of daily truck count and headway separations or gap. For each site the daily truck count will vary by day of week and by season. The study needs to be repeated for multiple WIM sites in several states with varying ADTTs (including very high ADTT > 5000) and on routes with a variety of functional classes. With a large dataset of MP statistics as a function of ADTT and highway class, guidelines for appropriate MP values for system-wide use may be developed.

To calculate and report multiple presence percentages, use the following procedure:

- For each site, each direction, lump all days with light volume (daily truck counts ≤ 1000) into one bin. Find the average MP for each gap increment.
- For each site, each direction, lump all days with Average volume (daily truck counts > 1000 but ≤ 2500) into one bin. Find the average MP for each gap increment.
- For each site, each direction, lump all days with Heavy volume (daily truck counts > 2500 but ≤ 5000) into one bin. Find the average MP for each gap increment.
- For each site, each direction, lump all days with Very Heavy volume (daily truck counts > 5000) into one bin. Find the average MP for each gap increment.

Tabulate and chart the variation of MP as a function of gap and traffic volume (light, average, heavy and very heavy).

Multiple-Presence Data from Published Literature (New Jersey WIM Sites)

Multiple truck presence (MP) statistics based on actual truck load data from New Jersey (NJ) highways is available in the published literature (Gindy, M. and Nassif, H. (2006)). The data consist of WIM measurements from various sites located throughout New Jersey and recorded over an 11-year period, between 1993 and 2003 (with some gaps). The database included twenty-five (25) sites which are geographically dispersed across NJ and which constitute a variety of functional classes including rural and urban principal and minor arterials. The sites represent a variety of site-specific conditions including truck volume, road and area type, and number of lanes. The study did not include heavy truck traffic sites with ADTT > 5000. Timestamps of truck arrivals to the hundredth of a second were recorded. Statistics for various truck loading cases including single, following, side-by-side, and staggered are presented (see Fig. 16).
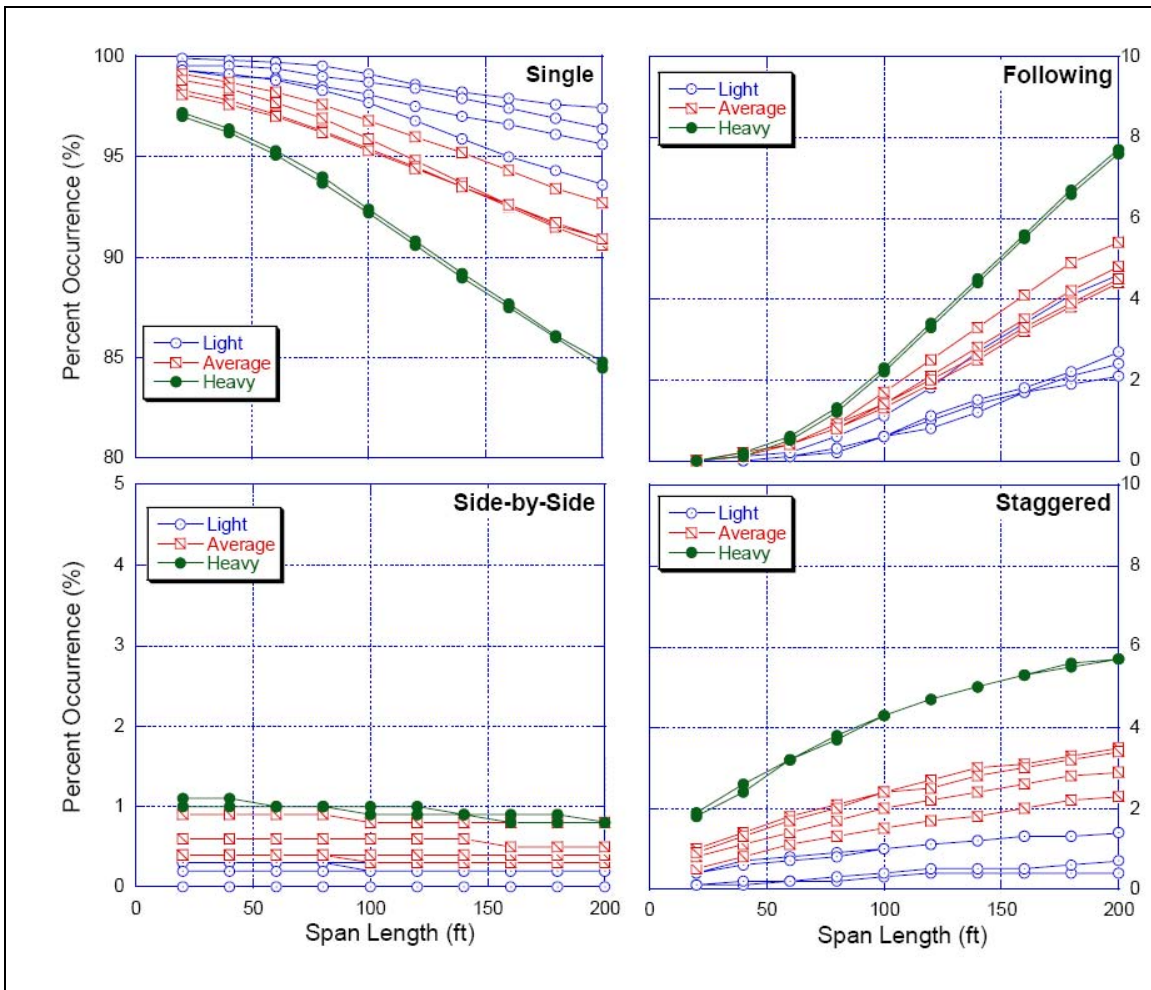
Figure 16   Variation of Multiple-Presence with Span Length – NJ WIM Sites

Multiple truck presence statistics depend on factors such as truck volume, and bridge span length. The position of all trucks in the near vicinity were checked to determine whether multiple trucks simultaneously occur on the bridge The statistics shown below in Table 13 for multiple truck occurrences were extracted from Fig. 16 for various truck volumes and span lengths. As the paper

did not provide a tabulation of MP statistics, the values are close approximations scaled from the charts. Use a linear interpolation for other spans.

Table 13 Maximum Observed Multiple Presence Probabilities as a Function of ADTT and Bridge Span Length – NJ Sites

Maximum Side-by-Side Trucks Percent Probabilities				
	Site Truck Traffic			
Span	Light: ADTT ≤ 1000	Average: 1000 < ADTT ≤ 2500	Heavy: 2500 < ADTT ≤ 5000	Very Heavy ADTT > 5000
All Spans	0.30	0.90	1.00	

Maximum Staggered Trucks Percent Probabilities				
	Site Truck Traffic			
Span	Light: ADTT ≤ 1000	Average: 1000 < ADTT ≤ 2500	Heavy: 2500 < ADTT ≤ 5000	Very Heavy ADTT > 5000
20	0.40	1.20	1.90	Not Available
40	0.60	1.60	2.30	Not Available
60	0.70	1.80	3.20	Not Available
80	0.80	2.00	3.80	Not Available
100	0.90	2.40	4.20	Not Available
120	1.00	2.60	4.60	Not Available
160	1.20	3.20	5.20	Not Available
200	1.40	3.60	5.90	Not Available

Maximum Following Trucks Percent Probabilities				
	Site Truck Traffic			
Span	Light: ADTT ≤ 1000	Average: 1000 < ADTT ≤ 2500	Heavy: 2500 < ADTT ≤ 5000	Very Heavy ADTT > 5000
20	0.00	0.00	0.00	Not Available
40	0.00	0.00	0.10	Not Available
60	0.10	0.50	0.60	Not Available
80	0.60	1.00	1.20	Not Available
100	1.20	1.80	2.20	Not Available
120	1.80	2.40	3.40	Not Available
160	3.40	4.00	4.80	Not Available
200	4.40	5.40	7.80	Not Available

Multiple-Presence Data from Current Research (New York WIM Sites)

By studying the occurrence of multiple trucks within a given headway separation at WIM sites with accurate time stamps, the effects of multiple trucks on a span can be simulated for WIM sites without accurate time stamps. Five WIM sites (ten directional sites) with free-flowing traffic in New York State were studied by the 12-76 Research Team in order to determine the maximum multiple presence probabilities for various truck traffic volumes. The sites chosen were Route 12 east bound and west bound (WIM site 2680), a rural state route, I-84 east bound and west bound (WIM sites 8280 and 8382), a rural interstate, I-81 north bound and south bound (WIM site 9121), a rural interstate, and Route 17 north bound and south bound (WIM site 9631), a rural state route. Two WIM sites on urban interstates (I-95and I-495) were studied, but not included in the results due to frequent traffic congestion which precludes free flowing traffic. Daily truck traffic volume was classified as light (less than 1000 trucks per day), average (more than 1000 trucks but less than 2500 trucks per day), heavy (more than 2500 trucks but less than 5000 trucks per day), and very heavy (more than 5000 trucks per day).

When considering multiple trucks on a given span, a multiple presence event is said to have occurred if the gap between two trucks, that is the distance between the last axle of the leading truck and the first axle of the trailing truck, is less than the span length. For instance, two trucks with a headway separation $H \leq 100$ ft will be simultaneously on span of length = 100' – truck length. Multiple presence probabilities were compiled for two trucks in adjacent lanes side-by-side, two trucks in adjacent lanes staggered, and two trucks in the same lane. For the purpose of simulating a multiple presence event, only the headway separation, that is the distance from the front axle of the lead truck to the front axle of the trailing truck, is important. Multiple presence probabilities were compiled for headway separations up to 300 feet, in 20-foot increments (Table 14).

For each day that truck data was captured at a WIM site, the number of multiple presence events that occurred in that day is recorded as a percentage of the total truck count for that day. The average multiple presence percentage is then calculated for all days with light truck volume, average truck volume, heavy truck volume, and very heavy truck volume, respectively. Each direction of traffic was considered separately. The maximum multiple presence percentages are summarized in the following tables.

Multiple-presence data at NY WIM sites were calculated in the NCHRP 12-76 Project using the same approach as the NJ statistics, to allow a direct comparison. The findings from the two states for side-by-side and staggered truck occurrences are quite comparable across most span lengths. The NJ values for following trucks are generally higher. The NY findings, defined in terms of headway separation intervals (Table 15), will be used in the interim to simulate multiple-presence events for sites where accurate time stamps are not available. This is achieved by categorizing the likelihood of trucks occupying various slots or headway intervals on the bridge either in the adjacent lane or in the same lane.

Table 14 Maximum Observed Multiple Presence Cumulative Probabilities as a Function of Headway Separation and ADTT – NY Sites

Maximum Side-by-Side Truck Multiple Presence Cumulative Probabilities				
Headway H (ft)	Site Truck Traffic			
	Light: ADTT < 1k	Average: 1k < ADTT < 2.5k	Heavy: 2.5k < ADTT < 5k	Very Heavy: ADTT > 5k
H ≤ 20	0.19	0.41	0.61	0.00
H ≤ 40	0.33	0.84	1.27	0.00
H ≤ 60	0.54	1.25	1.95	0.00
H ≤ 80	0.80	1.60	2.57	0.00
H ≤ 100	1.00	2.13	3.33	0.00
H ≤ 120	1.21	2.54	4.14	0.00
H ≤ 140	1.45	2.88	4.80	0.00
H ≤ 160	1.62	3.18	5.41	0.00
H ≤ 180	1.80	3.47	5.97	0.00
H ≤ 200	1.99	3.73	6.49	0.00
H ≤ 220	2.09	3.97	6.97	0.00
H ≤ 240	2.23	4.21	7.42	0.00
H ≤ 260	2.35	4.43	7.85	0.00
H ≤ 280	2.49	4.64	8.26	0.00
H ≤ 300	2.60	4.84	8.66	0.00

Maximum Following Truck Multiple Presence Cumulative Probabilities				
Headway H (ft)	Site Truck Traffic			
	Light: ADTT < 1k	Average: 1k < ADTT < 2.5k	Heavy: 2.5k < ADTT < 5k	Very Heavy: ADTT > 5k
H ≤ 20	0.00	0.00	0.00	0.00
H ≤ 40	0.00	0.00	0.00	0.00
H ≤ 60	0.01	0.00	0.00	0.00
H ≤ 80	0.02	0.00	0.00	0.00
H ≤ 100	0.08	0.04	0.03	0.00
H ≤ 120	0.20	0.19	0.19	0.00
H ≤ 140	0.41	0.52	0.64	0.00
H ≤ 160	0.77	1.09	1.37	0.00
H ≤ 180	1.25	1.76	2.28	0.00
H ≤ 200	1.71	2.51	3.26	0.00
H ≤ 220	2.22	3.19	4.20	0.00
H ≤ 240	2.70	3.86	5.11	0.00
H ≤ 260	3.12	4.51	5.98	0.00
H ≤ 280	3.53	5.11	6.83	0.00
H ≤ 300	3.92	5.70	7.63	0.00

Table 15 Maximum Observed Multiple Presence Probabilities by Headway Interval as a Function of ADTT – NY Sites

Maximum MP Probabilities based on 5 WIM sites (10 directional sites) in New York State				
Maximum Side-by-Side Truck Multiple Presence Probabilities				
	Site Truck Traffic			
Headway H (ft)	Light: ADTT ≤ 1k	Average: 1k < ADTT ≤ 2.5k	Heavy: 2.5k < ADTT ≤ 5k	Very Heavy: ADTT > 5k
H ≤ 20	0.19	0.41	0.61	0.00
20 < H ≤ 40	0.14	0.43	0.66	0.00
40 < H ≤ 60	0.21	0.41	0.68	0.00
60 < H ≤ 80	0.26	0.35	0.62	0.00
80 < H ≤ 100	0.20	0.53	0.76	0.00
100 < H ≤ 120	0.21	0.41	0.81	0.00
120 < H ≤ 140	0.24	0.34	0.66	0.00
140 < H ≤ 160	0.17	0.30	0.61	0.00
160 < H ≤ 180	0.18	0.29	0.56	0.00
180 < H ≤ 200	0.19	0.26	0.52	0.00
200 < H ≤ 220	0.10	0.24	0.48	0.00
220 < H ≤ 240	0.14	0.24	0.45	0.00
240 < H ≤ 260	0.12	0.22	0.43	0.00
260 < H ≤ 280	0.14	0.21	0.41	0.00
280 < H ≤ 300	0.11	0.20	0.40	0.00

Maximum Following Truck Multiple Presence Probabilities				
	Site Truck Traffic			
Headway H (ft)	Light: ADTT ≤ 1k	Average: 1k < ADTT ≤ 2.5k	Heavy: 2.5k < ADTT ≤ 5k	Very Heavy: ADTT > 5k
H ≤ 20	0.00	0.00	0.00	0.00
20 < H ≤ 40	0.00	0.00	0.00	0.00
40 < H ≤ 60	0.01	0.00	0.00	0.00
60 < H ≤ 80	0.01	0.00	0.00	0.00
80 < H ≤ 100	0.06	0.04	0.03	0.00
100 < H ≤ 120	0.12	0.15	0.16	0.00
120 < H ≤ 140	0.21	0.33	0.45	0.00
140 < H ≤ 160	0.36	0.57	0.73	0.00
160 < H ≤ 180	0.48	0.67	0.91	0.00
180 < H ≤ 200	0.46	0.75	0.98	0.00
200 < H ≤ 220	0.51	0.68	0.94	0.00
220 < H ≤ 240	0.48	0.67	0.91	0.00
240 < H ≤ 260	0.42	0.65	0.87	0.00
260 < H ≤ 280	0.41	0.60	0.85	0.00
280 < H ≤ 300	0.39	0.59	0.80	0.00

STEP 7   **PROTOCOLS FOR WIM DATA ANALYSIS FOR ONE-LANE LOAD EFFECTS FOR SUPERSTRUCTURE DESIGN (SINGLE EVENTS AND FOLLOWING EVENTS)**

Step 7.1   **Load Effects for Single Events for Superstructure Design**

a) Group data into bins by travel lane. Generate GVW relative and cumulative histograms for all trucks. Use 4 Kip bins.

b) Run the trucks (FHWA Class 6 and above – three or more axles) through moment and shear influence lines (or structural analysis program) for simple and two-span continuous spans. Use span lengths of: 20', 40', 60', 80', 100', 120', 160', and 200'.

c) Normalize maximum moment and shear values by dividing by the corresponding load effects for HL-93. Generate a database table of normalized load effects. Make sure that each record contains GVW, class, # of axles, date, arrival time, travel lane, in addition to load effects. The date, GVW and arrival time will serve as a truck record indicator.

Step 7.2   **Following Truck Events for Superstructure Design When Accurate Truck Arrival Time Stamps are Available**

Load effects for following trucks may be obtained directly from the WIM data where accurate time arrival stamps are collected together with truck weight data. The load effects analysis is performed with the following trucks in their proper relative positions.

       For estimating the maximum daily load effects for two random following trucks crossing the bridge as follows:

a) Combine the two trucks by superimposing the second truck on the truck first truck with the axles offset by the measured headway separation.
b) Run the combined truck through moment and shear influence lines for simple and two-span continuous spans. Use span lengths of: 20', 40', 60', 80', 100', 120', 160', and 200'.
c) Repeat the process for each following truck event.
d) Normalize the results by dividing by the effects of HL-93.

Step 7.3   **Simulation of Following Truck Events When Accurate Truck Arrival Time Stamps are not Available**

Load effects for following trucks may be obtained directly from the WIM data where accurate time arrival stamps are collected together with truck weight data. The load effects analysis is performed with the following trucks in their proper relative positions. Where accurate truck arrival time stamps are not available, generalized MP Statistics obtained in Step 6 may be used to simulate following trucks in their likely relative positions:

1. From Step 6, obtain the probabilities for following trucks in the same lane with varying headway separations (given in 20 ft increments) as a function of ADTT in each direction (see Table 15).

2. The number of expected multiple presence events in each direction for each headway separation interval, H, can be determined from the equation:

$$\text{Number of MP Events} = \text{MP Probability} \times \text{ADTT}$$

3. Randomly select two trucks from the entire population of trucks in the desired direction. Being that there is no correlation between the truck population and travel lane, any two randomly selected trucks can be considered, regardless of lane, as long as the trucks are traveling in the desired direction.

4. Randomly select a headway separation within the desired headway separation interval.

5. With the randomly selected truck pair separated by the randomly selected headway separation, maximum load effects can be calculated in the same manner as for trucks with accurate time stamps and measured headway separation (Step 7.2).

6. Repeat steps 3 through 5 for each headway separation interval and each direction of travel until the expected number of multiple-presence events have been generated for each headway separation and each direction of travel.

7. Normalize by dividing the results by the effects of HL-93 loading.

STEP 7.4   Group Load Effects into STRENGTH I and STRENGTH II (One-Lane)

Overloaded trucks seen in the WIM data could be either illegal overloads or authorized permit loads. It should be noted that separating permits from non-permit overloads in the WIM data is only viable where accurate permit records are available. In most jurisdictions only the special permit or single-trip permit moves are tracked in terms of their actual load configurations and travel routes. These heavy loads populate the upper tails of the load spectra and it would be beneficial to know which vehicles are authorized and which are illegal. Separating routine permits may not be possible due to the lack of necessary permit records at the state level and the sheer volume of permits in operation in most states. This is not considered a necessary requirement for live load modeling as routine permits can be taken as variations of the exclusion loads allowed under state law.

Legal loads and routine permits are grouped under STRENGTH I. Heavy special permits are grouped under STRENGTH II. For following events, if one of the trucks is a heavy special permit truck, group that loading event under STRENGTH II.

Step 7.5   Assemble Single-Lane Load Effects Histograms for STRENGTH I and STRENGTH II

a) Combine the normalized load responses of single truck events and following truck events into a single histogram for each load effect (M, V) and assemble in narrow bins of 0.02 increments for STRENGTH I and STRENGTH II. These combined histograms will represent the single lane load effects from a single truck or multiple trucks in the same lane.

b) These will constitute the single-lane measured load effects histograms without any filtering for WIM sensor errors (see Step 10).

STEP 8   **PROTOCOLS FOR WIM DATA ANALYSIS FOR TWO-LANE LOAD EFFECTS FOR SUPERSTRUCTURE DESIGN (SIDE-BY-SIDE & STAGGERED EVENTS)**

Step 8.1   **Truck Load Effects from Trucks in Adjacent Lanes Using Accurate Truck Arrival Time Stamps to the 1/100 th of a Second.**

a) Determine the number of truck multiple presence (MP) events where trucks are in adjacent lanes in each direction for each day. During a MP event there could be more than one truck in a lane.
b) For each multiple-presence (MP) event obtain the headway separation between trucks in adjacent lanes and in the same lane using the WIM data.
c) For estimating the maximum daily load effects for two random trucks simultaneously crossing the bridge, proceed as follows:

1. Combine the two trucks by superimposing the second truck in the adjacent lane on the truck first truck with the axles offset by the headway separation.
2. Run the combined truck through moment and shear influence lines for simple and two-span continuous spans. Use span lengths of: 20', 40', 60', 80', 100', 120', 160', and 200'.
3. Keep track of the normalized M and V
4. For each MP event, repeat the process

Step 8.2   **Simulation of Load Effects of Trucks in Adjacent Lanes Using Generalized MP Statistics.**

1. From Step 6, obtain the probabilities for side-by-side/staggered trucks in adjacent lanes with varying headway separations (given in 20 ft increments) as a function of ADTT in each direction (see Table 15).

2. The number of expected multiple presence events in each direction for each headway separation interval, H, can be determined from the equation:

Number of MP Events = MP Probability x ADTT

3. Randomly select two trucks from the entire population of trucks in the desired direction. Being that there is no correlation between the truck population and travel lane, any two randomly selected trucks can be considered, regardless of lane, as long as the trucks are traveling in the desired direction.

4. Randomly select a headway separation within the desired headway separation interval.

5. With the randomly selected truck pair separated by the randomly selected headway separation, maximum load effects can be calculated in the same manner as for trucks with accurate time stamps and measured headway separation (Step 8.1).

6. Repeat steps 3 through 5 for each headway separation interval and each direction of travel until the expected number of multiple-presence events have been generated for each headway separation and each direction of travel.

STEP 8.3   Group Load Effects into STRENGTH I and STRENGTH II (Two-Lane)

Overloaded trucks seen in the WIM data could be either illegal overloads or authorized permit loads. It should be noted that separating permits from non-permit overloads in the WIM data is only viable where accurate permit records are available. In most jurisdictions only the special permit or single-trip permit moves are tracked in terms of their actual load configurations and travel routes. These heavy loads populate the upper tails of the load spectra and it would be beneficial to know which vehicles are authorized and which are illegal. Separating routine permits may not be possible due to the lack of necessary permit records at the state level and the sheer volume of permits in operation in most states. This is not considered a necessary requirement for live load modeling as routine permits can be taken as variations of the exclusion loads allowed under state law.

Legal loads and routine permits are grouped under STRENGTH I. Heavy special permits are grouped under STRENGTH II. For multiple-presence events, if one of the trucks is a heavy special permit truck, group that loading event under STRENGTH II.

Step 8.4   Assemble Two-Lane Load Effects Histograms for STRENGTH I and STRENGTH II

a) Assemble normalized load effects frequency histograms for two-lane load effects for STRENGTH I and STRENGTH II in narrow bins of 0.02 increments

c) These will constitute the two-lane measured load effects histograms without any filtering for WIM sensor errors (see Step 10).

STEP 9   ASSEMBLE AXLE LOAD HISTOGRAMS FOR DECK DESIGN

Step 9.1   One-Lane Axle Loads for Deck Design

a) Separate trucks into STRENGTH I and STRENGTH II groups.
b) For each group, generate axle weight relative frequencies histograms for axle types: Single, Tandem, Tridem, and Quad axles. Use a 2 Kip interval for the bins. Axles spaced at less than 6 ft to be considered as part of the same axle group.

c) This will constitute the measured axle load histogram without any filtering for WIM sensor errors (see Step 10).

d) Assuming normal distribution models for axle weight data for the filtered histogram, determine the mean and standard deviation for: all axles, top 20% axles, top 5% axles. For each axle type report the 99th percentile statistic W_{99}.

Step 9.2   Side-by-Side Axle Events for Two-Lanes.

Multiple-presence studies specifically for axles loads are performed for the two-lane loaded case. There will be a greater probability of side-by-side axle events than side-by-side truck events, due to the fact that each truck has two or more axles. However, an axle with a headway separation greater than the effective strip width for the slab as defined in the LRFD Specifications would not have an influence on the load effect of the axle in the adjacent lane and may be neglected. With

these key differences recognized, the process for multiple-presence computations for axle loads will follow an approach similar to that used for truck multiple presence studies.

a) Determine the number of side-by-side axle events in each direction for the following combinations:

- Single – Single
- Single – Tandem
- Tandem – Tandem
- Other

STEP 10   FILTERING OF WIM SENSOR ERRORS / WIM SCATTER FROM MEASURED HISTOGRAMS

The live load modeling protocols presented in this project rely on the weight histograms and the histograms of the corresponding load effects as collected from Weigh-In-Motion stations at various highway sites.   Current WIM systems are known to have certain levels of random measurement errors that may affect the accuracy of the load modeling results. This section proposes an approach to filter out WIM measurement errors from the collected WIM data histograms.   To execute the filtering process, a calibration of the results of the WIM system should be made by comparing the results of the WIM system to those of a static scale.   The calibration process should be repeated several times within the WIM data collection time frame. The results of this calibration will be the basis for filtering out WIM measurement errors for each WIM data site.

10.1   WIM System Calibration

Typical WIM calibration procedures consist of taking several WIM measurements from representative calibration trucks and compare the WIM measurements to those obtained from a certified static scale.   Traditionally, it has been common to use a single truck for the calibration process although it would be advisable to use different trucks having different characteristics to ensure that the accuracy of the results remain consistent independent of the truck characteristics. As an example, Table 16 gives a summary sheet of the calibration data assembled for the northbound lane of site No. 7100 on I-87 in New York. The table shows the actual axle weight along with the weights estimated from the piezo-loop WIM system installed at the site. The WIM data was collected for 10 different crossings of the same calibration truck.   The truck's speeds were approximately 40 mph. Table 17 shows the ratio of the WIM weight divided by the actual weight for each of the 5 axles for the 10 crossings. The average of the ratios from all the 50 measurements is 0.97 with a standard deviation of 10%.   The plot in Figure 17 of WIM error versus axle weight demonstrates that the correlation between the bias value and the axle weight is practically negligible.   There appears to be a difference in the standard deviations as the axle weights change. However, more data is needed to analyze this trend more accurately. Similarly, it is not clear why the readings for axles 2 and 3 (or axles 4 and 5), which respectively have somewhat similar weights, are leading to large differences in their standard deviations.

Table 16 Typical WIM calibration results for NY State DOT installations.

SITE: ___7100___   LOCATION: I87 Champlain Exit 42 Rt 11 (BIN 1009070) - Acc Rt 9

DATE: 5/25/2006

			Lane: 1 Northbound											
	Sensor configuration Piezo-Loop_Piezo				Contract#/Sales Order									
		Drive				Trailer			60-ft					
	Steer	2nd Axle	3rd Axle	Total	4th Axle	5th Axle	Total	GVW	Moment	Axle 1-2	Axle 2-3	Axle 3-4	Axle 4-5	Length
Actual	12.61	16.10	15.85	31.95	20.28	18.75	39.03	83.58	275.37	12.83	4.50	37.25	4.13	58.71
Pass	1st Axle	2nd Axle	3rd Axle	Total	4th Axle	5th Axle	Total	GVW	Moment	Axle 1-2	Axle 2-3	Axle 3-4	Axle 4-5	Length
1	11.60	17.20	14.20	31.40	21.70	19.30	41.00	84.0	287.2	12.3	4.6	37.3	4.10	58.30
2	11.90	14.10	14.40	28.50	17.90	18.40	36.30	76.7	254.3	12.3	4.6	37.2	4.00	58.10
3	10.20	14.20	15.00	29.20	28.00	19.00	47.00	86.4	332.2	12.8	4.5	37.1	4.00	58.40
4	11.50	15.70	14.30	30.00	21.50	17.60	39.10	80.6	275.2	12.80	4.50	37.20	4.00	58.50
5	12.50	18.20	15.50	33.70	17.00	19.30	36.30	82.5	288.3	12.8	4.5	37.2	4.00	58.50
6	12.70	13.90	15.60	29.50	21.20	19.20	40.40	82.6	283.7	12.8	4.6	37.3	4.00	58.70
7	12.80	19.00	17.00	36.00	18.00	17.50	35.50	84.3	292.8	16.7	4.4	33.2	4.10	58.40
8	11.20	16.20	13.80	30.00	23.10	20.20	43.30	84.5	303.8	12.8	4.6	37.2	4.10	58.70
9	11.80	15.90	14.40	30.30	21.00	19.20	40.20	82.3	281.6	12.8	4.5	37.2	4.10	58.60

Table 17. WIM errors expressed as a ratio of measured values over actual values.

Pass	1st Axle	2nd Axle	3rd Axle	4th Axle	5th Axle	Moment on 60-ft span			
1	0.92	1.07	0.90	1.07	1.03	1.04			
2	0.94	0.88	0.91	0.88	0.98	0.92			
3	0.81	0.88	0.95	1.38	1.01	1.21			
4	0.91	0.98	0.90	1.06	0.94	1.00			
5	0.99	1.13	0.98	0.84	1.03	1.05			
6	1.01	0.86	0.98	1.05	1.02	1.03			
7	1.02	1.18	1.07	0.89	0.93	1.06			
8	0.89	1.01	0.87	1.14	1.08	1.10			
9	0.94	0.99	0.91	1.04	1.02	1.02			
10	0.97	0.86	0.97	0.96	0.97	0.96	Overall	Axle	Moment
Average	0.94	0.98	0.94	1.03	1.00	1.04	Average	0.97	1.04
Stdev	0.062	0.116	0.059	0.157	0.046	0.078	Stdev	0.100	0.078
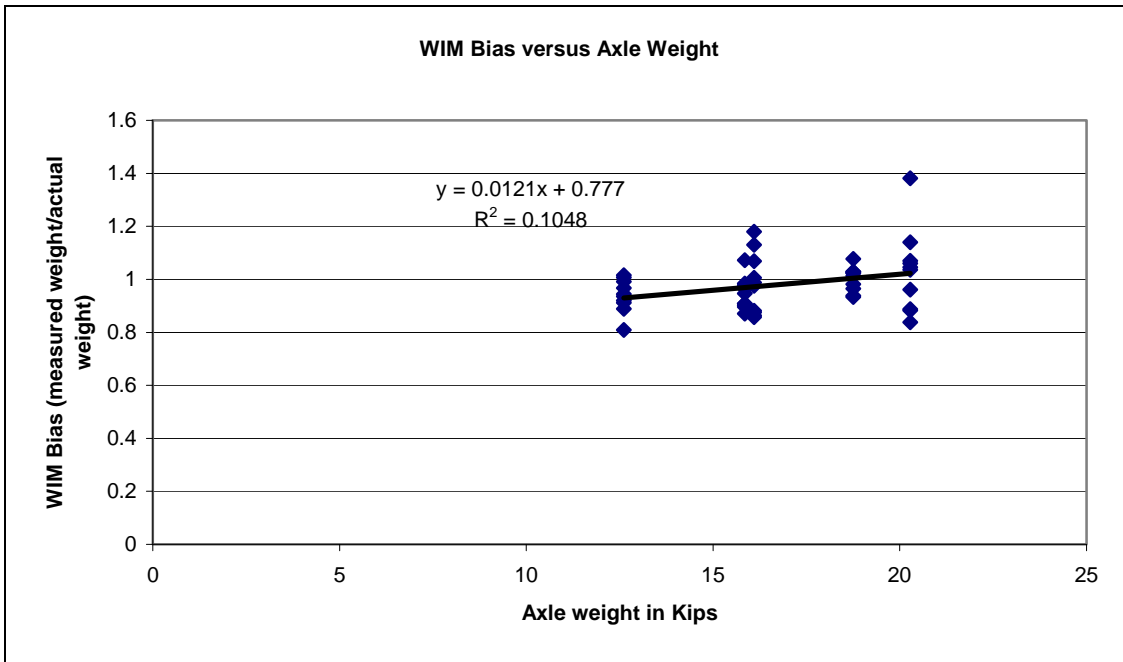
Figure 17   Plot of WIM error ratio versus axle weight for I-84 site

Axle weight histograms are needed for modeling the live loads for deck design, while the design of main bridge members requires the maximum bending moment and shear force effect. Thus, for main bridge members, it is more important to study the influence of WIM errors on the load effect rather than on the axle weights. Because main member load effects are influenced by the weight and spacing of several axles, some of the axle weight errors will cancel out and thus the overall error may have a lower standard deviation than that for individual axles. For example, for the calibration data of the same I-87 site studied above, the maximum moment effect of the calibration truck for a 60-ft simple span beam would be equal to 275.4 kip-ft, if the actual axle weights and axle spacings were used. The maximum moment effect for the values obtained from the eighth pass would be 303.8 kip-ft. The maximum moment from the 10 different passes are provided in Table 16 showing an overall average error ratio of 1.04 and a standard deviation of 7.8%.   These are compared to an average error of 0.97 and a standard deviation of 10% for the axle weights. The information provided in Table 16 can be used to filter out the errors from the axle weight and moment effect histograms as described in the next section.

The variation of the ratio with each truck crossing indicates that the measured axle weight to actual axle weight ratio is a random variable designated as ε with a mean value of 0.97 and a standard deviation of 10% for this particular site. Figure 18, shows a plot of the axle error ratio data on a Normal probability plot. With only one exception, all the data lies within the 95% confidence levels indicating that the data can be reasonably well represented by a Normal probability distribution function. This information will be required to execute the WIM error filtration as will be discussed in the next section. In the following we are assuming that these results are valid for all the trucks collected at the WIM sites independent of truck type, vehicle speed and time at which the WIM measurements were taken.   A sensitivity analysis is the performed in Appendix E to study how the standard deviation of the error would affect the results.
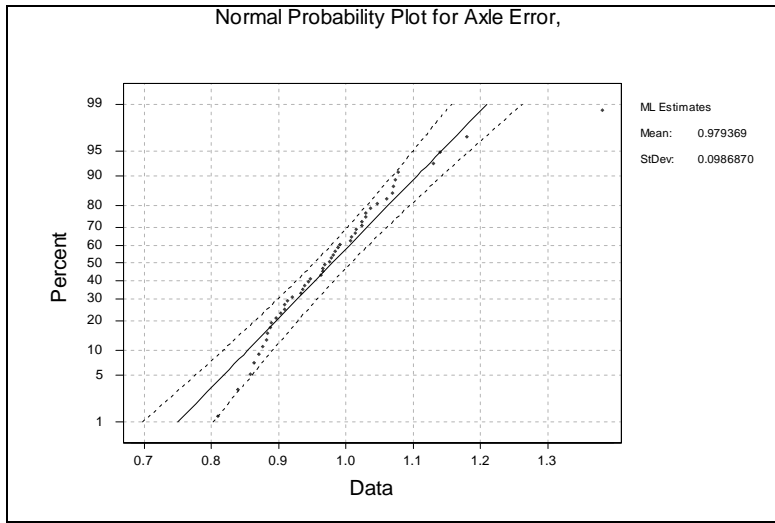
Figure 18   Plot of WIM axle error ratio on Normal Probability Plot.

10.2   WIM Error Filtration Procedure

Let us assume that the actual weight of an axle, or the actual moment effect of a truck, is denoted by x_r, while the measured value using the WIM system is x_m.   Because of WIM system measurement errors, the difference between the measured value and the actual value can be represented by a calibration factor or an error ratio, ε. Because the error may depend on various random factors related to the WIM system's characteristics and truck/structure/WIM system dynamic interaction as well as some truck features including tire size and pressure, the calibration factor ε is a random variable that relates the measured WIM data results to the "true" weight through the equation:

$$x_m = x_r \varepsilon \tag{16}$$

If the histogram and statistical information for ε are obtained from the calibration of the WIM system, these statistics can be used to filter out the errors in the measured raw WIM truck weight histogram collected at a given site. Our goal then is to obtain the histogram of x_r given that the measured data give the histogram of x_m and given the statistics of ε using the equation:

$$x_r = \frac{x_m}{\varepsilon} \tag{17}$$

Since the error ε varies randomly, it will not be possible to obtain x_r for each particular truck. Instead, an algorithm can be developed to obtain a histogram for all the actual truck weights given the histogram of the measured weights and the probability distribution of the error ratio ε.

The WIM data collected at a site will produce a histogram for x_m which can be related to the probability distribution function of x_m represented by $f_{xm}(\ldots)$.

Similarly, the calibration of the WIM system will provide information on the distribution function of ε represented by $f_\varepsilon(\ldots)$. For example, the WIM calibration of the I-84 NB lane 4 indicates that the error of the WIM system axle weights can be modeled as a Normal probability

65

distribution with a probability function $f_\varepsilon(\varepsilon)$ with mean value $\bar{\varepsilon} = 0.97$ and a standard deviation $\sigma_\varepsilon = 0.10$.

Since x_r is the ratio of two random variables with known probability distribution functions, the probability distribution function of the actual weight x_r, $f_{xr}(\dots)$, can be obtained using the expression (Ang & Tang 2007):

$$f_{X_r}(z) = \int_{-\infty}^{\infty} |y| f_{X_m,\varepsilon}(zy, y)\,dy \qquad (18)$$

The analysis of the correlation of the error with the actual magnitude of the axle weight, as illustrated in Figure 17, has shown that they are practically independent i.e. the percent error does not depend on the magnitude of the actual truck weight. One should note however, that the number of readings is limited to those of a single truck. Actual statistics for ε should be obtained from runs of different trucks at normal highway speeds. If one assumes that the measured truck weight x_m and the error ε are also independent random variables, then Equation 18 can be expanded as:

$$f_{X_r}(z) = \int_{-\infty}^{\infty} |y| f_{X_m}(zy) f_\varepsilon(y)\,dy \qquad (19)$$

10.3   WIM Error Filtration Algorithm

The integration of Equation 19 can be executed numerically using a simple algorithm so that the integration is changed into a simple summation and the equation can be represented as:

$$f_{X_r}(z) = \sum_{\text{all values of } \varepsilon=y} |y| f_{X_m}(zy) f_\varepsilon(y) \Delta y \qquad (20)$$

Recalling that the probability distribution functions of ε, x_r, and x_m are related to the histograms by:

$$H_\varepsilon(y) = f_\varepsilon(y)\Delta y$$
$$H_{x_r}(z) = f_{x_r}(z)\Delta z \qquad (21)$$
$$H_{x_m}(zy) = f_{x_m}(zy)\Delta(zy)$$

where $\Delta(\dots)$ is the bin size for each histogram. If the bin sizes for the histogram of the actual weight x_r and that of the measured weight x_m are taken to be the same, so that $\Delta z = \Delta(zy)$, then Equation 20 can be expressed as:

$$f_{X_r}(z)\Delta(z) = \sum_{\text{all values of } \varepsilon=y} |y| f_{X_m}(zy)\Delta(z) f_\varepsilon(y)\Delta y \qquad (22)$$

$$H_{x_r}(z) = \sum_{\text{all values of } \varepsilon=y} |y| H_{x_m}(zy) f_\varepsilon(y)\Delta y \qquad (23)$$

Thus, given the histogram of the measured WIM data, x_m, and the probability distribution of the calibration factor, ε, the integration of Equation 19 for all possible values of $x_r=z$ can be executed numerically using software tools.

The protocols for calculating L_{max} should then be executed using the filtered histogram $H_{xr}(z)$.

Implementation of the above WIM Error Filtration Algorithm, based on NY calibration data, is given in Appendix E.

STEP 11   ACCUMULATED FATIGUE DAMAGE AND EFFECTIVE GROSS WEIGHT FROM WIM DATA

WIM data can be used to study the stress range produced by individual trucks on a bridge component. Damage accumulation laws such as Miner's rule can then be used to estimate the fatigue damage for the whole design period for the expected truck population at a site.

Obtain cumulative fatigue damage from WIM population and compare to LRFD fatigue truck (Fig. 19, 54 Kip gross weight) moments for each span. Use span lengths of: 20', 40', 60', 80', 100', 120', 160', and 200'. Determine fatigue damage adjustment factor K, defined as:

$$K \times M_{FT} = \left[\frac{\sum (M_i)^3}{\#Trucks} \right]^{1/3} \tag{24}$$

M_{FT} = Moment from LRFD fatigue Truck, includes 0.75 load factor
K = Fatigue Damage Adjustment factor
M_i = Moment range of trucks measured
Trucks = Total number of trucks measured.
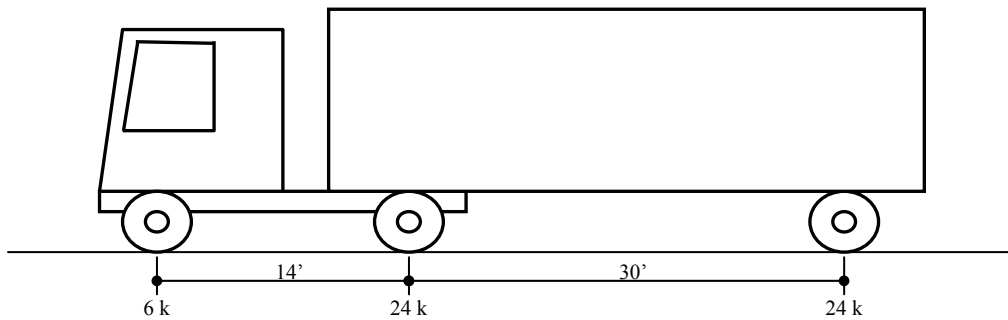
Figure 19   LRFD Design Fatigue Truck (54 Kips)

Obtain K for each span. For varying spans, determine the effective gross weight for trucks measured at the site using the Equation:

$$W_{eq} = \left(\sum f_i W_i^3 \right)^{1/3} \tag{25}$$

Where f_i is the fraction of gross weights within interval i, and W_i is the mid-width of interval i. In this calculation use trucks only with three or more axles (Class 6 and above).

STEP 12 **LIFETIME MAXIMUM LOAD EFFECT L$_{max}$ FOR SUPERSTRUCTURE DESIGN (STRENGTH I)**

Step 12.1 **Methods for Estimating Lmax**

In order to check the calibration of load models and/or load factors for a specification, it is necessary to estimate the mean maximum loading or load effect L$_{max}$. If further calibration of the Specification is to be carried out, the corresponding COV should also be found. The estimation of the maximum load effect L$_{max}$ expected over a 75-year bridge design period can be executed through a variety of methods. Simplified analytical methods or simulations may be used to estimate the maximum loading over a longer period, from short-term WIM data. This has to be done from a limited set of data that is collected for truck weights and truck configurations as well as truck traffic headways over relatively short periods of time. These methods can be categorized as:

a) Convolution or Numerical Integrations,
b) Monte Carlo Simulations,
c) Simplified Statistical Projections

The models require as input the WIM data collected at a site after being scrubbed for data quality and filtered for WIM errors as described in the previous steps. The design of bridges requires the estimation of the maximum load effect over periods of 75 years. The convolution method uses numerical integrations of the collected WIM data histograms to obtain projections of the expected maximum load effect within a given return period (e.g. 75-years). The WIM data collected cannot reasonably be accurate enough in the tail of the distributions to obtain good estimates of the parameters for such extended return periods. Hence, the only possible means to obtain the parameters of the distributions of the 75-year maximum load effect is by using statistical projections. The probability distribution of the maximum value of a random variable will asymptotically approach an extreme value distribution as the number of repetitions increases. Generally a Gumbel fit can be executed on the tail of the short-term maximums for statistical projections.

An alternative to the convolution approach consists of using a Monte Carlo simulation to obtain the maximum load effect. The Monte Carlo simulation uses random sampling from the collected data to obtain the maximum load effect. A Monte Carlo simulation requires the performance of an analysis a large number of times and then assembling the results of the analysis into a histogram that will describe the scatter in the final results. Each iteration is often referred to as a cycle. The process can be executed for the single lane-loading situation or the side-by-side loading. The Monte Carlo Simulation may be performed to find L$_{max}$ in one of two ways:

- Use the empirical histogram to find L$_{max}$ by simulation for a short period and then project for a longer period (use an extreme value distribution such as Gumbel distribution). As mentioned earlier, the probability distribution of the maximum value of a normal random variable will asymptotically approach the Gumbel distribution.

- Alternatively, use a smoothed tail end of the WIM histogram by fitting the tail with a known probability distribution function (such as the Normal distribution) and use that fitted distribution with the Monte Carlo simulation. This will require a very large number of repetitions.

It should be emphasized however, that the Monte Carlo simulation would be very inefficient for projections over long return periods when the number of repetitions are very high. (Algorithms such as Markov Chain Monte Carlo modeling may allow improved performance in such cases). Furthermore, one should make sure not to exceed the random number generation limits of the software used, otherwise the generated numbers will not be independent and the final results will be erroneous.

Simplified statistical projections for estimating the maximum load effect in a given return period can be developed based on the assumption that the tail end of the moment load effect for the original population of trucks as assembled from the WIM data approaches a Normal distribution. The method uses the properties of the extreme value distribution. Equations in closed form provide such a projection, requiring much less effort than the convolution approach. The estimation of the maximum load effect for two side-by-side trucks improves as the return period increases. This is again due to the asymptotic nature of the solution, which yields good results only as the number of load repetitions increases and as the sampling is made from the tail end of the raw WIM histogram.

Step 12.2 Procedure for calculating L_{max} from WIM data Using an Extreme Value Distribution for the Upper Tail

There are several possible methods available to calculate the maximum load effect for a bridge design period from truck WIM data. The one implemented in these protocols is found to be one of the easiest methods that provide results comparable to many other methods including Monte Carlo simulations. This method is based on the assumption that the tail end of the histogram of the maximum load effect over a given return period approaches a Gumbel distribution as the return period increases. The method assumes that the WIM data is assembled over a sufficiently long period of time to ensure that the data is representative of the tail end of the truck weight histograms and to factor in seasonal variations and other fluctuations in the traffic pattern. The use of WIM data for a whole year will satisfy this requirement. In a separate analysis this study will investigate how the confidence intervals in the projection results are affected by the number of samples collected and the number of days for which the WIM data is available, especially when only limited data is available at a site.

Sensitivity analyses have shown that the most important parameters for load modeling are those that describe the shape of the tail end of the truck load effects histogram. Current WIM technology has certain levels of random measurement errors that may affect the accuracy of the load modeling results. To bring uniformity in the load modeling process, a standardized approach to executing the error filtering procedure that utilizes calibration statistics for the WIM scale is described in Step 10. This procedure should be executed on the raw data prior to calculating $L_{max.}$

Step 12.2.1 Protocols for calculating maximum load effect L_{max}

The process begins by assembling the WIM truck weight data and load effects for single lane events and two-lane events and filtering the data for WIM sensor errors.

- Assemble the measured load effects histograms (moment effect or shear force effect) in narrow bins of 0.02 increments.

- Execute a statistical algorithm to filter out WIM scatter / sensor errors from the load effect s histograms as described in Step 10.

- Find the cumulative distribution function $F_x(x)$ = cumulative distribution function value for each event x sample by dividing the number of samples in a bin by the total number of samples and adding the value to the value in the previous bin.

- Calculate the standard deviate of the cumulative function for each bin. In MS EXCEL this can be achieved by taking NORMSINV(F(x)).

- Take the upper 5% of the values and plot the Normal deviate versus X.

- Take the trend line and find the slope, m, and the intercept, n, of the regression line.

- Find the mean of Normal that best fits the tail end of the distribution as μ_{event} = -n/m.

- Find the standard deviation of the best fit Normal to be σ_{event} = (1-n)/m- μ_{event}.

- Take the number of events per day, n_{day}

- Find, N, the total number of events for the return period of interest. For 75-years take N= n_{day}*365*75

- The most probable value, u, for the Gumbel distribution that models the maximum value in 75 years L_{max} is given as:

$$u_N = \mu_{event} + \sigma_{event} \times \left[\sqrt{2\ln(N)} - \frac{\ln(\ln(N)) + \ln(4\pi)}{2\sqrt{2\ln(N)}} \right] \qquad (26)$$

- The dispersion coefficient for the Gumbel distribution that models the maximum load effect L_{max} is given as:

$$\alpha_N = \frac{\sqrt{2\ln(N)}}{\sigma_{event}} \qquad (27)$$

- The mean value of L_{max} is given as:

$$L_{max} = \mu_{max} = u + \frac{0.577216}{\alpha_N} \qquad (28)$$

- Calculate the standard deviation of the Gumbel distribution that best models the maximum daily effect as:

$$\sigma_{max} = \frac{\pi}{\sqrt{6}\alpha_N} \qquad (29)$$

70

Step 12.3   Alternate Method for Calculating Maximum Load Effect L_{max} Using Monte-Carlo Simulation

An alternative to the statistical projections approach described in Step 12.2 consists of using a Monte-Carlo simulation to obtain the maximum load effect. If there are not enough multiple events recorded in the WIM data, one could utilize simulations to generate MP events that conform to the measured statistical MP probabilities. In this approach, results of WIM data observed over a short period can be used as a basis for projections over longer periods of time. It should be noted that the Monte-Carlo method for single-lane events will not be able to give L_{max} for 75-years directly. At best a one-week or a one-month maximum single event could be obtained from a year's worth of WIM data as the Monte-Carlo simulation will not go beyond the maximum value measured at the site. A statistical projection technique must then be executed to extend the single event results to 75 years. Alternatively, one can use the fitted Normal distribution to represent the tail end of the histogram rather than use the raw data histogram and then the projection is automatically performed by the simulation. The same is not true for the two-lane loading cases as the Monte-Carlo procedure will simulate more samples of side-by-side events based on the observed multiple-presence probabilities.

A Monte-Carlo simulation requires the performance of an analysis a large number of times and then assembling the results of the analysis into a histogram that will describe the scatter in the final results. The process can be executed for the single lane-loading situation or the side-by-side loading. Figure 20 gives a schematic representation of the Monte Carlo Simulation, which follows the procedure described in the following steps:

Truck in Lane 1   **Truck in Lane 2**
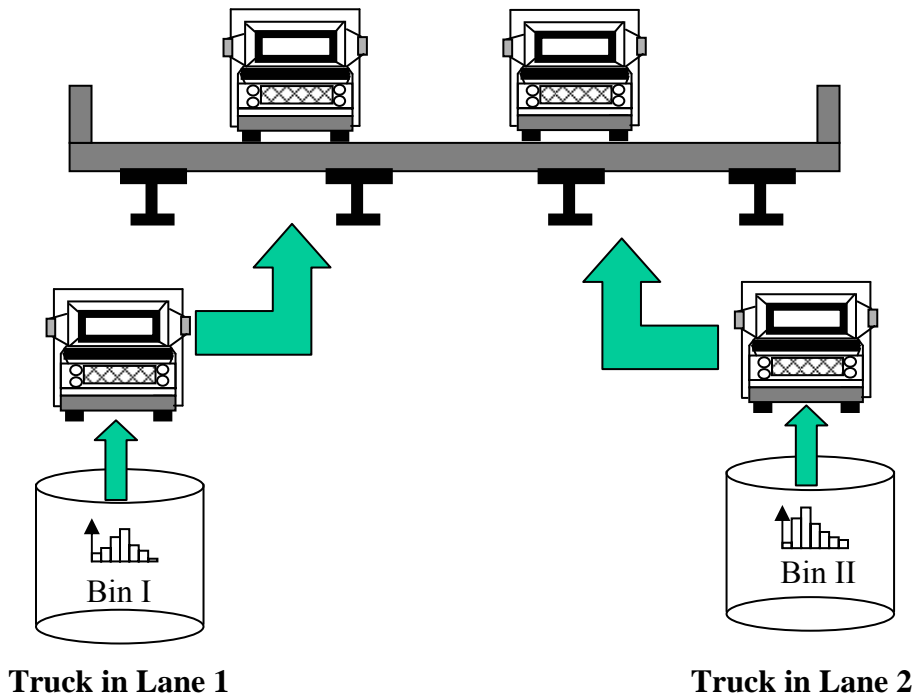
Figure 20   Schematic illustration of Monte Carlo simulation procedure.

1. Assemble the data representing the filtered load effects for the trucks in the drive lane into a histogram labeled Bin I in Figure 20.

2. Assemble the data representing the filtered load effects for the trucks in the passing lane into a histogram labeled Bin II in Figure 20.
3. Assemble the corresponding cumulative frequency curves for the two histograms.
4. Determine a main return period, t_{return}, for which the expected maximum moment is desired. For example, a one-week, one-month, a two-year, or a 75-year period may be selected. However, as noted earlier, it is unlikely that the sample size of the available WIM data will be sufficiently large to obtain results for the large return periods. Hence, it is expected that the process will be applicable for only short periods say a one-week or a one-month period the results of which can then be projected for longer periods using the extreme value projection. Alternatively, one can use the fitted Normal distribution to represent the tail end of the histogram rather than use the raw data histogram and then the projection is automatically performed by the simulation.
5. Use a uniform distribution random generator to produce a pseudo random number varying between 0 and 1. Such random generator routines are provided in all general-purpose computer software and programming tools (such as EXCEL, MATLAB).
6. The pseudo-random number of step 5 will serve to select a single value from Bin I representing the load effect of a truck arriving in the drive lane. The selection of the moment effect is executed by assuming that the pseudo-random number generated (call it ran_{1i}) represents the cumulative frequency of the moment for this truck. Thus, to find the value of the moment, X_{1i}, the cumulative distribution function needs to be inverted so that $X_{1i} = F_{x1}^{-1}(ran_{1i})$ where $F_{x1}^{-1}(...)$ is the inverse of the cumulative function for the effect of the trucks in the drive lane. (Figure 21).
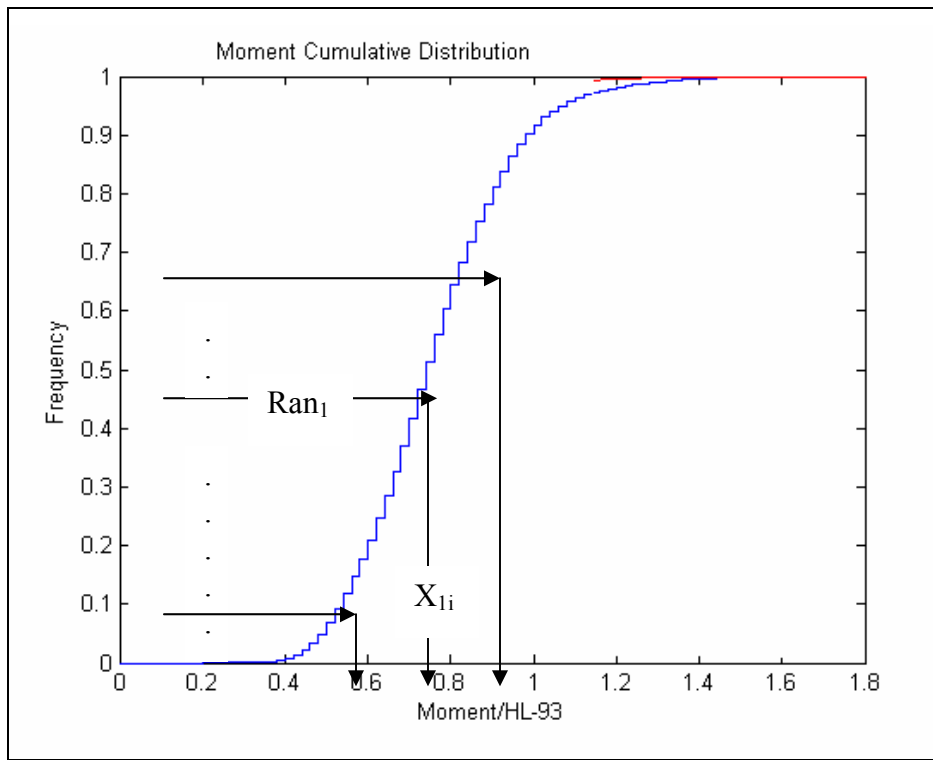
Figure 21 Schematic illustration of the random generation of a sample X_{1i}.

72

7. For estimating the maximum load effect for the trucks crossing the bridge in the drive lane, follow steps a through e, otherwise skip this step and go to step 8.

   a) Find the number of loading events in the drive lane, K_1, corresponding to the pre-selected return period t_{return}.
   b) Repeat steps 5 through 6 K_1 times to generate K_1 samples for the moments in the drive lane in the period t_{return}.
   c) Compare the K_1 values and choose the largest one of these. This will give you one estimate of the maximum expected value in t_{return}, which is designated as $X_{1mx\ K1}$.
   d) Repeat steps a through c for several cycles to generate several estimates of the maximum value $X_{1mx\ K1}$.
   e) Assemble the values collected in step d in a histogram. Also, find their average value and standard deviations.

8. For estimating the maximum response for two side-by-side trucks, do the following:

   a) Repeat steps 5 and 6 by generating a pseudo number ran_{2i}, which represents the cumulative frequency of the moment for trucks in the passing lane. Find the value of the moment, X_{2i}, by inverting the cumulative frequency, $F_{x2}(\ldots)$, for the load effects of the truck in the passing lane so that $X_{2i} = F_{x2}^{-1}(ran_{2i})$.
   b) Assuming that the maximum effect of the truck in the drive lane occurs at the same time that the maximum effect of the truck in the passing lane, add the moment effects of these two trucks to produce the moment effect of a single side-by-side event $X_{si}=X_{1i}+X_{2i}$.
   c) Repeat the process K_s times where K_s=number of side-by-side events expected in the basic return period t_{return}.
   d) Compare all the K_s moment effects $X_{s1} \ldots X_{sKs}$ and take the maximum value out of these K_s values. This will produce a single estimate of the maximum response corresponding to the basic return $X_{s\ max\ Ks}$.
   e) Repeat the whole simulation process m cycles to get m estimates of $X_{s\ max\ Ks}$.
   f) Obtain the histogram of the m estimates of $X_{s\ max\ Ks}$ and calculate the average value and standard deviation.

STEP 13   DEVELOP AND CALIBRATE VEHICULAR LOAD MODELS FOR BRIDGE DESIGN

Step 13.1   Superstructure Design live load Calibration (STRENGTH I)

There are two calibration methods that can be applied to calibrate a new live load model based on recent changes in truck weights:

  Method I: The first approach, which is relatively simple, is to focus on the mean or expected maximum live load variable, L_{max}. That is, assume that the present LRFD calibration and safety indices are adequate for the strength and load data then available, but update the load model or the load factor for current traffic conditions in a manner consistent with the LRFD calibration approach. One key assumption in this regard is that the site-to-site variability in L_{max} as measured by the COV (Coefficient of variation COV = STDEV/Mean) is the same as that used during the

AASHTO LRFD calibration. In AASHTO LRFD calibration, the overall live load COV was taken as 20%.

Method II: If the variability in the WIM data is much greater than that assumed in the calibration, then the entire LRFD calibration to achieve the target 3.5 reliability index may no longer be valid for that state and a simple adjustment of the live load factor as given above should not be done. The second approach, which is more robust, is to perform a reliability analysis using the new statistical data for live loads and determine the live load factors needed to achieve the same reliability target adopted in the LRFD calibration.

Method I: Simplified Adjustment of STRENGTH I Live Load Factor

The process adjusts the loading model and/or the corresponding live load factor by the ratio:

$$r_1 = \frac{L_{max} \text{ from WIM data projections for one-lane}}{L_{max} \text{ used in existing LRFD calibration for one-lane}} \tag{30}$$

$$r_2 = \frac{L_{max} \text{ from WIM data projections for two-lanes}}{L_{max} \text{ used in existing LRFD calibration for two-lanes}} \tag{31}$$

An increase in maximum expected live load based on current WIM data can be compensated in design by raising the live load factor in a corresponding manner. The basic steps are summarized as follows:

a) Obtain quality WIM data from a variety of jurisdictions and traffic conditions and Compute the expected lifetime maximum load, $L_{max,}$ for each data set for one-lane and for two-lane loadings
b) Compare L_{max} for a suite of bridges to this expected 75-year maximum load for a similar suite of bridges given by NCHRP 368.
c) Compute the average ratio, r (L_{max} WIM data, divided by L_{max} Ontario data) for one-lane and for two-lanes. Compute also the corresponding COV for all sites examined.
d) Adjust the design requirements by modifying the live load factor by the average ratio, r, as given above. If r is relatively uniform over the suite of bridges used to fix L_{max} then the HL-93 model can be maintained without adjustment. It is relatively easy to modify the live load factor γ_L but this cannot be done unless it applies to every span.

L_{max} Used in Existing LRFD Calibration

NCHRP Report 368 provides mean maximum moments and shears for various periods of time from one day to 75-years for simple span moments, shears and negative moments for continuous spans. Span lengths range from 10 ft to 200 ft (Table 18). Continuous spans are comprised of two equal spans. Continuous span positive moments and shears at the center pier have not been provided in the report. The maximum one lane load effect is caused either by a single truck or two or more trucks (with the weight smaller than that of the single truck) following behind each other. There was little data to verify statistical parameters for multiple presence. The maximum values of moments and shears were calculated by simulations. For two lane moments and shears, simulations indicated that the load case with two fully correlated side-by-side trucks will govern, with each truck equal to the maximum two-month truck. The ratio of the mean maximum 75-year moment (or shear) and a mean 2-month moment (or shear) is about 0.85 for all spans.

Table 18. L$_{max}$ Used in Existing LRFD Calibration

75-Year Lmax Used in LRFD Calibration (normalized by HL-93 load effects)						
Span (Ft)	75-Year Lmax					
	Simple Span Moment		Simple Span Shear		Negative moment	
	One-Lane	Two-Lane	One-Lane	Two-Lane	One-Lane	Two-Lane
20	1.30	2.12	1.23	2.12	1.27	2.28
40	1.35	2.34	1.23	2.18	1.30	2.40
60	1.32	2.30	1.23	2.22	1.25	2.30
80	1.32	2.28	1.27	2.26	1.21	2.24
100	1.31	2.26	1.28	2.28	1.20	2.22
120	1.29	2.24	1.22	2.20	1.20	2.22
160	1.24	2.18	1.20	2.14	1.20	2.22
200	1.23	2.16	1.17	2.08	1.20	2.22

Based on the above simple method, an increase in the maximum expected 75-year live load as estimated from current WIM data can be accounted for in the design equation by raising the live load factor in proportion to the ratio of the estimated live load projection from WIM data to the value used during the calibration of the AASHTO LRFD Specifications.

Method II   Reliability Analysis and Adjustment of STRENGTH I Live Load Factor

The simplified approach in Method I focuses on the maximum live load variable, L$_{max}$, assuming that the overall LRFD calibration, multiple presence factors, and target reliability indices are adequate. Hence, the approach only updates the load factors to better represent current truck traffic conditions. One key assumption in this regard is that the site-to-site variability in L$_{max}$ as measured by the COV (Coefficient of variation COV = STDEV/Mean) is the same as that used during the AASHTO LRFD calibration. In AASHTO LRFD calibration, the overall live load COV was taken as 20%. This 20% includes site-to-site variability, uncertainties in estimating the load distribution factors, uncertainties in estimating the dynamic allowance factor, the uncertainties in estimating L$_{max}$ due to the randomness of the parameter and the limitations in the data.

When implementing the draft protocols using recent WIM data in Task 8 from various States, it became evident that this procedure, while simple to understand and use, had certain limitations when applied to statewide WIM data. Using a single maximum or characteristic value for L$_{max}$ for a State would be acceptable if the scatter or variability in L$_{max}$ from site-to-site for the state was equal to (or less than to be conservative) the COV assumed in the LRFD calibration. If the variability in the WIM data is much greater than that assumed in the calibration, then the entire LRFD calibration to achieve the target 3.5 reliability index may no longer be valid for that state and a simple adjustment of the live load factor as given above should not be done. The site-to-site scatter in the L$_{max}$ values obtained from recent WIM data showed significant variability from span to span, state to state, and between one-lane and two-lane load effects as given in Table 19 for a sample set of states. For example, the data from Florida show a COV for the moments of simple span bridges under one-lane loadings that varies from 32.5% for the 20-ft simple spans to 22.3% for the 200-ft simple span. These COV's for site-to-site must be augmented by the COV's for the other variables that control the maximum load including within site variability, the effect of the Dynamic allowance factor, Load distribution factor, and WIM data sample size, leading to much higher overall COV for the live load than the 20% used during the AASHTO LRFD

calibration. For the same maximum moment of simple span bridges under one-lane loading, the site-to site variability for the data collected in California shows a COV that ranges between 19.3% for the 20-ft simple span bridges down to 5.9% for the 200-ft simple span bridges.

Table 19   Site-to-Site Variability in L_{max} Measured by Coefficient of Variation (COV)

State		Event Type	SPAN (ft)							
			20	40	60	80	100	120	160	200
	M-simple	1-Lane								
FL		COV	0.325	0.307	0.278	0.276	0.270	0.260	0.238	0.223
IN		COV	0.185	0.137	0.122	0.135	0.147	0.142	0.122	0.132
CA		COV	0.193	0.104	0.045	0.054	0.061	0.062	0.058	0.059
	M-simple	2-Lane								
FL		COV	0.201	0.187	0.213	0.213	0.207	0.207	0.206	0.212
IN		COV	0.150	0.139	0.132	0.125	0.116	0.113	0.116	0.119
CA		COV	0.112	0.125	0.136	0.146	0.133	0.126	0.121	0.113
	V-simple	1-Lane								
FL		COV	0.340	0.299	0.289	0.279	0.248	0.241	0.224	0.214
IN		COV	0.188	0.129	0.108	0.113	0.105	0.103	0.115	0.131
CA		COV	0.143	0.087	0.056	0.047	0.049	0.049	0.058	0.056
	V-simple	2-Lane								
FL		COV	0.203	0.204	0.205	0.183	0.174	0.175	0.180	0.189
IN		COV	0.140	0.119	0.122	0.133	0.134	0.136	0.135	0.140
CA		COV	0.109	0.127	0.137	0.120	0.113	0.112	0.107	0.109

Overall the results of Table 19 indicate that the Florida sites evidenced the highest variability in L_{max}, whereas California data was a lot more uniform. As shown by the data in Table 19, the site-to-site COV statistics alone for FL are greater than the overall live load COV used in the LRFD calibration. On the other hand, the site-to-site COV statistics for CA are lower. It should also be noted that the one-lane COV's for Florida are higher than the Two-lane COV, whereas in California the two-lane event have a higher site-to-site variability.

The maximum L_{max} values, site-to-site variability in L_{max} as well as the variability in one-lane vs. two-lane events are influenced by several factors that appear to be state-specific. These factors include:

1. The presence of exclusion vehicles that are state legal loads --- these heavy hauling vehicles usually operate mostly on state truck routes. There is likely to be a greater variation in truck weights on different routes in states with exclusion vehicles such as Florida. These heavy exclusion vehicles (and routine permits) may also be resulting in high L_{max} values for the one-lane loaded case. It should be noted that all trucks with six or fewer axles were grouped in the STRENGTH I calibration. This group included legal loads, exclusion loads, as well as non-flagged routine permits.
2. The load limit enforcement environment in a state will have an influence on the level of illegal overloading. For instance, California is known to have an effective truck weight monitoring (and enforcement) operation that effectively utilizes the network of weigh-in-motion systems throughout the state.
3. Site-to-site variability in truck weight data is also impacted by the quality and reliability of WIM data collected at the remote WIM sites. WIM data quality is highly dependant on the WIM quality assurance programs implemented by the State DOTs. Quality assurance programs must regularly check data for quality and require system repair or recalibration when suspect data is identified. Weighing accuracy is also sensitive to roadway conditions. Less variability in traffic data is expected when all WIM systems are maintained to the same standard of performance and data accuracy.

In order to incorporate the site-to-site statistical variations in WIM data collected in a given State, a reliability-based approach to adjusting the live load factors is proposed as described in this report.

RELIABILITY-BASED ADJUSTMENT OF LIVE LOAD FACTORS

AASHTO LRFD Background

The calculation of the L_{max} values is meant for use to adjust the live load factors in the LRFD design check equations. Since L_{max} is a random variable with high levels of uncertainties including site-to-site variability, the most appropriate procedure for adjusting the live load factor is by applying the principles of structural reliability. A reliability-based procedure for adjusting the live load factors would explicitly account for the variations in the L_{max} values as well as the other variables that control the loading of a bridge member and its capacity to resist the applied loads.

The variability in the L_{max} values are due to the random nature of L_{max} including the projection to the 75-year design life, the limitation in the data sample size collected within each site, and site-to-site variability. For developing a new design code, the L_{max} values for a wide range of nationally representative sites should be used as input. For adjusting the live load factors to reflect state-specific truck weights and truck traffic patterns, L_{max} values obtained from a representative sample of sites within the state should be used. This section illustrates how the reliability-based adjustment of the live load factor can be executed given a set of L_{max} values obtained from WIM data.

The LRFD design equation takes the form

$$\phi R_n \geq \gamma_{DW} D_W + \gamma_{DC} D_C + \gamma_L L_n \tag{32}$$

where ϕ and γ are the resistance and load factors, R_n is the nominal resistance, D_W is the dead load effect for wearing surface, D_C is the dead load effect for the components and attachments and L_n is the live load effect of the HL-93 load including dynamic allowance and load distribution factor. According to the LRFD specifications $\phi = 1.0$ for the bending moment capacities of steel and prestressed concrete members, $\gamma_{DW}=1.50$, $\gamma_{DC}=1.25$. The current live load factor is given as $\gamma_L=1.75$. The dynamic allowance factor is 1.33 times the truck moment effect and the load distribution factor is calculated as a function of span length and beam spacing for different numbers of loaded lanes. If the Weigh-In-Motion data in a particular state show large differences from the standard generic data used during the calibration of the AASHTO LRFD equations, it may be necessary to adjust the LRFD live load factor to maintain the same safety levels. The adjustment requires the modeling of the live load effects and the other random variables that control the safety of bridge members.

Modeling of Live Load Effect on a Single Beam

For bending of typical prestressed concrete and steel girder bridges loaded by one lane of traffic, the load distribution factor equation is given as (AASHTO, LRFD, 2007):

$$D.F. = 0.06 + \left(\frac{S}{14}\right)^{0.4} \left(\frac{S}{L}\right)^{0.3} \left(\frac{K_g}{12Lt_s^3}\right)^{0.1}$$

(33)

Where S is the beam spacing, L is the span length, t_s is the deck thickness, and K_g is a beam stiffness parameter. Note that Equation 33 already includes a multiple presence factor m=1.2 which accounts for the higher probability of having one heavy truck in one lane as compared to the probability of having two side-by-side heavy trucks in two adjacent lanes.

For two lanes loaded, the load distribution factor equation for bending becomes (AASHTO, LRFD, 2007):

$$D.F. = 0.075 + \left(\frac{S}{9.5}\right)^{0.6} \left(\frac{S}{L}\right)^{0.2} \left(\frac{K_g}{12Lt_s^3}\right)^{0.1}$$

(34)

Observing that the L_{max} values are for the normalized total static load effects on a bridge and observing that the D.F. of Equation 33 for a single lane already includes a multiple presence factor m=1.2, the final mean value for maximum load effect on a single beam can be calculated for one lane and two lanes loaded as:

For one lane $\quad \overline{LL} = L_{max\,beam} = L_{max} \times HL_{93} \times IM \times D.F. / 1.2$

(35)

For two lanes $\quad \overline{LL} = L_{max\,beam} = L_{max} \times HL_{93} \times IM \times D.F. / 2$

Dividing D.F. of one lane by 1.2 is done to remove the multiple presence factor, while dividing the D.F. of two lanes by 2 is done to account for the fact that the L_{max} values for two lanes calculated in this report are normalized by dividing by the effect of one lane of HL-93 loading

The COV of the maximum beam live load effect should account for the site-to-site variability represented by $V_{site-to-site}$, the variability within a site represented by $V_{projection}$, the uncertainty associated with the limited WIM data sample size represented by V_{data}, the variability in the dynamic amplification factor, V_{IM} and the variability in the load distribution factor V_{DF}. The final COV for the applied live load effect on a single beam can be obtained from:

$$V_{LL} = \sqrt{V_{site-to-site}^2 + V_{projection}^2 + V_{data}^2 + V_{IM}^2 + V_{DF}^2}$$

(36)

$V_{site-to-site}$ is obtained by comparing the L_{max} values from different WIM sites within the state. An analysis of the results of L_{max} projections show that the uncertainties within a site are associated with a COV on the order of $V_{projection}$=3.5% for the projection of the one-lane maximum effect and a COV of $V_{projection}$=5% for the two side-by-side load effect. Additional uncertainties are associated with L_{max} due to the limited number of data points used in the projections and the confidence levels associated with the number of sample points. Using the +/-95% confidence limits, it is estimated that the COV associated with the use of one year worth of WIM data is on the order of V_{data}=2% for the one-lane case and about V_{data}=3% for the two-lane case. Nowak (1999) also observed that the dynamic amplification factors augmented the L_{max} load effect by an average of 13% for one lane of traffic and by 9% for side-by-side trucks. The dynamic amplification also resulted in a COV of V_{IM}=9% on the one-lane load effect and V_{IM}=5.5% on the

two-lane effect.   In previous studies on live load modeling, Ghosn & Moses (1985) included the uncertainties in estimating the lane distribution factor which was associated with a COV equal to V_{DF}=8% based on field measurements on typical steel and prestressed concrete bridges.

Modeling of Other Random Variables

In addition to the live loads, the random variables that control the safety of a bridge member include the actual resistance and the applied dead loads. Nowak (1999) provided models to represent the mean values and the COV's or standard deviations of these random variables that can be summarized as follows for the dead loads:

$$\overline{D_{C1}} = 1.03\ D_{C1} \qquad V_{DC1} = 8\%$$
$$\overline{D_{C2}} = 1.05\ D_{C2} \qquad V_{DC2} = 10\%$$
$$\overline{D_W} = 1.0\ D_W \qquad V_{DW} = 25\% \tag{37}$$

For the bending moment resistance the mean and COV are given as:

$$\overline{R} = 1.12\ R_n \qquad V_R = 10\% \qquad \text{For composite steel beams} \tag{38}$$
$$\overline{R} = 1.05\ R_n \qquad V_R = 7.5\% \qquad \text{For prestressed concrete beams}$$

Calculation of Reliability Index and Adjustment of Live Load Factor

In the LRFD specifications, safety is measured using the reliability index, β, which accounts for the uncertainties in estimating the effects of the applied loads and the resistance of bridge members. The reliability index, β, is related to the probability of failure, P_f, by:

$$\beta = \Phi^{-1}\left(-P_f\right) \tag{39}$$

where $\Phi^{-1}(\ )$ is the inverse of the cumulative Normal distribution function. If all the random variables representing the resistance, dead load and live load follow Gaussian (Normal) probability distributions, the reliability index, β, can be calculated as:

$$\beta = \frac{\overline{R} - \overline{DL} - \overline{LL}}{\sqrt{\sigma_R^2 + \sigma_{DL}^2 + \sigma_{LL}^2}} \tag{40}$$

Where the mean of the total dead load is given by:

$$\overline{DL} = \overline{D_{c1}} + \overline{D_{c2}} + \overline{D_w} , \tag{41}$$

the COV of the total dead load is

$$\sigma_{DL} = \sqrt{\sigma_{DC1}^2 + \sigma_{DC2}^2 + \sigma_{DW}^2} \tag{42}$$

and the standard deviations are obtained as:

$$\sigma_R = \overline{R} \times V_R$$
$$\sigma_{DL} = \overline{DL} \times V_{DL}$$
$$\sigma_{LL} = \overline{LL} \times V_{LL}$$

(43)

The AASHTO LRFD was calibrated so that all bridge members designed using the specified load and resistance factors produce a uniform level of risk expressed in terms of a reliability index β equal to a preset target value β$_{target}$. The AASHTO LRFD calibration was based on a standard set of L$_{max}$ values and live load standard deviations. If the L$_{max}$ values or their COV's within a state are different than those used during the AASHTO LRFD calibration it may be necessary to adjust the live load factors in order to maintain the same β$_{target}$. The adjustment of the live load factors requires the calculation of the reliability index for different values of the live load factor γ$_L$ and adopting the γ$_L$ that produces reliability index values as close to the target as possible for all material types, spans and geometric configurations..

During the calibration of the AASHTO LRFD, Nowak (1999) assumed that the resistance is Lognormal while the combined effect of the dead and live loads is Normal. The reliability index calculations were then executed using a First Order Reliability Method (FORM) algorithm instead of using Eq. (40). However, in order to illustrate the procedure and keep the calculations as simple as possible, it is herein assumed that all the random variables representing the resistance, dead load and live load follow Gaussian (Normal) probability distributions. In such a case, the reliability index, β, can be directly calculated from equation (40). Note that the data and models used by Nowak (1999) led to a target reliability index β$_{target}$=3.5.

Method II   Reliability Based Adjustment Procedure for Live Load Factors

1. Assemble a set of representative bridge samples for the state comprising steel and concrete bridges of different span lengths, number of beams and beam spacing.
2. Assume a value for γ$_L$
3. Choose one bridge from the representative sample of bridges
4. Find the nominal dead loads of components, and wearing surface: D$_{C1}$, D$_{C2}$ and D$_W$.
5. Find the nominal live load effect for the HL-93 loading.
6. Apply the new value of γ$_L$ into Eq. 32 to obtain the required nominal resistance value R$_n$.
7. Find the mean resistance $\overline{R}$ using Eq. (38)
8. Find the COV V$_R$ also using Eq. (38)
9. Find the mean dead load effects using Eq. (37)
10. Find the COV for the dead loads using Eq. (37) and find the standard deviations $\sigma_{DC1} = V_{DC1}\overline{DC_1}$ $\sigma_{DC2} = V_{DC2}\overline{DC_2}$ $\sigma_{DW} = V_{DW}\overline{DW}$

11. Use the protocols for the WIM data analysis to get L$_{max}$ for 75 years for one-lane loadings and two-lane loadings for several sites within the state.
12. Take the average L$_{max}$ and find V$_{site-to-site}$ the COV for one-lane loading and two-lane loading for site-to-site variability.

13. Find the mean value of the live load effect for one lane and two lanes using Eq. 35
14. Find the COV of the live load effect for one-lane loading and two-lane loading using Eq. 36

The proposed adjustment of the live load factor is based on the following assumptions:

- The target reliability index β_{target}=3.50 is a satisfactory target and does not need to be modified. This target was established by the AASHTO LRFD code writers based on the generic live load data available at the time. Future research could lead to selecting of a different target.
- Although the changes in γ_L would lead to different bridge member capacities R_n, it is assumed that these changes would not lead to changes in the dead loads applied on the bridge members.
- Equation (40) is based on the assumption that the resistance, dead load effects and live load effects follow Normal (Gaussian) probability functions. Otherwise one should use a First Order Reliability Method (FORM) algorithm as described by Nowak (1999).
- The models used to obtain the statistical data on the mean values and COV's of the moment and shear capacity of steel composite and prestressed concrete members as well as the dynamic amplification factors and load distribution factors used during the AASHTO LRFD calibration are still valid.
- The goal of the calibration is to adjust the live load factor only so that the representative sample of bridges would on the average match the target reliability index. In general, the target reliability index should be matched as closely as possible for all representative span lengths and bridge configurations. However, this may not be always possibly by changing the live load factor only.

Step 13.2   Deck Design Load Calibration (STRENGTH I)

The data base upon which the present AASHTO LRFD deck provisions were fixed is less defined than for bending and shear in longitudinal members. LRFD design loads for decks represented by a 32 kip axle or a pair of 25.0 Kip axles (Fig. 22) were not based on the Ontario WIM data. The design truck has the same weights and axle spacing as the HS20 load model, which was adopted in 1944 for bridge design, and has been carried over from the Standard Specifications. WIM data was not used to validate these axle load models during the LRFD development. NCHRP Report 368 on LRFD calibration is focused on bridge loads for superstructure design and does not specifically address calibration of loads models for deck design, fatigue design or overload permitting.
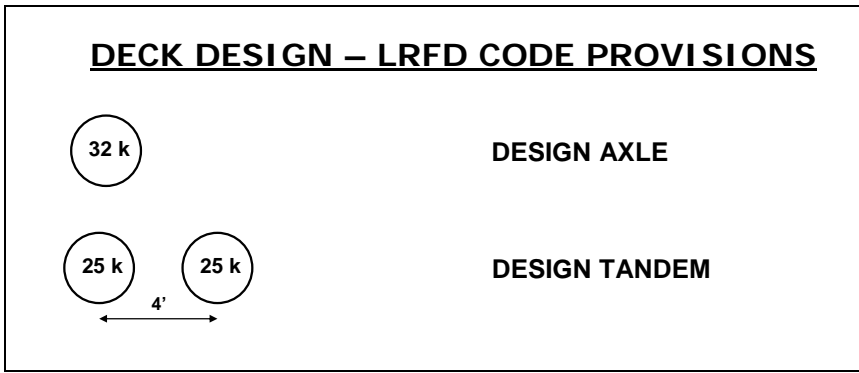
Figure 22 LRFD Deck Design Loads

Axle groups with more than two axles are currently not considered for deck design in LRFD. However, LRFD commentary C3.6.1.3.3 states "*Individual owners may choose to develop other axle weights and configurations to capture the load effects of the actual loads in their jurisdiction based upon local legal load and permitting policies. Triple axle configurations of single unit vehicles have been observed to have load effects in excess of the HL-93 tandem axle load*".
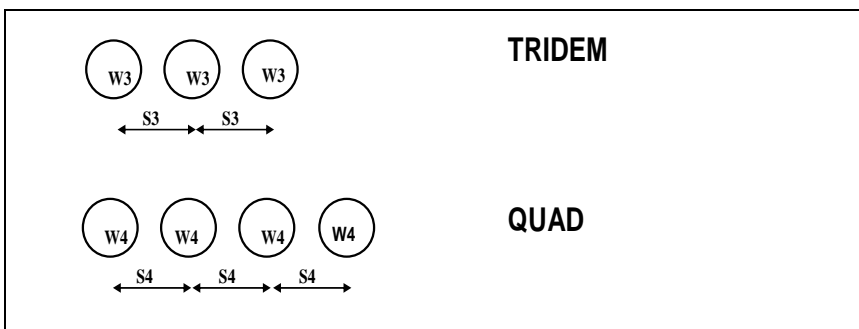
Figure 23   Common Axle Group Loads

A relevant issue which is beyond the scope of this project is the conservative nature of the present checking rules on the resistance side. The simple strip flexural model is conservative with respect to the true capacity of a deck which actually fails in a punching shear mode. Introducing an accurate strength model would require a change in nominal strength formulas as well as the calibrated factors, which require research beyond the current scope. Resistance factors vary with design methods and are not constant.

Rigorous calibration of load and resistance factors for deck design requires the availability of statistical data beyond live loads. LRFD did not specifically address deck components in the calibration. It is important to note that there are no β calculations or database of loads/load effects used for the calibration of decks in the LRFD available for use in this project.

One reasonable approach to calibration of deck design loads is to assume the present LRFD safety targets are adequate for the strength design of decks and establish new nominal loads for axles based on recent WIM data. The LRFD live load factors will remain unchanged, but the axle loads and axle types will be updated to be representative of current traffic data. For instance, tri-axles and quad-axles that are currently not included in the LRFD loadings may need to be considered.

Axle weight statistics from WIM data will first be assembled. The measured axle weights should be adjusted for WIM scatter and measurement errors as detailed in Step 10. This procedure will be repeated for multiple WIM sites to determine the governing nominal loads, taken as:

- For single axles, 32 Kips or the 99th percentile statistic $W_{99,}$ whichever is higher.
- For tandem axles, 50 Kips (2 x 25 Kips) or the 99th percentile statistic $W_{99,}$ whichever is higher.
- For tridem axles, the 99th percentile statistic W_{99}
- For quad axles, the 99th percentile statistic W_{99}

The nominal axle loads derived using WIM data are used instead of the code specified values, where the W_{99} statistic is higher than the code values. W_{99} represents an axle load with a 1% probability of exceedance in a year. This approach provides realistic axle loads for deck design based on current WIM data while keeping all other factors unchanged (load factor, deck dynamic load allowance, Table 20). It also allows the introduction of three and four axle configurations for deck design in a consistent manner. WIM data will also be applied to define nominal axle spacings for the multi-axle groups.

Table 20 Deck Design Load Calibration Using WIM

AXLE TYPE	DESIGN AXLE LOAD	AXLE SPACING	LOAD FACTOR
Single	W_{99} not less than 32 K	N/A	1.75
Tandem	W_{99} not less than 50 K	4 Ft	1.75
Tridem	W_{99} from WIM	4 Ft	1.75
Quad	W_{99} from WIM	4 Ft	1.75

Step 13.3   Repetitive live load Calibration (FATIGUE)

The LRFD fatigue truck configuration will be checked and updated to ensure that it produces fatigue damage similar to that obtained from actual trucks from the traffic data, for typical bridge configurations and fatigue details. Adjustments to the fatigue load model could include changes to:

- ❑   Effective gross weight
- ❑   Axle configuration and axle loads

Fatigue adjustment factor K for each span using site WIM data could provide the basis for calibrating fatigue design load models, as given below:

1. Use LRFD fatigue truck if K values are uniform and equal to 1.0
2. LRFD fatigue truck should be modified using the effective gross weight if K values are uniform but not equal to 1.0.
3. Recommend site-specific fatigue trucks if K varies from 1.0 for varying spans.

Step 13.4   Superstructure Design Overload Calibration (STRENGTH II)

Live Load Modeling for Strength II

The AASHTO LRFD Strength II limit state is used when checking the safety of bridge members under the effect of owner-specified special design vehicles or evaluation permit vehicles. The return period implicit in Strength II is equal to one year. To develop appropriate live load factors for the AASHTO LRFD Strength II limit state, three loading scenarios must be considered:

> I.   Permit vehicle alone
> II.   Permit vehicle along another permit
> III. Permit vehicle along random vehicle.

Case I is exclusively used if the permit vehicle is escorted and traffic is controlled such that no other heavy vehicle is allowed to cross the bridge when the permit is on. Otherwise, Case I should be compared to Cases II and III and the most critical case would govern. Case II may control the loading if a high number of permits are allowed over a certain route or are allowed to travel freely within a jurisdiction. Case III may control depending on the relative weights of the permit as compared to the heavy legal and illegal vehicles that normally cross the bridge.

Case I – Permit vehicle alone

In this case, we can assume that the axle weights and axle configuration of the permit truck are perfectly known so that the total maximum static live load effect on the bridge of the permit truck designated by P is a deterministic value. However, this does not imply that the total live load effect on a bridge member is deterministic due to the uncertainties in estimating the dynamic effect represented by the dynamic amplification factor, IM, and the uncertainties in the structural analysis process that allocates the fraction of the total load to the most critical member. For multi-girder bridges, the structural analysis is represented by the load distribution factor, D.F. The equations for the D.F. of multi-girder bridges loaded by a single lane given in the AASHTO LRFD specifications already include a multiple presence factor m=1.2. Therefore, the expression for the maximum load effect on the most critical beam when a single vehicle is on the bridge can be calculated from:

For case I
$$\overline{LL} = L_{\max\,beam} = P \times IM \times D.F./1.2$$
(44)

Nowak (1999) observed that the dynamic amplification factor augments the load effect by an average of 13% for one lane of traffic. Assuming that the weight and axle configuration of the permit vehicle are exactly known, the COV's of the maximum beam live load effect is obtained from the COV of IM and the COV of DF:

$$V_{LL} = \sqrt{V_{IM}^2 + V_{DF}^2}$$
(45)

Using the data for V_{IM} and V_{DF} for one lane proposed by Nowak (1999) and Ghosn & Moses (1985) the loading of a single permit vehicle, the live load COV becomes:
$$V_{LL} = \sqrt{(9\%)^2 + (8\%)^2} = 12\%$$

Case II – Two Permits side-by-side

In this case, we can assume that the axle weights and axle configurations of the two permit trucks are the same and are perfectly known so that the total maximum static live load effect on the bridge is a deterministic value equal to 2P. However, this does not imply that the total live load effect on a bridge member is deterministic due to the uncertainties in estimating the dynamic effect represented by the dynamic amplification factor, IM, and the uncertainties in the structural analysis process that allocates the fraction of the total load to the most critical member. The structural analysis is represented by the load distribution factor, D.F. The equations for the D.F. of multi-girder bridges loaded in two lanes given in the AASHTO LRFD specifications assume that the two lanes are loaded by the same vehicle and give the load on the most critical beam as a function of the load in one of the lanes. Thus, the live load effect on one member can be given as:

For case II
$$\overline{LL} = L_{max\,beam} = P \times IM \times D.F.$$
(46)

According to Nowak (1999), the dynamic amplification factor augments the load effect by an average of 9% for side-by-side trucks. The dynamic amplification also results in a COV of V_{IM}=5.5% on the two-lane effect. We will also assume that the same COV for the lane distribution factor V_{DF}=8% obtained by Moses & Ghosn (1986) from field measurements on typical steel and prestressed concrete bridges is still valid. Therefore, for the loading of a single permit vehicle, the live load COV becomes $V_{LL} = \sqrt{(5.5\%)^2 + (8\%)^2} = 9.71\%$.

The reliability index conditional on the arrival of two side-by-side permits on the bridge can then calculated using Eq. (40) where $\overline{R}$ is the mean resistance when the bridge member is designed for two side-by-side permits and $\overline{LL}$ is the live load effect on the beam due to two side-by-side permits.

The reliability index calculated from Eq. (40) in this case is conditional on having two side-by-side trucks. The probability that a bridge member would fail given that two permit vehicles are side-by-side can be calculated from the inverse of Eq. (39). However, the final unconditional probability of failure will depend on the conditional probability given two side-by-side events and the probability of having a situation with side-by-side permits. Thus:

$$P_f = P_{f\,/\,side-by-side\,events} \times P_{side-by-side}$$
(47)

The probability of having two-side-by-side permits depends on the number of permit trucks expected to cross the bridge within the return period within which the permits are granted. The percentage of these permits that will be side-by-side is related to the total number of permit crossings. Tables relating the percentage of side-by-side events, $P_{side-by-side}$ as a function of the number of truck crossings can be obtained from the WIM data. The final unconditional reliability index is then obtained by inserting the results of Eq. (47) into Eq, (39)

Case III –Permit Truck Alongside a Random Truck

For case III, the maximum live load effect is due to the permit truck alongside the maximum truck expected to occur simultaneously in the other lane. The maximum total load effect depends on the number of side-by-side events expected within the return period.

To determine the number of side-by-side permit-random truck events that would occur within a one-year period we assume that N_P gives the number of permit truck crossings expected in a return period T. The final number of random trucks along side a permit will be:

$$N_R = P_{side-by-side} \times N_P \tag{48}$$

where $P_{side-by-side}$ is the percentage of side-by-side events which depends on the ADTT and N_p is the number of permits within the return period of interest.

The maximum live load effect is obtained from:

$$\overline{LL} = \left(P \times DF_P + L_{max\,N_R} \times DF_R\right)IM \tag{49}$$

where P is the load effect of the permit truck, DF_P is the distribution factor for the load P, $L_{max\,N_R}$ is the maximum load effect of random trucks for N_R events which correspond to the one-year return period applicable for the Strength II case, DF_R is the distribution factor for the random load, and IM is the impact factor for side-by-side events. The problem in this case is that the DF tables provided in the AASHTO LRFD for two lanes assume that the two side-by-side trucks are of equal weight, which is clearly not the case. Following the AASHTO LRFD approach for permit trucks alongside random trucks, Moses (2001) suggested that DF_P be obtained from the AASHTO LRFD tables for single lane while DF_R be obtained from the difference between the DF of two lanes and that of a single lane.

The coefficient of variation for $L_{max\,N_R} \times DF_R$ is estimated as:

$$V_{L\max^*} = \sqrt{V_{site-to-site}{}^2 + V_{proejction}{}^2 + V_{data}{}^2 + V_{DF}{}^2} \tag{50}$$

where all the values are taken for the single lane case.

Assuming the effect of the permit load is deterministic, the coefficient of variation for $P \times DF_P$ is estimated as:

$$V_{P*}=8\% \tag{51}$$

which is the COV for the load distribution factor, DF_P. Hence, the standard deviation of LL without the Impact factor is:

$$\sigma_{LL^*} = \sqrt{\left(V_{P*} \times P \times DF_P\right)^2 + \left(V_{L\max^*} \times L_{max\,N_R} \times DF_R\right)^2} \tag{52}$$

and the COV for the live load effect on the critical beam including the effect of the impact IM is given by:

$$V_{LL} = \sqrt{\left(\frac{\sigma_{LL^*}}{LL^*}\right)^2 + V_{IM}^2}$$

(53)

where $LL^* = \left(P \times DF_P + L_{max\,NR} \times DF_R\right)$ is the static live load effect on the most critical bridge member.

The mean live load obtained form Eq. (49) and the COV obtained from Eq. (53) are then used to find the reliability index from Eq. (40).

The calibration of the appropriate live load factor would consist of finding the γ_L that will lead to reliability index values equal to the target value for Cases I, II and III.

Method II: Reliability Based Adjustment Procedure for Overload Live Load Factors

1. Assemble a set of representative bridge samples for the state comprising steel and concrete bridges of different span lengths, number of beams and beam spacing.
2. Determine the permit vehicle configuration.
3. Assume a value for γ_L
4. Choose one bridge from the representative sample of bridges
5. Find the nominal dead loads of components, and wearing surface: D_{C1}, D_{C2} and D_W.
6. Find the nominal live load effect, P, for the permit vehicle
7. Apply the new value of γ_L into Eq. 32 to obtain the required nominal resistance value R_n.
8. Find the mean resistance $\overline{R}$ using Eq. (38)
9. Find the COV V_R also using Eq. (38)
10. Find the mean dead load effects using Eq. (37)
11. Find the COV of the dead loads from Eq. (37) and Find the standard deviations $\sigma_{DC1} = V_{DC1}\overline{DC_1}$ $\sigma_{DC2} = V_{DC2}\overline{DC_2}$ $\sigma_{DW} = V_{DW}\overline{DW}$
12. Use the protocols for the WIM data analysis to get $L_{max\,NR}$ for one-lane loadings for a one year return period.
13. Calculate $\overline{LL}$ for Case I, Case II, and Case III from Equations 44, 46, and 49.
14. Find the COV for LL for each case using Eq. (45) or (53).
15. Find the standard deviations using Equations 42 and 43.
16. Apply the mean and standard deviation values of loads and resistance into Eq. (40) to calculate the reliability index, β, for the bridge configuration selected in step 4 for each of the three Cases.

87

- For Cases I and III the reliability index is obtained from Eq. (40) directly.
- For Case II, the conditional reliability index, β_{cond} is obtained from Eq. (40).   The final unconditional reliability index, β, is obtained from $\beta = \Phi^{-1}\left(-P_f\right)$ where P_f is obtained from Equation 47 and $P_{f/side-by-side} = \Phi\left(-\beta_{cond}\right)$ where Φ is the Standard Normal cumulative distribution function.

17. Go to step 4 to select another bridge and repeat steps 4 to 16   until you exhaust all the bridges in the representative sample.
18. Find the average β_{ave} of each load case for the representative sample of bridges.
19. If $\beta_{ave}=\beta_{target}=3.50$ stop otherwise go to step 3 and start the process over.
20. Determine the value of γ_L that leads to $\beta_{ave}=\beta_{target}=3.50$ for each of the three Cases.

DEMONSTRATION OF RECOMMENDED PROTOCOLS USING NATIONAL WIM DATA

Introduction

In this Chapter, draft protocols including step-by-step procedures for collecting and using traffic data in bridge design were developed. They are geared to address the use of national WIM data to develop and calibrate vehicular loads for LRFD superstructure design, fatigue design, deck design and design for overload permits.

The aim of this section is to give practical examples of using these protocols with national WIM data drawn from sites around the country with different traffic exposures, load spectra, and truck configurations. This will give a good cross-section of WIM data for illustrative purposes. This step will allow the updating and/or refinement of the protocols based on its applicability to WIM databases of varying quality and data standards currently being collected by the states. This section of the report discusses the results of the demonstration studies in more detail.

Selection of Sites for National WIM Data Collection

The protocols established in this Chapter were implemented using recent traffic data (either 2005 or 2006) from 26 WIM sites (47 directional sites) in five states across the country (Table 21). The sites were chosen to capture a variety of geographic locations and functional classes, from urban interstates, rural interstates and state routes.

Requests for WIM data needed for the studies were sent out to certain selected States based on the National survey findings. The requirements for selection of WIM sites were are as follows:

WIM data for a whole year (2006 or 2005) from the following highway functional classifications:

      a. Two WIM sites on Rural Interstates
      b. Two WIM sites on Urban Interstates
      c. Two WIM sites on Principal Arterials (non-Interstate routes)

Table 39 lists the sites studied along with their respective ADTT's. For consistency, lanes one and two are eastbound or northbound lanes; lanes three and four are westbound or south bound lanes.

Table 21 WIM Sites Studied in Task 8

State	Site ID	Route	Dir	# Truck Records	ADTT	State	Site ID	Route	Dir	# Truck Records	ADTT
CA	0001	Lodi	E/N	1537613	5058	MS	2606	I-55	N	564393	1622
CA	0001	Lodi	W/S	1470924	4839	MS	2606	I-55	S	604919	1733
CA	0003	Antelope	E	719834	2790	MS	3015	I-10	E	750814	2248
CA	0004	Antelope	W	806122	3149	MS	3015	I-10	W	667560	1999
CA	0059	LA710	S	4243780	11627	MS	4506	I-55	N	530517	2002
CA	0060	LA710	N	3806748	11432	MS	4506	I-55	S	477931	1804
CA	0072	Bowman	E/N	310596	2318	MS	6104	US-49	N	462301	1288
CA	0072	Bowman	W/S	289319	2159	MS	6104	US-49	S	498054	1387
FL	9916	US-29	N	175905	498	MS	7900	US-61	N	69996	220
FL	9919	I-95	N	939637	2708	MS	7900	US-61	S	68198	216
FL	9919	I-95	S	875766	2524	TX	0506	US-287	E/N	559663	1701
FL	9926	I-75	N	1096076	4136	TX	0506	US-287	W/S	520092	1581
FL	9926	I-75	S	1032680	3897	TX	0516	I-35	E/N	717666	2384
FL	9927	SR-546	E	204549	567	TX	0516	I-35	W/S	707744	2449
FL	9927	SR-546	W	168114	466	TX	0523	US-281	E/N	430227	1429
FL	9936	I-10	E	700774	1980	TX	0523	US-281	W/S	394804	1312
FL	9936	I-10	W	723512	2044	TX	0526	I-20	E/N	1330799	4070
IN	9511	I-65	N	2119022	5919	TX	0526	I-20	W/S	1174954	3593
IN	9511	I-65	S	2068073	5777						
IN	9512	I-74	E	931971	2596						
IN	9512	I-74	W	1003443	2795						
IN	9532	US-31	N	224506	629						
IN	9532	US-31	S	229532	643						
IN	9534	I-65	N	2128577	5929						
IN	9534	I-65	S	2162874	6025						
IN	9544	I-80/I-94	E	3786127	11235						
IN	9544	I-80/I-94	W	4032537	11966						
IN	9552	US-50	E	95900	278						
IN	9552	US-50	W	102212	296						

Data Filtering and Quality Control (Protocol Steps 5.1 and 5.2)

The same data scrubbing criteria established in Steps 5.1 and 5.2, were employed. That is, truck records that met any one of the following criteria were eliminated as unlikely or unwanted trucks for the purposes of this study. The following is a filtering protocol was applied for screening the WIM data used in this project. Truck records that meet the following filters were eliminated:

- Speed < 10 mph
- Speed > 100 mph
- Truck length > 120 ft
- Total number of axles > 12
- Total number of axles < 3
- Record where the sum of axle spacing is greater than the length of truck

- GVW < 12 Kips
- Record where an individual axle > 70 Kips
- Record where the steer axle > 25 Kips
- Record where the steer axle < 6 Kips
- Record where the first axle spacing < 5 feet
- Record where any axle spacing < 3.4 feet
- Record where any axle < 2 Kips
- Record which has GVW +/- sum of the axle weights by more than 10%

The two most common criteria used to eliminate records were "number of axles < 3" (2-axle light vehicles) and "steer axle < 6 kips". Typically, one of these two criteria was responsible for 75% to 90% of all scrubbed records at a given WIM site. Further more, the gross vehicle weight of these trucks tends to be low. Therefore, their removal from the study has very little effect on the analysis which tends to concentrate on the upper tail of the data. Table 22 shows the number of trucks, as well as the percentage of the total truck population, eliminated from each WIM site for meeting one or more of the above criteria. Also shown is the mean gross vehicle weight, in kips, of all the eliminated trucks.

Table 22 Trucks Eliminated by Data Filtering

State	Site	Number	%	GVW	State	Site	Number	%	GVW
CA	0001	1671347	35.7	12.0	IN	9511	984044	19.0	14.6
CA	0003	643461	47.2	11.2	IN	9512	421592	17.9	13.2
CA	0004	771032	48.9	11.4	IN	9532	839445	64.9	10.9
CA	0059	1242393	22.6	14.3	IN	9534	1952426	31.3	10.9
CA	0060	1366271	26.4	14.8	IN	9544	1855062	19.2	12.9
CA	0072	407724	40.5	10.9	IN	9552	162192	45.0	11.0
FL	9916	533513	73.0	16.5	MS	2606	380794	24.6	27.8
FL	9919	457426	20.1	22.5	MS	3015	1712866	53.4	25.9
FL	9926	1752902	45.2	13.7	MS	4506	458419	31.3	19.1
FL	9927	276965	42.6	16.5	MS	6104	488899	33.7	24.3
FL	9936	330745	18.8	26.3	MS	7900	86777	38.6	13.6
					TX	0506	584553	35.1	10.9
					TX	0516	881932	38.2	9.6
					TX	0523	465556	36.1	10.7
					TX	0526	1261244	33.5	11.4

The scrubbed WIM data was passed through various quality control checks. The quality control checks established in Step 5.2 were employed for each WIM site studied. The quality control checks look specifically at Class 9 trucks (5-axle semi-trailer trucks). Since Class 9 trucks are so prevalent in the population and their configurations are well defined, deviations from their expected characteristics can be noted and corrective measures taken.

The quality control checks are described as follows:

1. Percentage of trucks by class. Class 9 trucks should be the most prevalent truck class in the population.

2. Class 9 truck GVW histogram. The characteristic bi-modal shape of the GVW histogram should show an "unloaded" peak between 28 kips and 32 kips, and a "loaded" peak between 72 kips and 80 kips.
3. Over-weight Class 9 trucks. The percentage of Class 9 trucks over 100 kips should be small.
4. Class 9 truck steer axle weight histogram. The weight of the front axle of Class 9 trucks should be between 9 kips and 11 kips. There should not be a significant deviation from this range.
5. Class 9 drive tandem weight histogram. The weight of the drive tandem should not deviate significantly from the estimated values given in NCHRP Report 495.
6. Class 9 axle spacing histogram. The spacing between the steer axle and the drive tandem axle as well as the spacing between the drive tandem axles should be fairly consistent.

The traffic in each lane at a WIM site is recorded by it own sensor. If a sensor malfunctions or begins to lose its calibration it will manifest itself in one or more of the results of the quality control checks. By segregating the data of these quality control checks by lane and by month, deviations from the normal, expected values can be more easily identified and isolated. If a sensor appears to be malfunctioning or providing less reliable data, then the data collected by the offending sensor is eliminated from the population.

Of all the sites studied, only two required additional data scrubbing due to non-conformance during the quality control checks. At WIM Site 3015 in Mississippi, all data from Lane 3 during the months of January through June were eliminated. This accounted for 74,351 trucks, or 5.0% of the filtered truck data. At WIM Site 9916 in Florida, all data from Lane 1 during the month of January were eliminated. This accounted for 14,521 trucks, or 7.6% of the filtered truck data.

After this second round of data scrubbing due to sensor issues, all remaining data is considered reliable and ready for processing.

Truck Multiple-Presence (Protocol Step 6)

Accurate multiple presence data requires time stamps of truck arrival times to the hundredth of second. We did request this time stamp resolution, but the WIM data records were mostly to a second accuracy. Multiple-presence (MP) statistics need not be developed for each site. Multiple presence statistics are mostly transportable from site to site with similar truck traffic volumes and traffic flow. A relationship between MP and ADTT was developed in this Study, which could be applied to any given site without performing a site-specific analysis (see Step 7 below).

WIM Data Analysis for One-Lane Loading(Step 7)

Grouping Trucks into STRENGTH I

Protocols developed in Task 7 require that legal loads and routine permits be grouped under STRENGTH I and heavy special permits be grouped under STRENGTH II. The following approach to grouping trucks in the WIM databases was used:

- Do not attempt to classify NY trucks as permit or non-permits based on permit records when using large scale WIM databases. The permit data is not reliable, incomplete or not easily accessed to allow this to be achieved.
- Group all trucks with six or fewer axles in the STRENGTH I calibration. These vehicles include legal trucks and routine permits. These vehicles are considered to be enveloped by the HL-93 load model.

- Group all trucks with seven or more axles in the STRENGTH II calibration. These vehicles should include the heavy special permit loads, typically in the 150 Kip GVW and above category. An analysis of WIM data from several states indicates a big drop off in truck population for vehicles with seven or greater axles. Only a very small percentage of trucks belong to this permit group.

Gross Vehicle Weight Histograms (Step 7.1)

Gross Vehicle Weight (GVW) histograms were generated by direction of travel for each WIM site. Figure 24 shows, as a sample, the GVW histogram for WIM Site 9926 in Florida (I-75). Appendix C contains the GVW histograms for all other WIM sites studied in this task.
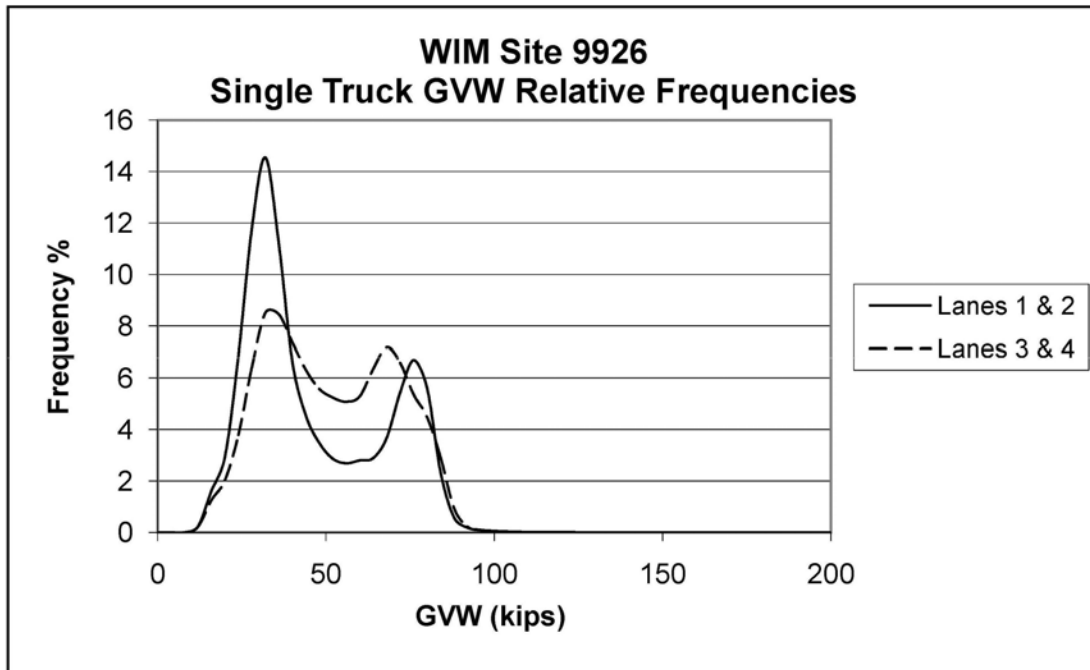
Figure 24 – GVW Histogram. WIM Site 9926 in Florida

The bi-modal shape of this histogram is typical of GVW histograms with the first major peak representing un-loaded or lightly loaded trucks and the second major peak representing trucks loaded near the legal limit of 80 kips.

One Lane Load Effects (Step 7.1)

The load effects of each truck individually were calculated for eight span lengths from 20 feet to 200 feet for both simple spans and two-span continuous spans. The load effects calculated were maximum mid-span moment for a simple span, shear at a support for a simple span, maximum positive moment for a two-span continuous span, maximum negative moment for a two-span continuous span, and shear at the center support of a two-span continuous span. All load effects were normalized to those of HL-93 loading. Figure 25 shows, as a sample, the single truck maximum mid-span moment histogram for a simple 60-ft span for WIM Site 9926 in Florida (I-75). Similarly, Figure 26 shows the single truck maximum shear histogram for a simple 60-ft span for WIM Site 9926. Appendix C contains the moment histograms for all other WIM sites studied in this task.
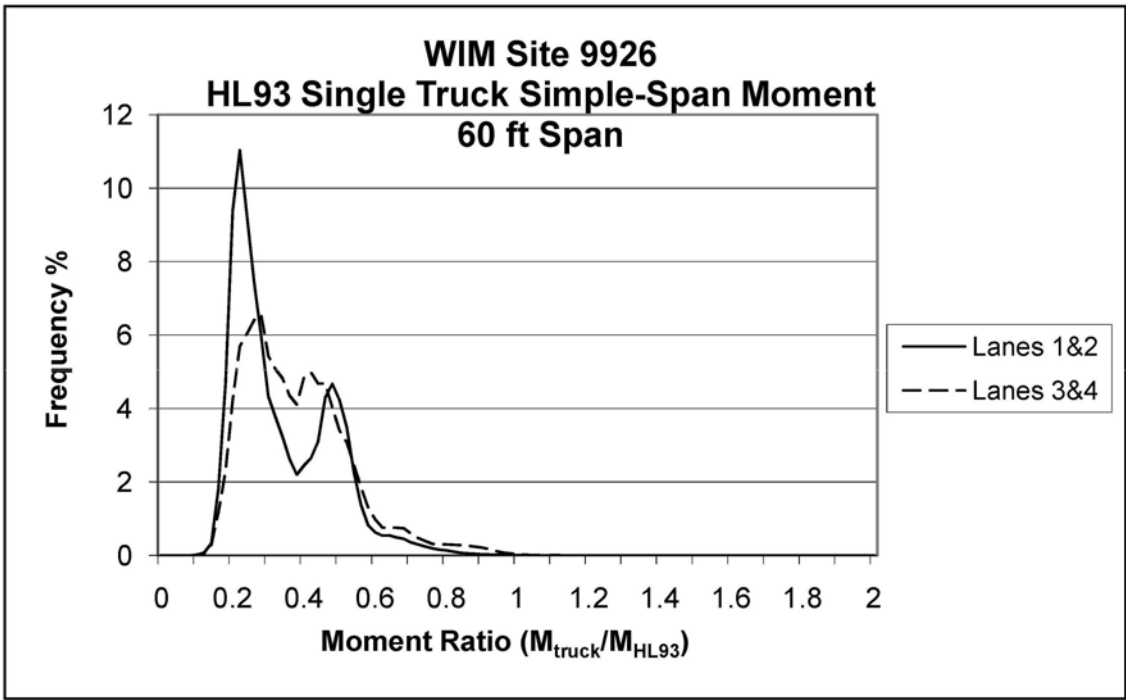
Figure 25 – Single Truck Simple-Span Moment Histogram. WIM Site 9926 in Florida
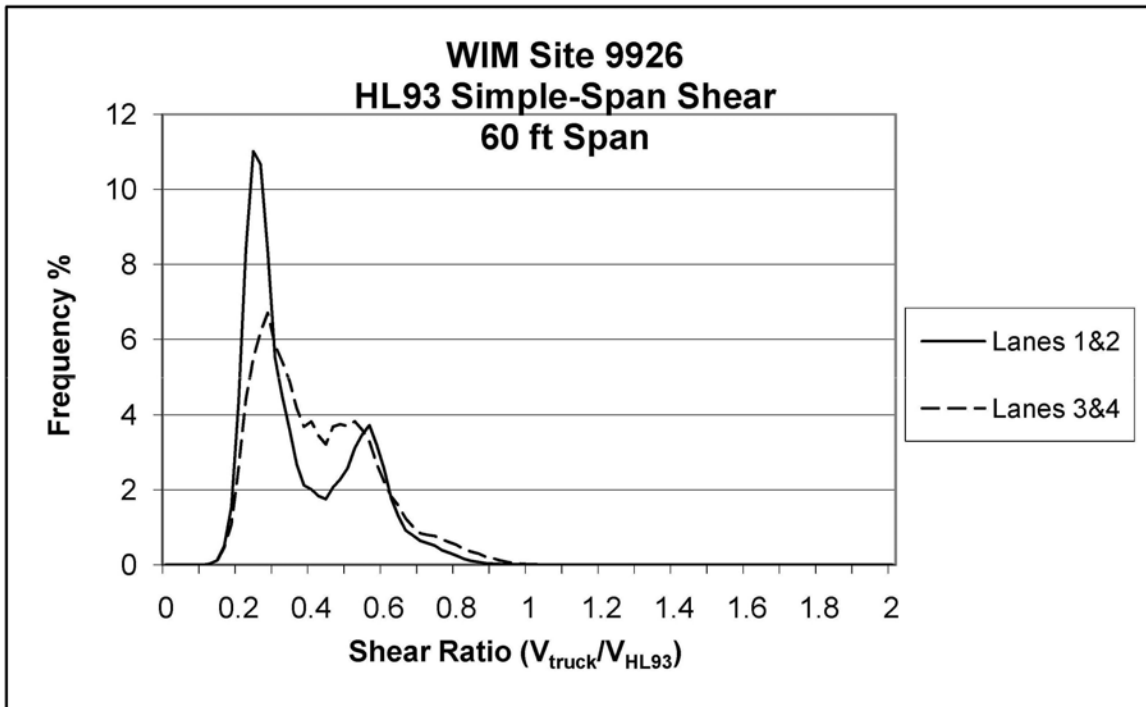
Figure 26 – Single Truck Simple-Span Shear Histogram. WIM Site 9926 in Florida

As would be expected, the general shape of these histograms is similar to that of the GVW histogram; that is, bi-modal with the first major peak representing unloaded or lightly loaded trucks and the second major peak representing trucks loaded near the legal limit.

WIM Data Analysis for Two-Lane Loading   (Step 8)

Simulation of Truck Events using Generalized Multiple Presence Statistics (Step 8.2)

All the New York WIM sites studied captured accurate time stamps with each truck record. This allowed for the analysis of two trucks existing simultaneously on a span. Additional data was also available from several WIM sites in New Jersey. None of the WIM sites included reported time stamps with sufficient precision (to the nearest $1/100^{th}$ of a second) to accurately model the relative positions of two trucks on a span. However, the probabilities of two trucks existing within various headway separations were determined. These probabilities, shown in Table 23, were used to simulate the simultaneous presence of two trucks on a span.

Table 23 – Multiple Presence Probabilities

	Multiple Presence Probabilities (%)							
	Two-Lane Events (Side-by-Side)				One-Lane Events (Following)			
Headway	Site Truck Traffic (ADTT)**				Site Truck Traffic (ADTT)**			
(ft)	Light	Average	Heavy	Very Heavy	Light	Average	Heavy	Very Heavy
0 to 20	0.19	0.41	0.61	0.60	0.00	0.00	0.00	0.00
20 to 40	0.14	0.43	0.66	0.63	0.00	0.00	0.00	0.00
40 to 60	0.21	0.41	0.68	0.66	0.01	0.00	0.00	0.01
60 to 80	0.26	0.35	0.62	0.64	0.01	0.00	0.00	0.09
80 to 100	0.20	0.53	0.76	0.74	0.06	0.04	0.03	0.49
100 to 120	0.21	0.41	0.81	0.64	0.12	0.15	0.16	1.81
120 to 140	0.24	0.34	0.66	0.61	0.21	0.33	0.45	3.04
140 to 160	0.17	0.30	0.61	0.56	0.36	0.57	0.73	3.29
160 to 180	0.18	0.29	0.56	0.53	0.48	0.67	0.91	3.03
180 to 200	0.19	0.26	0.52	0.50	0.46	0.75	0.98	2.74
200 to 220	0.10	0.24	0.48	0.48	0.51	0.68	0.94	2.52
220 to 240	0.14	0.24	0.45	0.43	0.48	0.67	0.91	2.28
240 to 260	0.12	0.22	0.43	0.41	0.42	0.65	0.87	2.18
260 to 280	0.14	0.21	0.41	0.39	0.41	0.60	0.85	1.98
280 to 300	0.11	0.20	0.40	0.36	0.39	0.59	0.80	1.87

** Light: ADTT $\leq$ 1000
Average: $1000 < ADTT \leq 2500$
Heavy: $2500 < ADTT \leq 5000$
Very Heavy: ADTT > 5000

Note that the very heavy ADTT MP was based only on one site in New York City and has some anomalies that should be addressed by additional studies at other U.S sites. Based on a WIM site's ADTT and the multiple presence probabilities established as shown in Table 23, the number of expected multiple presence events for the given WIM site were determined. For each expected multiple presence event two trucks traveling in the desired direction were chosen at random from the entire population of trucks traveling in that direction and positioned to achieve the required headway separation. The load effects of the simulated multiple presence events were calculated as for the single truck events.

For the purpose of design, in consideration of distribution factors, load effects were segregated into one-lane and two-lane; one-lane load effects are those due to a single truck as well as two trucks in the same lane, while two-lane load effects are those due to two trucks in

adjacent lanes. Figure 27 shows, as a sample, the one-lane and two-lane moment histograms for a 60-foot simple span for lanes one and two of WIM Site 9926 in Florida (I-75). Figure 28 and Figure 29 are similar, but show the histograms for simple span shear and negative moment, respectively. Appendix C contains the load effect histograms for all other WIM sites studied in this task.
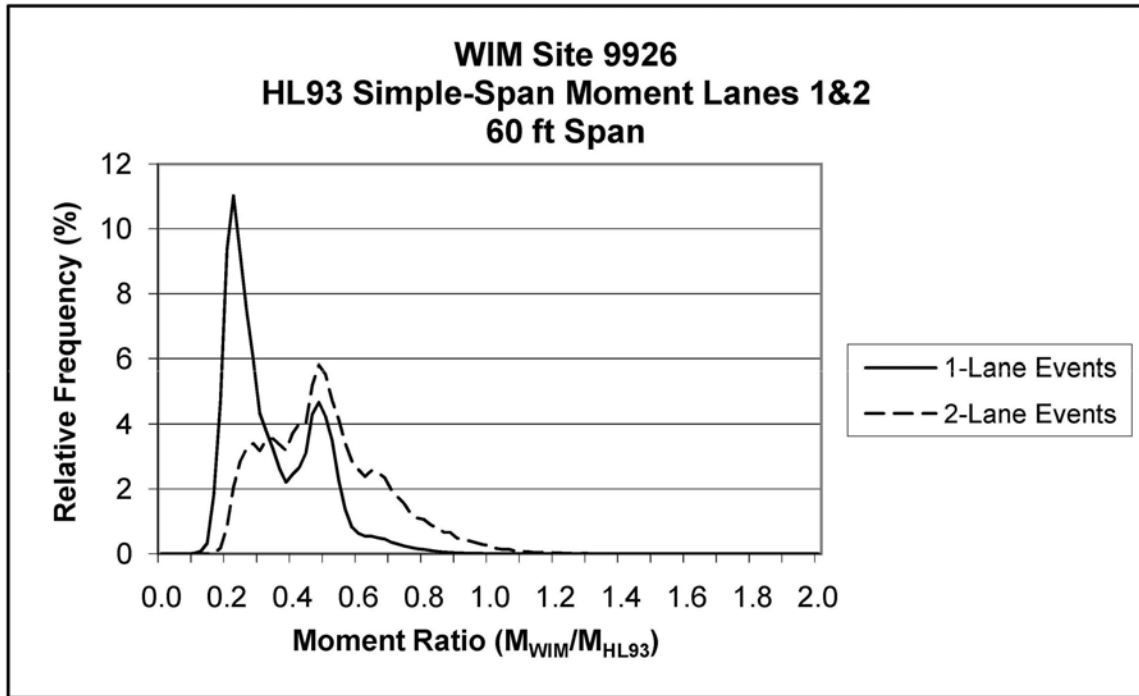
Figure 27 – Simple-Span Moment Histogram. WIM Site 9926 in Florida
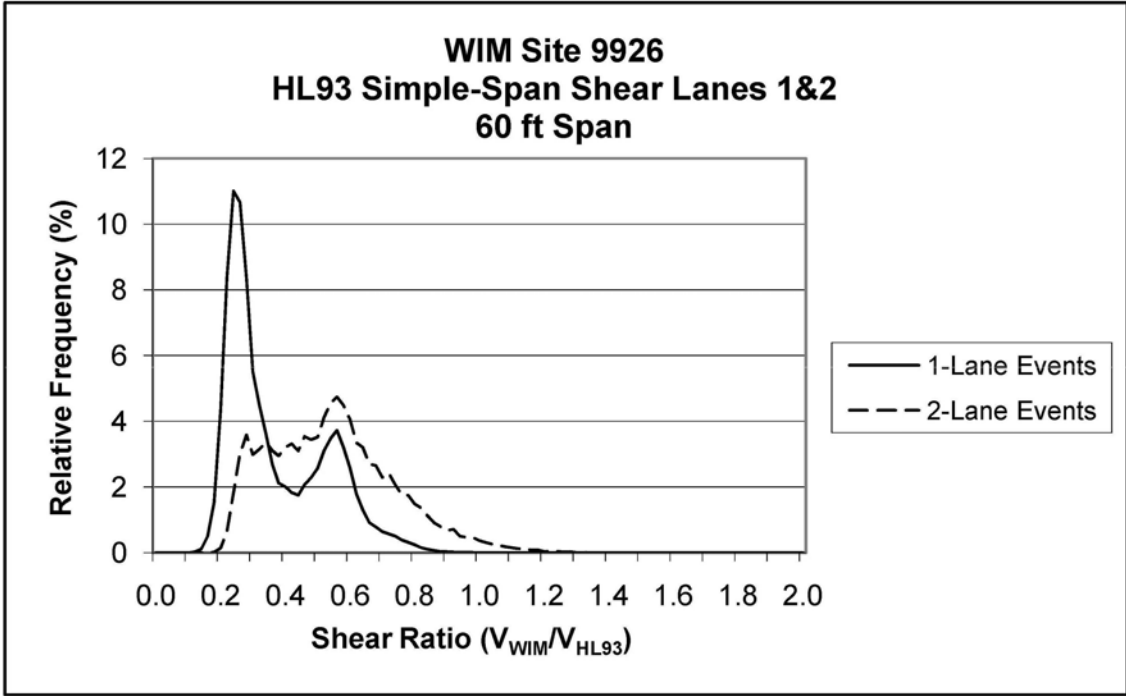
Figure 28 – Simple-Span Shear Histogram. WIM Site 9926 in Florida
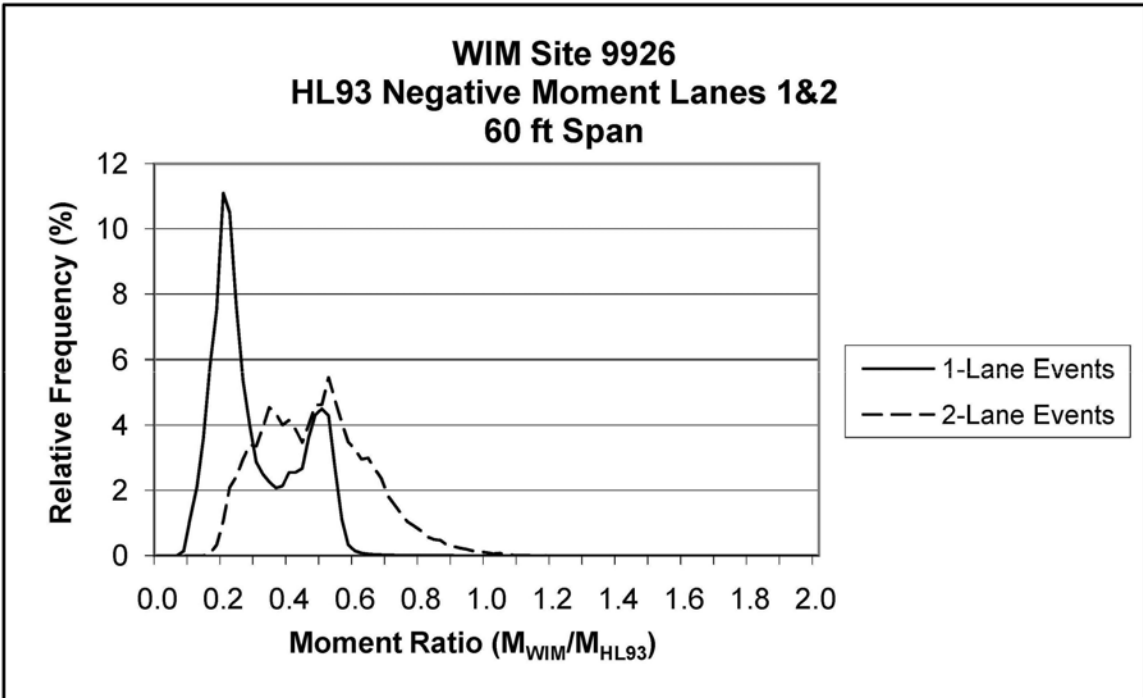
Figure 29 – Two-Span Continuous Negative Moment Histogram. WIM Site 9926 in Florida

Since it is unlikely that two trucks traveling in the same lane will be separated by less than 60 feet, the load effects histograms for the one-lane events are very similar to the single-truck load effects histograms; that is, they display the typical bi-modal shape. The same cannot be said of

the two-lane events. Here, the distinction between unloaded trucks and loaded trucks is blended resulting in a unimodal distribution.

Accumulated Fatigue Damage and Effective Gross Weight   (Step 11)

Damage accumulation laws such as Miner's rule can then be used to estimate the fatigue damage for the whole design period for the expected truck population at a site. For varying spans, the effective gross weight for trucks measured at the site was determined using the Equation:

$$W_{eq} = \left(\sum f_i W_i^3 \right)^{1/3}$$
(54)

Where f_i is the fraction of gross weights within interval i, and W_i is the mid-width of interval i. In this calculation use trucks only with three or more axles (Class 6 and above). The LRFD fatigue truck, has a 54 Kip effective gross weight. Table 24 shows the effective gross weights calculated for the various WIM sites.

Table 24 – Effective Gross Vehicle Weight for All WIM Sites Studied in Task 8

State	Site ID	Route	Dir	W_{eff}	State	Site ID	Route	Dir	W_{eff}
CA	0001	Lodi	E/N	61.5	MS	2606	I-55	N	73.7
CA	0001	Lodi	W/S	60.3	MS	2606	I-55	S	66.0
CA	0003	Antelope	E	56.3	MS	3015	I-10	E	56.9
CA	0004	Antelope	W	56.4	MS	3015	I-10	W	61.7
CA	0059	LA710	S	45.8	MS	4506	I-55	N	67.1
CA	0060	LA710	N	54.4	MS	4506	I-55	S	56.9
CA	0072	Bowman	E/N	56.0	MS	6104	US-49	N	65.5
CA	0072	Bowman	W/S	57.2	MS	6104	US-49	S	66.0
FL	9916	US-29	N	56.1	MS	7900	US-61	N	58.9
FL	9919	I-95	N	49.3	MS	7900	US-61	S	60.7
FL	9919	I-95	S	50.0	TX	0506		E/N	63.1
FL	9926	I-75	N	56.2	TX	0506		W/S	62.7
FL	9926	I-75	S	59.6	TX	0516		E/N	55.6
FL	9927	SR-546	E	52.9	TX	0516		W/S	58.4
FL	9927	SR-546	W	47.2	TX	0523		E/N	60.9
FL	9936	I-10	E	73.9	TX	0523		W/S	62.2
FL	9936	I-10	W	50.2	TX	0526		E/N	60.8
IN	9511	I-65	N	51.4	TX	0526		W/S	61.9
IN	9511	I-65	S	47.4					
IN	9512	I-74	E	64.5					
IN	9512	I-74	W	65.1					
IN	9532	US-31	N	47.4					
IN	9532	US-31	S	50.7					
IN	9534	I-65	N	49.0					
IN	9534	I-65	S	51.6					
IN	9544	I-80/I-94	E	53.5					
IN	9544	I-80/I-94	W	50.1					
IN	9552	US-50	E	55.7					
IN	9552	US-50	W	46.3					

Accumulated fatigue damage was studied, as in Step 11, by calculating the fatigue adjustment factor, K. The fatigue adjustment factor K was calculated relative to three reference trucks: the LRFD fatigue truck, the modified LRFD fatigue truck, and the site-specific fatigue truck.

$$K \times M_{FT} = \left[\frac{\sum (M_i)^3}{\#Trucks} \right]^{1/3} \tag{55}$$

The modified LRFD fatigue truck has the same number of axles, the same axle spacing, and the same axle weight distribution as the LRFD fatigue truck, but a GVW equal to the effective gross weight of the truck population at the WIM site. For the site-specific fatigue truck, the most common axle spacings and axle weight distributions were determined for the 5-axle trucks (the most common truck type) and used to define an equivalent 3-axle fatigue truck. That is, the drive tandem axles were combined into an equivalent single axle (with an axle weight equal to the combined weight of the tandem, located mid-way between the two tandem axles), and the trailer tandem axles were combined into an equivalent single axle. This is a slight adjustment to the definition of the site-specific fatigue truck used. The effective gross weight of the truck population was still used for the GVW of this fatigue truck. Table 24 shows the effective gross vehicle weight, in kips, used in calculating K for each directional WIM site studied in this task.

 The most common axle configuration of the five-axle trucks was gathered from histograms of axle weights and axle spacing for each WIM site. This information was used to define a site-specific fatigue truck for each site. Figure 30 shows, as a sample, the typical configuration of 5-axle trucks and the equivalent 3-axle fatigue truck derived from it for WIM Site 9926 in Florida (I-75). Table 25 shows, as a sample, the values of the fatigue adjustment factor, K, for the northbound lanes of WIM Site 9926. Appendix C contains the fatigue adjustment factor values for all other WIM sites studied in this task.

 The more closely the reference truck represents the actual truck traffic at a site, the closer the value of the fatigue adjustment factor is to unity. Values of K greater than 1.0 indicate that the reference truck underestimates the accumulated fatigue damage of the traffic, while values of K less than 1.0 indicate that the reference truck overestimates the accumulated fatigue damage. As would be expected, the site-specific fatigue truck most closely represents the entire truck population in regards to accumulated fatigue damage.
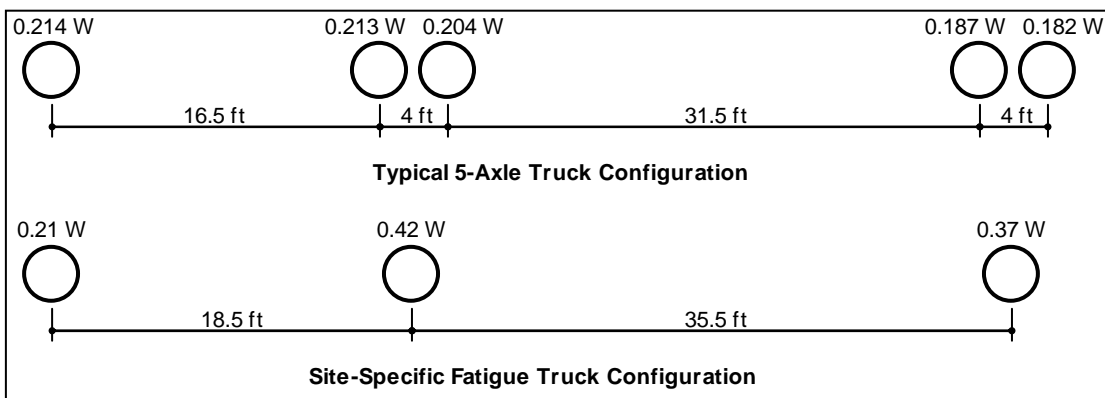
Figure 30 – Site Specific Truck Configurations. WIM Site 9926 in Florida (I-75)

Table 25 – Fatigue Adjustment Factor, K. WIM Site 9926 in Florida (I-75)

Lanes 1 and 2

LRFD Fatigue Truck		GVW =		54 kips					
Axle Weight:		Steer =		6 kips		Drive =		24 kips	Trailer =	24 kips
Axle Spacing:					14 ft				30 ft
Span (ft)	20	40	60	80	100	120	160	200	
K (simple)	0.8965	0.9933	1.0718	0.9749	0.9846	0.9944	1.0069	1.0142	
K (pos.)	0.875	0.9761	0.9988	0.967	0.9789	0.9885	1.0014	1.0094	
K (neg.)	1.1614	0.9462	1.0834	1.0868	0.9887	1.0004	1.0175	1.0257	

Modified LRFD Fatigue Truck		GVW =		56.203 kips	(effective gross weight)				
Axle Weight:		Steer =		6.245 kips		Drive =	24.979 kips		Trailer =	24.979 kips
Axle Spacing:					14 ft				30 ft
Span (ft)	20	40	60	80	100	120	160	200	
K (simple)	0.8613	0.9544	1.0298	0.9367	0.946	0.9554	0.9675	0.9745	
K (pos.)	0.8407	0.9378	0.9596	0.9291	0.9406	0.9498	0.9622	0.9698	
K (neg.)	1.1158	0.9091	1.0409	1.0442	0.95	0.9612	0.9777	0.9855	

Site-Specific Fatigue Truck		GVW =		56.203 kips	(effective gross weight)				
Axle Weight:		Steer =		11.803 kips		Drive =	23.605 kips		Trailer =	20.795 kips
Axle Spacing:					18.5 ft				35.5 ft
Span (ft)	20	40	60	80	100	120	160	200	
K (simple)	0.9115	1.0464	1.0364	1.0236	1.0072	1.0028	1.0002	0.9995	
K (pos.)	0.8896	1.0024	1.0203	1.0128	1.0051	1.0021	1	0.9994	
K (neg.)	0.9749	1.0111	0.9887	1.0052	1.029	1.0147	1.0073	1.0045	

Lanes 3 and 4

LRFD Fatigue Truck		GVW =		54 kips					
Axle Weight:		Steer =		6 kips		Drive =		24 kips	Trailer =	24 kips
Axle Spacing:					14 ft				30 ft
Span (ft)	20	40	60	80	100	120	160	200	
K (simple)	0.9928	1.1091	1.1941	1.0721	1.0701	1.0739	1.0804	1.0848	
K (pos.)	0.9649	1.0879	1.1129	1.0638	1.0657	1.0695	1.0763	1.0811	
K (neg.)	1.2809	1.0062	1.149	1.1622	1.0599	1.0688	1.0831	1.0901	

Modified LRFD Fatigue Truck		GVW =		59.573 kips	(effective gross weight)				
Axle Weight:		Steer =		6.619 kips		Drive =	26.477 kips		Trailer =	26.477 kips
Axle Spacing:					14 ft				30 ft
Span (ft)	20	40	60	80	100	120	160	200	
K (simple)	0.8999	1.0054	1.0824	0.9718	0.97	0.9734	0.9794	0.9833	
K (pos.)	0.8746	0.9861	1.0088	0.9643	0.966	0.9695	0.9756	0.9799	
K (neg.)	1.1611	0.9121	1.0415	1.0535	0.9607	0.9688	0.9818	0.9881	

Site-Specific Fatigue Truck		GVW =		59.573 kips	(effective gross weight)				
Axle Weight:		Steer =		12.51 kips		Drive =	25.021 kips		Trailer =	22.042 kips
Axle Spacing:					18.5 ft				35.5 ft
Span (ft)	20	40	60	80	100	120	160	200	
K (simple)	0.9523	1.1023	1.0894	1.0619	1.0327	1.0217	1.0125	1.0086	
K (pos.)	0.9255	1.0541	1.0726	1.0512	1.0323	1.0229	1.014	1.0099	
K (neg.)	1.0144	1.0143	0.9893	1.0142	1.0406	1.0228	1.0115	1.0071	

Lifetime Maximum Load Effect L_{max} for Strength I   (Step 12.2)

Statistical projections with a Gumbel distribution fit to the upper tail of the load effects histograms were used to determine the lifetime maximum load effects, L_{max}, for Strength I superstructure design. L_{max} was calculated for all five load effects, for all eight span lengths, for all 47 directional WIM sites, and segregated by one-lane and two-lane events.

The results of the calculation of L_{max} based on the data assembled from several WIM sites are provided in Tables 26 to 30 for different span lengths. The results show a slight decrease in the value of L_{max} with span length. The average value of L_{max} tends to be more closely related to its minimum value than to its maximum value indicating a bias to less heavily loaded spans. Where the information is available, the 75-year L_{max} values used in the LRFD calibration are also shown. With the exception of negative moment in a two-span continuous span, the L_{max} values used in the LRFD calibration are unconservative, being less than the maximum values observed in this study. The degree to which these values are unconservative is more pronounced in the one-lane events where the L_{max} values used in the LRFD calibration are less than the average values

observed in this study. Appendix B contains the L_{max} results for all the WIM sites studied in this task.

Table 26 through Table 30 show, for each state studied in this task respectively, the maximum values of L_{max} calculated for each load effect and span length (The maximum value shown in a cell in the table is the maximum for all WIM sites in that state.). Although in many cases the maximum L_{max} value for a 2-Lane event is larger than that of the equivalent 1-Lane event, this is not a generality that holds true for all load effects, all span lengths, or even all states. It is, however, evident that the truck traffic is state dependant resulting in a broad range of L_{max} values among the states.

Table 31 shows the 75-year L_{max} values used in the LRFD calibration. Here the L_{max} values remain fairly constant with span length and even with load effect. One apparent trend is for the L_{max} value of the 2-Lane event to be nearly 2x0.85 that of the equivalent 1-Lane event.

Table 26 – Maximum L_{max} Values for California

Maximum L_{max} Values of 8 Directional WIM Sites in California									
		Span (ft)							
Load Effect		20	40	60	80	100	120	160	200
M-simple	1-Lane	1.989	1.635	1.413	1.392	1.351	1.311	1.227	1.168
	2-Lane	1.955	1.823	1.844	1.891	1.859	1.783	1.676	1.544
V-simple	1-Lane	1.861	1.526	1.483	1.427	1.391	1.349	1.258	1.175
	2-Lane	1.930	1.843	1.904	1.870	1.842	1.796	1.662	1.549
M-positive	1-Lane	1.861	1.526	1.483	1.427	1.391	1.349	1.258	1.175
	2-Lane	1.867	1.859	1.859	1.894	1.854	1.806	1.697	1.564
M-negative	1-Lane	1.599	1.557	1.364	1.346	1.250	1.078	0.939	0.846
	2-Lane	2.017	2.013	1.446	1.086	1.020	0.973	0.895	0.812
V-center	1-Lane	1.752	1.508	1.506	1.439	1.344	1.208	1.020	0.915
	2-Lane	1.906	1.846	1.896	1.848	1.757	1.520	1.356	1.200

Table 27 - Maximum L_{max} Values for Florida

Maximum L_{max} Values of 9 Directional WIM Sites in Florida									
		Span (ft)							
Load Effect		20	40	60	80	100	120	160	200
M-simple	1-Lane	2.860	2.571	2.234	2.240	2.178	2.112	1.939	1.800
	2-Lane	2.511	2.478	2.471	2.451	2.405	2.365	2.244	2.141
V-simple	1-Lane	2.955	2.515	2.456	2.395	2.290	2.193	2.008	1.854
	2-Lane	2.444	2.467	2.493	2.380	2.297	2.273	2.199	2.101
M-positive	1-Lane	2.880	2.586	2.273	2.230	2.220	2.145	2.003	1.829
	2-Lane	2.407	2.423	2.496	2.497	2.429	2.361	2.260	2.151
M-negative	1-Lane	2.640	2.336	1.807	1.582	1.396	1.195	1.025	0.958
	2-Lane	2.480	2.577	1.814	1.615	1.489	1.361	1.279	1.128
V-center	1-Lane	2.851	2.436	2.404	2.306	2.204	1.903	1.588	1.421
	2-Lane	2.506	2.270	2.288	2.371	2.280	2.074	1.821	1.649

Table 28 - Maximum L$_{max}$ Values for Indiana

Maximum L$_{max}$ Values of 12 Directional WIM Sites in Indiana									
Load Effect		Span (ft)							
		20	40	60	80	100	120	160	200
M-simple	1-Lane	2.302	2.207	1.932	1.896	1.859	1.806	1.702	1.636
	2-Lane	2.219	1.958	1.814	1.765	1.706	1.749	1.740	1.669
V-simple	1-Lane	2.422	2.079	1.899	1.883	1.839	1.789	1.687	1.618
	2-Lane	2.134	1.820	1.885	2.019	2.057	2.034	1.914	1.798
M-positive	1-Lane	2.352	2.175	1.961	1.891	1.858	1.807	1.736	1.636
	2-Lane	2.278	1.952	1.800	1.735	1.739	1.768	1.742	1.672
M-negative	1-Lane	1.861	1.917	1.608	1.505	1.302	1.153	1.009	0.939
	2-Lane	1.841	2.335	1.853	1.324	1.076	1.073	1.017	0.934
V-center	1-Lane	2.392	2.024	1.831	1.810	1.764	1.581	1.395	1.302
	2-Lane	2.100	1.791	1.837	1.971	1.991	1.799	1.555	1.416

Table 29 - Maximum L$_{max}$ Values for Mississippi

Maximum L$_{max}$ Values of 10 Directional WIM Sites in Mississippi									
Load Effect		Span (ft)							
		20	40	60	80	100	120	160	200
M-simple	1-Lane	1.687	1.679	1.666	1.674	1.678	1.796	1.989	2.010
	2-Lane	2.255	2.156	1.930	1.935	2.025	2.031	1.954	1.856
V-simple	1-Lane	1.683	1.689	1.790	1.781	1.957	2.083	2.158	2.133
	2-Lane	2.309	2.135	2.054	2.097	2.104	2.093	1.981	1.861
M-positive	1-Lane	1.618	1.659	1.660	1.646	1.626	1.791	1.955	2.012
	2-Lane	2.237	2.182	1.979	1.989	2.034	2.035	1.973	1.873
M-negative	1-Lane	1.905	1.816	2.164	1.972	1.733	1.466	1.240	1.186
	2-Lane	2.059	2.490	1.911	1.353	1.228	1.193	1.118	1.015
V-center	1-Lane	1.711	1.702	1.853	1.839	1.940	1.920	1.824	1.764
	2-Lane	2.260	2.086	2.054	2.069	2.071	1.864	1.635	1.467

Table 30 - Maximum L$_{max}$ Values for Texas

Maximum L$_{max}$ Values of 8 Directional WIM Sites in Texas									
Load Effect		Span (ft)							
		20	40	60	80	100	120	160	200
M-simple	1-Lane	1.718	1.844	1.793	1.647	1.524	1.463	1.313	1.190
	2-Lane	1.966	1.763	1.598	1.557	1.600	1.611	1.559	1.462
V-simple	1-Lane	1.742	1.694	1.648	1.578	1.515	1.454	1.345	1.260
	2-Lane	1.996	1.655	1.706	1.776	1.785	1.759	1.666	1.554
M-positive	1-Lane	1.688	1.741	1.798	1.674	1.570	1.479	1.331	1.233
	2-Lane	1.937	1.698	1.579	1.561	1.609	1.612	1.575	1.490
M-negative	1-Lane	1.642	1.605	1.206	0.864	0.941	0.966	0.906	0.850
	2-Lane	1.567	2.028	1.536	1.098	0.978	0.993	0.952	0.838
V-center	1-Lane	1.666	1.706	1.670	1.569	1.447	1.242	1.057	0.966
	2-Lane	1.951	1.605	1.682	1.732	1.733	1.560	1.356	1.224

Table 31 – 75-year L$_{max}$ Values Used in LRFD Calibration

75-year L$_{max}$ Values Used in LRFD Calibration									
Load Effect		Span (ft)							
		20	40	60	80	100	120	160	200
M-simple	1-Lane	1.300	1.350	1.320	1.320	1.310	1.290	1.240	1.230
	2-Lane	2.120	2.340	2.300	2.280	2.260	2.240	2.180	2.160
V-simple	1-Lane	1.230	1.230	1.230	1.270	1.280	1.220	1.200	1.170
	2-Lane	2.120	2.180	2.220	2.260	2.280	2.200	2.140	2.080
M-negative	1-Lane	1.270	1.300	1.250	1.210	1.200	1.200	1.200	1.200
	2-Lane	2.280	2.400	2.300	2.240	2.220	2.220	2.220	2.220

Discussion and Analysis of L$_{max}$ results

- The ratio of 2-lane L$_{max}$ divided by one lane L$_{max}$ is reasonably constant for shear and moments within a range of 1.05 to 1.13 (Fig 31).

- The ratio of L$_{max}$ for 2-lane/L$_{max}$ for 1-lane for moments and shear of simple spans are relatively small, compared with the LRFD calibration data. This would indicate that in many cases the single event may govern design load effects. This would also depend on the LRFD live load distribution factors for one and two lane loaded conditions.

- Average L$_{max}$ seems to decrease with span length (Fig. 32) indicating that HL-93 loading is not entirely consistent with current truck weight data.
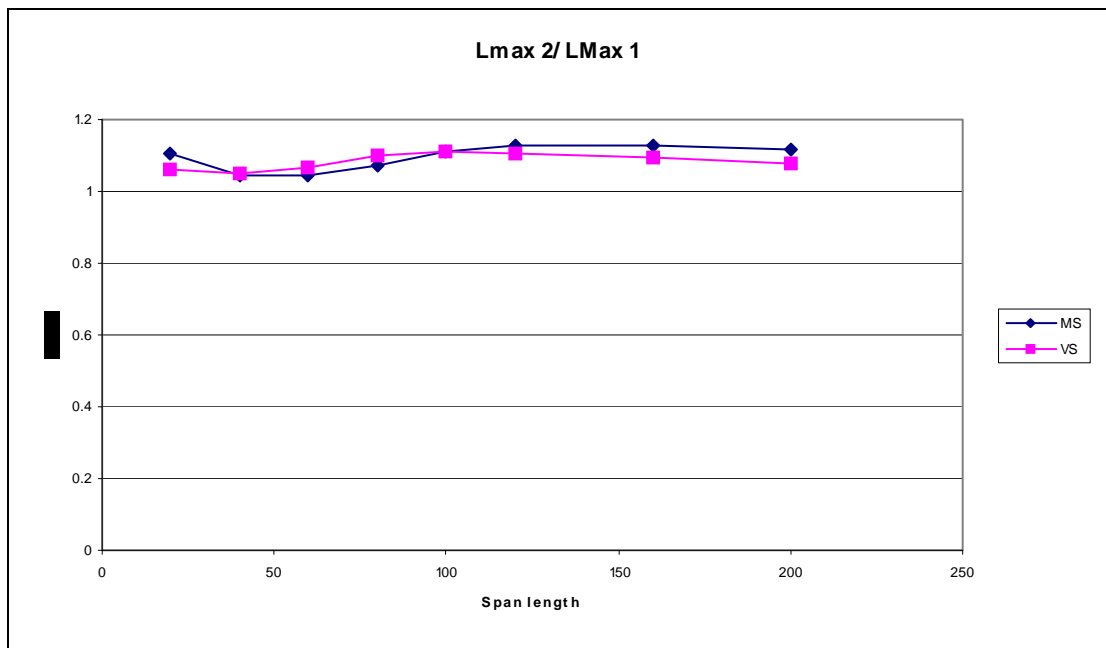
Figure 31 - L$_{max}$ for 2-lane / L$_{max}$ for 1-lane for moments and shear of simple spans
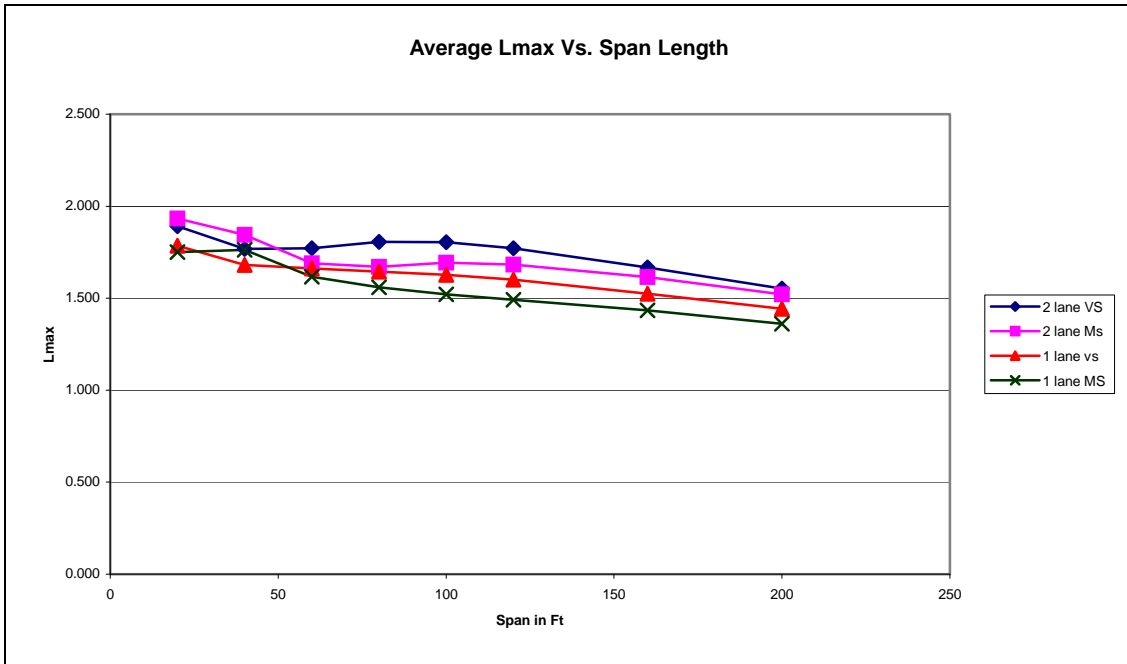
Figure 32 – Average L_{max} vs Span Length

- The spread in L_{max} is very high with a Coefficient of Variation (COV) 0.36 to 0.24 with a tendency to go lower with span length. This COV expresses the site-to-site variability. Also, the COV accounts for the extreme distribution property (obtained from the projections protocols). The one lane COV is lower and decreases faster with span length than the 2-lane COV.
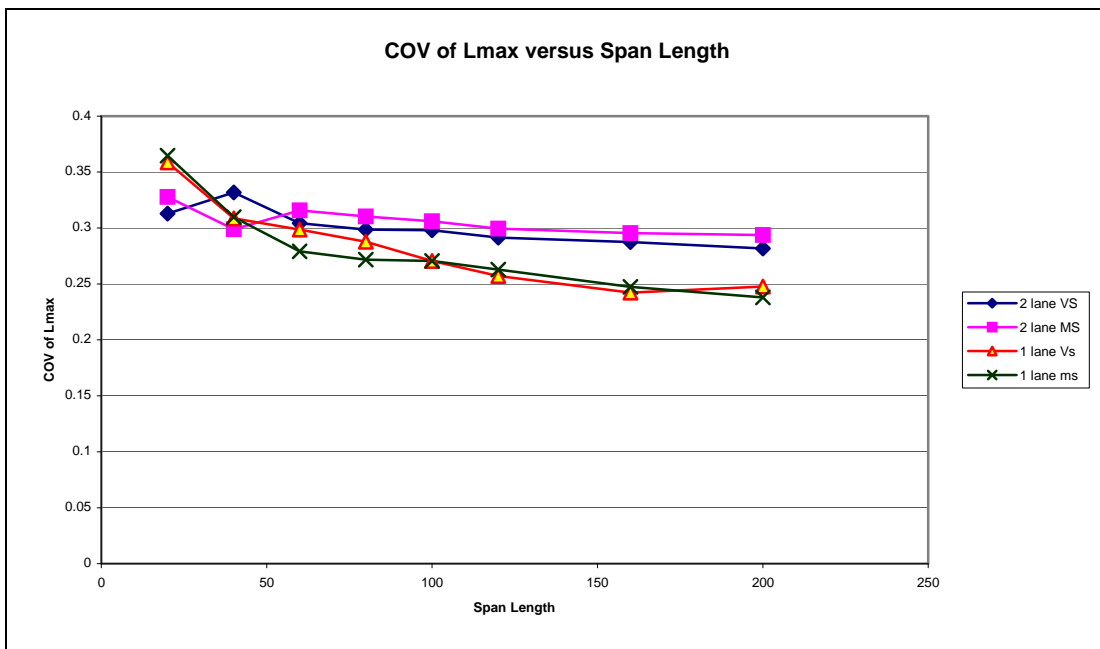
Figure 33 – COV of L_{max} vs Span Length

- There seems to be no correlation between L_{max} and ADTT. R^2 is approximately zero for all the cases (Figures 34 thru 37).
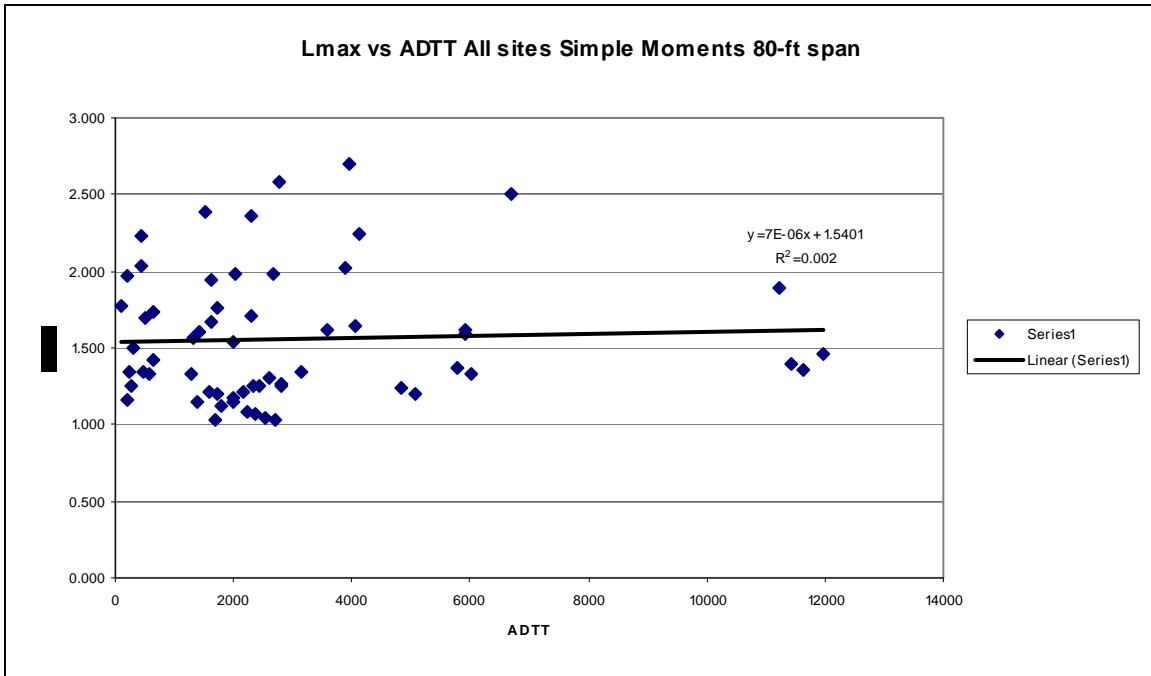
Figure 34 – L_{max} vs ADTT for One-Lane Simple Span Moment
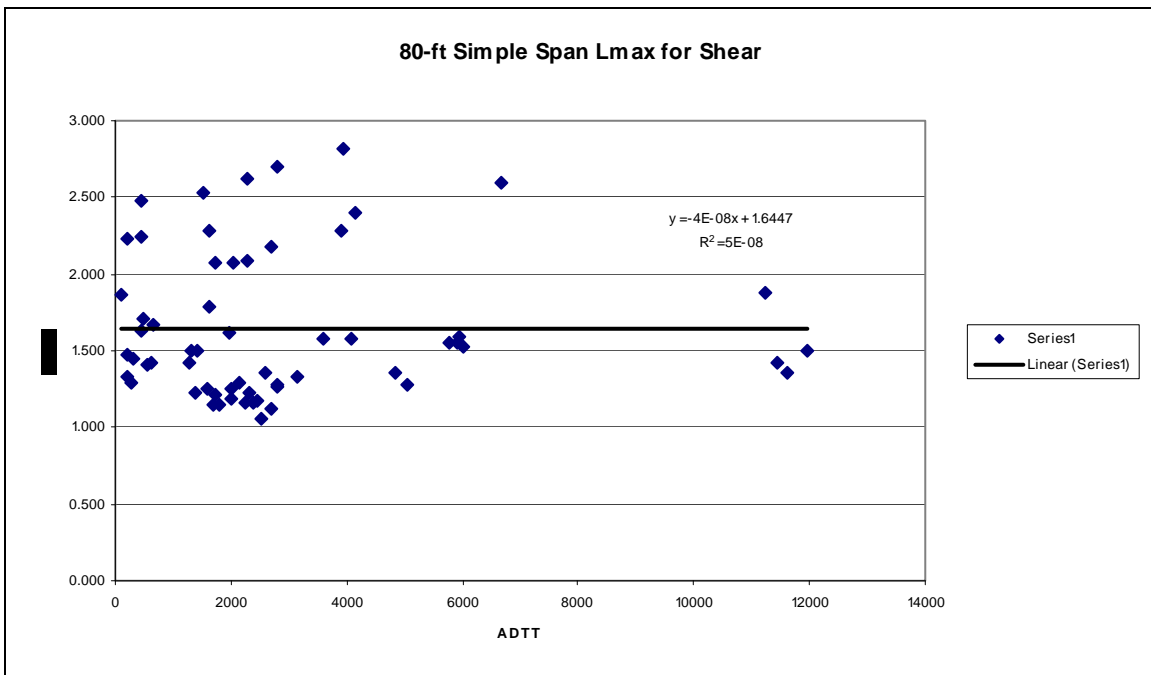
Figure 35 – L_{max} vs ADTT for One-Lane Simple Span Moment
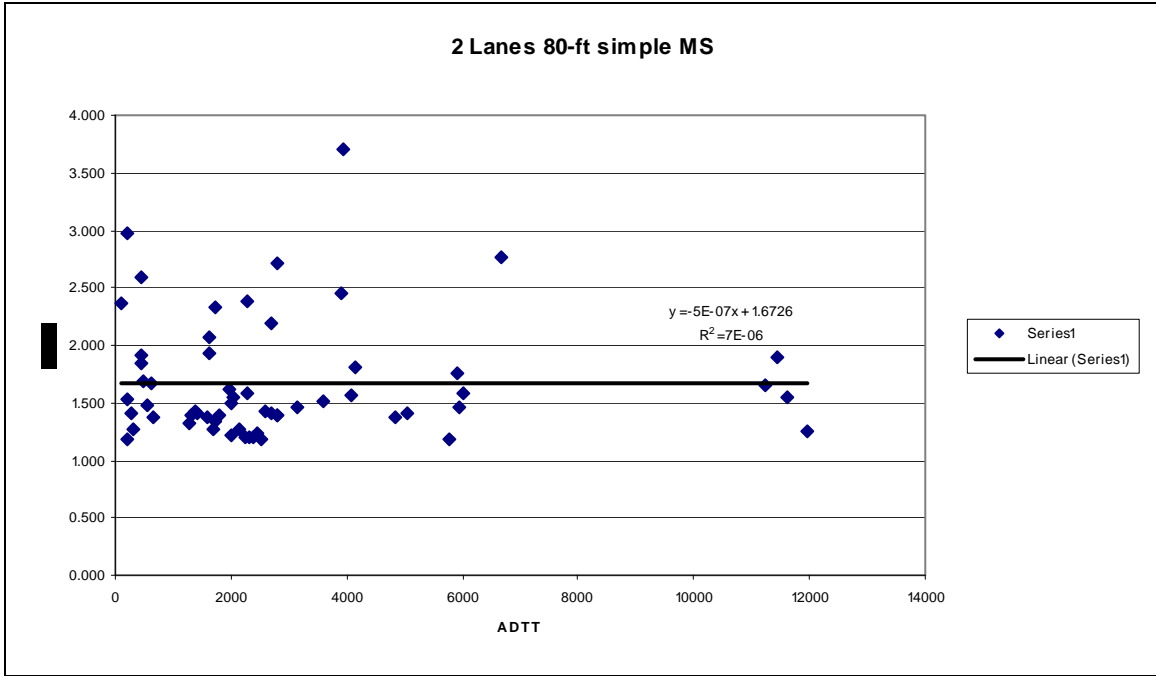
Figure 36 – L_{max} vs ADTT for Two-Lane Simple Span Moment
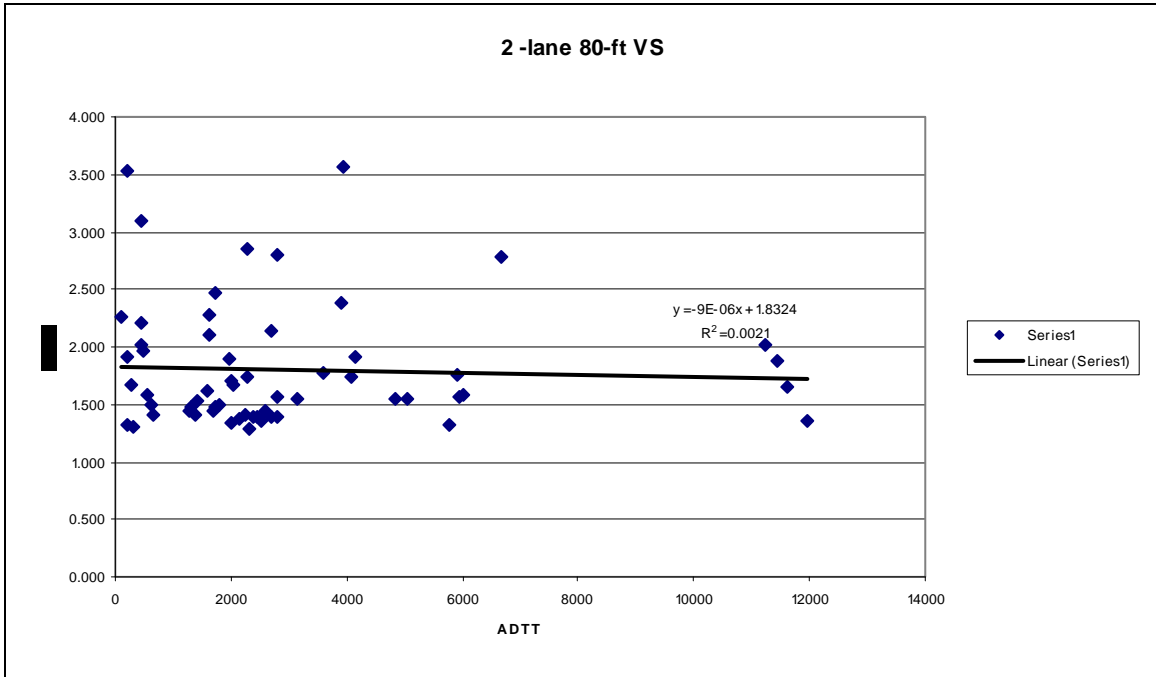
Figure 37 – L_{max} vs. ADTT for Two-Lane Simple Span Shear

Calibrate Vehicular Load Factors for Bridge Design Strength I (Step 13.1)

Method I

An increase in maximum expected live load based on current WIM data can be compensated in design by raising the live load factor in a corresponding manner. The calibration process adjusts the corresponding live load factor by the ratios r_1 and r_2 of Eq. (30) and (31):

$$\gamma_{L,StrengthI} = 1.75 \text{ x } r_{StrengthI} \tag{62}$$

The value r is taken to be the ratio of the L_{max} value as calculated from WIM data to the L_{max} value used in the LRFD calibration. It can be used to determine the effectiveness of HL93 for lifetime maximum loading. One key assumption with regard to this simplified procedure for adjusting live load factors is that the site-to-site variability in L_{max} as measured by the COV is the same as that used during the AASHTO LRFD calibration. In AASHTO LRFD calibration, the overall live load COV was taken as 20%.

Table 32 through Table 36 show, for each state studied in this task respectively, the maximum values of r calculated for each load effect and span length.

Table 32 - Maximum r Values for California

Maximum r Values of 8 Directional WIM Sites in California									
		Span (ft)							
Load Effect		20	40	60	80	100	120	160	200
M-simple	1-Lane	1.530	1.211	1.070	1.055	1.031	1.016	0.990	0.950
	2-Lane	0.922	0.779	0.802	0.829	0.823	0.796	0.769	0.715
V-simple	1-Lane	1.513	1.241	1.206	1.124	1.087	1.106	1.048	1.004
	2-Lane	0.910	0.845	0.858	0.827	0.808	0.816	0.777	0.745
M-negative	1-Lane	1.259	1.198	1.091	1.112	1.042	0.898	0.783	0.705
	2-Lane	0.885	0.839	0.629	0.485	0.459	0.438	0.403	0.366

Table 33 - Maximum r Values for Florida

Maximum r Values of 9 Directional WIM Sites in Florida									
		Span (ft)							
Load Effect		20	40	60	80	100	120	160	200
M-simple	1-Lane	2.200	1.904	1.692	1.697	1.663	1.637	1.564	1.463
	2-Lane	1.184	1.059	1.074	1.075	1.064	1.056	1.029	0.991
V-simple	1-Lane	2.402	2.045	1.997	1.886	1.789	1.798	1.673	1.585
	2-Lane	1.153	1.132	1.123	1.053	1.007	1.033	1.028	1.010
M-negative	1-Lane	2.079	1.797	1.446	1.307	1.163	0.996	0.854	0.798
	2-Lane	1.088	1.074	0.789	0.721	0.671	0.613	0.576	0.508

Table 34 - Maximum r Values for Indiana

Maximum r Values of 12 Directional WIM Sites in Indiana									
Load Effect		Span (ft)							
		20	40	60	80	100	120	160	200
M-simple	1-Lane	1.771	1.635	1.464	1.436	1.419	1.400	1.373	1.330
	2-Lane	1.047	0.837	0.789	0.774	0.755	0.781	0.798	0.773
V-simple	1-Lane	1.969	1.690	1.544	1.483	1.437	1.466	1.406	1.383
	2-Lane	1.007	0.835	0.849	0.893	0.902	0.925	0.894	0.864
M-negative	1-Lane	1.465	1.475	1.286	1.244	1.085	0.961	0.841	0.783
	2-Lane	0.807	0.973	0.806	0.591	0.485	0.483	0.458	0.421

Table 35 - Maximum r Values for Mississippi

Maximum r Values of 10 Directional WIM Sites in Mississippi									
Load Effect		Span (ft)							
		20	40	60	80	100	120	160	200
M-simple	1-Lane	1.298	1.244	1.262	1.268	1.281	1.392	1.604	1.634
	2-Lane	1.064	0.921	0.839	0.849	0.896	0.907	0.896	0.859
V-simple	1-Lane	1.368	1.373	1.455	1.402	1.529	1.707	1.798	1.823
	2-Lane	1.089	0.979	0.925	0.928	0.923	0.951	0.926	0.895
M-negative	1-Lane	1.500	1.397	1.731	1.630	1.444	1.222	1.033	0.988
	2-Lane	0.903	1.038	0.831	0.604	0.553	0.537	0.504	0.457

Table 36 - Maximum r Values for Texas

Maximum r Values of 8 Directional WIM Sites in Texas									
Load Effect		Span (ft)							
		20	40	60	80	100	120	160	200
M-simple	1-Lane	1.322	1.366	1.358	1.248	1.163	1.134	1.059	0.967
	2-Lane	0.927	0.753	0.695	0.683	0.708	0.719	0.715	0.677
V-simple	1-Lane	1.416	1.377	1.340	1.243	1.184	1.192	1.121	1.077
	2-Lane	0.942	0.759	0.768	0.786	0.783	0.800	0.779	0.747
M-negative	1-Lane	1.293	1.235	0.965	0.714	0.784	0.805	0.755	0.708
	2-Lane	0.687	0.845	0.668	0.490	0.441	0.447	0.429	0.377

Summary of Method I Results

As with L_{max}, the value of r is state dependant. Unlike L_{max}, however, there is a significant, and consistent, difference between the r-values for 1-Lane events and 2-Lane events. The r-values for 1-Lane events are significantly greater than those for 2-Lane events. Whereas the maximum r-values for 2-Lane events exceed 1.0 in some cases, its maximum value among all WIM sites is 1.184. This indicates that the HL93 loading defined in the LRFD specification is fairly adequate in modeling the lifetime maximum loading on a span with two lanes loaded. For 1-Lane events, the maximum r-values are often greater than 1.5 with a maximum value among all WIM sites of 2.402. This indicates that the HL93 loading defined in the LRFD specification underestimates the lifetime maximum loading on a span with only one lane loaded. It should be noted that HL-93 load effects are being compared with routine truck traffic at a site, defined as all trucks with six or fewer axles that will include legal loads and routine permits. These un-analyzed routine permits are a form of exclusion traffic for a particular state and should be enveloped by the HL-93 design live load model. This simplified procedure for adjusting live load factors assumes that the site-to-

site variability in L_{max} is within the AASHTO LRFD calibration limits. This needs to be verified as a precondition for the use of Method I.

Adjustment of Live Load Factors Using Method II

An example illustrating the application of the protocols for adjusting the load factors for Strength I using the reliability-based approach is presented. The illustration is provided for a set of bridges varying in span length between 60 ft to 200 ft with beam spacing varying between 4 ft and 12 ft. Composite steel and prestressed concrete simple span bridges are selected.

The procedure follows the protocols provided in Step 13.1 Method II using the equations of Chapter 2 and the results are given in Tables 37 through 46. For example, using the data provided by Nowak (1999) for a typical 60-ft simple span composite steel bridge with beams at 4-ft spacing, the wearing surface dead load is estimated to be D_W=49 kip-ft (referred to as D_3 in Tables 31 and 32), the other dead loads are combined into D_C=284 kip-ft (with D_{C1}=39 kip-ft for factory made members (referred to as D_1 in Tables 31 and 32, and D_{C2}=245 kip-ft for cast in place members referred to as D_2 in Tables 31 and 32). Assuming that $\left(\dfrac{K_g}{12Lt_s^3} \right) = 1.0$ as suggested by the AASHTO LRFD (2007) for the cases when the detailed design is not available, Eq. (34) will yield a distribution factor D.F. =0.42 for two lanes loaded and Eq. (33) gives D.F. =0.33 for one lane loaded. Given that the AASHTO HL-93 lane load moment for a 60-ft simple span is 288 kip-ft and the HL-93 truck load is 805 kip-ft and applying the dynamic allowance factor IM=1.33 on the truck load, Equation 32 would lead to a nominal required resistance for a single beam R_n=1430 kip-ft for the two-lane case and R_n=1210 kip-ft for the one lane case. Since in this case the R_n value for two lanes is higher than that obtained for one-lane loading, the two-lane case governs the design.

Similar calculations can be executed to find the required nominal bending moment capacity of steel and prestressed concrete bridges having different span lengths and beam spacings. For example, Tables 31 and 32 show the nominal bending moment resistances obtained using Equation 32 with the AASHTO LRFD specified live load factor γ_L=1.75 for a sample of simple span bridge configurations. The configurations selected and the corresponding values for the dead weights are adopted from the report of the AASHTO LRFD calibration study (Nowak; 1999).

Table 37. Calculation of Nominal Resistance, R_n, using current LRFD for a sample of typical composite steel bridges.

Composite steel		Dead Loads			HL-93		Required Nominal Resist.	
Span	Spacing	D1	D2	D3	Truck load	lane load	two lanes	one lane
ft	ft	kip-ft	kip-ft	kip-ft	kip-ft	kip-ft	kip-ft	kip-ft
60	4	39	245	49	805	288	1430.07	1210.44
60	6	48	335	73	805	288	1905.25	1580.00
60	8	70	414	97	805	288	2362.18	1931.67
60	10	84	521	122	805	288	2831.06	2295.99
60	12	103	639	146	805	288	3307.38	2668.51

Composite steel			Dead Loads		HL-93		Required Nominal Resist.	
Span	Spacing	D1	D2	D3	Truck load	lane load	one lane	two lanes
ft	ft	kip-ft	kip-ft	kip-ft	kip-ft	kip-ft	kip-ft	kip-ft
120	4	502	981	194	1882	1152	4552.49	3925.44
120	6	607	1341	292	1882	1152	6019.48	5112.16
120	8	650	1656	389	1882	1152	7302.59	6119.07
120	10	681	2083	486	1882	1152	8676.66	7220.72
120	12	773	2556	583	1882	1152	10158.57	8433.60

Composite steel			Dead Loads		HL-93		Required Nominal Resist.	
Span	Spacing	D1	D2	D3	Truck load	lane load	one lane	two lanes
ft	ft	kip-ft	kip-ft	kip-ft	kip-ft	kip-ft	kip-ft	kip-ft
200	4	2780	2725	540	3320	3200	12317.82	10987.92
200	6	3303	3725	810	3320	3200	16016.30	14116.20
200	8	3790	4600	1080	3320	3200	19422.06	16963.58
200	10	4190	5788	1350	3320	3200	23046.27	20039.36
200	12	4875	7100	1620	3320	3200	27132.98	23586.16

Table 38. Calculation of Nominal Resistance, R_n, using current LRFD for a sample of typical prestressed concrete bridges.

Prestressed Concrete			Dead Loads		HL-93		Required Nominal Resist.	
Span	Spacing	D1	D2	D3	Truck load	lane load	two lanes	one lane
ft	ft	kip-ft	kip-ft	kip-ft	kip-ft	kip-ft	kip-ft	kip-ft
60	4	262	245	49	805	288	1708.82	1489.19
60	6	262	335	73	805	288	2172.75	1847.50
60	8	262	414	97	805	288	2602.18	2171.67
60	10	262	521	122	805	288	3053.56	2518.49
60	12	262	639	146	805	288	3506.13	2867.26

Prestressed Concrete			Dead Loads		HL-93		Required Nominal Resist.	
Span	Spacing	D1	D2	D3	Truck load	lane load	one lane	two lanes
ft	ft	kip-ft	kip-ft	kip-ft	kip-ft	kip-ft	kip-ft	kip-ft
120	4	1899	981	194	1882	1152	6298.74	5671.69
120	6	1899	1341	292	1882	1152	7634.48	6727.16
120	8	1899	1656	389	1882	1152	8863.84	7680.32
120	10	1899	2083	486	1882	1152	10199.16	8743.22
120	12	1899	2556	583	1882	1152	11566.07	9841.10

Prestressed Concrete			Dead Loads		HL-93		Required Nominal Resist.	
Span	Spacing	D1	D2	D3	Truck load	lane load	one lane	two lanes
ft	ft	kip-ft	kip-ft	kip-ft	kip-ft	kip-ft	kip-ft	kip-ft
200	4	5650	2725	540	3320	3200	15905.32	14575.42
200	6	5650	3725	810	3320	3200	18950.05	17049.95
200	8	5650	4600	1080	3320	3200	21747.06	19288.58
200	10	5650	5788	1350	3320	3200	24871.27	21864.36
200	12	5650	7100	1620	3320	3200	28101.73	24554.91

Live Load Effect Modeling

The work performed as part of NCHRP 12-76 consisted of collecting WIM truck traffic data on various sites within the U.S. and using these data to project for the maximum expected live load effects, L_{max}, over the 75-year design life of a new bridge. For example, Table 33 provides a set of L_{max} values obtained for the maximum bending moments of 60-ft, 120-ft and 200-ft simple span bridges from 8 sites in California. The L_{max} values were calculated for one lane of traffic and for two lanes of traffic and they are normalized with respect to the effect of one lane of HL-93 loading. For example the results of Table 33 for the 60-ft span, show that on the average the 75-year maximum load effect will be equal to 1.321 times the static load effect of the HL-93 design load. The values vary from site to site showing a standard deviation for site-to-site variability of 0.060 or a Coefficient of Variation COV $V_{site-to-site}$=4.5%. Table 34 gives the calculated L_{max} values for the same sites for the cases when two lanes are loaded simultaneously. Notice that the 60-ft span the two-lane L_{max} is on the average equal to 1.44 times the effect of one lane of HL-93 with a site-to-site variability expressed through a COV, $V_{site-to-site}$=13.6%. The higher COV for the two-lane effects is partially due to the differences in the number of two-lane events collected at each site over the one year WIM data collection period as compared to the number of data samples collected for single truck events in the main traffic lane. Other factors that influence the differences in the COV's include the Average Daily Truck Traffic at the sites, the frequency of heavy legal and overloaded vehicles (illegal, exclusion, or permit) in the truck traffic stream, and the probability of having two lanes loaded by such vehicles.

Table 39. L_{max} values for one lane for the moment effect of simple span beams

1-Lane Event Lmax for Simple Span Moment											
				Span Length (ft)							Max
State	Site ID	Direction	ADTT	20	40	60	80	100	120	160	200	Value
CA	0001	E/N	5058	1.370	1.278	1.239	1.206	1.173	1.164	1.137	1.086	1.370
CA	0001	W/S	4839	1.400	1.354	1.305	1.237	1.174	1.161	1.124	1.069	1.400
CA	0003	E	2790	1.190	1.216	1.293	1.268	1.219	1.191	1.149	1.106	1.293
CA	0004	W	3149	1.365	1.354	1.382	1.337	1.253	1.189	1.114	1.051	1.382
CA	0059	S	11627	1.340	1.291	1.368	1.358	1.338	1.293	1.212	1.127	1.368
CA	0060	N	11432	1.989	1.635	1.413	1.392	1.351	1.311	1.227	1.168	1.989
CA	0072	E/N	2318	1.138	1.228	1.297	1.255	1.221	1.140	1.052	1.003	1.297
CA	0072	W/S	2159	1.217	1.227	1.272	1.213	1.149	1.094	1.046	0.976	1.272
			Min Value	1.138	1.216	1.239	1.206	1.149	1.094	1.046	0.976	
			Avg Value	1.376	1.323	1.321	1.283	1.235	1.193	1.132	1.073	
			Max Value	1.989	1.635	1.413	1.392	1.351	1.311	1.227	1.168	
			stand. Dev.	0.266	0.137	0.060	0.070	0.076	0.074	0.065	0.063	0.101
			COV	0.193	0.104	0.045	0.054	0.061	0.062	0.058	0.059	0.057

Table 40. L_max values for two lanes for the moment effect of simple span beams

| | | | | \multicolumn{8}{c}{Span Length (ft)} | Max |
State	Site ID	Direction	ADTT	20	40	60	80	100	120	160	200	Value
2-Lane Event Lmax for Simple Span Moment												
CA	0001	E/N	5058	1.663	1.706	1.515	1.412	1.456	1.450	1.386	1.299	1.706
CA	0001	W/S	4839	1.592	1.475	1.324	1.382	1.445	1.460	1.410	1.341	1.592
CA	0003	E	2790	1.447	1.421	1.429	1.392	1.374	1.332	1.281	1.213	1.447
CA	0004	W	3149	1.575	1.441	1.440	1.460	1.515	1.529	1.479	1.388	1.575
CA	0059	S	11627	1.678	1.665	1.490	1.553	1.562	1.578	1.506	1.419	1.678
CA	0060	N	11432	1.955	1.823	1.844	1.891	1.859	1.783	1.676	1.544	1.955
CA	0072	E/N	2318	1.368	1.235	1.172	1.199	1.224	1.233	1.177	1.122	1.368
CA	0072	W/S	2159	1.499	1.428	1.335	1.265	1.286	1.247	1.198	1.125	1.499
			Min Value	1.368	1.235	1.172	1.199	1.224	1.233	1.177	1.122	
			Avg Value	1.597	1.524	1.444	1.444	1.465	1.452	1.389	1.306	
			Max Value	1.955	1.823	1.844	1.891	1.859	1.783	1.676	1.544	
			stand. Dev.	0.179	0.191	0.196	0.211	0.195	0.183	0.168	0.148	
			COV	0.112	0.125	0.136	0.146	0.133	0.126	0.121	0.113	0.127

In addition to the site-to-site variability, the uncertainties associated with the estimated values for L_{max} include the uncertainties within a site due to the random nature of L_{max} and the fact that the WIM data histograms do not necessarily include all the extreme load events that may occur within the 75-year design period of the bridge. An analysis of the results of the projections show that the uncertainties within a site are associated with a COV on L_{max} on the order of $V_{projection}=3.5\%$ for the projection of the one-lane maximum effect and a COV of $V_{projection}=5\%$ for the two side-by-side load effect. $V_{projection}$ was obtained from the analysis of the WIM data described in the draft protocols, by taking the ratio of the standard deviation σ_{max} obtained from Eq. (29) divided by the mean $L_{max}=\mu_{max}=$of Eq. (28).

Additional uncertainties are associated with L_{max} due to the limited number of data points used in the projections and the confidence levels associated with the number of sample points. Using the +/-95% confidence limits, it is estimated that the COV is on the order of $V_{data}=2\%$ for the one-lane case and about $V_{data}=3\%$ for the two-lane case. V_{data} is an estimate obtained from the upper and lower 95% confidence intervals calculated as presented earlier in the report entitled under Step 5.3 "Assessing the Statistical Adequacy of WIM Data". We took the upper and lower 95% values and assumed that they fall within +/- 1.96 standard deviations from the mean. So, by dividing the difference between the mean value and the upper and lower 95% values by 1.96 we obtain estimates of the standard deviation which when divided by the mean value give estimates of the COV. For example, the upper and lower 95% limits for the WIM data collected at the I-81 site in New York State for L_{max} of the one lane loading for the moment at the midpoint a 60-ft simple span are 1.964 and 1.839. The mean L_{max} for the one lane loading case is obtained as 1.906. Thus, one estimate of the standard deviation is obtained as (1.906-1.839)/1.96=0.034. The estimate of the COV, V_{data}, becomes 0.034/1.906=0.018 or about 1.8%. Another estimate is obtained as (1.964-1.906)/1.96/1.906=1.6%. The final V_{data} used is rounded up to 2%. Similarly for the two-lane loading, the mean is $L_{max}=3.276$, the lower 95% limit is 3.058 and the upper 95% limit is 3.462. One estimate for the standard deviation is (3.276-3.058)/1.96=0.111 and the estimate for the COV is 0.111/3.276=3.40% another estimate is obtained as (3.462-3.276)/1.96/3.276=2.90% and the final V_{data} used is 3%. Strictly speaking, the approach followed for finding V_{data} is not exact, but the V_{data} calculated gives some measure of the uncertainty related to the size of the data sample.

Nowak (1999) also observed that the dynamic amplification factors augmented the L_{max} load effect by an average of 13% for one lane of traffic and by 9% for side-by-side trucks. The dynamic amplification also resulted in a COV of V_{IM}=9% on the one-lane load effect and V_{IM}=5.5% on the two-lane effect. In previous studies on live load modeling, Ghosn & Moses (1985) included the uncertainties in estimating the lane distribution factor which was associated with a COV equal to V_{DF}=8% based on field measurements on typical steel and prestressed concrete bridges. This information is used in Eq. (35) and (36) to find the mean value of the live load and the COV.

For example, the application of Equation (35) for the average load effect on a 60-ft simple span bridge with beams at 4-ft from the California sites would lead to:

For one lane:
$$\overline{LL} = L_{max\ beam} \times HL_{93} = 1.32 \times (288 + 805) \times 1.13 \times 0.33 / 1.2 = 448\ kip - ft$$
For two lanes:
$$\overline{LL} = L_{max\ beam} \times HL_{93} = 1.44 \times (288 + 805) \times 1.09 \times 0.42 / 2 = 360\ kip - ft$$

For the one-lane case, L_{max}=1.32 is obtained from Table 39 as the average value for the California sites for 60-ft spans. L_{max}=1.44 for two lanes is obtained from Table 40 as the average value for the 60-ft spans from all the sites.

Notice that the mean live load effect for the one lane case is higher than that of the two-lane case. This is due to the fact that the number of side-by-side events is generally low compared to the number of single lane events, thus the projection to the 75-year maximum for one lane of traffic would lead to the possibility of having a very heavy single truck load (1.32 times the effect of the HL-93 load) as compared to having two very heavy side-by-side trucks the maximum for each one being on the order of 0.72 (1.44/2) times the effect of the HL-93 live load. Also, the load distribution factor D.F. indicates that the effect of a single truck would more likely load a single beam by 27% of the weight of one truck (D.F.=0.33/1.2=0.27) as compared to the weights of two trucks side-by-side which would be more evenly spread over all the beams of the bridge such that the most loaded beam would carry 21% of the lane load (D.F=0.42/2=0.21). Furthermore, the dynamic amplification peaks of two trucks are not likely to coincide due to the different natural frequencies, which would lead to a lower overall dynamic allowance factor for the two-lane case (1.09) as compared to the one-lane case (1.13). Note, that in these calculations and following the procedure of Nowak (1999), it has been assumed that the load distribution factors provided by AASHTO LRFD are the expected (mean) values. It should also be mentioned that the data for the dynamic allowance and for the load distribution factors as used by Nowak (1999) are based on very limited data and much more research is needed on these topics to study how these factors change from site to site and how they relate to the truck weights and traffic data. However, these issues are beyond the scope of this study and in this case, this study uses the same data applied during the AASHTO LRFD calibration.

The application of Equation 36 for the 60-ft L_{max} yields:

For two lanes: $V_{LL} = \sqrt{(13.5\%)^2 + (5\%)^2 + (3\%)^2 + (5.5\%)^2 + (8\%)^2} = 18\%$

For one lane: $V_{LL} = \sqrt{(4.5\%)^2 + (3.5\%)^2 + (2\%)^2 + (9\%)^2 + (8\%)^2} = 13\%$

$V_{site-to-site}$ values of 4.5% and 13.5% for one-lane and two-lane cases are respectively obtained from Tables 39 and 40 for the 60-ft spans. The standard deviation for the two-lane case becomes $\sigma_{LL} = V_{LL} * \overline{LL} = 65$ kip-ft and for the one-lane case $\sigma_{LL}=58$ kip-ft.

Thus, the COV of the two-lane effect for the California sites is comparable to the $V_{LL}=19\%$ to 20% obtained by Ghosn & Moses (1985) and subsequently used by Nowak (1999) during the calibration of the AASHTO LRFD specifications. Note that the COV for the single lane effect is lower than that of the two-lane effect indicating that the estimation of the maximum load effect for one lane is associated with lower levels of uncertainty. The difference in the two V_{LL} COV's is primarily due to the site-to-site variability, which is much higher for the two-lane loading as compared to that for the one-lane loading.

Modeling of Other Random Variables

The application of Equations (37) and (38) for the beams of the 60-ft composite steel bridge at 4-ft spacing will yield mean dead loads: $\overline{D_{C1}} = 40$ kip-ft, $\overline{D_{C2}} = 257$ kip-ft and $\overline{D_w} = 49$ kip-ft. The standard deviations are: $\sigma_{DC1}=3.2$ kip-ft, $\sigma_{DC2}=25.7$kip-ft and $\sigma_{DW}=12.3$ kip-ft. The mean of the total dead load becomes $\overline{DL} = 346$ kip-ft and using the square root of the sum of the square, the standard deviation for the total dead load is $\sigma_{DL}=29$ kip-ft. The mean nominal resistance for a two-lane bridge is $\overline{R} = 1602$ kip-ft and for a one-lane bridge, $\overline{R} = 1355$ kip-ft. The standard deviation for the resistance for the two lane bridge is $\sigma_R=160$ kip-ft and for the one-lane bridge $\sigma_R=136$ kip-ft. For the maximum moment of the sample of simple span bridges studied in this report, Equations 37 and 38 will yield the mean and standard deviation values provided in Tables 35 and 36 for the bending moment of simple span composite steel and prestressed concrete bridges.

Calculation of Reliability Index and Calibration of Live Load Factor

The adjustment of the live load factors requires the calculation of the reliability index for different values of the live load factor γ_L. The γ_L that produces reliability index values as close to the target as possible for all material types, spans and geometric configurations will be adopted as the final γ_L. Using $\gamma_L=1.75$ for the one-lane 60-ft bridge with beams at 4-ft spacing the reliability index is calculated from Eq. (40) as:

$$\text{One lane:} \qquad \beta = \frac{1355 - 346 - 448}{\sqrt{136^2 + 29_L^2 + 58_L^2}} = 3.72$$

For the two-lane 60-ft bridge with beams at 4-ft spacing the reliability index is calculated as:

$$\text{Two lanes:} \qquad \beta = \frac{1602 - 346 - 360}{\sqrt{160^2 + 29^2 + 65^2}} = 5.12$$

The results for this example indicate that, based on the WIM data collected on the California sites, the use of the AASHTO LRFD strength design equation with a live load factor $\gamma_L=1.75$ and the HL-93 loading leads to a reliability index $\beta=3.72$ for the 75-year design life of a 60-ft simple span steel bridge with beams at 4-ft spacing. In this case, the one-lane load governs the safety of the bridge beams producing a reliability index value of $\beta=3.72$ which is higher than the target $\beta=3.50$ set during the calibration of the AASHTO LRFD specifications. It should be emphasized that the target $\beta=3.50$ was set during the AASHTO LRFD code calibration based on the

observation made at the time that under the generic live loading data, typical bridge configurations that were designed to satisfy the AASHTO LFD specifications, produced an average reliability index β=3.50.   Thus, the new LRFD code was developed in order for new designs to match this β=3.50 as closely as possible for all bridge spans, configurations and material types.

The two-lane loading leads to a much higher reliability index value of β=5.12.   This indicates that for the two-lane case, the AASHTO LRFD is conservative.

It is noted that for the sake of simplicity this report assumed that the resistance, dead load and live load follow Normal (Gaussian) distributions. The work of Nowak (1999) assumed that the resistance is lognormal while the combination of all the loads is Normal. A preliminary sensitivity analysis was performed indicating that the Normal model produces lower reliability index values than the LogNormal model. The calculation of the reliability index can be executed using Monte Carlo simulations (or other simulation techniques) if the probability distributions of all the random variables are available.   Previous sensitivity analyses performed by this research team has demonstrated that the calibration of LRFD design equations is not sensitive to the probability distribution type used as long as the new equations are designed to match an average reliability index calculated using the same models and probability distributions (Ghosn & Moses 1985 and 1986)

California Data

Tables 35 and 36 show the reliability index values obtained for the maximum bending moment of a sample of simple span steel composite and prestressed bridge configurations. The results show that for the California truck traffic conditions, the reliability index for one lane is on the average equal to β=3.55 which is close to the target β=3.50. For two lanes of truck traffic, the average reliability index is β=4.63. This indicates that for the two-lane loading of California bridges, the current AASHTO LRFD is conservative producing higher reliability index values than the target β=3.50 set by the AASHTO LRFD code writers. The range of the β's however is large varying between a β=5.32 for short span prestressed concrete bridges with closely spaced beams to β=4.0 for long span prestressed concrete bridges with closely spaced beams. The fact that the loading of the short span bridges is dominated by the live loads while the long span bridges' loading is dominated by the dead load indicates that for California bridges, the HL-93 nominal design live load is conservative.

If one wishes to reduce the reliability index for the two lane cases and achieve an average reliability index for the two-lane cases equal to the target β=3.5, then a live load factor γ_L=1.20 should be used. This would mean that the HL-93 loading should be associated with a multiple lane reduction factor =1.46 (1.75/1.20) when checking the design for two lanes of traffic. Alternatively, for the California WIM data, one could keep the current AASHTO LRFD live load factor γ_L=1.75 and accept the fact that the design will yield the target reliability index for one lane of traffic with the understanding that the design would be conservative for multiple lanes.

The adjusted γ_L=1.20 for the two-lane loading conditions is obtained by trial and error using the protocols steps 13.1 Method II. These steps are based on: 1) having established a representative sample of bridge configurations that represent the most common bridge spans, types, and configurations in the state; and 2) having pre-determined an appropriate reliability index target β_{target}, that bridges evaluated using the adjusted live load factor should meet.

In usual reliability-based adjustments of design and evaluation equations, the reliability index after adjusting the live load factor should match the target reliability, β_{target}, as closely as possible for all representative span ranges, bridge types, loading cases, etc.   Given the large

spread in the calculated reliability index values observed in Tables 35 and 36, this may not be possible to achieve by only adjusting the live load factor. Furthermore, the sample of bridges selected for analysis may not actually be representative of the California bridges. However, to illustrate the process, the steps provided in 13.1 outline a reliability-based live load adjustment procedure that assumes that the target reliability index has already been established as β_{target}=3.5 for the sample of bridges analyzed in the previous section, and the goal of the trial and error analysis process is to adjust the live load factor γ_L so that the average reliability index of the bridges analyzed after adjusting the live load factor will produce the target index.

Florida Data

The results presented above for the California WIM data may not be consistent with the data from other states or jurisdictions. The differences are mainly due to the legal truck weight limits or exemptions and the permit overload frequencies and weight regulations that may vary from state to state. For example, if the L_{max} values generated from the Florida WIM data sites are used as input for the live load modeling, the reliability index values shown in Tables 37 and 38 are obtained. These tables show that the reliability index for one lane of loading drops to an average of β=2.58. The two-lane L_{max} would lead to an average reliability index β=3.96. The latter value is still higher than the target β=3.5 while the one lane reliability is lower than the target. It is noted that the Florida data shows high variations from the results of different sites leading to a high COV for L_{max} and subsequently lower reliability index values than those observed from the California data. It is noted that if the live load factor is raised to γ_L=2.37 the reliability indexes for the Florida sites would increase to β=3.50 for the one-lane cases, and β=4.95 for the two-lane cases, bringing the reliability indexes more in line with the California results.

Indiana Data

Using the L_{max} values generated from the Indiana WIM data sites, the reliability index values shown in Tables 39 and 40 are obtained. These tables show that the reliability index for one lane of loading is on the average equal to β=3.16 for one-lane loading. The two-lane L_{max} would lead to an average reliability index β=4.71. The latter value is higher than the target β=3.5 while the one lane reliability is slightly lower than the target. The Indiana data shows a site-to-site variability in COV's on the order of 11% to 15% for both one-lane and two-lanes loadings. This is compared to the CA data that shows low site-to-site variability in the one-lane loading cases (typically less than 10% for spans greater than 40ft) and the Florida data that shows high COV's for both the one-lane and two-lane cases (typically greater than 20%).

Summary

Using a single maximum or characteristic value for L_{max} for a State would be acceptable if the scatter or variability in L_{max} from site-to-site for the state was equal to (or less than to be conservative) the COV assumed in the LRFD calibration. If the variability in the WIM data is much greater than that assumed in the calibration, then the entire LRFD calibration to achieve the target 3.5 reliability index may no longer be valid for that state and a simple adjustment of the live load factor as given in the Method I of Step 13.1 protocols should not be done. This example presented a reliability-based procedure to adjust the live load factors based on the L_{max} values assembled for each state. The results show that the average reliability index values vary considerably from state to state as a function of the average L_{max} values, the live load case that governs, and the site-to-site variability expressed in terms of the COV of L_{max}. Also, the results reflect the fact that current WIM data indicates that one-lane loadings are often dominating the

safety of bridge members due to the lower number of side-by-side events and the lower load effects produced by these events when compared to the data used during the calibration of the AASHTO LRFD. The Method II procedure outlined provides a more robust method for updating live load factors for LRFD design using recent WIM data.

Table 41. Reliability index calculation for bending moment of simple span composite steel bridges based on California WIM data

Span	spacing	Ave. Res. 1	Av. Res. 2	σ Res. 1	σ Res. 2	Mean DL	σ DL	Mean LL 1	Mean LL 2	σ LL 1	σ LL 2	beta 1-lane	beta 2-lane
60	4	1356	1602	136	160	346	28	447	362	60	64	3.73	5.11
60	6	1770	2134	177	213	474	38	567	476	76	84	3.71	5.09
60	8	2163	2646	216	265	604	48	675	583	91	103	3.69	5.07
60	10	2572	3171	257	317	756	61	776	684	105	121	3.66	5.02
60	12	2989	3704	299	370	923	74	870	782	117	138	3.63	4.97
Span	spacing	Ave. Res. 1	Av. Res. 2	σ Res. 1	σ Res. 2	Mean DL	σ DL	Mean LL 1	Mean LL 2	σ LL 1	σ LL 2	beta 1-lane	beta 2-lane
120	4	4396	5099	440	510	1741	117	949	904	134	153	3.60	4.50
120	6	5726	6742	573	674	2325	160	1193	1181	169	200	3.57	4.49
120	8	6853	8179	685	818	2797	199	1414	1440	200	244	3.57	4.50
120	10	8087	9718	809	972	3375	247	1618	1686	229	286	3.53	4.47
120	12	9446	11378	945	1138	4063	301	1811	1923	256	326	3.49	4.42
Span	spacing	Ave. Res. 1	Av. Res. 2	σ Res. 1	σ Res. 2	Mean DL	σ DL	Mean LL 1	Mean LL 2	σ LL 1	σ LL 2	beta 1-lane	beta 2-lane
200	4	12306	13796	1231	1380	6265	377	1630	1611	228	258	3.38	4.07
200	6	15810	17938	1581	1794	8123	500	2035	2095	285	335	3.36	4.08
200	8	18999	21753	1900	2175	9814	614	2401	2547	336	408	3.35	4.09
200	10	22444	25812	2244	2581	11743	749	2740	2977	384	476	3.32	4.06
200	12	26416	30389	2642	3039	14096	906	3059	3390	428	542	3.28	4.01

Table 42. Reliability index calculation for bending moment of simple span prestressed concrete bridges based on California WIM data

Span	spacing	Ave. Res. 1	Av. Res. 2	σ Res. 1	σ Res. 2	Mean DL	σ DL	Mean LL 1	Mean LL 2	σ LL 1	σ LL 2	beta 1-lane	beta 2-lane
60	4	1564	1794	125	144	576	34	447	362	60	64	3.78	5.32
60	6	1940	2281	155	183	695	44	567	476	76	84	3.80	5.40
60	8	2280	2732	182	219	802	52	675	583	91	103	3.82	5.45
60	10	2644	3206	212	256	939	64	776	684	105	121	3.80	5.45
60	12	3011	3681	241	295	1087	77	870	782	117	138	3.78	5.43

prestressed concrete

Span	spacing	Ave. Res. 1	Av. Res. 2	σ Res. 1	σ Res. 2	Mean DL	σ DL	Mean LL 1	Mean LL 2	σ LL 1	σ LL 2	beta 1-lane	beta 2-lane
120	4	5955	6614	476	529	3180	187	949	904	134	153	3.45	4.35
120	6	7064	8016	565	641	3656	215	1193	1181	169	200	3.53	4.51
120	8	8064	9307	645	745	4084	245	1414	1440	200	244	3.57	4.61
120	10	9180	10709	734	857	4629	285	1618	1686	229	286	3.58	4.64
120	12	10333	12144	827	972	5223	331	1811	1923	256	326	3.56	4.64

prestressed concrete

Span	spacing	Ave. Res. 1	Av. Res. 2	σ Res. 1	σ Res. 2	Mean DL	σ DL	Mean LL 1	Mean LL 2	σ LL 1	σ LL 2	beta 1-lane	beta 2-lane
200	4	15304	16701	1224	1336	9221	545	1630	1611	228	258	3.28	4.00
200	6	17902	19898	1432	1592	10541	620	2035	2095	285	335	3.36	4.17
200	8	20253	22834	1620	1827	11730	699	2401	2547	336	408	3.41	4.28
200	10	22958	26115	1837	2089	13247	808	2740	2977	384	476	3.41	4.32
200	12	25783	29507	2063	2361	14895	934	3059	3390	428	542	3.40	4.32

Table 43. Reliability index calculation for bending moment of simple span composite steel bridges based on Florida WIM data

Span	spacing	Ave. Res. 1	Av. Res. 2	σ Res. 1	σ Res. 2	Mean DL	σ DL	Mean LL 1	Mean LL 2	σ LL 1	σ LL 2	beta 1-lane	beta 2-lane
60	4	1356	1602	136	160	346	28	566	425	151	134	2.25	4.02
60	6	1770	2134	177	213	474	38	718	558	192	177	2.27	4.02
60	8	2163	2646	216	265	604	48	855	683	229	216	2.30	4.02
60	10	2572	3171	257	317	756	61	982	802	263	254	2.32	4.01
60	12	2989	3704	299	370	923	74	1102	916	295	290	2.34	3.99
Span	spacing	Ave. Res. 1	Av. Res. 2	σ Res. 1	σ Res. 2	Mean DL	σ DL	Mean LL 1	Mean LL 2	σ LL 1	σ LL 2	beta 1-lane	beta 2-lane
120	4	4396	5099	440	510	1741	117	1201	1036	315	269	2.69	4.01
120	6	5726	6742	573	674	2325	160	1510	1354	397	351	2.71	4.00
120	8	6853	8179	685	818	2797	199	1789	1651	470	429	2.71	4.01
120	10	8087	9718	809	972	3375	247	2048	1934	538	502	2.72	3.99
120	12	9446	11378	945	1138	4063	301	2292	2205	602	572	2.72	3.96
Span	spacing	Ave. Res. 1	Av. Res. 2	σ Res. 1	σ Res. 2	Mean DL	σ DL	Mean LL 1	Mean LL 2	σ LL 1	σ LL 2	beta 1-lane	beta 2-lane
200	4	12306	13796	1231	1380	6265	377	2120	1851	565	498	2.82	3.78
200	6	15810	17938	1581	1794	8123	500	2648	2407	706	648	2.83	3.79
200	8	18999	21753	1900	2175	9814	614	3123	2926	833	788	2.83	3.79
200	10	22444	25812	2244	2581	11743	749	3565	3420	950	921	2.83	3.78
200	12	26416	30389	2642	3039	14096	906	3980	3894	1061	1049	2.82	3.74

Table 44. Reliability index calculation for bending moment of simple span prestressed concrete bridges based on Florida WIM data

Span	spacing	Ave. Res. 1	Av. Res. 2	σ Res. 1	σ Res. 2	Mean DL	σ DL	Mean LL 1	Mean LL 2	σ LL 1	σ LL 2	beta 1-lane	beta 2-lane
60	4	1564	1794	125	144	576	34	1201	1036	151	134	2.21	4.07
60	6	1940	2281	155	183	695	44	1510	1354	192	177	2.20	4.09
60	8	2280	2732	182	219	802	52	1789	1651	229	216	2.19	4.10
60	10	2644	3206	212	256	939	64	2048	1934	263	254	2.20	4.10
60	12	3011	3681	241	295	1087	77	2292	2205	295	290	2.21	4.09

prestressed concrete

Span	spacing	Ave. Res. 1	Av. Res. 2	σ Res. 1	σ Res. 2	Mean DL	σ DL	Mean LL 1	Mean LL 2	σ LL 1	σ LL 2	beta 1-lane	beta 2-lane
120	4	5955	6614	476	529	3180	187	2120	1851	315	269	2.67	3.91
120	6	7064	8016	565	641	3656	215	2648	2407	397	351	2.68	4.01
120	8	8064	9307	645	745	4084	245	3123	2926	470	429	2.69	4.07
120	10	9180	10709	734	857	4629	285	3565	3420	538	502	2.69	4.09
120	12	10333	12144	827	972	5223	331	3980	3894	602	572	2.68	4.09

prestressed concrete

Span	spacing	Ave. Res. 1	Av. Res. 2	σ Res. 1	σ Res. 2	Mean DL	σ DL	Mean LL 1	Mean LL 2	σ LL 1	σ LL 2	beta 1-lane	beta 2-lane
200	4	15304	16701	1224	1336	9221	545	1630	1611	565	498	2.75	3.71
200	6	17902	19898	1432	1592	10541	620	2035	2095	706	648	2.79	3.84
200	8	20253	22834	1620	1827	11730	699	2401	2547	833	788	2.80	3.92
200	10	22958	26115	1837	2089	13247	808	2740	2977	950	921	2.80	3.94
200	12	25783	29507	2063	2361	14895	934	3059	3390	1061	1049	2.80	3.94

Table 45. Reliability index calculation for bending moment of simple span composite steel bridges based on Indiana WIM data

Span	spacing	Ave. Res. 1	Av. Res. 2	σ Res. 1	σ Res. 2	Mean DL	σ DL	Mean LL 1	Mean LL 2	σ LL 1	σ LL 2	beta 1-lane	beta 2-lane
60	4	1356	1602	136	160	346	28	508	376	62	50	3.31	5.17
60	6	1770	2134	177	213	474	38	644	495	79	65	3.30	5.14
60	8	2163	2646	216	265	604	48	767	606	94	80	3.29	5.12
60	10	2572	3171	257	317	756	61	881	711	107	94	3.28	5.07
60	12	2989	3704	299	370	923	74	988	812	121	107	3.26	5.01
Span	spacing	Ave. Res. 1	Av. Res. 2	σ Res. 1	σ Res. 2	Mean DL	σ DL	Mean LL 1	Mean LL 2	σ LL 1	σ LL 2	beta 1-lane	beta 2-lane
120	4	4396	5099	440	510	1741	117	1137	888	162	100	3.15	4.64
120	6	5726	6742	573	674	2325	160	1430	1161	203	131	3.14	4.62
120	8	6853	8179	685	818	2797	199	1695	1415	241	160	3.14	4.63
120	10	8087	9718	809	972	3375	247	1940	1657	275	187	3.12	4.59
120	12	9446	11378	945	1138	4063	301	2170	1890	308	214	3.09	4.54
Span	spacing	Ave. Res. 1	Av. Res. 2	σ Res. 1	σ Res. 2	Mean DL	σ DL	Mean LL 1	Mean LL 2	σ LL 1	σ LL 2	beta 1-lane	beta 2-lane
200	4	12306	13796	1231	1380	6265	377	1999	1598	264	190	3.08	4.11
200	6	15810	17938	1581	1794	8123	500	2496	2078	329	247	3.07	4.12
200	8	18999	21753	1900	2175	9814	614	2944	2526	389	301	3.07	4.13
200	10	22444	25812	2244	2581	11743	749	3360	2952	444	351	3.05	4.10
200	12	26416	30389	2642	3039	14096	906	3752	3362	495	400	3.02	4.05

Table 46. Reliability index calculation for bending moment of simple span prestressed concrete bridges based on IndianaWIM data

Span	spacing	Ave. Res. 1	Av. Res. 2	σ Res. 1	σ Res. 2	Mean DL	σ DL	Mean LL 1	Mean LL 2	σ LL 1	σ LL 2	beta 1-lane	beta 2-lane
60	4	1564	1794	125	144	576	34	508	376	62	50	3.34	5.40
60	6	1940	2281	155	183	695	44	644	495	79	65	3.35	5.50
60	8	2280	2732	182	219	802	52	767	606	94	80	3.36	5.55
60	10	2644	3206	212	256	939	64	881	711	107	94	3.36	5.55
60	12	3011	3681	241	295	1087	77	988	812	121	107	3.34	5.53

prestressed concrete

Span	spacing	Ave. Res. 1	Av. Res. 2	σ Res. 1	σ Res. 2	Mean DL	σ DL	Mean LL 1	Mean LL 2	σ LL 1	σ LL 2	beta 1-lane	beta 2-lane
120	4	5955	6614	476	529	3180	187	1137	888	162	100	3.05	4.46
120	6	7064	8016	565	641	3656	215	1430	1161	203	131	3.10	4.64
120	8	8064	9307	645	745	4084	245	1695	1415	241	160	3.13	4.76
120	10	9180	10709	734	857	4629	285	1940	1657	275	187	3.13	4.80
120	12	10333	12144	827	972	5223	331	2170	1890	308	214	3.12	4.80

prestressed concrete

Span	spacing	Ave. Res. 1	Av. Res. 2	σ Res. 1	σ Res. 2	Mean DL	σ DL	Mean LL 1	Mean LL 2	σ LL 1	σ LL 2	beta 1-lane	beta 2-lane
200	4	15304	16701	1224	1336	9221	545	1999	1598	264	190	2.99	4.04
200	6	17902	19898	1432	1592	10541	620	2496	2078	329	247	3.05	4.22
200	8	20253	22834	1620	1827	11730	699	2944	2526	389	301	3.09	4.34
200	10	22958	26115	1837	2089	13247	808	3360	2952	444	351	3.09	4.37
200	12	25783	29507	2063	2361	14895	934	3752	3362	495	400	3.08	4.38

Calibrate Overload Load Factors for Strength II (Step 13.4)

Reliability Analysis and Adjustment of Live Load Factor for Case I – Permit vehicle alone
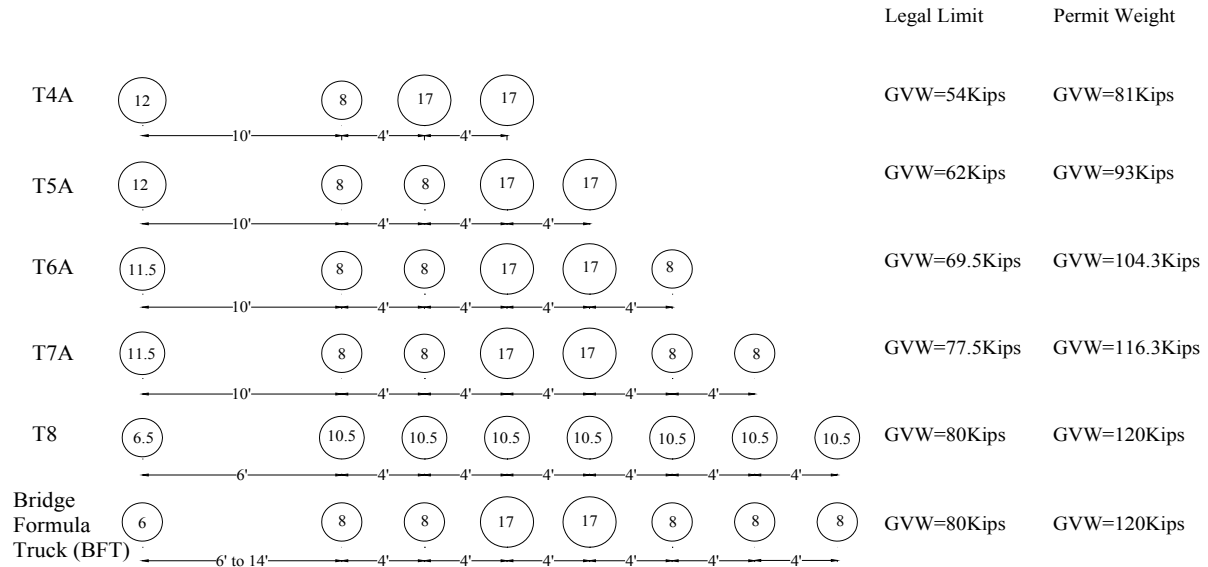
Figure 38. Examples of Permit Truck Configurations

To execute the reliability calculations, we will use a set of typical permit vehicles configurations as shown in Figure 38. These configurations are for typical Special Hauling Vehicles (SHV) and are adopted from the work performed for NCHRP 12-63 (Sivakumar et al; 2006). The weights of these SHV's are increased by 150% from the legal limits to be considered as special permit loads. For 60-ft, 120-ft and 200-ft simple spans, these hypothetical permit vehicles produce the maximum moments of Table 47.

Table 47. Moment Effect for Set of Permit Trucks

Span length	Moments in kip-ft					
	T4A	T5A	T6A	T7A	T8	BFT
60 ft	1016	1116	1240	1346	1336	1405
120 ft	2230	2508	2802	3090	3134	3205
200 ft	3850	4366	4887	5415	5534	5604

The nominal resistance that would be required for a set of multi-beam simple span steel bridges can be calculated by applying Eq. 32 with γ_D=1.25 for component dead weights and γ_D=1.50 for the wearing surface. In Eq. 32, the effect of the permit trucks is multiplied by a load factor γ_L=1.35 after applying the D.F. of Eq. 33 and the impact factor specified in the AASHTO LRFD as IM=1.33. The required nominal resistance values for the cases considered in this example are provided in Table 48. In these calculations we are assuming that the dead loads of the components remain essentially unchanged when the applied live loads are changed. The application of Eq. 40 leads to the reliability index values provided in Table 49.

Table 48. Nominal Resistance for Beams of Simple Span Bridges under a Single Permit

Composite steel		Dead weight effect (kip-ft)			R_N Nominal resistance (kip-ft)					
Span (ft)	space (ft)	DC_1	DC_2	D_W	T4A	T5A	T6A	T7A	T8	BFT
60	4	39	245	49	928	978	1038	1091	1086	1120
60	6	48	335	73	1222	1285	1362	1428	1422	1465
60	8	70	414	97	1506	1580	1672	1751	1743	1795
60	10	84	521	122	1806	1892	1998	2089	2080	2139
60	12	103	639	146	2119	2215	2334	2436	2426	2492
Span (ft)	space (ft)	DC_1	DC_2	D_W	T4A	T5A	T6A	T7A	T8	BFT
120	4	502	981	194	3074	3190	3312	3432	3450	3480
120	6	607	1341	292	4041	4187	4341	4491	4515	4552
120	8	650	1656	389	4850	5023	5205	5384	5411	5455
120	10	681	2083	486	5768	5966	6175	6379	6411	6461
120	12	773	2556	583	6808	7029	7263	7492	7527	7583
Span (ft)	space (ft)	DC_1	DC_2	D_W	T4A	T5A	T6A	T7A	T8	BFT
200	4	2780	2725	540	9116	9307	9500	9695	9740	9765
200	6	3303	3725	810	11779	12018	12259	12502	12558	12590
200	8	3790	4600	1080	14206	14488	14772	15060	15125	15163
200	10	4190	5788	1350	16893	17214	17538	17867	17941	17984
200	12	4875	7100	1620	20073	20432	20794	21160	21243	21292

Table 49. Reliability Index for a Single Permit with γ_L=1.35

Composite steel		Reliability index, β					
Span (ft)	space (ft)	T4A	T5A	T6A	T7A	T8	BFT
60	4	3.31	3.34	3.37	3.39	3.39	3.40
60	6	3.30	3.33	3.36	3.38	3.38	3.39
60	8	3.28	3.31	3.34	3.37	3.37	3.38
60	10	3.25	3.29	3.32	3.34	3.34	3.36
60	12	3.22	3.26	3.29	3.32	3.31	3.33
Span (ft)	space (ft)						
120	4	3.01	3.05	3.08	3.12	3.12	3.13
120	6	2.99	3.03	3.07	3.10	3.11	3.11
120	8	2.99	3.03	3.07	3.10	3.10	3.11
120	10	2.96	3.00	3.04	3.07	3.08	3.09
120	12	2.93	2.97	3.01	3.04	3.05	3.06
Span (ft)	space (ft)						
200	4	2.78	2.81	2.84	2.86	2.87	2.87
200	6	2.77	2.80	2.83	2.86	2.87	2.87
200	8	2.78	2.81	2.83	2.86	2.87	2.87
200	10	2.76	2.79	2.82	2.84	2.85	2.85
200	12	2.74	2.77	2.80	2.82	2.83	2.83

The results of Table 49 illustrate the following points:

- For a given span length and beam spacing, the different vehicle configurations produce little change in the reliability index. The largest difference in β being on the order of 0.11 when the range is between β=3.22 to β=3.33 for the 60-ft span with beams at 12ft.
- Increasing the beam spacing leads to slightly lower reliability index values.
- Increasing span length leads to lower reliability index values.
- The average reliability index for the span lengths and beam spacings considered is on the order of $β_{ave}$=3.07 with a minimum value of β=2.74 and a maximum value β=3.40.
- Using a live load factor $γ_L$=1.35 for Strength II produces an average reliability index $β_{ave}$=3.07 for a single permit on the bridge. This average value is lower than the $β_{target}$=3.50 used for the calibration of the AASHTO LRFD equations. If an average reliability $β_{ave}$=3.50 is desired for the bridge configurations considered in this example, then a $γ_L$=1.62 should be used when considering the case of a permit load alone on the bridge. The $γ_L$=1.62 is obtained using a trial and error procedure. The process is repeated until a $β_{ave}$=3.5 is obtained.
- An average reliability index $β_{ave}$=2.5 was used for the calibration of the operating rating live load factor in the LRFR code. If an average reliability $β_{ave}$=2.5 is desired for the bridge configurations considered in this example, then a $γ_L$=1.04 should be used when considering the case of a permit load alone on the bridge.

Reliability Analysis and Adjustment of Live Load Factor for Case II – Two Permits side-by-side

In this case, we can assume that the axle weights and axle configurations of the two permit trucks are the same and are perfectly known so that the total maximum static live load effect on the bridge L_{max} is a deterministic value. However, this does not imply that the total live load effect on a bridge member is deterministic due to the uncertainties in estimating the dynamic effect represented by the dynamic amplification factor, IM, and the uncertainties in the structural analysis process that allocates the fraction of the total load to the most critical member. The structural analysis is represented by the load distribution factor, D.F. The equations for the D.F. of multi-girder bridges loaded in two lanes given in the AASHTO LRFD specifications assume that the two lanes are loaded by the same vehicle and give the load on the most critical beam as a function of the load in one of the lanes. Thus, the live load effect on one member can be given from Equation (46). According to Nowak (1999), the dynamic amplification factor augments the load effect by an average of 9% for side-by-side trucks. The dynamic amplification also resulted in a COV of V_{IM}=5.5% on the two-lane effect. We will also assume that the same COV for the lane distribution factor V_{DF}=8% obtained by Moses & Ghosn (1986) from field measurements on typical steel and prestressed concrete bridges is still valid. Therefore, for the loading of a single permit vehicle, the live load COV becomes: $V_{LL} = \sqrt{(5.5\%)^2 + (8\%)^2} = 9.71\%$.

The reliability index conditional on the arrival of two side-by-side permits on the bridge can then calculated using Eq. (40) where $\overline{R}$ is the mean resistance when the bridge member is designed for

127

two side-by-side permits and $\overline{\overline{LL}}$ is the live load effect on the beam due to two side-by-side permits.

The reliability index calculated from Eq. (40) in this case is conditional on having two side-by-side trucks. The probability that a bridge member would fail given that two permit vehicles are side-by-side can be calculated from $P_{f\,/\,side-by-side} = \Phi\left(-\beta_{cond}\right)$. However, the final unconditional probability of failure will depend on the conditional probability given two side-by-side events and the probability of having a situation with side-by-side permits as shown in Eq. (47). The probability of having two-side-by-side permits depends on the number of permit trucks expected to cross the bridge within the return period within which the permits are granted. In this example, we will assume that all the permits will likely cross the same bridges so that the number of permits crossing a certain bridge within a one-year period is equal to the number of permits granted. The percentage of these permits that will be side-by-side is related to the total number of crossings as provided in Table 50. For example, assuming that the number of permit-vehicles expected on a bridge during the return period when the permits are in effect will be on the order of 1000 vehicles then, according to Table 50, the probability of having side-by-side events is 0.54% (=0.19+0.14+0.21). This value is obtained by conservatively assuming that trucks within a headway distance H<60 ft are actually side-by-side.

Table 50. Multiple presence probabilities for side-by-side events as a function of headway distance

Maximum MP Probabilities based on 5 WIM sites (10 directional sites) in New York State				
Maximum Side-by-Side Truck Multiple Presence Probabilities				
	Site Truck Traffic			
Headway H (ft)	Light: ADTT ≤ 1k	Average: 1k < ADTT ≤ 2.5k	Heavy: 2.5k < ADTT ≤ 5k	Very Heavy: ADTT > 5k
H ≤ 20	0.19	0.41	0.61	0.00
20 < H ≤ 40	0.14	0.43	0.66	0.00
40 < H ≤ 60	0.21	0.41	0.68	0.00
60 < H ≤ 80	0.26	0.35	0.62	0.00
80 < H ≤ 100	0.20	0.53	0.76	0.00
100 < H ≤ 120	0.21	0.41	0.81	0.00
120 < H ≤ 140	0.24	0.34	0.66	0.00
140 < H ≤ 160	0.17	0.30	0.61	0.00
160 < H ≤ 180	0.18	0.29	0.56	0.00
180 < H ≤ 200	0.19	0.26	0.52	0.00
200 < H ≤ 220	0.10	0.24	0.48	0.00
220 < H ≤ 240	0.14	0.24	0.45	0.00
240 < H ≤ 260	0.12	0.22	0.43	0.00
260 < H ≤ 280	0.14	0.21	0.41	0.00
280 < H ≤ 300	0.11	0.20	0.40	0.00

To execute the reliability calculations, we will use a set of typical permit vehicles configurations as shown in Figure 38. These configurations were adopted from the work performed for NCHRP 12-63 (Sivakumar et al; 2006) and multiplying the legal weights of each SHV by 150%. For 60-ft, 120-ft and 200-ft simple spans, these vehicles produce maximum moments as shown in Table 47.

Table 51. Conditional Reliability Index for Case II

Composite steel		Conditional Reliability index, , β					
Span (ft)	space (ft)	T4A	T5A	T6A	T7A	T8	BFT
60	4	3.65	3.69	3.72	3.74	3.74	3.76
60	6	3.64	3.68	3.71	3.74	3.73	3.75
60	8	3.64	3.67	3.70	3.73	3.73	3.74
60	10	3.61	3.65	3.68	3.71	3.71	3.72
60	12	3.59	3.62	3.66	3.69	3.68	3.70
Span (ft)	space (ft)						
120	4	3.29	3.34	3.39	3.43	3.44	3.45
120	6	3.29	3.34	3.39	3.43	3.43	3.44
120	8	3.29	3.35	3.39	3.44	3.44	3.45
120	10	3.27	3.33	3.38	3.42	3.42	3.43
120	12	3.25	3.30	3.35	3.39	3.40	3.41
Span (ft)	space (ft)						
200	4	2.97	3.02	3.06	3.10	3.11	3.12
200	6	2.98	3.03	3.07	3.11	3.12	3.13
200	8	2.99	3.04	3.08	3.12	3.13	3.13
200	10	2.98	3.02	3.07	3.11	3.12	3.12
200	12	2.96	3.00	3.04	3.08	3.09	3.10

Table 52. Final (unconditional) Reliability Index for Case II

Composite steel		Reliability index, β					
Span (ft)	space (ft)	T4A	T5A	T6A	T7A	T8	BFT
60	4	4.83	4.85	4.88	4.90	4.89	4.91
60	6	4.82	4.84	4.87	4.89	4.89	4.90
60	8	4.81	4.84	4.86	4.88	4.88	4.89
60	10	4.79	4.82	4.85	4.87	4.87	4.88
60	12	4.77	4.80	4.83	4.85	4.85	4.86
Span (ft)	space (ft)						
120	4	4.55	4.59	4.62	4.66	4.66	4.67
120	6	4.55	4.58	4.62	4.65	4.66	4.66
120	8	4.55	4.59	4.63	4.66	4.66	4.67
120	10	4.54	4.58	4.61	4.65	4.65	4.66
120	12	4.52	4.55	4.59	4.62	4.63	4.64
Span (ft)	space (ft)						
200	4	4.32	4.35	4.38	4.41	4.42	4.42
200	6	4.32	4.35	4.39	4.42	4.42	4.43
200	8	4.33	4.36	4.39	4.42	4.43	4.43
200	10	4.32	4.35	4.38	4.41	4.42	4.42
200	12	4.30	4.34	4.37	4.40	4.40	4.41

The nominal resistance that would be required for a set of multi-beam simple span steel bridges can be calculated by applying Eq. 32 with γ_D=1.25 for component dead weights and γ_D=1.50 for the wearing surface. In Eq. 32, the effect of the permit trucks is multiplied by a load factor γ_L=1.35 after applying the D.F. of Eq. 34 and the impact factor specified in the AASHTO LRFD as IM=1.33. In these calculations we are assuming that the dead loads of the components remain essentially unchanged when the applied live loads are changed. The conditional reliability index is given in Table 51. Eq.47 is then used to find the unconditional probability of failure that is then inverted using Eq. 39 to find the unconditional reliability index β. The final (unconditional) reliability index values are provided in Table 52 for the bridge configurations analyzed in this example.

The results of Tables 51 and 52 illustrate the following points:

- For a given span length and beam spacing, the different vehicle configurations produce little change in the reliability index. The largest difference in the unconditional β being on the order of 0.12 for the 120-ft span bridges.
- Increasing the beam spacing leads to small changes of less than 0.06 in the reliability index values.
- Increasing the span length leads to lower reliability index values.
- The average unconditional reliability index for the span lengths and beam spacings considered is on the order of β_{ave}=4.62 with a minimum value of β=4.30 and a maximum value β=4.91
- The higher reliability index obtained for the two side-by-side permits as compared to the single permit is primarily due to the low probability of having side-by-side events. If one looks at the conditional reliability index, then the average $\beta_{conditional}$=3.38 is closer to but still higher than the β_{ave}=3.07 obtained for a single permit truck. In this case, the still higher conditional reliability index value is partially due to the lower mean impact factor ($\overline{IM}$=1.09 versus 1.13) and the lower corresponding COV (V_{IM}=5.5% versus 9%) for side-by-side events which are justified by the low likelihood of having the peaks of the dynamic oscillations of the two side-by-side vehicles occur simultaneously.

Reliability Analysis and Adjustment of Live Load Factor for Case III –Permit Truck Alongside a Random Truck

For case III, the maximum live load effect is due to the permit truck alongside the maximum truck expected to occur simultaneously in the other lane. The maximum total load effect depends on the number of side-by-side events expected within the return period.

To determine the number of side-by-side permit-random truck events that would occur within a one-year period we will assume that the number of side-by-side events involving one random truck is obtained from Table 44 based on the ADTT. For example, we assume that N_P gives the number of permit truck crossings expected in a return period T. The average number of random trucks in one day is given by the ADTT. For ADTT between 1,000 and 2500 trucks per day, the percentage of side-by-side events involving a random truck (assumed to be those within a headway H $\leq$ 60 ft) is taken from Table 44 to be 1.25% (=0.41%+0.43%+0.41%). Thus, within a one-year return period, there will be 4.56 x ADTT (=1.25%x365xADTT) random trucks alongside another truck. Assuming that there will be 1000 permits on this route within this one-year period, the percentage of permits in the total truck population will be 2.74/ADTT

$\left(= \dfrac{1000}{ADTT \times 365} \right)$. This indicates that the number of random trucks alongside a permit truck will be on the average N_R=12.5 (=4.56x2.74) events within a one-year return period. The maximum live load effect expected within this one-year period will be due to the heaviest of these 12.5 random trucks combined with the effect of the permit. Table 53 gives the $L_{max\,NR}$ values for the maximum moment effect on simple spans obtained for the maximum of 12.5 events for single lanes for WIM data collected at 6 California sites. These are obtained by applying the protocls steps 12.2.1 with $N=N_r$=12.5 in Equations 26 and 27. The values in Table 53 are normalized as a function of the effect of the HL-93 vehicle.

Table 53. L_{max} values for the maximum moment effect on simple spans obtained for the maximum of 12.5 events for single lanes

Site	$L_{max\,N_R}$ for N_R=12.5 events		
	60-ft	120-ft	200-ft
Lodi 1	0.67	0.70	0.67
Lodi 2	0.69	0.71	0.63
Antelope 1	0.67	0.66	0.59
Antelope 2	0.72	0.70	0.62
LA710 1	0.70	0.68	0.63
LA 710 2	0.74	0.71	0.66
Bowman 1	0.64	0.62	0.56
Bowman 2	0.63	0.64	0.58
Average	0.68	0.68	0.62
Std. Dev.	0.04	0.03	0.04

The maximum live load effect is obtained from Eq. (49) where P is the load effect of the permit truck, DF_P is the distribution factor for the load P, $L_{max\,N_R}$ is the maximum load effect of random trucks for N_R events, DF_R is the distribution factor for the random load, and IM is the impact factor for side-by-side events. The coefficient of variation for $L_{max\,N_R} \times DF_R$ is estimated using Eq. (50) as:

$$V_{Lmax^*} = \sqrt{(5.6\%)^2 + (3.5\%)^2 + (2\%)^2 + (8\%)^2} = 10.6\%$$

where the 5.6% is the COV for site to site variability, the 3.5% is due to randomness in the WIM data and the 2% is due to the limitation in the WIM sample size, the 8% is due to the uncertainties in estimating DF_R

Assuming the effect of the permit load is deterministic, the coefficient of variation for $P \times DF_P$ is estimated as V_{P^*}=8% which is the COV for the load distribution factor, DF_P. Hence, the standard deviation of LL without the Impact factor is obtained using Eq. (52):

$$\sigma_{LL^*} = \sqrt{(8\% \times P \times DF_P)^2 + (10.6\% \times L_{max\,N_R} \times DF_R)^2}$$

and the COV for the live load effect on the critical beam including the effect of the impact IM is given by Eq. (53).

The live load mean obtained from Eq. (49) and the COV obtained from Eq. (53) are then used to find the reliability index from Eq. (40). In these example calculations, the same bridge configurations used fro Case II are assumed and the nominal R_n values are obtained from two side-by-side permit loads as traditionally done. The reliability calculations produce the results shown in Table 54.

The results in Table 54 show a large range for β varying between 2.93 and 4.51 with an average $\beta=3.72$. To reduce the average to $\beta_{target}=3.5$, the live load factor would need to be reduced from $\gamma_L=1.35$ to 1.25.

Table 48. Reliability Index for Case III

Composite steel		Reliability index, β					
Span (ft)	space (ft)	T4A	T5A	T6A	T7A	T8	BFT
60	4	4.03	4.16	4.30	4.41	4.40	4.47
60	6	4.04	4.17	4.32	4.44	4.43	4.49
60	8	4.04	4.18	4.33	4.45	4.44	4.51
60	10	4.01	4.16	4.32	4.43	4.42	4.49
60	12	3.98	4.13	4.29	4.41	4.40	4.47
Span (ft)	space (ft)						
120	4	3.37	3.52	3.67	3.80	3.82	3.85
120	6	3.37	3.53	3.68	3.81	3.83	3.86
120	8	3.38	3.54	3.70	3.84	3.86	3.89
120	10	3.36	3.52	3.68	3.82	3.84	3.87
120	12	3.33	3.49	3.65	3.79	3.81	3.84
Span (ft)	space (ft)						
200	4	2.95	3.07	3.18	3.28	3.30	3.31
200	6	2.96	3.08	3.19	3.30	3.32	3.33
200	8	2.97	3.09	3.20	3.31	3.34	3.35
200	10	2.95	3.08	3.19	3.30	3.32	3.34
200	12	2.93	3.05	3.16	3.27	3.30	3.31

Summary

The reliability analysis executed in this report for the limit state of Strength II with a live load factor $\gamma_L=1.35$ shows large variations in the reliability index depending on whether the permit load crosses the bridge with no other trucks alongside of it, or the permit is alongside another permit, or the permit is alongside a random truck. When the permit crossing is controlled such that no other trucks are alongside, the average reliability index for the span lengths and beam spacings considered in this report is on the order of $\beta_{ave}=3.07$. The average reliability index for two permits side by side is on the order of $\beta_{ave}=4.62$. The results for a permit alongside a random truck is on average $\beta=3.72$. A high average reliability index for two side-by-side permits is due to the low probability of the occurrence of such cases. If the number of permits is such that the chances of their side-by-side occurrences is close to 100%, then the average reliability index becomes $\beta=3.38$ which is lower than the random-permit reliability index of 3.72. In this latter

case, the reliability index β=3.38 is lower than the 3.72 because in the random-permit case it is unlikely that the random truck will be as heavy as the permit truck.

Adjustments to the live load factor γ_L=1.35 can be made to match a target reliability index. It should be noted that the determination of the target reliability index and the sample of bridge configurations for which the adjustment of the live load factor need to be made should be based on the experience of bridge owners with the performance of the bridges in their jurisdiction. The calculations performed as part of this report assume that the resistance, dead loads and live loads follow normal (Gaussian) probability distributions. This assumption was made to illustrate the procedure and can be adjusted as more information on these variables is assembled from on going and recent research studies.

Axle Loads for Deck Design from WIM Data (Step 9)

Axle Group Weight (Step 9.1 and 9.2)

One-lane (single truck) and two-lane (side-by-side trucks) axle events were analyzed for the purpose of calibrating deck design loads. For the one-lane events, single, tandem, tridem and quad axle groups were considered. For the two-lane events, single-single, single-tandem and tandem-tandem axle group combinations were considered. All other axle group combinations were consolidated into one group. Single axles and tandem axles are, by far, the most common axle groups.

Figure 39 shows, as a sample, the one-lane axle group weight histograms for WIM Site 9926 in Florida (I-75). Table 55 shows summary statistics for the data. Figure 40 shows the two-lane axle group weight histograms for the same site and Table 56 shows summary statistics for this data. In addition to the mean and standard deviation of the entire population, top 20% of the population, and top 5% of the population, the 99th percentile is shown. This upper extreme is taken in this project as the maximum anticipated load for design. Table 57 shows the 99th percentile of the one-lane axle group weights for all the WIM sites studied in this task. Table 58 shows the 99th percentile of the two-lane axle group weights for all the WIM sites studied in this task. As would be expected, the combined load of the two-lane events is less than sum of the constituent one-lane events indicating that the heaviest axles loads are not, necessarily, involved in side-by-side events. Appendix C contains axle group weight histograms for all other WIM sites studied in this task.

Rigorous calibration of load and resistance factors for deck design requires the availability of statistical data beyond live loads. LRFD did not specifically address deck components in the calibration. In the protocols developed in this study, the nominal axle loads derived using WIM data are used instead of the code specified values, where the W_{99} statistic is higher than the code values. All other factors are kept unchanged (load factor, deck dynamic load allowance). The governing nominal axle loads for LRFD deck design, are taken as:

- For single axles, 32 Kip load given in LRFD or the 99th percentile statistic W_{99}, whichever is higher
- For tandem axles, 50 Kips (2 x 25 Kips given in LRFD) or the 99th percentile statistic W_{99}, whichever is higher
- For tridem axles, the 99th percentile statistic W_{99}
- For quad axles, the 99th percentile statistic W_{99}

133

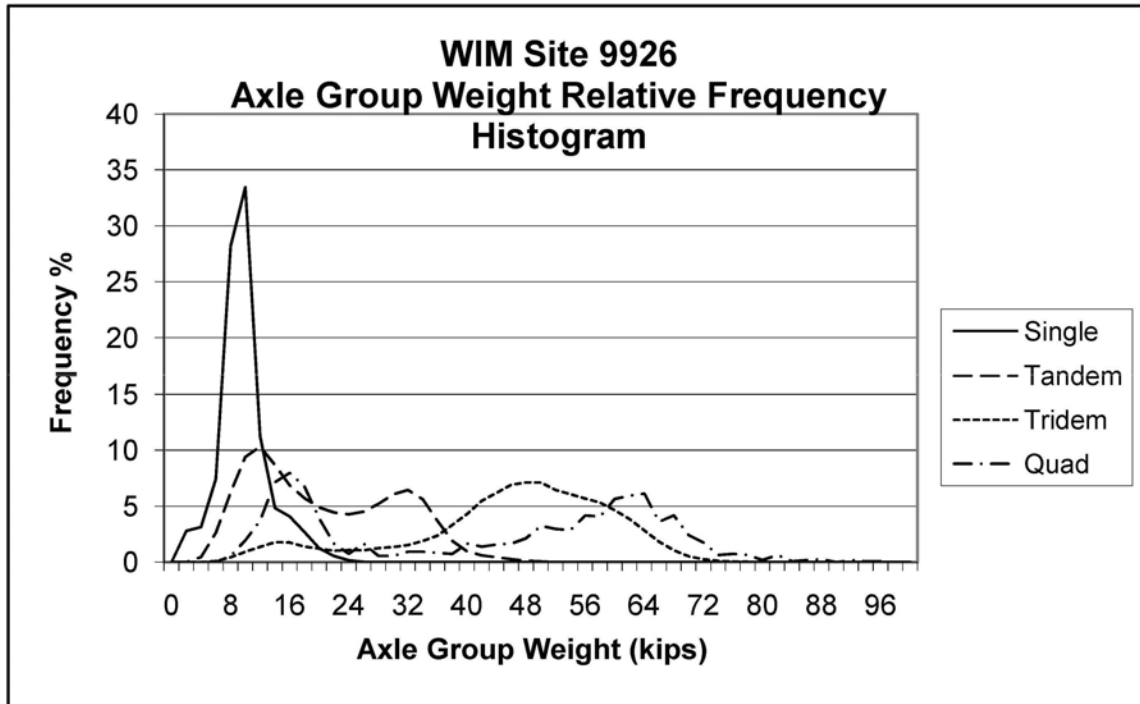The 99th percentile axle weights are as given in the tables for each axle type at each WIM site.

Figure 39 – 1-Lane Axle Group Weight Histogram. WIM Site 9926 in Florida

Table 55– 1-Lane Axle Group Weight Statistics. WIM Site 9926 in Florida

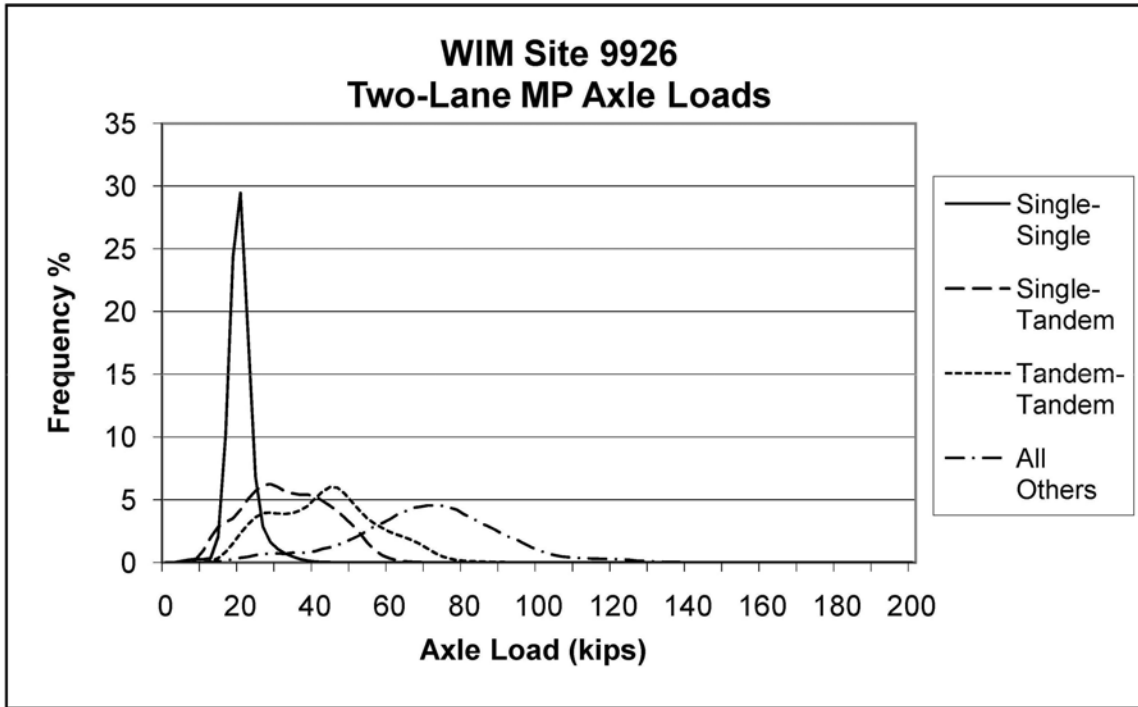| WIM Site 9926 Axle Group Weight Statistics				
Statistics	Single	Tandem	Tridem	Quad
Axle Count	2986536	3293111	94115	1077
Mean All Axles	10.831	21.773	46.649	43.899
Std Dev All Axles	3.494	9.847	13.955	22.070
COV All Axles	0.323	0.452	0.299	0.503
Mean Top 20% Axles	16.039	36.285	63.111	70.777
Std Dev Top 20% Axles	2.932	3.763	3.976	6.282
COV Top 20% Axles	0.183	0.104	0.063	0.089
Mean Top 5% Axles	20.152	41.357	68.343	79.444
Std Dev Top 5% Axles	2.008	3.913	3.817	6.380
COV Top 5% Axles	0.100	0.095	0.056	0.080
99th Percentile	20	42	68	82

Figure 40 - 2-Lane Axle Group Weight Histogram. WIM Site 9926 in Florida

Table 56 - 2-Lane Axle Group Weight Statistics. WIM Site 9926 in Florida

WIM Site 9926 Two-Lane Multiple Presence Axle Load Statistics				
Statistics	Single-Single	Single-Tandem	Tandem-Tandem	All Others
Event Count	13124	29735	16306	1801
Mean All Events	21.585	32.535	43.445	63.314
Std Dev All Events	4.994	10.486	14.111	17.759
COV All Events	0.231	0.322	0.325	0.280
Mean Top 20% Events	29.141	47.916	64.044	87.483
Std Dev Top 20% Events	3.345	4.509	6.522	8.462
COV Top 20% Events	0.115	0.094	0.102	0.097
Mean Top 5% Events	33.655	54.181	72.988	99.089
Std Dev Top 5% Events	3.003	4.094	5.088	7.489
COV Top 5% Events	0.089	0.076	0.070	0.076
99th Percentile	34	54	74	102

Table 57 – 99th Percentile One-Lane Axle Group Weight

State	Site ID	Route	Single	Tandem	Tridem	Quad
CA	0001	Lodi	18	36	50	40
CA	0003	Antelope	16	32	52	62
CA	0004	Antelope	18	34	56	64
CA	0059	LA710	16	34	46	54
CA	0060	LA710	18	36	46	60
CA	0072	Bowman	16	32	50	54
FL	9916	US-29	20	46	78	88
FL	9919	I-95	14	32	50	62
FL	9926	I-75	20	42	68	82
FL	9927	SR-546	18	38	58	64
FL	9936	I-10	22	44	74	94
IN	9511	I-65	14	30	52	62
IN	9512	I-74	18	38	58	68
IN	9532	US-31	16	34	58	72
IN	9534	I-65	16	34	56	66
IN	9544	I-80/I-94	16	34	54	64
IN	9552	US-50	16	34	56	62
MS	2606	I-55	20	48	76	78
MS	3015	I-10	16	36	52	68
MS	4506	I-55	18	40	60	78
MS	6104	US-49	16	36	52	74
MS	7900	US-61	16	40	56	78
TX	0506		18	36	56	--
TX	0516		18	36	56	--
TX	0523		18	36	62	--
TX	0526		18	36	60	--

Table 58 - 99th Percentile Two-Lane Axle Group Weight

State	Site ID	Route	Single-Single	Single-Tandem	Tandem-Tandem	Other
CA	0001	Lodi	34	50	66	76
CA	0003	Antelope	30	46	62	82
CA	0004	Antelope	32	48	64	78
CA	0059	LA710	26	44	62	72
CA	0060	LA710	30	48	66	74
CA	0072	Bowman	30	46	62	80
FL	9916	US-29	36	60	78	90
FL	9919	I-95	26	42	58	74
FL	9926	I-75	32	58	74	120
FL	9927	SR-546	30	50	70	76
FL	9936	I-10	38	60	84	106
IN	9511	I-65	26	40	54	78
IN	9512	I-74	34	52	72	90
IN	9532	US-31	28	46	64	84
IN	9534	I-65	28	44	58	86
IN	9544	I-80/I-94	28	46	60	80
IN	9552	US-50	28	46	64	70
MS	2606	I-55	36	62	86	92
MS	3015	I-10	28	46	66	78
MS	4506	I-55	34	54	72	84
MS	6104	US-49	32	50	68	90
MS	7900	US-61	32	52	68	76
TX	0506		32	50	68	84
TX	0516		30	48	66	82
TX	0523		30	50	70	96
TX	0526		32	50	68	96

CHAPTER 4

CONCLUSIONS AND SUGGESTED RESEARCH

CONCLUSIONS

The present HL-93 load model, and in fact the calibration of the AASHTO LRFD specifications, is based on the top 20% of trucks in an Ontario truck weight database assembled in 1975 from a single site over only a two-week period. It reflects truck configurations and weights taken in the mid-1970s, which primarily consisted of five-axle semi trailer trucks. In the past 30 years, truck traffic has seen significant increases in volume and weight. Therefore, current AASHTO specified live load models, that are based on past Canadian traffic data, may not represent modern and future traffic conditions in some US jurisdictions.

Bridge engineers often focus on enhancing the knowledge of member and system resistances with less effort expended on understanding the live load demand on bridge elements and systems. Enhancement of bridge live load models needs representative samples of unbiased truck weight data that meet accepted quality standards. It also requires information on simultaneous presence of multiple trucks on bridges. Traditionally, the latter has been assembled from headway data, and has not been collected in a manner suitable for the development of design live loads. Due to the development of various weigh-in-motion technologies, the quality and quantity of WIM data has greatly improved in recent years. Unbiased truckloads are now being collected at normal highway speeds, in large quantity, and without truck driver's knowledge. Modern WIM data loggers have the capability to record and report truck arrival times to an accuracy of 0.01 second, sufficient for estimating multiple presence probabilities. This information, however, has not been used to update the bridge design loads. In this regard, the lack of nationally accepted protocols may have been a contributing factor.

The goal of this project, therefore, was to develop a set of protocols and methodologies for using available recent truck traffic data collected at different US sites and recommend a step-by-step procedure that can be followed to obtain live load models for LRFD bridge design. The protocols are geared to address the collection, processing and use of national WIM data to develop and calibrate vehicular loads for LRFD superstructure design, fatigue design, deck design and design for overload permits. The study also gives practical examples of implementing these protocols with recent national WIM data drawn from states/sites around the country with different traffic exposures, load spectra, and truck configurations.

Truck traffic data should be collected through Weigh-In-Motion systems that can collect simultaneously headway information as well as truck weights and axle weights and axle configurations while remaining hidden from view and unnoticed by trucks drivers. Truck data surveys collected at truck weigh stations and publicized locations are not reliable for use in live load modeling, because, they are normally avoided by illegal overweight vehicles that could control the maximum loads applied on bridge structures.

The selection of WIM systems sites should focus on sites where the owners maintain a quality assurance program that regularly checks the data for quality and requires system repair or recalibration when suspect data is identified. Weighing accuracy is sensitive to roadway conditions. Roadway conditions at a WIM site can deteriorate after a system is installed and calibrated. Regular maintenance and recalibrations are essential for reliable WIM system performance. Quality information is more important than the quantity of traffic data collected. It is far better to collect small amounts of well-calibrated data than to collect large amounts of data from poorly calibrated scales. Even small errors in vehicle weight measurements caused by poorly calibrated sensors could result in significant errors in measured loads. For long duration

counts, the scale should be calibrated initially, the traffic characteristics at that site should be recorded, and the scale's performance should be monitored over time. The State should also perform additional, periodic on-site calibration checks (at least two per year). These steps will ensure that the data being collected are accurate and reliable. Site-specific calibration is the only way that the dynamic effects of the pavement leading to the scale can be accounted for in the WIM scale calibration. This calibration process should be executed for a whole range of truck and axle weight types and configurations.

In many spans, the maximum lifetime truck-loading event is the result of more than one vehicle on the bridge at a time. Obtaining reliable multiple presence statistics requires large quantities of continuous WIM data with refined time stamps, which may not be available at every site. Studies done using New York WIM data during this project show that there is a strong correlation between multiple presence and ADTT. The multiple presence statistics are mostly transportable from site to site with similar truck traffic volumes and traffic flow and need not be repeated for each site. The site ADTT could serve as a key variable for establishing a site multiple presence value. The multiple-presence probabilities for permit trucks are significantly different from those used for normal traffic. Information on loads and multiple-presence probabilities for permits need to be obtained locally or regionally through WIM measurements and considered in the STRENGTH II design process since the data used for calibration of national codes are unlikely to be representative of all jurisdictions.

DRAFT RECOMMENDED PROTOCOLS FOR USING TRAFFIC DATA IN BRIDGE DESIGN

An aim of these processes is to capture weight data appropriate for national use or data specific to a state or local jurisdiction where the truck weight regulations and/or traffic conditions may be significantly different from national standards. The objective is to use data from existing WIM sites to develop live load models for bridge design. The models will be applicable for the strength, serviceability and fatigue design of bridge members, including bridge decks and design vehicles for overload permitting. Based on the research findings of this project, step-by-step protocols for collecting and using traffic data in bridge design have been developed. The recommended protocols are summarized as follows:

STEP 1   DEFINE WIM DATA REQUIREMENTS FOR LIVE LOAD MODELING

This step defines the types of traffic data and WIM sensor calibration statistics needed for live load modeling of superstructure design load models (STRENGTH I), overload permitting (STRENGTH II), deck design, and for calibration of fatigue load models.

STEP 2   SELECTIONS OF WIM SITES FOR COLLECTING TRAFFIC DATA FOR BRIDGE DESIGN

This step defines the criteria to be used for selecting WIM sites for national, state-specific, route-specific, and for site-specific design live load modeling. National study of truck loads can be conveniently handled by dividing the country into five regions. Representative states are selected from each region and the sites and routes for WIM data collection are selected based on roadway functional classifications. Some of the criteria for selecting WIM sites include: remote WIM sites away from weigh stations with free flowing traffic; sites that can provide a year's worth of continuous data; sites that have been recently calibrated and are subject to a regular maintenance and quality assurance program; and sites equipped with

current sensor and equipment technologies (preferably able to capture and record truck arrival times to the nearest $1/100^{th}$ of a second or better).

STEP 3   QUANTITIES OF WIM DATA REQUIRED FOR LOAD MODELING

There are several possible methods available to calculate the maximum load effect for a bridge design period from truck WIM data. The one implemented in these protocols is based on the assumption that the tail end of the histogram of the maximum load effect over a given return period approaches a Gumbel distribution as the return period increases. The method assumes that the WIM data is assembled over a sufficiently long period of time, preferably a year, to ensure that the data is representative of the tail end of the truck weight histograms and to factor in seasonal variations and other fluctuations in the traffic pattern. Sensitivity analyses have shown that the most important parameters for load modeling are those that describe the shape of the tail end of the truck load effects histogram. Step 3 provides recommendations for the quantity of WIM data to be collected from each site. They include: 1) A year's worth of recent continuous data at each site to observe seasonal changes of vehicle weights and volumes is preferable; 2) If continuous data for a year is unavailable seek a minimum of one month data for each season for each site; 3) Data from all lanes in both directions of travel.

STEP 4   WIM CALIBRATION & VERIFICATION TESTS

WIM devices used for collecting data for live load modeling should be required to meet performance specifications for data accuracy and reliability. Field tests to verify that a WIM system is performing within the accuracy required is an important component of data quality assurance for bridge load modeling applications. Steps to ensure that the data being collected are accurate and reliable include: 1) Initial calibration of WIM equipment 2) Periodic monitoring of the data reported by WIM systems as a means of detecting drift in the calibration of weight sensors, and 3) Periodic on-site calibration checks for long duration counts, where, in addition to Steps 1 and 2 above, the scale is subjected to periodic on-site calibration checks at least two per year and the calibration statistics retained for use in filtration of sensor errors.

STEP 5   PROTOCOLS FOR DATA SCRUBBING, DATA QUALITY CHECKS & STATISTICAL ADEQUACY OF TRAFFIC DATA

High speed WIM is prone to various errors, which need to be recognized and considered in the data review process to edit out unreliable data and unlikely trucks to ensure that only quality data is made part of the load modeling process. It is also important to recognize that unusual data is not all bad data. The WIM data should therefore be scrubbed to include only the data that meet the quality checks. Filtering protocols provided in this step should be applied for screening the WIM data prior to use in the live load modeling and calibration processes. Adjustments to the data scrubbing rules may need to be made to accommodate changes in truck configurations from state to state. Reviewing a sampling of trucks that were eliminated during the data scrubbing process is also recommended to check if the process is performing as intended. Ongoing simple quality checks are also performed on the WIM data to detect any operational problems with the sensors.

STEP 6   GENERALIZED MULTIPLE-PRESENCE STATISTICS FOR TRUCKS AS A
                FUNCTION OF TRAFFIC VOLUME

In many spans, the maximum lifetime truck-loading event is the result of more than one
vehicle on the bridge at a time. Refined time stamps are critical to the accuracy of MP
statistics for various truck loading cases including: single, following, side-by-side, and
staggered. However, multiple presence statistics are mostly transportable from site to site
with similar truck traffic volumes and traffic flow. A relationship between MP and traffic
volume could be developed to utilize the MP values from national data to any given site
without performing a site-specific analysis. In this step, relationship between the trucks
weights in the drive lane and passing lanes must be established to determine whether passing
trucks characteristics are similar to those in the main traffic lane and if there is a correlation
between the truck properties.

STEP 7   PROTOCOLS FOR WIM DATA ANALYSIS FOR ONE-LANE LOAD
                EFFECTS FOR SUPERSTRUCTURE DESIGN

In this step single lane load effects for single truck events and for following truck events for
superstructure design are determined. Load effects for following trucks may be obtained
directly from the WIM data where accurate time arrival stamps are collected. Generalized MP
Statistics obtained in Step 6 may be used for simulation of load effects where accurate truck
arrival time stamps are not available. The trucks are grouped into bins by travel lane and run
through moment and shear influence lines (or structural analysis program) for simple and
two-span continuous spans. The results are normalized by dividing by the corresponding load
effects for HL-93.
     Legal loads and routine permits are grouped under STRENGTH I. Heavy special permits
are grouped under STRENGTH II. In most states permit records are either not specific
enough or detailed enough to allow separation of permit loads from non-permit loads in a
large WIM database. The protocols recommend that in such cases to group trucks with six or
fewer axles in the STRENGTH I calibration. Vehicles in this group include legal trucks and
routine permits or divisible load permits. These vehicles (legal loads and un-analyzed
permits) are considered to be enveloped by the HL-93 load model. Group all trucks with
seven or more axles in the STRENGTH II calibration.

STEP 8   PROTOCOLS FOR WIM DATA ANALYSIS FOR TWO-LANE LOAD
                EFFECTS FOR SUPERSTRUCTURE DESIGN

Determine the number of side-by-side or staggered truck multiple presence events
where trucks are in adjacent lanes in each direction. Run the combined truck with the
trucks offset by their actual headway separation through moment and shear influence lines for
simple and two-span continuous spans. Estimate the maximum daily load effects for two
random trucks simultaneously crossing the bridge. The results are normalized by
dividing by the corresponding load effects for HL-93. Where accurate time arrival stamps are
not available, generalized MP Statistics obtained in Step 6 may be used for simulation of load
effects. Legal loads and routine permits are grouped under STRENGTH I. Heavy special
permits are grouped under STRENGTH II. As in Step 7, the protocols recommend that in
cases where reliable permit record are unavailable to group trucks with six or fewer axles in
the STRENGTH I calibration and trucks with seven or greater axles in the STRENGTH II
calibration.

STEP 9   ASSEMBLE AXLE LOAD HISTOGRAMS FOR DECK DESIGN

As before, separate trucks into STRENGTH I and STRENGTH II groups for single events and for two-lane loaded cases. For each group, generate axle weight relative frequencies histograms for axle types: Single, Tandem, Tridem, and Quad axles. Multiple-presence probabilities are determined for side-by-side axle events.

STEP 10   FILTERING OF WIM SENSOR ERRORS / WIM SCATTER FROM WIM HISTOGRAMS

Current WIM systems are known to have certain levels of random measurement errors that may affect the accuracy of the load modeling results.   This step proposes an approach to filter out WIM measurement errors from the collected WIM data histograms. To execute the filtering process, calibration data for the WIM system for a whole range of trucks should be obtained. The results of these sensor calibration tests will be the basis for filtering out WIM measurement errors for each WIM data site. The Protocols present a procedure to filter out the WIM calibration errors from the measured WIM histograms of gross weights (or load effects) to obtain WIM data histograms that reflect the actual truck weights rather than the measured weights.

STEP 11   ACCUMULATED FATIGUE DAMAGE AND EFFECTIVE GROSS WEIGHT FROM WIM DATA

Updating the LRFD fatigue load model using recent WIM data is described in this step. Damage accumulation laws such as Miner's rule can then be used to estimate the fatigue damage for the whole design period for the truck population at a site. Cumulative fatigue damage from the WIM population is compared to the LRFD fatigue truck to determine the fatigue damage adjustment factor K. Based upon the results of the WIM study changes may be proposed to the LRFD fatigue truck model, its axle configuration and/or its effective weight.

STEP 12   LIFETIME MAXIMUM LOAD EFFECT L_{max} FOR SUPERSTRUCTURE DESIGN

In order to check the calibration of load models and/or load factors for strength design, it is necessary to estimate the mean maximum lifetime loading or load effect L_{max}. There are several possible methods available to calculate the maximum load effect for a bridge design period from truck WIM data. Simplified analytical methods or simulations may be used to estimate the maximum loading over a longer period (75 years), from short-term WIM data. The approach implemented in these protocols is found to be one of the easiest methods that provide results comparable to many other computationally intensive methods, including Monte Carlo simulations. This statistical projection method is based on the assumption that the tail end of the histogram of the maximum load effect over a given return period approaches a Gumbel (extreme value) distribution as the return period increases.

STEP 13   DEVELOP AND CALIBRATE VEHICULAR LOAD MODELS FOR BRIDGE DESIGN

Various levels of complexity are available for utilizing the site-specific truck weight and traffic data to calibrate live load models for bridge design. A simplified calibration approach (Method I) is proposed that focuses on the maximum live load variable, L_{max} for

updating the live load model or the load factor for current traffic conditions, in a manner consistent with the LRFD calibration. The ratio, r (L_{max} WIM data, divided by L_{max} Ontario data) for one-lane and for two-lanes is used to adjust the live load factor. This procedure assumes that the present LRFD calibration and safety indices are adequate for the load data and that the site-to-site variability (COV) of the present data and the data then available are consistent. A more robust reliability-based approach (Method II) is also presented that considers both the recent load data and the site-to-site variations in WIM data in the calibration of live loads.

During the development of the step-by-step protocols, recent long-term WIM data collected at several NY WIM sites by NYSDOT were obtained and used to test the validity and applicability of the protocols. The testing process was very helpful in ensuring that the recommended draft protocols were practical and could be effectively implemented using already available national WIM data.

DEMONSTRATION OF PROTOCOLS USING NATIONAL WIM DATA

The draft recommended protocols were implemented using recent traffic data for a whole year (either 2005 or 2006) from 26 WIM sites in five states across the country. The states were: CA, TX, FL, IN, and MS. The states and WIM sites were chosen to capture a variety of geographic locations and functional classes, from urban interstates, rural interstates and state routes. An aim of this task was to give practical examples of using these protocols with national WIM data drawn from sites around the country with different traffic exposures, load spectra, and truck configurations. Adjustments and enhancements were made to the several protocol steps based on the experience gained from this demonstration task.

The lifetime maximum L_{max} and r values (ratio of L_{max} values) determined using Step 12 and Method I of Step 13 showed a significant, and consistent difference between the r-values for the 1-Lane events and 2-Lane events. The r-values for 1-Lane events are significantly greater than those for 2-Lane events. Whereas the maximum r-values for 2-Lane events had a maximum value of 1.184, the 1-Lane events had a maximum r-value among all WIM sites of 2.402. This seems to indicate that the live loading defined in the LRFD specification is fairly adequate in modeling the lifetime maximum loading on a span with two lanes loaded, but underestimates the lifetime maximum loading on a span with only one lane loaded. However, as discussed in Step 13, using a single maximum or characteristic value for L_{max} for a State would be acceptable if the scatter or variability in L_{max} from site-to-site for the state was equal to or less than the COV assumed in the LRFD calibration. The site-to-site scatter in the L_{max} values obtained from recent WIM data showed significant variability from span to span, state to state, and between one-lane and two-lane load effects, well above the overall 20% COV used during the LRFD calibration. For example, the data from Florida show a COV for the moments of simple span bridges under one-lane loadings that varies from 32.5% for the 20-ft simple spans to 22.3% for the 200-ft simple span. (On the other hand, the site-to-site COV statistics for California are lower). Live load modeling using Method II was then implemented to reflect the site-to-site variability.

The results show that for the California truck traffic conditions, the reliability index for one lane is on the average equal to $\beta=3.55$ which is close to the LRFD target $\beta=3.50$. For two lanes of truck traffic, the average reliability index is $\beta=4.63$. This indicates that for the two-lane loading of California bridges, the current AASHTO LRFD is conservative producing higher reliability index values than the target $\beta=3.50$ set by the AASHTO LRFD code writers. If the intent is to reduce the reliability index for the two lane cases to the target $\beta=3.5$, then an adjusted live load factor $\gamma_L=1.20$ would result using the steps provided in the protocols. The reliability index for Florida for one lane loading drops to an average of $\beta=2.58$. The two-lane L_{max} would

lead to an average reliability index β=3.96. The latter value is still higher than the target β=3.5 while the one lane reliability is lower than the target. If the live load factor is raised to γ_L=2.37 then the reliability indices for the Florida sites would increase to β=3.50 for the one-lane cases. For Indiana, the reliability index for one lane of loading is on the average equal to β=3.16 for one-lane loading and the two-lane loading would lead to an average reliability index β=4.71. The Indiana data shows a site-to-site variability in COV's on the order of 11% to 15% for both one-lane and two-lanes loadings.

Both calibration methods indicate that the live loading defined in the LRFD specification is generally adequate or even conservative in modeling the lifetime maximum loading on a span with two lanes loaded, but it underestimates the lifetime maximum loading for the one lane loaded case. This could be attributable to the increasing presence of heavy exclusion vehicles and/or routine permits in the traffic stream. The load limit enforcement environment in a state will also have a more discernible influence on the maximum single-lane loading than the maximum two-lane loading, which results from the presence of two side-by-side trucks. Additionally, with more multiple presence and WIM data currently available, the projections of L_{max} for two-lane events as undertaken in this study are based on actual side-by-side events rather than based on simulations using conservative assumed side-by-side multiple-presence probabilities as done during the AASHTO LRFD code calibration. The WIM data collected as part of this study show that the actual percentage of side-by-side multiple truck event cases is significantly lower than assumed by the AASHTO LRFD code writers who had to develop their models based on a limited set of multiple presence data.

Knowing the actual truck weight distribution in each lane allowed the determination of the relationship between the trucks weights in the main traffic lane (drive lane) and adjacent lanes and if there is a correlation between the truck properties. This study seems to indicate that there is some negative correlation between the weights of side-by-side trucks. This means that when a heavy truck is in one lane, the other lane's truck is expected to be lighter. Here again, the conservative assumptions used during the LRFD calibration were not adequately supported by field measurements.

SUGGESTED RESEARCH AND IMPROVEMENTS IN DATA COLLECTION

Developing and calibrating bridge live load models requires large amounts of quality WIM data. Improvements in WIM data collection is needed to allow the effective implementation of these protocols. Suggested research on this topic for the future and recommendations for improving WIM data collection are as follows:

- States should evaluate their WIM data collection equipment to ascertain if it can provide the quantity and quality of data to implement these protocols. It may be necessary to upgrade the WIM technology and data collection system at specific sites selected for data collection.
- DOT's should carefully consider the locations of WIM sites within a state. Remote WIM sites away from weigh stations are needed to provide un-biased WIM data. Availability of WIM sites on heavy freight routes, hauling routes, or routes known to have significant permit traffic is important for live load modeling purposes.
- WIM devices should be required to meet ASTM performance specifications for data accuracy and reliability. The WIM sites should be subject to a regular maintenance and quality assurance program. The system components should be reliable enough to be able to provide a year's worth of continuous data.
- The WIM system should be able to capture and record truck arrival times to the nearest $1/100^{th}$ of a second or better to allow the determination of truck headway separations.

144

Sensors should be placed in the drive lane and passing lanes at sites used for data collection.

- The WIM system should not cut off trucks having more than a certain number of axles or heavier than a certain upper weight limit. It is important to record the long heavy superloads that may have a dozen or more axles and weigh over 200 Kips. These trucks populate the upper tail of the truck weight distribution and have a significant influence on bridge safety.

- WIM calibration and verification testing requirements defined in Step 4 should be implemented as part of an overall Quality Assurance Program. Regular maintenance and periodic recalibration of any WIM system is critical for obtaining reliable traffic data. Initial calibration and periodic recalibration every six months are recommended for sites selected for data collection. Calibration of WIM equipment should follow LTPP calibration procedures or ASTM 1318 standards. Periodic monitoring and quality check of the data reported by WIM systems should be performed as a means of detecting drift in the calibration of weight sensors. Calibration statistics should be maintained for each WIM site for use in the error filtration process during the data analysis.

- Separating permit vehicles from non-permit traffic in large scale WIM data requires the availability of reliable electronic permits database/records of special permits authorized in a given period for a State. DOT surveys have indicated that such permit databases are not currently being maintained, at least in an electronic form. States should make necessary changes to their permit operations / management to create and maintain a comprehensive electronic database of overweight permits authorized that will allow these vehicles to be properly grouped as either STRENGTH I or STRENGTH II for live load modeling.

REFERENCES

1. American Association of State Highway and Transportation Officials (AASHTO). (2007). *LRFD Bridge Design Specifications, 4th Edition*. With Interims, Washington, D.C.

2. Lichtenstein Consulting Engineers, Inc. (2006): NCHRP Project 12-63 *Legal Truck Loads and AASHTO Legal Loads for Posting*, Final Report to the Transportation Research Board.

3. Lichtenstein Consulting Engineers, Inc. (2000). "NCHRP Web Document 28 (NCHRP Project 12-46): *Manual for Condition Evaluation and Load Rating of Highway Bridges Using Load and Resistance Factor Philosophy*. Final Report to the Transportation Research Board.

4. NCHRP Report 368 (1999): *Calibration of LRFD Bridge Design Code* National Cooperative Highway Research Program (NCHRP), Transportation Research Board.

5. NCHRP Report 299 (1987): *Fatigue Evaluation Procedures for Steel Bridges.*

6. AASHTO (1987): *Guide for Maximum Dimensions and Weights of Motor Vehicles and for the Operation of Non-Divisible Load Oversize and Overweight Vehicles.*

7. NCHRP Synthesis 241 (1997): *Truck Operating Characteristics, A Synthesis of Highway Practice.*

8. NCHRP 12-51 Final Report (2002): *Effect of Truck Weight on Bridge Network Costs.*

9. TRB Special Report 267 (2002): *Regulation of Weights, Lengths, and Widths of Commercial Motor Vehicles.*

10. NCHRP Report 509 (2004): *Equipment for Collecting Traffic Load Data*

11. NCHRP Report 575 (2007): Legal *Truck Loads and AASHTO Legal Loads for Posting*

12. ARA Inc. (2004): NCHRP Project 1-37A Final Report; *Guide for Mechanistic-Empirical Design of New and Rehabilitated Pavement Structures, Parts I & II*, Transportation Research Board.

13. Washington State University (1995): NCHRP Project 3-39(2) Final Report; *On-Site Evaluation and Calibration Procedures for Weigh-in-Motion Systems.*

14. TRB Special Report 225 (1990): *Truck Weight Limits: Issues and Options*

15. TRB Special Report 227 (1990): *New Trucks for Greater Productivity and Less Road Wear.*

16. USDOT (2001): *Traffic Monitoring Guide.*

17. USDOT (2000): *Comprehensive Truck Size and Weight Study, Volumes I, II & III*

18. AASHTO (1987): *Guide for Maximum Dimensions and Weights of Motor Vehicles and for the Operation of Non-Divisible Load Oversize and Overweight Vehicles.*

19. FHWA/RD-85/012: *Loading Spectrum Experienced by Bridge Structures in the United States*

20. FHWA/OH-85/005 (1985): *Comprehensive Study of Bridge Loads and Reliability*

21. FHWA Office of Transportation Policy Studies; *Analysis of the Vehicle Inventory and Use Survey for Trucks with Five-Axles or More*, May, 2001,

22. NCHRP Project 12.28 (1992): *Development of Sit-Specific Load Models for Bridge Rating*

23. *Traffic-Load Forecasting Using Weigh-in-Motion Data*, Center for Transportation Research, University of Texas at Austin, March 1997.

24. Buckland, P., *North American and British Loan-Span Bridge Loads*, ASCE Journal of Structural Engineering, October 1991.

25. Gindy, M. and Nassif, H. (2006). "Multiple Presence Statistics for Bridge Live Load Based on Weigh-in-Motion Data," Transportation Research Board 86th Annual Meeting, Washington, D.C.)

26. Lui, W. D., C. A. Cornell, and R. A. Imbsen, "Analysis of Bridge Truck Loads," *Probabilistic Methods in Civil Engineering, Proceedings of the 5th ASCE Specialty Conference,* Blacksburg, VA USA, May 25-27 1998, p 221-224.

27. Moses, F., M. Ghosn, and R. E. Snyder, "Application of Load Spectra to Bridge Rating," *Transportation Research Record,* n 950, 1984, p 45-53.

28. Moses, F. (2000). *Calibration of Load Factors for LRFR Bridge Evaluation*. National Cooperative Highway Research Program (NCHRP). Transportation Research Board. NCHRP Report 454.

29. Bakht, B. and L. G. Jaeger, "Bridge Evaluation for Multipresence of Vehicles," *Journal of Structural Engineering,* v 116, n 3, Mar, 1990, p 603-618.

30. Miao, T. J. and T. H. T. Chan, "Bridge Live Load Models from WIM Data," *Engineering Structures,* v 24, n 8, Jul, 2002, p 1071-1084.

31. Minervino, C. M., Sivakumar, B., Moses, F., Mertz, D., Edberg, W., New AASHTO Guide Manual for Load and Resistance Factor Rating of Highway Bridges, ASCE Journal of Bridge Engineering, January 2004.

32. Heywood, R. J. and A. S. Nowak, "Bridge Live Load Models," *Proceedings of ICOSSAR '89, the 5th International Conference on Structural Safety and Reliability,* San Francisco, CA USA, Aug 7-11 1989, p 2147-2154.

33. Nowak, A. S. and Y.-K. Hong, "Bridge Live-Load Models," *Journal of Structural Engineering,* v 117, n 9, Sept, 1991, p 2757-2767.

34. Nowak, A. S. and M. M. Szerszen, "Bridge Load and Resistance Models," *Engineering Structures,* v 20, n 11, Nov, 1998, p 985-990.

35. Moses, F., "Calibration of Load Factors for Load and Resistance Factor Evaluation," *Proceedings of the 1999 Structures Congress "Structural Engineering in the 21st Century",* New Orleans, LA USA, Apr 18-21 1999, p 292-295.

36. Nowak, A. S. and H. N. Grouni, "Calibration of the Ontario Highway Bridge Design Code 1991 Edition," *Canadian Journal of Civil Engineering,* v 21, n 1, Feb, 1994, p 25-35.

37. Buckland, P. G. and R. G. Sexsmith, "Comparison of Design Loads for Highway Bridges," *Canadian Journal of Civil Engineering,* v 8, n 1, Mar, 1981, p 16-21.

38. Sivakumar, B. *New AASHTO Load Models for Load Rating & Posting*, 23rd Annual International Bridge Conference, Pittsburgh, June 2006.

39. Sivakumar B. LRFR for More Uniform Safety in Bridge Load Ratings and Postings. TRB Sixth International Bridge Engineering Conference, July 2005, Boston, MA.

40. Sivakumar B, *Recommendation of a New Truck Model for Bridge Evaluation*, Journal of Bridge Structures, 2005

41. Sivakumar, B., Minervino, C.M., *Load Rating and Permit Review Using Load and Resistance Factor Philosophy*, TRB, 8th International Bridge Management Conference, Denver, Colorado, April 1999.

42. Sivakumar, B., and Minervino, C.M., *Bridge Evaluation using Load and Resistance Factor Philosophy,* 1999 ASCE Structures Congress, New Orleans, April, 1999.

43. Kulicki, J. M, "Development of Bridge Live Load Models," *Proceedings of the ASCE Structures Congress '94,* Atlanta, GA USA, Apr 24-28 1994, p 532-537.

44. Kulicki, John M.; Mertz, Dennis R. *New Live Load Model for Bridge Design,* Proceedings of the 8th Annual International Bridge Conference, Jun 10-12 1991, Pittsburgh, PA.

45. Nowak, A. S., "Development of Bridge Load Model for LRFD Code," *Structural Engineering in Natural Hazards Mitigation, Proceedings of the Symposium on Structural Engineering in Natural Hazards Mitigation,* Irvine, CA USA, Apr 19-21 1993, p 1041-1046.

46. Agarwal, A. and M. S. Cheung, "Development of Loading-Truck Model and Live-Load Factor for the Canadian Standards Association CSA-S6 Code," *Canadian Journal of Civil Engineering,* v 14, n 1, Feb, 1987, p 58-67.

47. Ghosn, M. and F. Moses, "Effect of Changing Truck Weight Regulations on U.S. Bridge Network," *Journal of Bridge Engineering,* v 5, n 4, Nov, 2000, p 304-310.

48. Nowak, A. S., "Live Load Model for Highway Bridges," *Structural Safety,* v 13, n 1-2, Dec, 1993, p 53-66.

49. Nowak, A. S. and H. Nassif, "Live Load Models Based on WIM Data," *Probabilistic Mechanics and Structural and Geotechnical Reliability, Proceedings of the 6th ASCE Specialty Conference,* Denver, CO USA, Jul 8-10 1992, p 587-590.

50. Heywood, R. J., "Multiple Presence Load Model for Bridges," *Probabilistic Mechanics and Structural and Geotechnical Reliability, Proceedings of the 6th ASCE Specialty Conference,* Denver, CO USA, Jul 8-10 1992, p 579-582.

51. Jaeger, L. G. and B. Bakht, "Multiple Presence Reduction Factors for Bridges," *Bridges and Transmission Line Structures, Proceedings of the Sessions at Structures Congress '87,* Orlando, FL USA, p 47-59.

52. Fu, G. and O. Hag-Elsafi, "New Safety-Based Checking Procedure for Overloads on Highway Bridges," *Transportation Research Record,* n 1541, Nov, 1996, p 22-28.

53. Fu, G. and O. Hag-Elsafi, "Overweight Trucks and Safety of Bridges," *Proceedings of the ASCE Structures Congress '94,* Atlanta, GA USA, Apr 24-28 1994, p 284-289.

54. Fujino, Y. and M. Ito, "Probabilistic Analysis of Traffic Loading on Highway Bridges," *National Bureau of Standards,* Special Publication, v 2, 1979, p 539-550.

55. Kulicki, J. M., "Rating Bridges for Special Permit Loadings with Considerations of Future Life – Case Studies," *Reports of the Working Commissions (International Association for Bridge and Structural Engineering),* v 38, 1982, p 91-112.

56. Ghosn, M. and F. Moses, "Reliability Calibration of Bridge Design Code," *Journal of Structural Engineering,* v 112, n 4, Apr, 1986, p 745-763.

57. Ghosn, M. and D. M. Frangopol, "Site-Specific Live Load Models for Bridge Evaluation," *Probabilistic Mechanics and Structural and Geotechnical Reliability, Proceedings of the 7th ASCE Specialty Conference,* Worcester, MA USA, Aug 7-9 1996, p 30-33.

58. Laman, J. A. and A. S. Nowak, "Site-Specific Truck Loads on Bridges and Roads," *Proceedings of the Institution of Civil Engineers: Transport,* v 123, n 2, May, 1997, p 119-133.

59. Harman, D. J. and A. G. Davenport, "Statistical Approach to Traffic Loading on Highway Bridges," *Canadian Journal of Civil Engineering,* v 6, n 4, Dec, 1979, p 494-513.

60. Brameld, G. H., "Statistical Formulation of Highway Bridge Live Loads," *Pitagora Editrice,* v 2, 1983, p 1073-1084.

61. Harman, D. J., A. G. Davenport, and W. S. S. Wong, "Traffic Loads on Medium and Long Span Bridges," *Canadian Journal of Civil Engineering,* v 11, n 3, Sept, 1984, p 556-573.

62. Nowak, A. S. and D. M. Ferrand, "Truck Load Models for Bridges," *Proceedings of the 2004 Structures Congress – Building on the Past: Securing the Future,* Nashville, TN USA, May 22-26 2004, p 1147-1156.

63. Frangopol, D. M., G. G. Goble, and N. Tan, "Truck Loading Data for a Probabilistic Bridge Live Load Model," *Probabilistic Mechanics and Structural and Geotechnical Reliability, Proceedings of the 6th ASCE Specialty Conference,* Denver, CO USA, Jul 8-10 1992, p 340-343.

64. Jacobsohn, A. P., "Truck Weights: A Long and Winding Road," *Waste Age,* v 28, n 6, Jun, 1997, p 58-60, 62, 64-66, 68.

65. Fu, G. and O. Hag-Elsafi, "Vehicular Overloads: Load Model, Bridge Safety, and Permit Checking," *Journal of Bridge Engineering,* v 5, n 1, Feb, 2000, p 49-57.

66. Kim, S., A. S. Nowak, and R. Till, "Verification of Site-Specific Live Load on Bridges," *Probabilistic Mechanics and Structural and Geotechnical Reliability, Proceedings of the 7th ASCE Specialty Conference,* Worcester, MA USA, Aug 7-9 1996, p 214-217.

67. Laman, J. A. and A. S. Nowak, "Verification of Truck Loads for Girder Bridges," *Proceedings of the 13th Structures Conference, Part 1 of 2,* Boston, MA USA, Apr 3-5 1995, p 907-920.

68. Daniels, J. H., J. L. Wilson, B. T. Yen, L. Y. Lai, and R. Abbaszadeh, "WIM Plus Response Study of Four In-Service Bridges," *Engineer's Society of Western Pennsylvania, Official Proceedings – 3rd Annual International Bridge Conference,* Pittsburgh, PA USA, p 136-142.

69. Bez, R., R. Cantieni, and J. Jacquemoud, "Modeling of Highway Traffic Loads in Switzerland," *IABSE Proceedings P-117/87,* 1987, p 153-168. Publisher: International Association for Bridge and Structural Engineering.

70. Ghosn, M., F. Moses, and F. Gabriel, "Truck Data for Bridge Load Modeling," *Second Workshop on Bridge Engineering Research in Progress,* Reno, Nevada USA, Oct 29-30 1990, p 71-74.

71. Lui, W. D., C. A. Cornell, and R. A. Imbsen, "Analysis of Bridge Truck Loads," *Proceedings of the 5th ASCE Specialty Conference, Probabilistic Methods in Civil Engineering,* P.D. Spanos, ed., Blacksburg, Virginia USA, May 25-27 1988, p 221-224.

72. Kulicki, J. M. and D. R. Mertz, "New Live Load for Bridge Design," *Proceedings of the 8th Annual International Bridge Conference,* Pittsburgh, PA USA, Jun 10-12 1991, p 238.

73. Hwang, E.-S., H.-M. Koh, and D.-B. Bae, "A Proposal for New Design Live Load Model in Korea," *Structural Safety and Reliability: Proceedings of the Eighth International Conference, ICOSSAR'01,* Newport Beach, CA USA, Jun 17-22 2001, 1 page abstract (paper on CD-ROM).

74. Najafi, F. T. and B. Blackadar, "Analysis of Weigh-in-Motion Truck Traffic Data," *Proceedings of the 40th Annual Meeting of the Transportation Research Forum,* Philadelphia, PA USA, Oct 29-31 1998, p 139-162.

75. Nyman, W. E., "Calibration of Bridge Fatigue Design Model," *Journal of Structural Engineering,* v 111, n 6, Jun, 1985, p 1251-1266.

76. Gindy, M., and H. H. Nassif, "Comparison of Traffic Load Models Based on Simulation and Measured Data," *Joint International Conference on Computing and Decision Making in Civil Engineering*, Montreal, Canada, Jun 14-16 2006.

77. Caprani, C. C., S. A. Grave, E. J. O'Brien, and A. J. O'Connor, "Critical Loading Events for the Assessment of Medium Span Bridges," *ICCST '02: Proceedings of the 6th International Conference on Computational Structures Technology,* Prague, Czech Republic, Sept 4-6 2002, p 343-344 (abstract) (paper on CD-ROM). Editor: B.H.V. Topping and Z. Bittnar, Publisher: Civil Comp Press.

78. Laman, J. A. and A. S. Nowak, "Fatigue-Load Models for Girder Bridges," *Journal of Structural Engineering,* v 122, issue 7, Jul, 1996, p 726-733.

79. Au, A., C. Lam, A. C. Agarwal, and B. Tharmabala, "Bridge Evaluation by Mean Load Method per the Canadian Highway Bridge Design Code," *Canadian Journal of Civil Engineering,* v 32, n 4, Aug, 2005, p 678-686.

80. Laman, J. A. and A. S. Nowak, "Live Load Spectra for Bridge Evaluation," *Proceedings of the Symposium on Practical Solutions for Bridge Strengthening and Rehabilitation,* Des Moines, IA USA, Apr 5-6 1993, p 13-22.

81. van de Lindt, J. W., G. Fu, Y. Zhou, and R. M. Pablo Jr., "Locality of Truck Loads and Adequacy of Bridge Design Load," *Journal of Bridge Engineering,* v 10, issue 5, Sept, 2005, p 622-629.

82. Kim, S., A. F. Sokolik, and A. S. Nowak, "Measurement of Truck Load on Bridges in Detroit, Michigan Area," *Transportation Research Record 1541,* 1996, p 58-63.

83. Cohen, H., G. Fu, W. Dekelbab, and F. Moses, "Predicting Truck Load Spectra Under Weigh Limit Changes and its Application to Steel Bridge Fatigue Assessment," *Journal of Bridge Engineering,* v 8, n 5, Sept, 2003, p 312-322.

84. Moses, F., "Probabilistic Load Modeling for Bridge Fatigue Studies," *International Association for Bridge and Structural Engineering,* 1982, p 883-889.

85. Wu, S-S, "Procedure to Estimate Loading from Weigh-In-Motion Data," *Transportation Research Record 1536,* 1996, p 19-24.

86. Cheung, M. S. and W. C. Li, "Reliability Assessment in Highway Bridge Design," *Canadian Journal of Civil Engineering,* v 29, n 5, Oct, 2002, p 799-805.

87. Stamatiadis, N. and D. L. Allen, "Seasonal Factors Using Vehicle Classification Data," *Transportation Research Record 1593,* 1997, p 23-28.

88. Jones, D., "Summary of U.S. National and Regional Trends in Truck Loading," *Proceedings of the Third International Conference on Weigh-in-Motion (ICWIM3),* Orlando, FL USA, May 13-15 2002, p 277-280.

89. Wang, T-L, C. Liu, D. Huang, and M. Shahawy, "Truck Loading and Fatigue Damage Analysis for Girder Bridges Based on Weigh-In-Motion Data," *Journal of Bridge Engineering,* v 10, issue 1, Jan, 2005, p 12-20.

90. O'Connor, A. J., E. J. O'Brien, and B. Jacob, "Use of WIM Data in Development of a Stochastic Flow Model for Highway Bridge Design and Assessment," *Proceedings of the 3rd International Conference on Weigh-In-Motion (ICWIM3),* Orlando, FLA USA, May 13-15 2002, p 315-324.

91. Grundy, P. and G. Boully, "Fatigue Design in the New Australian Bridge Design Code," *Proceedings of the Austroads 5th Bridge Conference*, Hobart, Tasmania, May 19-21 2004, 12 pages.

92. Jamera, F. et al., "FHWA Study Tour for European Traffic-Monitoring Programs and Technologies," U.S. Department of Transportation Federal Highway Administration, Aug, 1997, 112 pages.

93. Qu, T., C. E. Lee, and L. Huang, "Traffic-Load Forecasting Using Weigh-In-Motion Data," *Research Report 987-6,* Mar, 1997, 133 pages.

94. Hwang, E.-S. and H.-M. Koh, "Simulation of Bridge Live Load Effects," *16th Congress of IABSE,* Lucerne, 2000, 8 pages.

95. Lu, Q., J. Harvey, T. Le, J. Lea, R. Quinley, D. Redo, J. Avis, "Truck Traffic Analysis Using Weigh-In-Motion (WIM) Data in California," Jun, 2002, 303 pages.

96. O' Brien, E. and A. Znidaric, "Report of Work Package 1.2 - Bridge WIM systems (B-WIM)," *Weighing In-Motion of Axles and Vehicles for Europe (WAVE)*, Jun, 2001, 100 pages.

97. Chotickai, P. and M. D. Bowman, "Truck Models for Improved Fatigue Life Predictions of Steel Bridges," *Journal of Bridge Engineering*, v 11, n 1, Jan, 2006, p 71-80.

98. Tallin, A. G. and T. Petreshock, "Modeling Fatigue Loads for Steel Bridges," *Transportation Research Record*, n 1275, p 23-26.

99. Ang & Tang (2007) *Probability Concepts in Engineering*", 2nd edition, Wiley, New York

100. Lee, C. E. and N. Souny-Slitine, "Final Research Findings on Traffic-Load Forecasting Using Weigh-In-Motion Data," *Research Report 987-7,* Sept, 1998, 39 pages.

101. O'Brien, E. J. and C. C. Caprani, "Headway Modeling for Traffic Load Assessment of Short to Medium Span Bridges," *The Structural Engineer,* Aug 16, 2005, p 33-36.

102. van de Lindt, J. W., G. Fu, R. M. Pablo Jr., and Y. Zhou, "Investigation of the Adequacy of Current Design Loads in the State of Michigan," *Research Report RC-1413,* Jul, 2002, 60 pages.

103. Stone, J. R., "North Carolina Forecasts for Truck Traffic," 19 pages.

104. Nichols, A. P. and D. M. Bullock, "Quality Control Procedures for Weigh-in-Motion Data," *FHWA/IN/JTRP-2004/12 – Final Report,* Jun, 2004, 238 pages.

105. O'Connor, A., and E. J. O'Brien, "Traffic Load Modelling and Factors Influencing the Accuracy of Predicted Extremes," *Canadian Journal of Civil Engineering,* v 32, 2005, p 270-278.